
# Global review of human-induced earthquakes

Gillian R. Foulger, Miles Wilson, Jon Gluyas, Bruce R. Julian, Richard Davies

PII: S0012-8252(17)30003-X
DOI: doi: 10.1016/j.earscirev.2017.07.008
Reference: EARTH 2456

To appear in: *Earth-Science Reviews*

Received date: 5 January 2017
Revised date: 19 July 2017
Accepted date: 23 July 2017

Please cite this article as: Gillian R. Foulger, Miles Wilson, Jon Gluyas, Bruce R. Julian, Richard Davies , Global review of human-induced earthquakes, *Earth-Science Reviews* (2017), doi: 10.1016/j.earscirev.2017.07.008

# GLOBAL REVIEW OF HUMAN-INDUCED EARTHQUAKES

Gillian R. Foulger[1], Miles Wilson[1], Jon Gluyas[1], Bruce R. Julian[1] & Richard Davies[2]

[1]Department of Earth Sciences, Durham University, Durham, DH1 3LE, U.K.

[2]School of Civil Engineering and Geosciences, Newcastle University, Newcastle upon Tyne NE1 7RU, UK

*Abstract*

The Human-induced Earthquake Database, *HiQuake*, is a comprehensive record of earthquake sequences postulated to be induced by anthropogenic activity. It contains over 700 cases spanning the period 1868 - 2016. Activities that have been proposed to induce earthquakes include the impoundment of water reservoirs, erecting tall buildings, coastal engineering, quarrying, extraction of groundwater, coal, minerals, gas, oil and geothermal fluids, excavation of tunnels, and adding material to the subsurface by allowing abandoned mines to flood and injecting fluid for waste disposal, enhanced oil recovery, hydrofracturing, gas storage and carbon sequestration. Nuclear explosions induce earthquakes but evidence for chemical explosions doing so is weak. Because it is currently impossible to determine with 100% certainty which earthquakes are induced and which not, *HiQuake* includes all earthquake sequences proposed on scientific grounds to have been human-induced regardless of credibility. Challenges to constructing *HiQuake* include under-reporting which is ~30% of M ~4 events, ~60% of M ~3 events and ~90% of M ~2 events. The amount of stress released in an induced earthquake is not necessarily the same as the anthropogenic stress added because pre-existing tectonic stress may also be released. Thus earthquakes disproportionately large compared with the associated industrial activity may be induced. Knowledge of the magnitude of the largest earthquake that might be induced by a project, $M_{MAX}$, is important for hazard reduction. Observed $M_{MAX}$ correlates positively with the scale of associated industrial projects, fluid injection pressure and rate, and the yield of nuclear devices. It correlates negatively with calculated inducing stress change, likely because the latter correlates inversely with project scale. The largest earthquake reported to date to be induced by fluid injection is the 2016 M 5.8 Pawnee, Oklahoma earthquake, by water-reservoir impoundment the 2008 M ~8 Wenchuan, People's Republic of China, earthquake, and by mass removal the 1976 M 7.3 Gazli, Uzbekistan earthquake. The minimum amount of anthropogenic stress needed to induce an earthquake is an unsound concept since earthquakes occur in the absence of industrial activity. The minimum amount of stress *observed* to modulate earthquake activity is a few hundredths of a megapascal and possibly as little as a few thousandths, equivalent to a few tens of centimeters of water-table depth. Faults near to failure are pervasive in the continental crust and induced earthquakes may thus occur essentially anywhere. In intraplate regions neither infrastructure nor populations may be prepared for earthquakes. Human-induced earthquakes that cause nuisance are rare, but in some cases may be a significant problem, *e.g.*, in the hydrocarbon-producing areas of Oklahoma, USA. As the size of projects and density of populations increase, the potential nuisance of induced earthquakes is also increasing and effective management strategies are needed.

## 1 Introduction

Natural processes that modulate the spatial and temporal occurrence of earthquakes include tectonic stress changes, migration of fluids in the crust, Earth tides, surface ice and snow loading, heavy precipitation, atmospheric pressure changes, sediment unloading and groundwater loss [e.g., Kundu *et al.*, 2015]. Such processes perturb stress on faults by only small amounts but, since rock failure in earthquakes is a critical process, nucleation of each event is ultimately brought about by a final, incremental change in stress. It is thus unsurprising that anthropogenic activity that perturbs stress in the crust, even slightly, can modulate seismicity. In most cases such effects probably go unnoticed (Section 7.1) but as industrial projects proliferate and grow in scale the number of cases where a link is obvious is increasing.

Mining- and dam-induced earthquakes have been recognized for several decades. Now concern is growing about earthquakes induced by hydraulic fracturing for shale-gas extraction, waste-water disposal by injection into boreholes. Seismicity may also increase in hydrocarbon reservoirs as they enter their tertiary phases of production. The full extent of human activities that may induce earthquakes is, however, wider than generally appreciated. We conducted an extensive search to build as complete a catalog as possible of cases of induced seismicity reported to date. Our work expands previous reviews that include a general overview by McGarr et al. [2002], lists by Nicol *et al.* [2011] and Suckale [2009], and a review of $M \geq 1$ events by Davies *et al.* [2013] listed 198 cases. Our new database of human-induced earthquakes, *HiQuake*, contains over 700 cases of anthropogenic projects postulated to induce earthquake activity. It is publically available at www.inducedearthquakes.org [Wilson *et al.*, 2017].

We constructed *HiQuake* by searching for case histories in published papers, conference abstracts, books, reports, the world-wide web and personal knowledge. The credibility of individual cases made varies from extremely low to overwhelming, with most cases in between. There is no rigorous way of quantifying the likelihood that a particular claim for human induction is correct, and many arguments for anthropogenesis are presented as tentative by authors and challenged by other researchers, *e.g.*, the 1983 $M_W$ 6.2 Coalinga, California, event (Section 3.3.2). There is thus no rigorous way of defining a "credibility cut-off" below which a

case history should be excluded from the database. For this reason we adopted the only reliable policy which was to include all cases without regard to plausibility. *HiQuake* thus lists all projects proposed on scientific grounds (not religious or moral) to have induced earthquakes and judgment regarding the credibility of any individual case is the responsibility of the user. *HiQuake* thus comes with a *caveat emptor*. It is up to the database user to judge the strength of arguments for anthropogenic induction of any particular case included. For convenience, details of our information sources are included in the database.

In this paper we present the basics of relevant, fundamental, but sometimes-misunderstood background issues. Following this we give examples of seismicity postulated to be related to:

a) Surface operations,
b) Extraction of mass from the subsurface,
c) Introduction of mass into the subsurface, and
d) Explosions.

We sub-divide each category. In some cases, categorization is tentative because more than one anthropogenic process preceded or was ongoing at the time of the earthquakes, *e.g.*, fluid extraction and injection are often conducted simultaneously in hydrocarbon reservoirs. Finally, we summarize features of the database and comment on related issues with which scientists are currently grappling.

### *1.1 Intraplate earthquakes*

Plate tectonic theory in its simplest form considers plates to be rigid and expects most large earthquakes to occur in plate boundary zones. The fact that intraplate earthquakes occur, and may be large, is *prima facie* evidence that the plates are not rigid but also deform in their interiors. Intraplate stress changes cyclically as stress diffuses through them following the great[1] earthquakes and volcanic events that sum to bring about what geologists model as smooth plate

[1] Earthquakes are classified as Great (8 or more), Major (7 - 7.9), Strong (6 - 6.9), Moderate (5 - 5.9), Light (4 - 4.9) and Minor (3 -3.9).

movements [Foulger *et al.*, 1992; Heki *et al.*, 1993]. The configuration of plate boundaries is geometrically unstable and evolving. For example, in Europe the formation of extensional features such as the Rhine Graben (Germany) is likely a consequence of southerly migration of the collision zone between Africa and Europe ("slab roll-back"). Intraplate European seismicity is probably related to the same process (Figure 1) [Nielsen *et al.*, 2007].

Intraplate seismicity is commonly assumed to be spatially stable so future earthquakes occur where events have occurred in the past. This assumption has recently been re-visited as a result of geodetic work done in the New Madrid Seismic Zone, USA [e.g., Newman *et al.*, 1999; Stein *et al.*, 2009]. There, it is generally expected that future large earthquakes will follow the damaging 1811-1812 sequence of four $M \geq 7$ earthquakes [e.g., Johnston & Schweig, 1996]. As a result, significant resources have been invested in earthquake hazard mitigation. Recent GPS surveying has, however, failed to detect any ongoing strain build-up [Stein *et al.*, 2009]. This led to the proposal that the spatial distribution of intraplate earthquakes in general is not stationary and that the locations of past large earthquakes are not a good predictors of future earthquakes [Liu & Stein, 2016]. Wrong forecasts of the location of future large earthquakes may lead to inefficient deployment of hazard-reduction resources thus has significant implications for public safety.

A non-stationary spatial pattern of seismicity accords with evidence that the crust is critically stressed in most intraplate regions. Stress measurements made in boreholes commonly show that stress is close to the depth-dependent strength of the crust as estimated by laboratory experiments [e.g., Brudy *et al.*, 1997; Zoback & Healy, 1984]. The ambient pore pressure is generally close to hydrostatic, the crust is pervasively faulted, and faults that are well oriented for slip in the ambient stress field are commonly close to failure. This is consistent with observations that human-induced seismicity may occur, and even be large, in regions that have been historically aseismic.

### *1.2 Induced, triggered, stimulated, and nuisance earthquakes*

Many if not all earthquakes induced by human activity release more stress than artificially added to the crust. McGarr et al. [2002] suggested the terms "induced" for earthquakes where the stress change caused by human activity is comparable to the shear stress causing a fault to slip,

"triggered" where the anthropogenic stress change is much smaller, and "stimulated" where there are insufficient data to make the distinction.

It is beyond dispute that in many cases seismic strain energy released in earthquakes is many orders of magnitude larger than that introduced into the crust by the industrial activity. In this paper, however, we use the term "induced" for all earthquakes related to human activity because:

a) All earthquakes probably release some pre-existing strain energy and are thus likely to be "triggered". Only where rock is entirely unstressed initially could this not be so and that is not possible in a heterogeneous, gravitating half-space. Even nuclear tests, which are purely explosive sources, trigger the release of some regional tectonic stress as shown by shear components in their focal mechanisms [e.g., Toksöz & Kehrer, 1972].

b) The amount of tectonic strain energy loaded into the crust that is relieved seismically, on what time-scale, and the amount released aseismically are poorly understood. In rapidly deforming regions aseismic deformation can be measured geodetically [e.g., Heki *et al.*, 1997] and surface subsidence is commonly observed above producing reservoirs [e.g., the Wilmington Oilfield, California; Kovach, 1974; Nagel, 2001]. Only a fraction of the total strain energy is relieved seismically but it is difficult to determine what this fraction is. Surface geodetic data have low sensitivity to fault motion at depth. Estimates of the percentage of strain energy dissipated aseismically varies from ~20% to 1000% of that released seismically [Villegas-Lanza *et al.*, 2016]. The recent under-prediction of the magnitude of the 2011 $M_W$ 9 Tohoku-oki, Japan, earthquake which killed > 18,000 people and did incalculable economic damage, showed that our assumptions regarding the length of the "seismic cycle" may be incorrect. Even large earthquakes may not relieve all the stress on a fault so our ability to estimate long-term stress buildup in the crust is limited.

   The same considerations hold true for industrial projects. If the timescale of energy release is underestimated, and with it the size of the largest expected earthquake (which dominates the energy budget because of the fractal nature of earthquake magnitudes), the maximum expected earthquake magnitude ($M_{MAX}$) may be underestimated.

c) It is at best impractical and at worst fundamentally impossible to determine how much of the strain energy released in a seismic event pre-existed. Even in cases where the energy released is comparable to that industrially added [e.g., McGarr, 1991], much of the latter may have been relieved by aseismic deformation such as ground subsidence or inflow of water at depth. These processes may themselves trigger earthquakes or load adjacent regions to seismic failure [e.g., Guglielmi *et al.*, 2015].

We use the term "induced" neutrally, and without implications for the origin of the total seismic stress change, in accord with the usage of the Committee on Induced Seismicity Potential [Hitzman, 2013]. That committee uses the term "induced" to mean "earthquakes related to human activities".[2]

We use the term "nuisance" earthquakes for those that cause societal inconvenience. This inconvenience may be physical or psychological. It includes objectionable damage to infrastructure or the environment, public concern, annoyance or distress about ground shaking, noise or environmental effects such as hydrological changes. Clearly no seismological parameter, *e.g.*, magnitude or intensity of ground shaking, can quantify nuisance because it is dependent on the culture of those affected. Nuisance earthquakes are those that need health-and-safety management. That requires an evidence base to which it is hoped the present review will contribute.

### *1.3 Factors involved in the nucleation of earthquakes*

Shear slip on fault planes, with or without crack-opening or closing components, is the most common earthquake source process. Factors involved in nucleation, i.e. the onset of motion, include:

the coefficient of friction on the fault plane;

[2] "*Some researchers (e.g., McGarr et al., 2002) draw a distinction between "induced" seismicity and "triggered" seismicity. Under this distinction, induced seismicity results from human-caused stress changes in the Earth's crust that are on the same order as the ambient stress on a fault that causes slip. Triggered seismicity results from stress changes that are a small fraction of the ambient stress on a fault that causes slip. Anthropogenic processes cannot "induce" large and potentially damaging earthquakes, but anthropogenic processes could potentially "trigger" such events. In this report we do not distinguish between the two and use the term "induced seismicity" to cover both categories."* Hitzman, M. W. (Ed.) (2013), Induced Seismicity Potential in Energy Technologies x+248 pp., National Academies Press, Washington, D.C..

compressive normal stress on the fault plane;

pore pressure in the fault zone; and

- shear stress on the fault.

According to the widely used Coulomb Theory, the shear stress required for failure $\tau$ is

$$\tau = \tau_0 + \mu(\sigma_n - p) \qquad \textit{Eq. 1}$$

where $\tau_0$ is the cohesion, $\mu$ is the coefficient of friction, $\sigma_n$ is the normal stress across the fault, and $p$ is the pore pressure in the fault zone [e.g., McGarr *et al.*, 2002]. The onset of an earthquake may thus result from reduction of the cohesion or normal stress on the fault plane or increase in the shear stress or pore pressure.

The loss or gain of overlying mass, introduction of fluid into a fault zone, or the imposition of vertical and/or horizontal stress by other means *e.g.*, stress transfer from nearby earthquakes, can bring a fault closer to failure. Where there are rapid temperature changes, *e.g.*, where cold water is injected into geothermal areas, thermal effects may also be a significant.

Both the addition and removal of material industrially is associated with earthquakes. Removal of water from aquifers (Section 3.1) and rock from mines (Section 3.2) may reduce the confining stress on fault planes. Introduction of water via reservoir impoundment (Section 2.1.1) or injection (Section 4.1) may alter the fluid pressure in fault zones. Cessation of groundwater pumping, *e.g.*, out of mines, may result in influx of groundwater and increase in pore pressure (Section 4.1.7). Addition of solid mass at the surface may also alter hydrological conditions (Section 2.1.2).

Theories for the mechanism of induced earthquakes include the asperity model of Pennington *et al.* [1986] which suggests that fluid extraction results in differential compaction or aseismic fault motion, increasing stress on locked faults. This stress is eventually relieved when asperities break. The poroelastic model of Segall [1985; 1992] suggests that declining pore pressures resulting from fluid extraction cause contraction of the reservoir rocks and stress build-up. *Ad hoc* theories for individual earthquakes may provide candidate explanations *a posteriori*. However, developing a method that can reliably predict *a priori* which industrial projects will

induce earthquakes and which not remains a work in progress.

### *1.4 Earthquake locations*

Earthquakes in the *HiQuake* database span the period 1868 to 2016. Seismological technology has improved vastly during this period, but even today the standard of monitoring is non-uniform. Many projects may not be monitored at all until nuisance seismicity begins. In contrast, others may be monitored by dense seismic networks installed well in advance to obtain a pre-operational baseline [e.g., Cladouhos *et al.*, 2013]. As a result, data in *HiQuake* such as locations, magnitudes and focal mechanisms are non-uniform in quality.

Inaccurate hypocentral locations hamper efforts to associate earthquakes with operations, especially if the errors are larger than the separation between boreholes or producing horizons. An example is the case of the Crooked Lake, Alberta, earthquake sequences, thought to have been induced by shale-gas hydrofracturing (Section 4.1.6) [Schultz *et al.*, 2015]. A pre-operational seismic baseline was not available for medium-magnitude earthquakes, there was little information on local crustal structure, and most of the seismic data were from stations > 100 km away. As a result, it is unclear whether the lack of spatial correlation of some events with operations is real or a consequence of inaccurate locations.

The largest source of hypocentral uncertainty is imperfect knowledge of crustal structure. This factor is not included in the error estimates computed by many commonly used hypocenter-location programs which typically base uncertainty estimates on root-mean-square arrival-time residuals, assuming no errors in the crustal model used. Such residuals may be unrealistically small for systematically mislocated hypocenters. Advanced earthquake location methods using relative locating ["double-differencing"; Waldhauser & Ellsworth, 2000] or waveform cross-correlation [Got *et al.*, 1994] can improve the accuracy of locations *relative to one another* but do not reduce systematic errors in the absolute locations. Accurate depths may be out of reach if geometrically strong data are unavailable because errors in hypocentral depth are typically 2-3 times the error in horizontal (epicentral) location. Insufficient stations and sparse networks are also hindrances (Section 4.2.1).

Obtaining accurate local crustal velocity models in the neighborhood of small-scale industrial

projects may be challenging. Information may be limited to well-logs, global or national crustal models, or models from analogous geological areas [e.g., Schultz *et al.*, 2015]. Such models are not adequate for reducing location uncertainties to sub-hectometer (100 m) levels. Ideally, high-quality crustal models based on active-source seismic surveying and/or one- and three-dimensional inversions of local earthquake data will be available. Projects will be monitored by dense networks of seismic stations with stations every 1-2 $km^2$. Experimental designs of this kind can return locations accurate to about a hectometer. Reducing errors still further requires calibration shots [Foulger & Julian, 2014].

In order to inform discussions regarding whether earthquakes are induced or natural, a pre-operation baseline is required. For this purpose, seismic networks must be deployed prior to commencement of operations. An effort to establish such a baseline for the entire UK prior to possible expansion of shale-gas hydrofracturing was recently made by Wilson *et al.* [2015].

### *1.5 Earthquake magnitudes*

Magnitudes given for earthquakes often differ by up to a whole magnitude unit because:

- Traditional scales such as local magnitude ($M_L$) use measurements of the amplitudes of certain seismic phases recorded on seismic stations. Amplitudes are a poor measure of the size of an earthquake because they are influenced by factors such as the orientation of the fault that slipped and source-to-station crustal structure. For these and other factors, measurements at different stations may yield different magnitudes for the same earthquake.

- Different magnitude scales such as $M_L$ and surface-wave magnitude ($M_s$) use different types of seismic waves, resulting in both systematic and random differences in the magnitudes calculated. For example, shallow earthquakes excite stronger surface waves than deep earthquakes, so $M_S$ underestimates the sizes of deeper earthquakes compared with $M_L$.

- Seismological practice is notoriously non-standard in respect of magnitudes, and local magnitude scales and practices often depart considerably from those originally defined.

Many local seismic stations and networks use their own customized magnitude scales, often constructed by calibrating them using a few earthquakes measured in common with the nearest permanent or calibrated station. That station may in turn have been calibrated in the same way. $M_L$ technically refers to recordings made on Wood-Anderson seismographs, but such instruments are now rare. As a result, magnitudes reported from one seismic network may not be comparable to those reported from another, even if the same magnitude scale has, in theory, been used.

It is beyond the scope of this paper to render all magnitudes to a single scale and in this paper we therefore do not discriminate between magnitude types reported. We record the information currently available in the *HiQuake* database, *e.g.*, $M_L$ (local magnitude), $m_b$ (body-wave magnitude), $M_S$ (surface-wave magnitude), $M_d$ (duration magnitude) and $M_W$ (moment magnitude). Where magnitude type is not specified we use the notation M. Where several different estimates are published, we preferentially cite $M_W$. If $M_W$ is not available, and more than one other magnitude has been published, we cite the largest. Rendering all the magnitude to $M_W$ is a task for future work.

### *1.6 Earthquake counts*

The total number of earthquakes detected for a sequence depends on the density of seismic monitoring. This may change with time, *e.g.*, if additional seismic stations are installed after nuisance seismicity has begun. Earthquakes are a fractal phenomenon, and their numbers increase by about an order of magnitude for each reduction in magnitude unit. If earthquake counts are to be meaningfully compared, they must thus be related to a common low-magnitude cut-off threshold.

The numbers of earthquakes induced may be of interest where monitoring networks are stable since this parameter may serve as a sensitive strainmeter. As a result, earthquake counts have been particularly useful for monitoring active volcanoes. The availability of many earthquakes is an advantage for purposes such as tracking injected fluids. From the point of view of potential damage from large earthquakes, however, those of most relevance are the relatively few large-magnitude events and possibly only the largest ($M_{MAX}$).

### *1.7 The database*

The approach we used to construct the database is described in detail by Wilson et al [2017]. Challenges intrinsic to the task included:

Incomplete reporting (Section 7.1);

- Ambiguous reporting, *e.g.*, "Seismicity is not reported";
- Lack of reported data, *e.g.*, operational parameters not given;
- Uncertainty regarding whether or not the earthquakes were induced, *e.g.*, some postulated associations are based simply on short-term temporal correlations or weak spatial correlations unsupported statistically and possibly coincidences. We dealt with this by including all cases (Section 1);
- Multiple possible induction processes ongoing simultaneously, *e.g.*, hydrocarbon extraction and wastewater injection;
- Non-uniformity of magnitude reporting (Section 1.5). We report $M_W$ if available, and if not the largest other magnitude;
- Lack of suitable networks to detect earthquakes. For some studies, instruments were installed only after the onset of seismicity (Section 1.4);
- Poor location accuracies (Section 1.4).

A list of database column headings is given in Table 1. The full *HiQuake* database is available as an Excel spreadsheet and references use as an EndNote library at http://www.inducedearthquakes.org.

### *1.8 Earthquakes and belief systems*

Public attitudes to induced earthquakes may have major implications for industrial projects, but human reactions to earthquakes may not be based on science. Because of their apparently random and spontaneous nature, and lack of obvious direct causes, earthquakes have for millennia been explained in terms of folklore, religion, and other belief systems [e.g., Harris, 2012]. This includes Chinese, Russian and Japanese folklore and the religions of the ancient Greeks and Polynesians. All three mainstream Abrahamic religions–Christianity, Islam and

Judaism–are based on ancient texts that attribute earthquakes to shortfalls in human moral behavior.

Recent cases where belief-system-based explanations for earthquakes have had significant societal impacts include:

- In 2015, the Malaysian government attributed a $M_W$ 6.0 earthquake that killed 18 people to tourists posing nude on Mt. Kinabalu, one of the country's sacred mountains.
- In 2014 local people in the Altai Mountains, Siberia, attributed earthquakes to the removal of the mummified remains of a 5$^{th}$-century BC noblewoman for archaeological research.
- In 2010, the American evangelist Pat Robertson allegedly attributed the devastating $M_W$ 7.0 Haiti earthquake to the successful 1791-1804 anti-slavery insurrection on the island.

These examples illustrate the importance of public information and outreach when planning industrial projects that might induce earthquakes.

## 2 Surface operations

### *2.1 Adding mass*

Earthquakes have been postulated to have been induced by three kinds of surface-mass addition. These are water impoundment behind dams (168 cases), erecting heavy buildings (1 case), and engineering coastal sediments (1 case).

Seismic events in mines have been known for centuries. The earliest report of earthquakes induced by water reservoir impoundment is from Lake Mead, Nevada and Arizona, USA [Carder, 1945]. Several probable water-reservoir-induced earthquakes have resulted in fatalities and extensive property damage. The largest earthquake claimed to have been induced in this way is the 2008 M ~8 Wenchuan, China, earthquake, which has been associated with impoundment of the reservoir behind the Zipingpu dam. Reports of earthquakes induced by erecting heavy buildings and engineering coastal sediments are, in comparison, rare.

2.1.1 Water impoundment behind dams

A well-studied example is that of the Koyna Dam, India (Figure 2). A detailed overview of this case, along with a review of dam-induced earthquakes, is given by Gupta [2002]. The 103-m-high Koyna Dam was raised in 1962 and contains a reservoir up to 75 m deep and 52 km long. Five years after it was completed, a sequence of earthquakes with magnitudes up to $M_S$ 6.3 occurred causing ~200 deaths and slightly damaging the dam. The largest earthquake nucleated at shallow depth, probably < 5 km, and its epicenter was ~10 km downstream from the dam. Earthquake activity has continued subsequently, correlating to some extent with water level in the reservoir (Figure 3) [Talwani, 1995]. A M > 5 event occurs there about every four years.

A second notable example is the Nurek dam, Tadjikistan [Keith *et al.*, 1982; Leith *et al.*, 1981; Simpson & Soboleva, 1977; Simpson & Negmatullaev, 1981]. Building of this dam began in 1961 and, at 317 m, it is currently the highest in the world. It contains a reservoir ~10 $km^3$ in volume (Figure 4). The largest earthquake to have occurred there to date is the 1972 $M_S$ 4.6 event [Simpson & Negmatullaev, 1981]. Seismicity is ongoing and there is evidence for correlation with periods of increase in water depth (Figure 5).

The largest-volume reservoir in the world is 1.64 x $10^{11}$ $m^3$ and is contained by the 111-m-high Aswan dam, Egypt. Earthquakes induced there are thought to occur in two depth intervals i.e. ~0-10 km and ~15-25 km (Figure 6 and Figure 7). This vertical separation is postulated to indicate two different processes/environments of induction [Awad & Mizoue, 1995]. The largest earthquake observed there to date is the 1981 M 5.7 earthquake, thought to have nucleated in the deeper zone.

A rare case where induced seismicity damaged the dam itself is that of the 105-m-high Xinfengjian Reservoir, China. Impoundment of the 1.39 x $10^{10}$ $m^3$ volume reservoir began in 1959 and seismic activity started a month later. A $M_S$ 6.1 earthquake occurred in 1962 which caused minor cracking of the dam.

A case of particular interest is that of the May 2008 $M_W$ ~8 Wenchuan, China, earthquake (Figure 8). This earthquake was so large relative to the height of the nearby Zipingpu dam (156 m) and the volume of the reservoir (~$10^9$ $m^3$) that it is controversial whether it was induced or

not. It occurred ~20 km from the dam within months of full reservoir impoundment. The earthquake caused ~90,000 deaths, collapsed roads and bridges, and serious damaged more than 100 towns.

The activated zone lies at the transition between the low-strain-rate (< $10^{-10}$ per year), stable Sichuan Basin and the tectonically active Tibet plateau where strain rates are > $10^{-8}$/year. The transition is marked by the multi-stranded Longmenshan fault zone which accommodates thrust and strike-slip motion. Paleoseismic work suggests an earthquake recurrence time of ~7,000 years for M 7-8 earthquakes [Klose, 2012].

Prior to impoundment of the reservoir there had been ~40 recorded earthquakes per month in the vicinity of the dam. In October 2005, seismicity increased as impoundment started and the water level rose rapidly by ~80 m. The water level peaked in October 2006 at ~120 m above pre-impoundment levels. Earthquake activity surged to ~90 events per month but reduced thereafter (Figure 9).

The 2008 $M_W$ ~8 mainshock nucleated at ~16 km depth and thrust motion propagated up toward the surface beneath the reservoir. Rupture transitioned to strike-slip motion and propagated laterally along the fault in both directions, rupturing > 300 km of the Longmenshan thrust belt with an average slip of 2.4 m, peaking at 7.3 m. The source time function, which lasted 90 s, indicated that failure occurred in five sub-events that sequentially released 9%, 60%, 8%, 17% and 6% of the total moment (Figure 9) [Zhang *et al.*, 2008, Yong Zhang, personal communication]. The average stress drop during the earthquake was 18 MPa, peaking at 53 MPa. Like other great earthquakes, this event owed its large size to progressive activation of adjacent fault segments in a chain of sub-events.

The increase in shear and normal stresses, caused by the reservoir, that were orientated to encourage slip on the fault were no more than a few kPa [Klose, 2012]. This is small, even compared with the stress changes associated with Earth tides (Section 7.3). Klose [2012] suggests that the additional stress modulated the timescale on which the earthquake occurred, advancing it in time by ~60 years. It has been much disputed whether such a small stress perturbation was sufficient to trigger such a large earthquake. A more relevant question is whether the reservoir could have induced the initial $M_W$ ~7.5 sub-event, since it is that sub-event

which started the cascade of segment failures that grew the earthquake to $M_W$ ~8.

An unusual dam-related seismic sequence occurred in association with the Beni Haroun hydraulic complex in the Mila region, 30 km west of the city of Constantine, Algeria [Semmane *et al.*, 2012]. This complex comprises a main dam 120 m high and a reservoir with a capacity of ~$10^9$ $m^3$. It is connected by pipelines to the secondary Oued Athmania reservoir, ~15 km south of the main dam (Figure 10). A 6-km section of pipeline passes through a mountain as a lined tunnel 1.4-3.6 m in diameter. To reach this part of the pipeline water is pumped up ~600 m higher than the Beni Haroun reservoir. The pipeline has a capacity of 600,000 $m^3$/day.

In 2007, a sequence of earthquakes up to $M_d$ 3.9 occurred. It is thought to have been induced by leakage into the ground of ~400,000 $m^3$ of water as it was being pumped between the reservoirs. More than 7,200 earthquakes were recorded over a ~2-month period. The water leaked from the tunnel via defective joints and penetrated deep into the ground via fractures, faults and karst cavities. Earthquakes started within days of the leakage (Figure 10). The area had no prior record of such swarm activity and installation of the complex in 2000 had not been associated with an increase in seismicity. The events did no damage but were heard loudly and alarmed local people unaccustomed to earthquakes [Semmane *et al.*, 2012].

The Colorado River, USA, contains numerous dams. The two largest are the 220-m-high Glen Canyon dam, a concrete arch that impounds Lake Powell, Arizona, and the Hoover dam, ~600 km further downstream, that impounds Lake Mead, mostly in Nevada. Glen Canyon dam is built in Mesozoic sedimentary rocks whereas the Hoover dam is built in Tertiary volcanics, part of the tectonically active basin-range province. In keeping with expectations, the latter is seismogenic but the former is not (Figure 11).

Currently, attention is focused on the 181-m-high Three Gorges dam, China (). Its 40 $km^3$ water reservoir was fully impounded in 2010 and power generated came online in 2012. Total generation capacity is 22,500 MW. The area lies in a seismogenic region that includes two major fault lines. The reservoir is not the largest in the world, but earthquakes are already being

reported with a $M_L$ 4.6 event occurring in 2014.[3]

2.1.2 Erecting tall buildings

Lin [2005] suggested that erection of the ~500-m high Taipei 101 building, Taiwan, influenced the pattern of seismicity in the immediate neighborhood of the building. This 7 x $10^8$ kg building increased stress on the ground at its base by ~0.47 MPa. In the eight-year period prior to building, nine earthquakes with $M_L \leq 2.0$ occurred whereas during the eight-year period that spanned construction and followed it, 20 earthquakes up to M 3.8 occurred. Earthquakes were unusually frequent during the construction period (Figure 12).

This is the only published case to date proposing earthquakes were induced by erecting a heavy building. Taiwan lies in a convergent plate boundary zone where the Philippine Sea plate subductings beneath the Eurasian plate at the Manila trench. As a consequence it is seismically active.

This case raises the question of whether other such examples exist, *e.g.*, in Japan. The building that is currently the tallest in the world, the 825-m-high Burj Khalifa, Dubai, weighs less than the Taipei 101 building, at only 4.5 x $10^8$ kg. There are no known reports of changes in earthquake activity from the New York or Tokyo regions where large buildings are common, though to our knowledge the issue has not been studied in detail.

2.1.3 Coastal land gain

Klose [2007b] suggested that the 2007 $M_L$ 4.2 Folkestone, Kent, UK, earthquake was triggered by geo-engineering of shingle accumulation in the harbor since 1806. There is substantial coastal land loss as a result of erosion to the southwest and northeast of Folkestone, but land gain by artificial shingle accumulation in Folkestone harbor has been ongoing for ~200 years. An estimated total of ~2.8 x $10^9$ kg had accumulated by 2007, four times the mass of the Taipei 101 building. This altered the stress by an estimated 0.001-0.03 MPa at 2 km depth. The earthquake epicenter lay ~1 km (epicentral error ~5 km) from the shingle, and nucleated at shallow depth.

[3] https://journal.probeinternational.org/2014/04/07/three-gorges-dam-triggers-frequent-seismic-activities/

### *2.2 Surface operations: Removing mass*

Operations that remove mass from the surface and are reported to induce earthquakes are limited to quarrying. *HiQuake* contains 16 such cases. The largest earthquake that has been associated with quarrying is the 2013 M 6.1 Kuzbass, Siberia, event [Emanov *et al.*, 2014; Yakovlev *et al.*, 2013]. It occurred in the Bachatsky open-cast coal mine which is 10 km long, 2.2 km wide, excavated up to 320 m deep, and produces > 9 x $10^6$ tonnes of coal per year. The earthquake collapsed buildings in local communities and was felt in neighboring provinces.

Moderate earthquake activity had been detected in the mine in early 2012 when a $M_L$ 4.3 event and associated aftershocks occurred. A dense local seismic network was installed, and recorded a low level of small earthquakes with magnitudes up to ~$M_L$ 2. Event magnitudes increased with time, and 15 months later a $M_L$ 3.9 event occurred followed a month later by the M 6.1 mainshock.

### *2.3 Surface operations: Summary*

The impoundment of water in reservoirs behind dams induces earthquakes in abundance and accounts for 168 (24%) of all cases in *HiQuake*. Ignoring natural lakes where dams have made minor changes to the water level, reservoirs are up to 8,502 $km^2$ in area (Lake Volta, behind the Akosombo Dam, Ghana). Earthquakes may thus be induced throughout relatively large regions.

Eight cases of induced earthquakes with M > 6 have been proposed, associated with the dams at Zipingpu (China), Lake Hebgen (USA) [Klose, 2013], Polyphyto (Greece), Koyna (India), Kariba (Zambia/Zimbabwe), Kremasta (Greece), Hsingfengkiang (China) and Killari (India). In China there are 348 reservoirs with volumes exceeding 0.1 $km^3$. Of these, 22 (6.3%) are reported to be seismogenic.

Gupta [2002] reviews theories for the mechanism of triggering. Stresses induced by reservoirs at the depths where earthquakes occur are small, perhaps of the order of 0.1 MPa. This is much smaller than the 1-10 MPa stress drops that are typical in earthquakes. They are, nevertheless, larger than seismogenic Earth tidal stresses (Section 7.3). The mechanism of induction may be that the surface load alters hydraulic conditions at depth, causing fluid to migrate into fault zones and increase pore pressure. This may also explain the seismicity postulated to have been induced

by the Taipei 101 building, Taiwan (Section 2.1.2) and shingle accumulation at Folkstone, UK (Section 2.1.3).

## 3 Extraction from the subsurface

### *3.1 Groundwater extraction*

Five cases of earthquakes associated with artificial lowering of the water table have been postulated. The 2011 $M_W$ 5.1 Lorca, Spain, event, suggested to have been induced by groundwater extraction (Figure 13) [González *et al.*, 2012], caused extensive damage to the town of Lorca, seriously damaging both modern and historic buildings, killing nine people and injuring several hundred (Figure 14).

The region lies in a transpressive shear zone containing thrust- and strike-slip faults, in the Nubia-Eurasia plate boundary. The $M_W$ 5.1 mainshock nucleated on the Alhama de Murcia fault at unusually shallow depth (~3 km). This fault has generated several large earthquakes over the past few centuries. Geodetic data from radar interferometry and GPS surveying constrained co-seismic deformation that was consistent with slip of up to ~15 cm on a ~10 x 10 km section of the fault in the depth interval ~1-4 km (Figure 15).

To the southeast, groundwater pumping 1960-2010 had lowered the water table by > 250 m. The surface had concurrently subsided > 10 cm/year, totaling > 2 m. Significant environmental effects had occurred as a result (Figure 16).

A slip deficit of up to ~12 cm had probably accumulated in the Alhama de Murcia fault since the previous large earthquake on the fault segment ~200 years earlier. Calculated Coulomb stress changes induced by water removal were consistent with a crustal unloading process that enabled tectonically accumulated stress to be released in the 2011 event. González *et al.* [2012] concluded that cumulative long-term hydraulic unloading, coupled with the location and type of the fault with respect to the depleting aquifer, contributed to the stress conditions that precipitated the earthquake.

Other cases of induced seismicity of this kind include the 2015 $M_W$ 7.8 Gorkha, Nepal, earthquake which has been linked to groundwater depletion beneath the Indo-Gangetic Plain to

the south [Kundu *et al.*, 2015]. This thrust earthquake caused ~8000 deaths and ~$10 billion of economic loss, ~50% of the Gross Domestic Product of Nepal.

The Indo-Gangetic Plain is the most intensely irrigated region in southeast Asia and has the highest population density. It covers ~2.5 x $10^6$ $km^2$ and is home to ~0.5 billion people. Groundwater is extracted at a rate of ~23 x $10^{12}$ $m^3$/year, equivalent to a drop in the water table of ~1 m/year (Figure 17). This load is being removed from the footwall of the Main Himalayan Thrust and encourages slip in the fault zone in a similar way to the Lorca case (Figure 18) [Kundu *et al.*, 2012].

The Coulomb failure stress change has been ~0.003-0.008 MPa since 1960 [Kundu *et al.*, 2012]. This is at the lower limit of those induced by Earth tides (Section 7.3) but is comparable to the natural rate of stress accumulation on the Main Himalayan Thrust of ~0.001-0.002 MPa/year. Dewatering of the Indo-Gangetic Plain is thus accelerating stress accumulation on the Main Himalayan Thrust by 4.5-20%.

Groundwater beneath the San Joaquin Valley, California, has been depleted by ~1.6 x $10^{11}$ $m^3$ over the past ~150 years [Amos *et al.*, 2014; McGarr, 1991]. The most rapid depletion occurs during the summer agricultural growing months and the most rapid natural recharge during the winter and spring. Annual fault-normal seasonal stress variations on the San Andreas fault zone from this source are ~0.001 MPa, encouraging earthquakes in summer and autumn. The stress rate is similar to that calculated for the Main Himalayan Thrust from dewatering the Indo-Gangetic Plain and the predicted seasonality in seismicity is seen in earthquakes with M > 1.25.

A similar process was suggested to modulate seismicity in the Gran Sasso chain in the central Apennines, Italy [Bella *et al.*, 1998]. There, tunneling for construction of a highway 1970-1986 significantly changed the hydrology of natural springs. Changes in the spatial pattern of local seismicity, an increase in seismic rate, and the occurrence of three M > 3 events were postulated to be linked to the hydraulic changes. Klose [2007a] attributes the 1989 $M_L$ 5.6 Newcastle, New South Wales, Australia, event to the dewatering of deep coal mines.

### *3.2 Mining*

Mine excavations perturb stresses in surrounding rocks and may reduce some components from

values initially of the order of 100 MPa to atmospheric (0.1 MPa). The resulting stress differences can exceed the strength of competent rocks and cause earthquakes. These are traditionally known as “rock bursts” or “coal bumps”.

Lately, excellent seismic data have been recorded on dense, multicomponent arrays installed for hazard mitigation purposes. Propagation paths are often short, pass through homogeneous rock, and data are free from the effects of the weathered surface layer that degrade surface observations. Significant advances in understanding the source physics of earthquakes have been achieved using these data. It has been shown that many mining-induced earthquakes have net implosive source mechanisms, consistent with partial closure of the artificial voids created by the removal of mass [e.g., Feignier & Young, 1992; Kusznir *et al.*, 1982; Rudajev & Sileny, 1985; Wong & McGarr, 1990; Wong *et al.*, 1989]. Miller *et al.* [1998a, Section 3.4] give a detailed review of this.

### 3.2.1 Traditional mining

Mining seismicity may be disproportionately serious because of the large loss of life and resources caused. This includes environmental damage such as surface subsidence which may render buildings beyond repair. Mitigating mining-induced seismicity is a major technical challenge, and might also become a limiting factor to the industry [e.g., Tang *et al.*, 2010].

During the ~50-year period 1949-1997, over 2000 coal bursts occurred in 33 mines in China, killing several hundred people and costing > 1300 days in lost production [Tang *et al.*, 2010]. In 2007 some 102 coal mines and 20 other mines reported seismicity (Figure 19). Seven of these were associated with events of $M > 4.0$ and 27 with events of $M \geq 3.0$ [Li *et al.*, 2007]. Earthquakes are shallow, occurring at 0-7 km depth. The largest coal mining event that has occurred in China is the 1977 $M_L$ 4.3 event at Taiji mine, Beipiao, Liaoning [Li *et al.*, 2007].

Coal mining in China is increasing in depth of extraction and volume removed, and the problem of mining-induced seismicity is increasing also (Figure 20 and Figure 21). The demand for coal and other minerals requires, in the absence of other solutions, that this trend continues. The problem of mining-induced earthquakes may thus grow unless management solutions are found.

Perhaps the most spectacular case of mining-induced seismicity occurred in 1989 in the

Volkershausen Ernst Thaelmann/Merkers potash mine, Germany. An event with $M_L$ 5.6 [Bennett *et al.*, 1994; Knoll, 1990] was associated with the collapse of ~3,200 pillars throughout an area of ~6 $km^2$ in the depth range 850-900 m. A large part of the local town of Düren was devastated, damaging several hundred buildings and totally destroying 19. Three people were killed and several injured. The event was probably multiple, with three main sub-events of $M_L$ 4.4, 5.1 and 5.5. The $M_L$ 5.5 sub-event was attributed partly to fluid waste injection which increased pore pressure by ~0.3-1.1 MPa, and this may have initiated an earthquake which led to collapse of the pillars [Knoll, 1990].

An case that involved litigation over the cause of a fatal mine-related earthquake is the 2007 $M_W$ 4.1 Crandall Coal Mine, Utah, event. Nine miners and rescuers were killed by a gallery collapse. The cause of the collapse was variously attributed to triggering by a natural earthquake or unsafe back-stripping mining practices. The seismic moment tensor of the event was not consistent with shear slip on a fault, as expected for a natural earthquake, but with a rapidly closing crack, as expected for a gallery collapse (Figure 22) [Dreger *et al.*, 2008]. The following year, the US Mine Safety and Health Administration levied fines totaling $1.85 million for unsafe mining practices at Crandall Coal Mine.

The UK has a long history of mining dating from the Neolithic period that includes flint, lead, copper, coal, tin and gold (Figure 23). During the 19th and 20th centuries coal mining reached its peak and in 1913, 292 million tonnes were extracted from 3024 mines. Some of these were excavated to depths of ~1200 m and extended several kilometers offshore beneath the North Sea[4,5]. *HiQuake* includes the largest earthquake recorded in each major UK coalfield.

Wilson *et al.* [2015] reviewed UK earthquakes to determine a national baseline for seismicity in advance of possible future shale-gas hydrofracturing. They used the earthquake database of the British Geological Survey. Of the ~8000 onshore British earthquakes in that catalog for 1970-2012 they estimated ~21% to have been anthropogenic, the majority caused by coal mining (Figure 24). Coal production and earthquakes correlate (Figure 25) [Wilson *et al.*, 2015]. A large

[4] https://www.gov.uk/government/statistical-data-sets/historical-coal-data-coal-production-availability-and-consumption-1853-to-2011

[5] http://www.dmm.org.uk/mindex.htm

reduction in seismicity accompanied a fall in production during the 1984-85 miners' strike. The economic cost of that strike is estimated to have been several billion pounds, from which it can be calculated that mitigation of each earthquake cost ~£10 million. The earthquake rate recovered in line with coal production when the strike ended 1985.

The region most renowned for large mining-induced earthquakes is South Africa. There, two of the world's richest ore bodies are mined–the gold-bearing conglomerates of the Witwatersrand Basin and the platinum-bearing pyroxenites of the Bushveld Complex. Both bodies extend to depths of several kilometers, and mining depths exceed 3.5 kilometers [Durrheim, 2010]. The current regional stress field is extensional but tectonically inactive. Mining-induced earthquakes are accompanied by collapses of up to ~1 m in the vertical that contract galleries in the form of horizontal tabular voids for up to several kilometers of their lengths. Earthquakes up to $m_b$ 5.6 have occurred (President Brand mine, Welkom, in 1994).

The problem of induced seismicity in South Africa became apparent early in the 20$^{th}$ century when mining penetrated to several hundred meters depth. It is now a major issue and great efforts are made to mitigate the risk. These include development of the safest possible mining techniques, optimal design of equipment, and seismological monitoring. Fatality rates have been reduced but still number several tens of deaths per year [e.g., Amidzic *et al.*, 1999; Boettcher *et al.*, 2015; deBruyn & Bell, 1997; Durrheim, 2010; Durrheim *et al.*, 2013; Durrheim *et al.*, 2006; Heesakkers *et al.*, 2005; Jaku *et al.*, 2001; Julià *et al.*, 2009; Kozlowska *et al.*, 2015; Lippmann-Pipke *et al.*, 2011; Milev & Spottiswoode, 2002; Richardson & Jordan, 2002; Wright *et al.*, 2003; Yabe *et al.*, 2015; Ziegler *et al.*, 2015].

An example is a $M_L$ 4.0 event that occurred in Western Deep Levels East gold mine in 1996. It nucleated in complex geology ahead of mining and extensively damaged the area. Work had involved removing a large pillar left by earlier, smaller-scale mining. This damaging earthquake had a significant impact and resulted in improved seismicity management strategies [Amidzic *et al.*, 1999].

An even larger event, with $M_L$ 5.3, occurred in the Klerksdorp district, South Africa, in 2005. It seriously damaged the nearby town of Stilfontein, injuring 58 people. Two mineworkers in a nearby gold mine were killed and thousands of others were evacuated. This earthquake was

attributed to stress loading by past mining [Durrheim *et al.*, 2006]. It highlighted the problem of poor documentation of historic mining activities, a problem for all nations with long traditions of mining. It also showed that earthquakes induced by one industrial project can endanger others nearby. Its delayed occurrence illustrates that seismic hazard may remain a problem after mine closure.

McGarr [1992a] used the exceptionally high-quality data collected on the state-of-the-art monitoring networks installed in deep South African gold mines to derive full moment tensors for 10 Witwatersrand mining-induced earthquakes with M 1.9-3.3. The earthquakes were of two types. Seven involved substantial coseismic volumetric reduction combined with normal faulting and three had no significant volumetric component. Those with volumetric components probably involved interaction between a mine stope and a shear fault [McGarr, 1992a].

These conclusions were confirmed by later workers. Julià *et al.* [2009] obtained focal mechanisms for 76 mine tremors with M 0.5-2.6 at the deep AngloGold Ashanti Savuka gold mine. These events were recorded on 20 high-frequency geophones in the mine. The largest principal stress was vertical and was relieved by a combination of volumetric closure and normal faulting, consistent with the vertical closure of galleries. Richardson and Jordan [2002] studied seismicity associated with five deep mines in the Far West Rand district using data recorded 1994-2000 on in-mine arrays. Seismic rates exceeded 1,000 events/day. Some earthquakes occurred within 100 m of active mining faces. Those events were attributed to blasting, stress perturbations from the excavation, and closure of stopes. Other events were distributed throughout the mining region, had M > 3, and were similar to regional tectonic earthquakes.

### 3.2.2 Solution mining

Solution mining recovers minerals via boreholes drilled into the deposit. A lixiviant–a liquid used to dissolve the target mineral–is pumped into the resource via an injection borehole, circulates through the rock dissolving the mineral, and is extracted via a production well. The lixiviant may be water (*e.g.*, to extract salt), or acid or sodium bicarbonate to extract metals, *e.g.*, uranium, copper, gold or lithium. Roughly half the world's uranium is produced by solution mining.

*HiQuake* contains eight cases of seismicity postulated to be associated with solution mining. At the Vauvert Field, France, brine is produced from a layer at 1900-3000 m depth comprising ~50% salt. Water is circulated through fractured zones via a well doublet. Some cavities created dissipate by salt creep but earthquakes occur where this process cannot keep up with mass removal. Seismicity also results from hydraulic fracturing used to create porosity. Over 125,000 earthquakes with M -3 to -0.5 occurred 1992-2007 have been located [Godano *et al.*, 2010].

In the USA three cases are documented, from Attica and Dale (New York) and Cleveland (Ohio). Of three $M_L$ ~5 events that occurred near Attica, in 1929, 1966 and 1967, two had hypocentral depths as shallow as 2-3 km [Herrmann, 1978]. They are postulated to have been induced by salt solution mining [Nicholson & Wesson, 1992].

In China, a $M_L$ 4.6 earthquake occurred in 1985 in association with solution mining of salt from depths of 800–1800 m at the Zigong salt mine, Sichuan Province [Li *et al.*, 2007]. This earthquake induced the highest intensity of ground shaking measured for any mining-induced earthquake in China. It is the largest mining-related event of any kind known from China.

At Mishraq, Iraq, earthquakes occurred in association with mining of sulfur by injecting hot (~150˚C) water at pressures of 0.6-0.8 MPa into layers up to 190 m deep [Terashima, 1981]. Surface subsidence of up to several mm/day resulted in surface cracking. Felt earthquakes occurred 1973-1975 and were most numerous at times of high injection rate.

### 3.2.3 Tunnel excavation

Earthquakes accompanying excavation of tunnels and cavities have been reported in 20 cases. These include excavations for power-station housing (*e.g.*, the underground powerhouse of the Pubugou, China hydroelectric station), water transport at hydro-electric and nuclear power stations (*e.g.*, the Yuzixi hydro-electric station, China, and the Forsmark nuclear plant, Sweden), road and railway transport (*e.g.*, the Ritsem tunnel, Sweden, and the Qinling railway tunnel, China) [Tang *et al.*, 2010].

The 57-km-long Gotthard Base Tunnel, Switzerland, part of the New Alpine Traverse through the Swiss Alps [Husen *et al.*, 2012] was excavated for freight and passenger rail transport 2002-2006 using drilling and blasting. Three “Multi-Function Stations” (MFSs) divide the tunnel into

five sections.

A series of 112 earthquakes with $M_L$ -1.0 to 2.4 occurred 2005-2007 in association with excavation of the southernmost station, MFS Faido. The largest event was just 0.5-1.0 km deep and felt strongly at the surface. The station cavity was damaged including flaking of the reinforced walls and upwarping of the floor by ~0.5 m. The seismicity correlated spatially and temporally with excavation of the station (Figure 26 and Figure 27). Accurate locations obtained using a dense, temporary seismic network showed that the earthquakes occurred at a similar depth to the tunnel. Some correlated with rockbursts in the tunnel shortly after blasting.

The focal mechanism of the largest earthquake indicated normal faulting on a steep plane 50-170 m long belonging to the local fault system. The tunnel traverses igneous and metamorphic rocks and it crosses a complex of structures with different rheological properties, including faulted and heavily fractured sections. Modeling suggested the earthquakes resulted from an unfavorable juxtaposition of rocks with different rheologies in a fault zone. The horizontal stresses added by the excavations were relieved by shrinking of the tunnel which reactivated the fault zone.

### *3.3 Hydrocarbons*

Suckale [2009; 2010] reviews of seismicity induced by hydrocarbon production. There are ~67,000 hydrocarbon fields worldwide [Li, 2011] including ~1500 giant and major fields, and ~1,000,000 producing oil and gas wells. Seismic response to production varies and no seismicity is reported for most fields. Reporting is, however, incomplete, and many fields are not instrumented (Section 7.1). Earthquakes account for only a small percentage of the deformation associated with reservoir compaction with the majority being taken up by ground subsidence or counteracted by fluid recharge from the sides. The earthquakes reported often occur on faults that were either previously unknown or considered to be inactive.

#### 3.3.1 Gas

There are 36 cases of seismicity postulated to have been induced by extraction of natural gas. These are from Canada (1 case), China (1 case), France (2 cases) Germany (7 cases), Italy (1 case), the Netherlands (18 cases), Oman (1 case), the USA (4 cases) and Uzbekistan (1 case).

The most extreme case is that of the Gazli reservoir, Uzbekistan. In 1976 and 1984, three $M_S$ ~7 earthquakes occurred, seriously damaging the local town of Gazli and causing one death and ~100 injuries [Simpson & Leith, 1985]. An additional $M_S$ 5.7 event occurred in 1978. Events occurred as follows:

| | |
|---|---|
| 1956 | the Gazli field was discovered; |
| 1963 | pipelines to the Urals industrial region were completed; |
| 1966 | production of ~20 x $10^9$ $m^3$/year of gas began. Reservoir pressure was ~7 MPa; |
| 1968-71 | production peaked; |
| 1976 | pressure had declined to 3-3.5 MPa; two $M_S$ ~7 earthquakes occurred; |
| 1978 | a $M_S$ 5.7 earthquake occurred; |
| 1984 | a $M_S$ ~7 earthquake occurred; |
| 1985 | pressure had declined to 1.5 MPa. |

Gas was produced from a reservoir at ~2 km depth, hosted in an open anticline of tight Paleogene sandstones. This structure is cut by several blind faults and the $M_S$ ~7 earthquakes are thought to have occurred on one of these (Figure 28). Fault-plane solutions suggest that they occurred on a north-dipping, easterly striking thrust fault, consistent with regional tectonics. Extrapolation of this fault to shallow depth suggests that it intersects with the gas reservoir. In addition to this geometric correspondence, Simpson and Leith [1985] cite as additional evidence that these events were induced:

previous seismic quiescence;

an anomalous magnitude distribution which involved three $M_S$ ~7 events rather than a mainshock-aftershock sequence;

the large decrease in pressure in the reservoir; and

unusual downwards rupture propagation.

That these earthquakes were induced has been challenged, *e.g.*, by Bossu *et al.* [1996], on the grounds that the stress perturbation on the fault was too small to have triggered such large earthquakes.

Possible analyses of this case are limited because data on operations are sparse. However, the Gazli case is important because of its implications for the maximum possible magnitude of earthquakes that could be induced by gas extraction.

The largest such postulated earthquake in Europe is the 1951 M 5.5 event that occurred in the previously aseismic Caviaga Gasfield, Po Valley, Italy [Caloi *et al.*, 1956]. There, large-scale extraction of methane at pressures > 10 MPa had been underway. The earthquake cannot be well studied because limited instrumentation was in place at the time. Simple analysis of paper recordings suggested that the largest, $M_L$ 5.5 event, nucleated at ~5 km depth and had a thrust mechanism.

The case of Caviaga is the only $M \geq 5$ gas-extraction-induced earthquake reported for Europe. Several other European gas-extraction projects are associated with $M \geq 4$ seismicity. The Lacq Gasfield, France, has generated earthquakes up to $M_L$ 4.2 and > 2000 were located there from 1974-1997 [Bardainne *et al.*, 2008].

Production at Lacq started in 1957 with extraction of gas from 3.2-5 km, beneath a 600-m-deep oilfield. The reservoir occupies a 20-km-long fractured anticline in Mesozoic limestones sealed by Cretaceous marl. Reservoir pressure decreased from 66 MPa to 2.3 MPa 1957-2008 and the surface subsided ~6 cm.

The first earthquake noticed, the 1969 M 3-4 event, occurred after the gas pressure had declined to 36 MPa. This, and the subsequent seismicity, is unlikely to have been natural because of its concentration in the gasfield and because Lacq is 30 km north of the nearest seismically active structure, the Pyrenean Frontal Thrust (). About 70% of the earthquakes located above the gas reservoir, many on faults optimally-oriented with respect to the stress perturbation caused by gas removal. Poorly oriented faults tended to be aseismic. There is poor correlation between the surface subsidence and the seismicity. Seismicity migrated from the center to the periphery of the reservoir (Figure 29). Comparison of the distribution of hypocenters with deformation models favored the model of Odonne et al. [1999] rather than that of Segall [1989] (Figure 30).

In The Netherlands, ~300 gasfields are produced. Of these, just a few percent are seismically active but globally this is a high rate of reported seismogenesis. The induction mechanism is

thought to be differential compaction [Gee *et al.*, 2016].

One of the largest earthquakes attributed to induction in The Netherlands is the 2012 Groningen $M_L$ 3.6 event. In addition to this a further 8 events with M > 3.0 have occurred in that field (Figure 31). Seismicity was first recorded in December 1991 when the reservoir reached ~28% depletion, some 28 years after the start of gas extraction in 1962 (Figure 32).

The Netherlands has a low rate of historic seismicity compared with neighboring countries where much higher rates are associated with the Upper Rhine Graben (Figure 33 and Figure 34) [van Eck *et al.*, 2006]. Currently, the majority of earthquakes in the northern Netherlands is associated with gas extraction. Several hundred have been recorded in the Groningen Field. This reservoir, the largest natural gasfield in Europe and the tenth-largest in the world, originally contained ~3 x $10^9$ $m^3$ of gas in a porous sandstone formation up to 300 m thick and 45 x 25 km in area. Both the seismic rate and the magnitudes of the largest earthquakes have increased with time (Figure 32). An apparent increase in the slope of the Gutenberg-Richter distribution (the "*b*-value") with time is consistent, however, with a progressive reduction in the proportion of large to small earthquakes [van Eck *et al.*, 2006; Van Wees *et al.*, 2014]. Reservoir compaction is greatest in two northwesterly trending zones of the reservoir and the earthquakes correlate with the southernmost of these (Figure 35).

A renowned case in the USA is the Fashing Gasfield, Texas (Figure 36) [Pennington *et al.*, 1986]. Production there started in 1958 from 3.2 km depth. By 1983 the pressure had decreased by ~7 MPa and a M 3.4 earthquake occurred (Figure 37). The depleting reservoir was replenished by water recharge produced water was reinjected. In 1992 a M 4.3 earthquake occurred and in 2011 a $M_W$ 4.8 event. This case is usually considered jointly with the nearby Imogene Oilfield (Section 3.3.2).

### 3.3.2 Oil

In many oilfields multiple processes are underway simultaneously including oil and gas extraction, waste-water disposal, water injection to aid oil recovery and hydrofracturing or thermal fracturing. It may thus be difficult to attribute unambiguously any seismicity to oil extraction alone (Section 1.7). Nevertheless, we have identified eight cases where earthquakes

have been postulated to be associated with oil extraction. These are from the USA, Iran, Russia and Norway. This is very few compared with the ~1,000,000 producing oilfields worldwide (Section 3.3).

One of the earliest reports of earthquakes accompanying oil production is from Goose Creek, Texas, where small earthquakes occurred in the 1920s (Figure 38). Following the extraction of several million barrels of oil an area ~10 $km^2$ in size subsided by up to 1 m over an ~8-year period [Nicholson & Wesson, 1992; Pratt & Johnson, 1926]. Goose Creek is a coastal region and a substantial area sank below sea level requiring industrial infrastructure to be adapted to the flooded conditions.

The largest earthquake attributed to oil extraction in *HiQuake* is the $M_W$ 6.2 1983 Coalinga, California, event. This event, along with the 1985 $M_W$ 6.1 Kettleman North Dome earthquake and the 1987 $M_L$ 5.9 Montebello Fields (Whittier Narrows) earthquake, both in California, were attributed to the removal of oil from fields in uplifting anticlines [McGarr, 1991]. The Coalinga and Whittier Narrows events were widely felt and caused multiple deaths and injuries (Figure 39).

All three events nucleated at ~10 km depth. McGarr [1991] suggested that net extraction of oil and water reduced the average density of the upper crust, and that the seismic deformation approximately restored isostatic equilibrium (Figure 40). This was challenged by Segall [1989] who concluded that depletion of the reservoir would have only loaded the nucleation region by ~0.01-0.03 MPa. Nicholson and Wesson [1992] suggested that the earthquake might have occurred in response to larger stresses imposed by fluids migrating into the mid-to-lower crust. They suggested changes in pressure resulting from withdrawal of oil induced fluid migration and brought the fault closer to failure. The Coalinga earthquake has also been attributed to extraction of groundwater for irrigation from the nearby San Joaquin valley (Section 3.1) [Amos *et al.*, 2014]. The Coalinga earthquake contributed to stress released six years later in the 1989 $M_W$ 6.9 Loma Prieta earthquake. This event ruptured a section of the San Andreas fault system 96 km south of San Francisco causing 63 deaths, 3,757 injuries and $5.6–6 billion of damage [Reasenberg & Simpson, 1992]. The 1933 $M_L$ 6.3 Long Beach, California, earthquake which killed > 100 people and did $40 million of damage may have resulted from oil production in the

nearby Wilmington and Huntington Beach Oilfields (Section 4.1.3) [Nicholson & Wesson, 1992].

There is little dispute that earthquakes were induced primarily by oil extraction from the Imogene Oilfield, Texas [Pennington *et al.*, 1986]. This field lies ~25 km from the seismogenic Fashing Gasfield (Section 3.3.1; Figure 36). In 1984 a $M_L$ 3.9 earthquake occurred in the Imogene Oilfield, followed by aftershocks 2-3 km deep near the reservoir bounding fault.

The Imogene Oilfield occupies Cretaceous limestone bounded by high-angle faults that splay at shallow depth. Production began in 1944 from a 33-m-thick horizon at 2.4 km depth. By 1973 reservoir pressure had dropped from 25 MPa to ~10 MPa. It was flooded 1972-1978 with 55,000 $m^3$ of water via injection wells to mitigate this pressure reduction. This is, however, much less than the ~1 million $m^3$ of oil and gas produced, and flooding ceased several years before the 1984 earthquake. As a consequence, the seismicity has been attributed to depressurization of the field as a result of oil depletion.

The most spectacular example of subsidence and induced earthquakes associated with a producing oilfield is that of the Wilmington Field, California (Figure 41 and Figure 38). Oil production began in 1936 and over the following 30 years up to 9 m of subsidence and 3.6 m of horizontal contraction occurred. Strain rates were > 1000 times greater than along locked sections of the San Andreas fault [Kovach, 1974; Segall, 1989].

Earthquakes began to occur above and below the reservoir when reduction in pressure reached ~10 MPa. Eight earthquakes with $M_L$ 2.4-5.1 occurred on shallow, low-angle bedding planes. The largest, which occurred in 1949, sheared off hundreds of production wells causing > $9 million of damage. An area of ~5.7 $km^2$ was affected and up to 20 cm of ground deformation occurred [Nicholson & Wesson, 1992; Segall, 1989]. Seven of the earthquakes occurred during the oil production period and one after significant water flooding began in 1958 to mitigate the subsidence. No further earthquakes occurred after 1961 and subsidence had been arrested by 1966. In this case seismicity may have been stopped, rather than induced, by the introduction of fluids.

Despite large quantities of oil produced in the Middle East there are only two accounts of

earthquakes postulated to have been induced by extraction there. One reports hundreds of earthquakes up to $M_L$ 4.24 in the Uthmaniyah-Hawaiyah and Haradh divisions of the Ghawar oil/gas field, Saudi Arabia. These earthquakes occurred below production levels and are attributed to fluid extraction. Focal mechanisms suggest the active elements are crust-penetrative basement faults [Mogren & Mukhopadhyay, 2013].

The other example is from Kuwait, where 465 M 0.3-4.3 earthquakes occurred 1997-2007. A large percentage occurred in the oilfields, including the Sabiriyah, Raudhatain, Bahra, Minagish, Umm Gudair, Wafra, Abduliyah and Dharif Fields (Figure 42). Some of this activity is likely associated with oil extraction [Al-Enezi *et al.*, 2008]. The largest proposed induced event related to Middle Eastern oilfields is the 1993 M 4.7 event in Kuwait. It may have been induced by the 1990 gushing and burning of oil wells by Iraqi armed forces leading to rapid pore pressure reduction and changes in subsurface stress [Bou-Rabee & Nur, 2002].

### *3.4 Geothermal production (heat/fluids)*

Small, natural earthquakes are common in wet, high-temperature geothermal areas, and were known in Iceland as “hverakippur” (trans: “hot-spring bump”) before they were studied scientifically. They are likely caused by a combination of active tectonics in plate-boundary zones and volcanoes, and natural geothermal heat loss. The latter causes cooling and contraction of the geothermal heat source and stress is relieved by rock fracturing with a component of tensile failure. Both the opening and closing of voids have been identified seismically [Foulger, 1988a; b; Foulger & Long, 1984; Foulger *et al.*, 1989; Miller *et al.*, 1998a; Miller *et al.*, 1998b; Ross *et al.*, 1999]. Production from geothermal fields by extraction of hot fluids will enhance natural fluid- and heat-loss and may increase seismic rates.

As for hydrocarbon reservoirs, it may be difficult to attribute confidently earthquakes in exploited geothermal areas where multiple processes are underway. They may also be induced by natural recharge, either shallow, cold groundwater or deep hot water. *HiQuake* contains only six cases where earthquakes are postulated to have been induced by geothermal production. These cases are the Cerro Prieto Field, Mexico [Glowacka & Nava, 1996], the Reykjanes and Svartsengi Fields, Iceland [Keiding *et al.*, 2010], Larderello, Italy [Batini *et al.*, 1985], The Geysers, USA [Eberhart-Phillips & Oppenheimer, 1984] and Olkaria, Kenya [Simiyu & Keller,

2000].

The largest were strike-slip events in the Imperial Valley (1979, $M_L$ 6.6), Victoria (~30 km southeast of the Cerro Prieto field; 1980, M 6.1), and at Cerro Prieto (1987, M 5.4) (Figure 43). Glowacka and Nava [1996] base this proposal on qualitative correlations between increased fluid extraction and seismic moment release, with delays of ~1 year (Figure 44).

Electrical power production at Cerro Prieto began in 1973. Steam and water at 250-350˚C is produced from 1500-3000 m depth. Over1 $km^3$ of fluid was extracted 1973-1996. The region is part of the plate boundary between the Pacific and North America and tectonics are dominated by the strike-slip Imperial fault which has a history of M > 6 earthquakes. Glowacka and Nava [1996] found the numerical data insufficient to support statistically a correlation between production and large earthquakes but argue that pore pressure decreases of a few MPa in the geothermal field were sufficient to have triggered them. Majer and McEvilly [1981; 1982] suggested, on the basis of data from local, temporary seismic networks, that earlier increases in production correlated with increases in small earthquakes.

Correlation between geothermal production and earthquakes has been proposed at the Reykjanes and Svartsengi geothermal areas, Iceland [Keiding *et al.*, 2010]. In areas, deformation associated with extension along the plate boundary and ~5 cm/a of subsidence resulting from geothermal fluid extraction were detected 1992-2009 using Interferometric Synthetic Aperture Radar (InSAR) and GPS data. Swarms of earthquakes up to $M_L$ 4.1 occurred on the flanks of the rifts containing the geothermal areas. The events were postulated to have been induced by stress changes from geothermal fluid extraction (Figure 45) but it is not possible to rule out a tectonic origin.

The Geysers geothermal field, California, is a vapor-dominated field that has been exploited for over 150 years, lately generating electricity. It is intensely seismically active (Figure 46) and earthquakes occurred even before large-scale fluid injections began (Figure 47). The pre-injection seismicity, and current seismicity, is likely production-related [Eberhart-Phillips & Oppenheimer, 1984]. It is difficult to distinguish production- from injection-related seismicity because both processes are underway. Over the last 50 years or so, the seismic rate has, however, correlated grossly with injection (Section 4.1.5).

### *3.5 Extraction from the subsurface: Summary*

Mining is the commonest cause of extraction-related earthquakes and contributes 267 cases to *HiQuake*. Five cases relate to groundwater and six to geothermal resources. The largest earthquakes postulated to be induced by subsurface extraction are the $M_W$ 7.8 Gorkha, Nepal, earthquake, the $M_L$ 6.1 Bachatsky, Russia, earthquake, the $M_S$ 7.3 Gazli, Uzbekistan earthquake and the $M_L$ 6.6 Cerro Prieto, Imperial Valley, Mexico, earthquake.

In the case of groundwater-withdrawal cases, stress changes as small as 0.001 MPa have been postulated to induce events [e.g., for the 2015 MW 7.8 Gorkha, Nepal, earthquake; Kundu *et al.*, 2015]. This is small even compared with Earth tides (Section 7.3). The ability of such small stresses to induce earthquakes is theoretically in keeping with the self-similar, critical earthquake nucleation process. However, such small effects may be comparable to many other natural and anthropogenic processes such as weather and the expansion of cities.

The sizes of postulated gas-extraction induced earthquakes are shown in Figure 48 for the 35 cases of where this parameter is reported. There is a continuous spectrum of sizes with the exception of the $M_S$ 7.3 Gazli, Uzbekistan, event, which is 1.8 magnitude units larger than the second largest.

Although oil extraction removes large masses from the crust, few earthquakes have been attributed to this process. Possible reasons are:

the process is only weakly seismogenic, perhaps because natural aquifer influx (peripheral or bottom water) partially replaces mass extracted;
under-reporting; and
ambiguity of induction process, since fluid injection often accompanies production.

## 4 Injection into the subsurface

The burgeoning issue of injection-related earthquakes was highlighted by Ellsworth [2013] who pointed out the recent dramatic increase in earthquake rate for $M \geq 3$ events in the central and eastern USA. More than 100 such earthquakes occurred annually, on average, 2010-2012 compared with just 21 events/year on average 1967-2000. Despite incomplete reporting,

*HiQuake* shows that increasing incidence of injection-related earthquakes is not confined to the USA.

Fluids are injected into the ground for diverse reasons including (Table 2):

solution mining (Section 3.2.2);
disposal of by-products;
enhancing oil recovery;
fracturing rock (i.e. the very process that causes earthquakes);
research into the earthquake nucleation process;
disposing of hot waste water;
underground storage of natural gas, hydrogen and compressed air; and
$CO_2$ geostorage to reduce emissions.

In addition, passive groundwater inflow may occur when reservoirs are produced, or pumping to suppress groundwater levels is terminated in abandoned mines.

*HiQuake* contains 180 projects where injections have been postulated to induce seismicity. Whereas in general, the removal of mass from the crust is expected to reduce the normal stress that prevents slip on faults, the introduction of fluids into faulted rock is expected to increase the pore pressure that encourages failure. Both these changes thus, capriciously, are expected to induce earthquakes. In the case of injections, in addition to the direct hazard from earthquakes, there is the added risk that if the target formation or its caprock are ruptured the injected fluid might escape. This could add to hazard, *e.g.*, where the injectate is polluted water, natural gas or $CO_2$.

### *4.1 Liquid*

#### 4.1.1 Military waste

Our database contains only one case where seismicity was, to a high degree of confidence induced by the injection of military waste. This is the legendary case of the so-called Denver earthquakes. They resulted in widespread awareness among seismologists and the general public

that human activity can induce earthquakes.

The incident began in 1961 when the Army Corps of Engineers drilled a 3.7-km deep well into highly fractured crystalline Precambrian basement at the Rocky Mountain Arsenal, northeast of Denver, Colorado [Evans, 1966; Hsieh & Bredehoeft, 1981]. The purpose of the well was disposal of contaminated wastewater which was done by injection into the bottom, unlined, 21 m. Disposal began in March 1962 at pressures ranging from atmospheric to ~7.2 MPa above formation pressure. In the four-year period up to 1966 a total of 625,000 $m^3$ of fluid were injected.

Minor earthquakes started to occur in the Denver area shortly after injection began and by 1967 over 1500 earthquakes, some of which were M 3-4, had been recorded (Figure 49). The correlation between volume injected and frequency of earthquakes, along with epicenters located < 8 km from the well, led Evans [1966] to suggest they had been induced.

Although waste disposal ceased in 1966, earthquake activity continued and in 1967 three earthquakes with $M_L > 5$ occurred, damaging infrastructure in Denver. Seismicity then declined and by the early 1980s had essentially ceased. Ironically, the large earthquakes that occurred after the end of injection weakened the temporal correlation between earthquakes and injection and thus the case argued for induction. Diffusion of the fluid would have continued after injection stopped, however, and could account for the ongoing seismicity [Healy *et al.*, 1968].

### 4.1.2 Wastewater disposal

Large quantities of connate brine, sometimes mixed with water, are typically co-produced with oil, especially as fields age. Water-to-oil ratios may exceed 20 [Gluyas & Peters, 2010]. It is commonly re-injected into depleted oilfields for disposal, to maintain reservoir pressure, and to promote sweep thus aiding oil recovery. Injected cold water commonly leads to thermal fracturing, especially in low-permeability reservoirs. Thermal fracturing is a desirable outcome as it facilitates lower injection pressures (and thus lower pump power requirements and costs) to be used. In California alone there are currently ~2,300 wastewater injection wells.

*HiQuake* contains 33 cases of induced seismicity attributed to waste fluid injection. Of these, three are in Canada, two in China, one in Italy and 27 in the USA. An interesting case is that of

Paradox Valley, Colorado, so-named because the Dolores River runs transversely across the valley. This case is noteworthy because of the apparently large distances from the injecting well of some of the postulated induced earthquakes [Ake *et al.*, 2005; Block *et al.*, 2015; King *et al.*, 2014; Yeck *et al.*, 2015].

At Paradox Valley, brine is injected into a sub-horizontal layer of Mississippian-age limestone at the bottom of a 4800-m-deep well. The objective is to reduce the salinity of Dolores River water and, as a consequence, the Colorado River into which it flows. Salt enters the Dolores River by inflow of groundwater ~8 times more saline than sea water. To manage this, shallow brine is extracted from the ground from nine production wells and re-injected at greater depth via a single disposal well at surface pressures up to 35 MPa [Yeck *et al.*, 2015]. Continuous injection has been underway since 1996. In the following two decades > 5,700 earthquakes surmised to have been induced were located, including a M 4.3 event in 2000 (Figure 50). Some epicenters lie > 10 km from the disposal well and a few are up to ~25 km distant.

The 1986 $M_W$ 4.9 Painesville, Ohio, earthquake was possibly induced and occurred close to critical infrastructure [Ahmad & Smith, 1988; McGarr, 2014; Nicholson *et al.*, 1988]. This event, which was felt in 11 states and parts of Canada, occurred in Precambrian basement. It was within 17 km of the Perry Nuclear Power Plant on the edge of Lake Erie, and ground acceleration reached 0.23 g. The injection of $1.2 \times 10^6$ $m^3$ of liquid agricultural waste into three wells ~12 km away was implicated. These injections began in 1976. The mainshock and associated M < 2.5 aftershocks thus occurred a decade after injections began by which time pressure had increased by 11.8 MPa at the injection location.

Whether this earthquake sequence was induced is controversial. Prior to instrumentation, similar earthquakes occurred in 1906, 1928, 1943 and 1958 (i.e. about every ~20 years) in the area. The 1986 earthquakes thus may have been natural. The long delay of seismicity after the start of injection also erodes confidence that the two processes were linked [Hitzman, 2013]. However, the many cases of postulated delayed earthquake induction that have occurred subsequently render it more plausible that the 1986 Painesville earthquakes were induced.

A European case is that of the 2012 $M_L$ 5.9 Emilia-Romagna, Italy, earthquake sequence which resulted in 27 fatalities [Cartlidge, 2014]. It was postulated that hydrocarbon exploitation at the

Mirandola Field and geothermal exploitation at Casaglia contributed to stress changes that induced this sequence.

Because of serious impact to people and infrastructure a commission was established to investigate whether it was induced [Styles *et al.*, 2014]. The commission found statistical correlations with production parameters in the weeks before the earthquakes but concluded stress changes resulting from reservoir depletion had not contributed. It concluded that, while an anthropogenic effect could not be ruled out, it was "highly unlikely" that the sequence had been induced.

A link between injection pressure and induced earthquakes is reported for the Huangjiachang Gasfield, Sichuan Basin, China [Lei *et al.*, 2013]. Few earthquakes occurred there until injection wellhead pressure exceeded 2 MPa. After that, more than 5000 M > 1.0 earthquakes occurred close to reservoir depth, the largest with $M_L$ 4.4.

The Sichuan Basin is relatively tectonically stable with sparse historic seismicity. Gas occupies shallow, high-porosity Paleozoic and Mesozoic limestone/dolomite anticlines. Faults cross both reservoirs and basement. The Huangjiachang Gasfield is small and hosted in fractured, jointed, karstified Permian limestone at 2500 m depth. Wastewater injection began there in 2007. For the first two years, water was introduced under atmospheric pressure and seismic rates were low. In 2009 injection pressures were increased, ultimately reaching 2.1 - 2.9 MPa, and earthquakes began to occur.

Particularly vigorous seismicity was reportededly induced by wastewater disposal in the Rongchang Field, also in the Sichuan Basin [Lei *et al.*, 2008]. Starting in 1989, two months after water injection began more than 32,000 earthquakes up to $M_L$ 5.2 were recorded. The largest event reactivated a thrust fault in the basement and earthquake locations suggested that failure occurred in both reservoir and basement.

An unprecedented surge in seismic rate occurred in Oklahoma in 2009 (Figure 51) [Ellsworth, 2013]. During 2008-2013 Oklahoma was the most seismically active state in the USA for M > 3 earthquakes exceeding even California, which hosts the San Andreas fault zone, and the New Madrid Seismic Zone, formerly considered to be the most hazardous intraplate seismic zone in

the USA. The largest event since 1950 in the New Madrid Seismic Zone has been M 4.9. In Oklahoma a $M_W$ 5.8 occurred in 2016.

Faulting in Oklahoma is widespread but only one is known to have been active historically. This is the Meers fault, which is thought to have generated M 6.5-7 earthquakes over the last 3,500 years [McNamara *et al.*, 2015]. The injection of water for enhanced oil recovery has been practiced in Oklahoma since the 1930s and the 1952 M ~5.6 event (the El Reno earthquake) may have been related to oil and gas extraction [Nicholson & Wesson, 1992]. Hough and Page [2015] investigated whether the population of Oklahoma has been sufficiently stable historically for comparable earthquake activity to have been noted. The population has been large and well-distributed since the early 20$^{th}$ century, suggesting that that knowledge of M ≥4 earthquakes is nearly complete (Figure 52). Industrially induced earthquakes in Oklahoma currently are essentially beyond doubt.

As elsewhere, multiple industrial processes are underway simultaneously in the hydrocarbon fields of Oklahoma so it is difficult to be certain which induced any particular earthquake. In addition to production there are ~7,000 injection wells that are used for:

- disposal of produced brine (the dominant use);
- enhanced oil recovery;
- hydrofracturing to increase permeability in shale; and
- disposal of hydrofracture fluid.

Most of the fluid is injected into the Arbuckle Group, a sequence of carbonates and sandstones overlying Precambrian crystalline basement (Figure 53).

The largest and most damaging earthquake to have occurred in Oklahoma is the 2016 $M_W$ 5.8 Pawnee earthquake. This exceeded the 2011 $M_W$ 5.7 Prague earthquake which is confidently associated with wastewater disposal into a depleted oilfield [e.g., Keranen *et al.*, 2013]. The Prague earthquake was felt in 17 states and in Chicago, 1,000 km away. It caused considerable damage, destroying 14 houses and injuring two people. This and the Pawnee earthquakes are the largest in the world associated with waste-water disposal and have led to re-assessment of the potential size of injection-induced earthquakes and the delay time following the onset of

operations.

Earthquake activity in the Prague area began in February 2010 with a $M_W$ 4.1 earthquake in the Wilzetta Oilfield. This lies within the ~200-km-long Pennsylvanian Wilzetta fault zone (Figure 54). In 2011 the activity culminated in the Prague sequence that included three earthquakes with $M_W$ 5.0, 5.7, and 5.0 in November, and prolific aftershocks. Hypocentral locations and focal mechanisms from 1,183 aftershocks clarified the geometry of the hypocentral zone (Figure 55) [Keranen *et al.,* 2013]. Strike-slip motion occurred on steeply dipping planes that intersect sedimentary layers and basement. The tip of the initial rupture plane lay within ~200 m of active injection wells at ~1 km depth.

In the Wilzetta zone, oil is contained in fault-bounded structural traps that are barriers to fluid migration through the porous limestone host formation. Where the Prague sequence occurred, production had been ongoing since the 1950s but has now declined. Three waste-disposal injection wells which came online in 1993 are nearby (Figure 55). They inject water into sealed rock compartments at ~1.3 - 2.1 km depth.

Over the 17-year period 1993-2011 injection pressure increased from atmospheric to 3.6 MPa by 2006. Seismicity may have started when the injected volume exceeded that extracted from the fault-bounded compartment. Once the compartment had been refilled ongoing injection may have reduced confining stress on the reservoir-bounding faults which failed as a consequence. More stress was released than corresponds to the total volume injected, so tectonic stress was likely also released. Both injection and M > 3 earthquakes continue in the Wilzetta Field.

Figure 56 shows seismicity and oil production in Oklahoma over the last century. Between 2009 and 2014, 26 M ≥ 4 events occurred in the state with over 100 M ≥ 3.5 events in 2014 alone. Monthly statewide wastewater injectate volume has doubled since 1997 [Walsh & Zoback, 2015]. Correlations between earthquakes and injection or production are rare.  and Figure 57 show earthquakes and fluid injections for the entire state and for individual study areas. Earthquakes do not correlate with faults and most earthquakes occur in the least faulted part of Oklahoma.

Faults that fail in Oklahoma are probably those favorably oriented relative to the regional stress

direction. Most events occur at 5-6 km depth in the basement, on faults kilometers or tens of kilometers in length. Such faults can maximally sustain M 5-6 earthquakes. Some earthquakes occur on well-known faults that have larger seismic potentials. The length of segments activated can be determined from aftershock distributions.

Oklahoma earthquake activity exhibits both similarities and differences to other induced seismicity. No short-term monthly correlation with injection is apparent and seismicity surged long after the start of injections, 17 years in the case of the Prague sequence. In this it resembles the Wilmington Oilfield, California, where induced seismicity began years after water injection started for enhanced oil recovery (Section 4.1.3). However, it is unlike the "Denver earthquakes" sequence (Section 4.1.1) where seismicity began almost immediately after injections. Induced earthquake sequences do not necessarily start with the largest event, and stress from earlier events may trigger larger ones.

In addition to inducion by hydrocarbon-related operations, earthquakes in Oklahoma are also be triggered by natural regional earthquakes ("remote triggering"). Van der Elst *et al.* [2013] noted that a $M_W$ 4.1 event near Prague occurred following the 27 February 2010 $M_W$ 8.8 Maule, Chile, earthquake (Figure 58). Stress changes resulting from distant earthquakes can be calculated and can reveal the failure susceptibilities of faults.

### 4.1.3 Water injected for enhanced oil recovery

Oil recovery is enhanced by injecting low-salinity water, water-alternating-gas and water viscosifiers and by thermal and chemical methods to modify either the viscosity of the fluids or the surface properties of the host reservoir. Distinguishing earthquakes induced by these processes from events induced by oil extraction is not straightforward if both are underway simultaneously. Temporal associations are persuasive, *e.g.*, if seismicity surges shortly after water injection commences in producing oilfields that were previously aseismic.

*HiQuake* contains 38 cases of seismicity proposed to have been induced by enhanced oil recovery. Of these, 24 are from the USA and the rest from Canada, China, Denmark, France, Kuwait, Norway, Romania, Russia and Turkmenistan.

The classic example is that of the Rangely Oilfield, Colorado, where induced earthquakes could

be controlled (Section 4.1.8) [Raleigh *et al.*, 1976]. Water was injected in wells up to 2 km deep where formation pressure was ~17 MPa. The seismic rate could be increased or decreased by varying the pore pressure around 26 MPa. This case raised hopes that earthquakes might be controlled, including damaging events on the San Andreas fault system. However, it was quickly realized that the fractal nature of earthquakes is such that the stress released by a few moderate earthquakes cannot substitute for a single large earthquake. Thus, hopes that damaging earthquakes might be averted by using engineering means were not realized.

The largest earthquakes postulated to have been induced by enhanced oil recovery are the M 6.2 1983 Coalinga event, the 1985 $M_W$ 6.1 Kettleman North Dome event, and the 1987 $M_L$ 5.9 Montebello Fields (Whittier Narrows) event, all in California. The primary cause for these earthquakes is, however, most likely oil extraction (Section 3.3.2) [McGarr, 1991].

More clear-cut examples come from the Newport-Inglewood fault zone, Los Angeles Basin, California. Of the 3 billion barrels of original reserves in the giant Wilmington Oilfield, 2.7 billion (~440,000,000 $m^3$) have been removed. Early production may have contributed to the damaging 1933 $M_L$ 6.3 Long Beach, California, earthquake, and the events of 1947, 1949, 1951, 1954, 1955, and 1961 (Section 3.3.2) [Kovach, 1974].

Water flooding for enhanced oil recovery and to counteract massive subsidence started in the Wilmington Oilfield in 1954. Earthquakes thought to have correlated with injection volumes up to M 3.0 occurred in 1971. Injection was continued at approximately the same volumetric rate as production and seismicity did not continue [Nicholson & Wesson, 1992].

A more persuasive case of water-flooding-induced seismicity which caused significant damage and loss of life is that of the Inglewood Field, ~20 km further north along the Newport-Inglewood fault zone. In 1963 an earth dam containing the nearby Baldwin Hills Reservoir failed, releasing 11 x $10^6$ $m^3$ of water into a residential area. This flood damaged over 1,000 homes, killed five people and caused $12 million of damage. Failure of the dam was attributed to cumulative fault displacements that resulted from water flooding of the Inglewood Oilfield for enhanced oil recovery [Castle & Yerkes, 1976; Hamilton & Meehan, 1971].

Discovered in 1924, the Inglewood Oilfield occupies an anticline within a zone of faults and

folds. Reserves were initially 430 million barrels but the field is now ~93% depleted. For the first three decades production occurred under only exsolution-gas- (pressure depletion) and peripheral-water drive. Some 83 x $10^6$ $m^3$ of oil, water and sand were extracted. Pressures declined from 3.9 to 0.34 MPa by the 1950s. A well-defined subsidence bowl centered on the oilfield developed. Subsidence was up to 1.75 m during 1911-1963. Horizontal displacements were up to 0.68 m 1934-1961 with radially oriented extension. The Baldwin Hills reservoir lay on the edge of this subsidence bowl.

In 1954 a water-flood program for enhanced oil recovery began. Deformation accelerated immediately. A sharp reduction in subsidence occurred in the eastern part of the field. Horizontal displacements and strain were consistent with the operations and f tectonic origin for the deformation could be rejected to a high degree of certainty.

Shallow seismicity increased in 1962 and the following year the Baldwin Hills dam ruptured. It was deduced that movement on one of the faults allowed water to flow into the soil under the dam, resulting in failure. This case, and that of the Wilmington Oilfield, highlight the risk of major hydrocarbon operations near to dense populations, particularly where prior tectonic activity is known.

#### 4.1.4 Enhanced Geothermal Systems (EGS)

Extraction of geothermal heat from rock with insufficient natural water was pioneered in the 1970s by the "hot dry rock" projects of Fenton Hill, New Mexico, and Cornwall, UK. These did not lead to economic development and were abandoned. The technology was resurrected early in the 21st century as "Enhanced Geothermal Systems" (EGS). An important milestone in this was the report "*The Future of Geothermal Energy*", prepared by the Massachusetts Institute of Technology for the U.S. Department of Energy [Tester & al., 2006][6].

The fundamental concept of EGS is to pump high-pressure fluid into a well to hydrofracture and thermofracture hot rock, enhancing permeability and creating an underground heat exchanger. Cold water is pumped down an injection well, it circulates through the hot rock, and hot water

[6] http://geothermal.inel.gov and http://www1.eere.energy.gov/geothermal/egs_technology.html

and steam are extracted via production wells drilled into the fractured rock.

The objective of injection is to produce a network of fractures in the otherwise low-permeability target formation. As for shale-gas hydrofracturing, earthquakes are an inevitable consequence of a successful EGS project. Dense seismometer networks are installed prior to hydrofracturing to enable the best possible earthquake earthquake locations, magnitudes and source mechanisms. Such state-of-the-art projects are advancing basic seismology.

Notable EGS projects have been conducted at:

Fenton Hill, New Mexico [e.g., Ferrazzini *et al.*, 1990];
Cornwall, UK [e.g., Turbitt *et al.*, 1983];
Soultz-sous-Forêts, France [e.g., Baisch *et al.*, 2010; Calo *et al.*, 2014];
Basel, Switzerland [e.g., Zang *et al.*, 2014a];
Newberry volcano, Oregon [Cladouhos *et al.*, 2013];
the Coso geothermal area, California (Section 4.1.5) [Julian *et al.*, 2010];
Desert Peak, Nevada [Chabora *et al.*, 2012]; and
Cooper Basin, Australia [e.g., Asanuma *et al.*, 2005].

The Fenton Hill, New Mexico, hot dry rock project was the first of its kind. It was completed in 1977 in rock at ~2.6 km depth 185˚C. Work continued into the 1990s, achieving production of ~10 MW thermal, but was terminated because of lack of funding.

An early modern EGS project commenced at Soultz-sous-Forêts, in the central Upper Rhine Graben, France in 1987 (Figure 59) [Baisch *et al.*, 2010; Calo *et al.*, 2014]. The site lies in highly fractured granite overlain by ~1,400 m of sediments. It contains three ~5,000 m deep injection wells and several shallower wells. Massive hydraulic stimulations were performed at depths > 4,000 m. In 2000, well GPK2 was stimulated with ~23,000 $m^3$ of water at flow rates of 30–50 l/s and overpressures of up to 13 MPa. Well GPK3 was stimulated in 2003 with ~37,000 $m^3$ of water at similar flow rates and overpressures. Well GPK4 was stimulated twice with a total of ~22,000 $m^3$ of fluid. In 2010 the project began to deliver 1.5 MW to the grid.

The injections were monitored using a sparse seismic network of multi-component, down-hole sensors at 1500-3500 m depths. More than 114,000 earthquakes were detected at rates up to 8000 events per day (Figure 60). Activity migrated away from the injection wells with time and the largest events occurred after injection stopped. Such behavior causes problems for "traffic light" systems for adjusting injection strategies to avoid large earthquakes on the basis of ongoing seismicity. Earthquake magnitudes eventually reached $M_L$ 2.9 and caused public concern. After the largest event in 2003 the flow rates and injected volumes were reduced. The project demonstrated that better understanding of induced seismicity is needed if it is not to jeopardize commercial implementation of EGS technology.

The most infamous example of nuisance seismicity induced by EGS operations is from Basel, Switzerland. The city of Basel lies where the Upper Rhine Graben intersects the Jura Mountains fold/thrust belt (Figure 1). Basel has a history of large earthquakes, including the largest historical event in NW Europe, the M ~6.5 earthquake of 1356 which destroyed the city. There may have been additional M ~7 events post-Pleistocene.

A summary of this project is provided by Häring *et al.* [2008] and a 2014 Special Issue of Geothermics [Zang *et al.*, 2014a]. The project was designed to provide power to Basel. A seismic network was installed in 2006 and the Basel-1 well drilled to 5 km depth. The wellbore intersects 2.4 km of sedimentary rocks and 2.6 km of granitic basement.

The granite in the open hole below 4629 m was hydraulically stimulated by injecting 11,570 $m^3$ of fluid. It was planned to inject for 21 days. However, seismicity became intense during the first 6 days, with events up to $M_L$ 2.6 occurring at ~4.6-5.0 km depth. These events precipitated cessation of injection in response to a pre-approved procedure. Five hours later an earthquake with $M_L$ 3.4 occurred and a further three M > 3 events followed over the next 56 days (Figure 61). There was considerable citizen anxiety and the project is now abandoned.

EGS has been extensively conducted in Cooper Basin, Australia, where the largest earthquake induced to date was $M_W$ 3.7. Cooper Basin is ideal for EGS. It lies in the interior of Australia, remote from population centers. Significant oil and gas resources explored and exploited since the 1960s have left industrial infrastructure in place that was used from 2002 when geothermal exploration started. The target heat source is granitic rocks with temperatures up to 240˚C at 3.5

km depth. These are the hottest known granitic rocks in the world at economic drilling depths that are not near active volcanoes.

Six wells were drilled into the granite to 3629-4852 m depths. Four are in the Habanero Field and the other two are 9 and 18 km away in the Jolokia and Savina Fields. EGS fluid injections were conducted 2003-2012 [e.g., Asanuma *et al.*, 2005; Baisch *et al.*, 2009; Baisch *et al.*, 2006a; Baisch *et al.*, 2006b; Baisch *et al.*, 2015; Kaieda *et al.*, 2010]. These induced up to 20,000 earthquakes well-recorded by dense, modern seismic networks.

Although all the stimulations were conducted in the same granite formation, they induced variable seismic responses (Figure 62). These are exemplified by two carried out in 2010 and 2012 [Baisch *et al.*, 2015]. The 2010 stimulation injected fluid into the Jolokia well at > 4000 m depth. It induced only minor seismic activity, even at extremely high fluid pressures (~120 MPa), and the injection rate achieved was only ~1.0 l/s, one to two orders of magnitude less than typical. Only 73 earthquakes with $M_L$ −1.4 to 1.0 were recorded over an eight-day stimulation period and an additional 139 over the next six months. The largest was M 1.6 which occurred 127 days after injection ceased–another case where the largest event occurred after injection finished. Hypocenters clustered around the injection well a few tens or hundreds of meters away, suggesting that they occurred on fractures poorly oriented for slip in the regional stress field.

The 2012 stimulation in well Habanero 4 injected 34,000 $m^3$ of water at 4100-4400 m depths with flow rates > 60 l/s, and wellhead pressures of ~50 MPa. This induced > 29,000 earthquakes with $M_L$ -1.6 to 3.0 recorded on a local 24-station network. Of these, 21,720 locations and 525 focal mechanisms were derived. This may be the most prolific EGS-induced earthquake dataset ever collected. In contrast to the well-hugging, sub-vertical fracture activated by stimulation of well Jolokia 1, the Habanero 4 stimulation activated a single, sub-horizontal fault zone only a few meters thick, extending > 1.5 km from the well. Failure was consistent with the regional stress field.

These remarkably different seismic responses characterized injections in different wells penetrating the same granite formation. This exemplifies the challenge of predicting the behavior of formations under stimulation, even when excellent geological knowledge is available. Despite the major technological advances achieved in the Cooper Basin project, due to low oil prices and

changing government priorities, the project was decommissioned in 2016.

Despite the challenges that currently face development of EGS, much has been learned recently that will underpin the future of the industry. Because it is known beforehand that projects induce seismicity, exemplary seismic monitoring and public outreach practices have been developed. These include installing custom-designed networks of three-component borehole instruments well in advance of operations to obtain a pre-operational baseline for seismic activity. Data are streamed to public websites and outreach includes town-hall meetings, seismometers in public buildings in nearby communities, distributing information to the public by talks, printed materials and the internet, and involving local communities in the commercial activity.

#### 4.1.5 Geothermal reinjection

Water is re-injected into exploited geothermal fields to maintain pressure. Although classified technically as renewable resources geothermal fields are, in reality, not so. If large quantities of hot fluid are removed at high rates for many years, exceeding natural recharge, the resource becomes depleted and progressive reduction in reservoir pressure leads to reduced production. To maintain pressure water is re-injected whilst avoiding cooling production wells.

The most remarkable case of seismicity attributed to geothermal reinjection is The Geysers field, California (Figure 46). The Geysers is a rare vapor-dominated reservoir that lies in the strike-slip regime of the San Andreas fault system, California. Exploitation began in the 1860s. Steam was first used to generate electricity in 1922 when 1 kW was produced. Production peaked in 1987 at about $3.5 \times 10^3$ kg $s^{-1}$ of steam from which 1800 MW of electricity was generated (Figure 47).

Power production decreased thereafter because the modest amount of reinjection done could not maintain declining steam pressure. Condensate was the main re-injectate and less was available than the amount of water produced. Reservoir pressure is sub-hydrostatic and thus the water could be reintroduced at atmospheric pressure, i.e. it was poured into boreholes and drained back into the reservoir under gravity.

The US Geological Survey routinely locates > 10,000 earthquakes/year at The Geysers. The annual seismic rate is currently 200-300 M 2 earthquakes and 1-2 M 4 earthquakes. The Geysers earthquake dataset is without doubt the richest set of induced earthquake data available in the

world with > 250,000 located events in the catalog of the Northern California Earthquake Data Center[7].

For many years it was not acknowledged that the industrial activity induced the earthquakes. However, as data accumulated the link could not be denied. It was initially assumed that the earthquakes resulted from the contracting reservoir collapsing in on itself. Surface subsidence rates are up to 5 cm/year [Lofgren, 1978; Mossop & Segall, 1999; Vasco *et al.*, 2013].

It is now clear that seismicity correlates better with reinjection than production [e.g., Majer & Peterson, 2007; Stark, 1990]. It has been possible to make this link since 1998 when the first of two major water-acquisition and reinjection projects began. The South East Geysers Effluent Project (SEGEP) began to re-inject water via a 46-km-long pipeline from Lake County that delivers up to 22 x $10^6$ l/day of grey water. In 2003 the second project came online, the Santa Rosa Geysers Recharge Project (SGRP), which delivers up to 41 x $10^6$ l/day via a 64-km-long pipeline from Santa Rosa (Figure 47) [Majer & Peterson, 2007]. Surges in earthquake rate correlate with the increases in water injection with those projects. Surges of earthquakes also correlate withindividual injections and injection wells [Majer & Peterson, 2007; Stark, 1990], *e.g.*, in the high-temperature northwest Geysers in 2004 (Figure 63).

Ground shaking from earthquakes with Modified Mercalli intensities of II – VI are felt daily in settlements near The Geysers. The largest earthquake that has occurred is the 2014 $M_W$ 4.5 event. On the basis of historical seismicity, the absence of long faults in the reservoir, and the lack of epicentral alignments, Majer *et al.* [2007] estimated that the largest earthquake that could occur was M ~5.0. An extensive review of The Geysers seismicity is provided by Majer and Peterson [2007]. They conclude that the seismicity results from a diverse set of processes that may work independently or together and either enhance or possibly reduce seismicity. To the processes listed in Section 1.3, thermal contraction from cooling the rock matrix can be added.

A second example of particularly rich geothermal-induced seismicity is from the Coso geothermal field. This field lies in the southwestern corner of the Basin and Range province in eastern California, at a right releasing step-over in the southern Owens Valley fault zone

[7] http://www.ncedc.org

[Monastero *et al.*, 2005]. It lies on a US Navy weapons test site, and is thus uninhabited and not generally accessible to the public. Electricity has been generated since the 1980s, producing about 250 MW. Because there is a shortage of local water, only about half the volume produced is replaced by reinjection and the local water table lowered greatly.

Tectonic seismicity is intense in the region, but even in this context the geothermal field is anomalously seismogenic. Several thousand locatable earthquakes per year occur within the ~5 x 5 km production field, the majority of which must be induced. These earthquakes have been used for detailed research [e.g., Julian *et al.*, 2004; Julian *et al.*, 2007; Kaven *et al.*, 2014; Monastero *et al.*, 2005]. Most production and reinjection data are proprietary, so published correlations between operations and seismicity are rare.

One of these rare cases is described by Julian *et al.* [2007]. In 2005 an existing well was used for an EGS experiment. Fluid was injected at rates of up to 20 l/s into well 34-9RD2 in order to increase permeability and enhance production in nearby producing wells. 34-9RD2 was re-worked prior to the injection to deepening it and replace the existing slotted liner with an un-slotted one.

Major unexpected circulation-loss zones were encountered resulting in a total loss of up to 20 l/s of drilling mud at 2672 m depth. The planned EGS project thus instantly metamorphosed into an unplanned reinjection operation. A vigorous earthquake swarm began immediately. High-resolution locations, relative locations, and full moment tensors were determined using an exceptionally high-quality dataset acquired on 36 digital, three-component seismic stations of the permanent network operated by the Geothermal Program Office of the US Navy augmented by temporary stations..

The swarm opened, in tensile mode, several hundred meters of a preexisting fault immediately adjacent to the well. The existence of this structure deduced from the seismic evidence was confirmed by surface geological mapping and a borehole televiewer log. This was an early demonstration of the potential of earthquake techniques to study the detailed subsurface fracture network in a geothermal reservoir.

In Europe, three geothermal projects have been associated with M > 3 induced earthquakes, all in

Italy:

- the Larderello-Travale area ($M_{MAX}$ 3.2);
- the Monte Amiata geothermal field ($M_{MAX}$ 3.5); and
- the Torre Alfina Field ($M_{MAX}$ 3.0).

Of these, the most notable case is Larderello-Travale, Tuscany which, like The Geysers, is a rare vapor-dominated system. Tuscany is tectonically active with transcurrent-transtensional-strike-slip deformation, high thermal gradients and temperatures up to 400˚C. There are several geothermal fields of economic interest. The shallower Larderello-Travale reservoirs occuply Triassic carbonate and evaporite rocks and the deeper ones fractured metamorphic basement.

Larderello-Travale has generated electricity almost continuously since 1904, and is thought to have a long history of seismicity. In the early 1970s, injection of cold condensate from the power plants started to recharge the upper reservoir and a seismic network was installed [Batini *et al.*, 1985; Batini *et al.*, 1980].

Seismicity is variable in rate and *b*-values. The events are mostly < 8 km deep, with 75% 3.0-5.5 km deep. The largest event reported was M 3.2 and occurred in 1977. Events have significant non-shear focal mechanism components, indicating tensile failure [Kravania *et al.*, 2000]. Because of the long history of seismic activity many events are thought to be natural. Nevertheless, a clear correlation between injected volume and seismic rate is reported [Batini *et al.*, 1985; Evans *et al.*, 2012].

#### 4.1.6 Shale-gas hydrofracturing

Gas-bearing shale formations are hydrofractured (“fracked”) to increase permeability and release the contained gas. It is typically done by drilling shallow horizontal wells into the target formation. Fluids are injected containing chemicals and solids designed to propagate fractures and prop them open. It is extensively applied in the USA where it has brought about a major reduction in the cost of natural gas (Figure 64). As a result of this success there is widespread interest in the technology in other countries. However, in regions where population density is high there may be public concern about potential environmental effects, including ground-water

pollution, industrialization and induced earthquakes.

Although over 2.5 million shale-gas hydrofracturing jobs have been completed worldwide, maximum earthquake magnitudes for only 21 cases have been reported. Of these cases, eight are from the USA, 12 from Canada, and one from the UK [Baisch & Vörös, 2011; de Pater & Baisch, 2011]. This is only 0.001% of all shale-gas hydrofracturing jobs (Section 7.1). Of those cases, moderately large earthquakes are reported from British Columbia (M 4.4, 4.4 and 3.8 events) and Alberta ($M_L$ 4.4), both in Canada [Kao *et al.*, 2015; Schultz *et al.*, 2015]. In the USA the largest shale-gas hydrofracturing-related earthquakes reported have been four M > 3 events in Oklahoma and Ohio [Darold *et al.*, 2014; Skoumal *et al.*, 2015].

These statistics are misleading because the fundamental purpose of hydrofracturing in gas-bearing shale is to crack the rock. Thus, all successful hydrofracturing jobs induce earthquakes but the aim is that they do not cause nuisance. Meeting this objective is helped in the USA and Canada by operating in regions of low population density. Seismic monitoring is often done because the earthquake locations indicate location and volume of the fracture network created. However, if nuisance seismicity is not induced there is little reason to report it. Seismic analyses focus on investigating the spatial distribution and mode of fracturing, the results are not of public interest, and they are likely to remain proprietary.

A remarkable case was associated with injection operations in 2013 near Crooked Lake, Alberta. There, the largest shale-gas hydrofracturing-related earthquakes on record were induced. The target formation was Devonian Duvemay organic-rich shale. Operations involved multi-stage, high-pressure injections of proppant-weight-in-well ~60 MPa and volumes of a few thousand cubic meters. Of ~3000 hydrofracturing operations in Alberta in 2013, only three (0.1%) are reported to have been accompanied by noteworthy seismicity, with 160 events up to $M_L$ 4.4 being observed over a ~2-year period [Schultz *et al.*, 2015].

The quality of information about the sequences is limited because there were no local seismic stations. Data from distant stations was subject to sophisticated processing and suggested close spatial and temporal correlation with the shale-gas hydrofracturing (Figure 65). Correlation also occurred between injection stages, a “screen-out” (i.e. interruption in slurry flow causing shutdown of injection) and seismicity. Associations between screen-outs and seismicity are

reported from elsewhere [Clarke *et al.*, 2014a; Skoumal *et al.*, 2015]. The seismicity may have hampered operations at Crooked Lake.

The Horn River Basin, British Columbia, is a major shale gas production area. Fracking commenced in 2006 and gas production peaked in 2010 and 2011 [Farahbod *et al.*, 2015]. Prior to the hydrofracturing, seismicity rates were low. Only 24 earthquakes with M 1.8-2.9 were located locally in a ~2-year period. When hydrofracturing started the seismic rate increased to >100 earthquakes/year and correlated with hydrofracturing (Figure 66). A logarithmic correlation between seismic moment, maximum magnitude and volume injected was observed (Figure 67).

For the entire Horn River Basin, injected volume was more closely related to seismicity than injection pressure. Increases in volume increased earthquake frequency but not magnitude. Large earthquakes ($>10^{14}$ N m, i.e., $M_W$ ~3.5) occurred only when ~150,000 $m^3$ of fluid were injected per month. Time lags between injections and seismicity ranged from days to months.

The embryonic UK shale-gas industry began with the unfortunate case of the 2011 Preese Hall, Lancashire, earthquake sequence. There, the first UK dedicated multi-stage shale-gas hydrofracturing operation was conducted in a 1000-m section of the Carboniferous gas-bearing Bowland Shale. Following the injection of 2245 $m^3$ of fluid and 117 tonnes of proppant, a nearby $M_L$ 2.3 earthquake was reported by the British Geological Survey. The earthquake was felt, and was unusual in that location. The nearest monitoring station was 80 km away. Additional seismic stations were deployed rapidly but no aftershocks recorded. UK shale-gas hydrofracturing thus started with a rare phenomenon–the suspected induction of a nuisance earthquake.

Operations continued, but about six weeks later a second felt event of $M_L$ 1.5 occurred ~1.0 km from the well. Citizen disquiet followed and operations were suspended. A total of 52 earthquakes in the magnitude range $M_L$ -2.0 to 2.3 were detected with similar waveforms to the two largest events. A government enquiry and 18-month suspension of operations ensued while the problem was investigated. The close relationship between hydrofracturing and seismicity left little doubt that the earthquakes had been induced (Figure 68).

The UK Department of Energy and Climate Change (DECC) commissioned a review and

recommendations for mitigation of seismic risk associated with future shale-gas hydrofracturing operations in the UK. Recommendations included monitoring test injections prior to the main injections, monitoring fracture growth during injections, near-real-time seismic monitoring, and halting or changing injection strategy at the occurrence of seismicity with a threshold magnitude of $M_L$ 0.5 [Green *et al.*, 2012].

Detailed studies of the locations and fault mechanisms of the poorly recorded seismicity, combined with seismic reflection data, showed that the earthquakes probably occurred a few hundred meters below the well perforations on a fault that was not previously known [Clarke *et al.*, 2014b; Green *et al.*, 2012]. The fault does not intersect the borehole but was close enough that hydrofracture fluid may have leaked into it. The structure is an ancient transpressional fault that formed at the end of a Carboniferous basin inversion and which had been inactive for 260 Ma. This case showed that even long-inactive faults, which are common in most continental crust, are close to failure and may be induced to slip by nearby injections.

#### 4.1.7 Allowing mines to flood

Removal of rock from mines lowers confining stress on nearby faults and brings them closer to failure. The simultaneous pumping out of water during mining lowers pore pressure, increasing the strength of faults and counteracting the effect of rock removal. These process roughly balance until a mine is abandoned and pumping stopped. After this, natural groundwater recharge may encourage seismicity.

A classic case is that of the 1994 Cacoosing Valley, Pennsylvania, earthquake sequence (Figure 69) [Seeber *et al.*, 1998]. Groundwater recharge is implicated in a $M_L$ 4.4 earthquake that occurred beneath an 800-m-wide carbonate quarry from which ~4 x $10^6$ $m^3$ had been removed. The earthquake caused ~$2 million of damage to nearby homes. The quarry had been excavated to an average depth of 50 m over the 58-year time period 1934-1992. Groundwater pumping done during the mining period stopped after mining ceased and the water table rose by ~10 m in a few months. The rock is permeable karstic carbonate and depletion of groundwater, along with subsequent recharge, likely extended over a wider area than the footprint of the quarry.

Earthquake activity commenced approximately five months after pumping ceased. A rapidly

deployed temporary seismometer recorded 67 aftershocks. They occurred in the upper 2.5 km in a planar pattern interpreted as the fault plane that slipped. Focal mechanisms suggested the mainshock had a thrust mechanism. The earthquakes occurred in the hanging-wall block such that unloading by rock removal would have encouraged slip. Surprisingly, the seismicity did not activate any of the plentiful, known, large-displacement faults in the region. Instead, stress was released on a set of small, unmapped faults which probably had a more suitable orientation. The mining had reduced confining stress by ~0.13 MPa, while the $M_L$ 4.4 mainshock had a stress drop of 1-4 MPa.

The Cacoosing Valley event may have been similar to one that occurred two decades earlier beneath a large quarry at Wappingers Falls, New York [Pomeroy *et al.*, 1976]. A $m_b$ 3.3 earthquake occurred there in 1974. Again, the mainshock and aftershocks nucleated at exceptionally shallow depth with some as shallow as 0.5 km. Slip occurred on a reverse fault immediately below the quarry and had a source mechanism consistent with the regional stress field. Over the preceding ~75 years ~30 x $10^6$ $m^3$ of rock had been removed by open-casting down to a depth of ~50 m. This changed the stress by ~1.5 MPa at the surface and reduced the normal stress on faults below.

#### 4.1.8 Research projects

In the wake of the Denver, Colorado earthquakes (Section 4.1.1) there was speculation that earthquakes might be controllable. Partly as a result, a series of earthquake-induction experiments have been conducted for research purposes. These have investigated the physical properties of natural fault zones and the processes that accompany earthquake occurrence. *HiQuake* contains 13 cases of earthquakes induced by research projects.

The first such project was conducted in 1969 at the Rangely Oilfield, Colorado [Raleigh *et al.*, 1976]. This oilfield occupies Mesozoic and Paleozoic sedimentary rocks at ~1700 m depth and is underlain by crystalline basement at ~3000 m. There is little local faulting, but earthquake activity had occurred with water flooding for enhanced recovery (Section 4.1.3). A seismograph array and prior earthquake record were therefore available. Fluid pressure in wells near the earthquakes was experimentally cycled to investigate the effect on the seismicity. There was close correlation between seismicity and high pore pressure and events up to $M_L$ 3.1 were

induced (Figure 70).

In 1970 another experiment was conducted at Matsushiro, Japan. A volume of 2883 $m^3$ of water at wellhead pressures of 1.4-5.0 MPa was pumped into an 1800-m-deep well to test whether earthquakes were induced by increasing pore pressure in a fault zone. After several days of injection earthquake activity started within a few kilometers of the well [Ohtake, 1974].

After a hiatus in experimenting of 16 years, in 1990, perhaps the best known research experiment to study fluid-induced seismicity was begun–the Kontinentales Tiefbohrprogramm der Bundesrepublik Deutschland (KTB)–the German Continental Deep Drilling Program. Extensive literature documents this project including a 1997 special section of Journal of Geophysical Research (No. 102) [e.g., Baisch & Harjes, 2003; Baisch *et al.*, 2002; Bohnhoff *et al.*, 2004; Erzinger & Stober, 2005; Fielitz & Wegler, 2015; Grasle *et al.*, 2006; Jahr *et al.*, 2005; Jahr *et al.*, 2007; Jahr *et al.*, 2008; Jost *et al.*, 1998; Shapiro *et al.*, 2006; Zoback & Harjes, 1997].

The main borehole was drilled 1990-1994 to a depth of 9.1 km. The first hydraulic stimulation was conducted in 1994 at depths and pressures close to the brittle-ductile transition. About 400 earthquakes up to $M_L$ 1.2 were induced at about 8.8 km depth (Figure 71). Focal mechanisms were consistent with stress measured in the borehole. Seismicity began within a few hours of pumping and a few tens of meters from the borehole. Modeling suggested that the earthquakes occurred in response to pressure perturbations of < 1 MPa, i.e. less than 1% of the ambient, hydrostatic pore pressure at the nucleation depth.

An important conclusion of this experiment was that differential stress in the crust is limited by the frictional strength of well-oriented, pre-existing faults ("Byerlee's Law") and the crust is in brittle failure equilibrium even at great depth in stable intraplate areas. Hydraulic experiments at the site have continued up to recent years [e.g., Jahr *et al.*, 2008].

A 1997 project in the Phillipines injected 36,000 $m^3$ of water into a well intersecting a creeping portion of the Philippine Fault at the Tongonan geothermal field. The water entered the formation at 1308-2177 m below the surface [Prioul *et al.*, 2000]. Several hundred earthquakes occurred but all were away from the fault in the geothermal reservoir. Prioul *et al.* [2000] concluded that tectonic stress on the fault is relieved aseismically and as a consequence there

was no differential shear stress to be released by the water injection.

In the same year, a water-injection experiment was conducted in the Nojima fault zone, Japan, shortly after it ruptured in the 1995 M 6.9 Kobe earthquake [Tadokoro *et al.*, 2000]. This experiment gathered information on the physical properties of a fault plane in the immediate post-rupture period. Over periods of a few days, 258 $m^3$ of water were injected into an 1800-m-deep borehole at a pressure of ~4 MPa at the surface, entering the fault zone at 1480-1670 m depth. An increase in M -2 to 1 seismicity occurred a few days after each injection. It was concluded that the fault zone was highly permeable and could slip with pore-fluid pressure increases of less than 10%.

Two additional experiments have been conducted in recent years, the first in 2013 as part of the Wenchuan Earthquake Fault Science Drilling (WFSD) project [Ma *et al.*, 2015]. This project studied the fault healing process. Over a four-month period 47,520 $m^3$ of water at 10-15 MPa was injected at rates of up to 1.7 l/s into a 552-m-deep well that intersected a fault zone at 430 m depth. The fault was activated and over 20,000 earthquakes up to M ~1 were detected by downhole observations. The hypocentral zone suggested failure in the same sense as the regional stress.

A similar phenomenon was reported by Guglielmi *et al.* [2015] in an experiment that stimulated an inactive fault in a carbonate formation. The experiment injected 0.95 $m^3$ of water into a 518-m-deep underground experimental facility in southeastern France where a vertical well intersected a fault at 282 m depth. Aseismic shear slip started at a pressure of ~1.5 MPa, and ~80 earthquakes occurred a few meters from the injection point. These accounted for only a small fraction of the slip on the fault, however. The accumulated moment at the end of the experiment was $M_o$ = 65 x $10^9$ Nm, (equivalent to an event with $M_W$ 1.17). This was far larger than the moment released by the seismicity, which totalled $M_o$ < -2 N m. Aseismic slip dominated deformation in the fault zone and the earthquakes occurred in rock mass outside the pressurized zone. Other experiments have been performed in a salt solution mine at Cerville-Buissoncourt in Lorraine, France [Kinscher *et al.*, 2015; Mercerat *et al.*, 2010] and the Wairakei geothermal field, New Zealand [Allis *et al.*, 1985; Davis & Frohlich, 1993].

This multi-decade, multi-national research endeavor has answered some critical questions, not

always those originally posed and not always with the preferred answer. Relieving in a controlled way the stress naturally released in large earthquakes is scientifically challenging. The continental crust is near to failure, even to great depths and where large faults are not known. Earthquakes can be induced by relatively small stress perturbations, but in some cases stress on a targeted fault is relieved aseismically. In these cases, motion on that fault may induce secondary earthquakes in the surrounding rock mass. Fluid injection may thus induce primarily aseismic slip, and seismicity may be a secondary effect, with imperfect spatial correlation with the injection activities. In many cases of induced seismicity more stress is released than is loaded on faults artificially, since pre-existing tectonic stress is also released. However, the Wenchuan and southeastern France experiments illustrate that the reverse sometimes occurs–some of the anthropogenically loaded stress may be released aseismically.

### *4.2 Gas*

#### 4.2.1 Natural gas storage

To stabilize supply and increase energy security nations store natural gas reserves, often underground. In May 2015, 268 underground gas storage facilities existed or were planned in Europe (Figure 72) and over 400 in the USA.

Depleted hydrocarbon reservoirs, aquifers, and salt cavern formations are obvious repositories because they are usually well understood geologically and engineering infrastructure including wells and pipelines may already be in place. They may also be conveniently close to consumption centers.

*HiQuake* contains seven cases of induced seismicity reported to have been associated with underground gas storage:

Gazli, Uzbekistan [Simpson & Leith, 1985];
the Castor project (in the old Amposta Field), Spain [Cesca *et al.*, 2014; Gaite *et al.*, 2016];
Bergermeer, Norg and Grijpskerk, Netherlands [Anonymous, 2014];
Háje, Czech Republic [Benetatos *et al.*, 2013; Zedník *et al.*, 2001]; and
Hutubi, China [Tang *et al.*, 2015].

At the Bergermeer Gasfield, a few earthquakes up to M 0.7 occurred in 2013 in association with the injection of cushion gas. Up to 15 earthquakes per month up to M 1.5, several of which were felt, were reported for the Háje storage facility. Larger earthquakes were occurre in association with gas storage at Hutubi, with over 700 earthquakes up to M 3.6 in the period 2009-2015.

The Gazli Gasfield, Uzbekistan, is primarily renowned for the three damaging $M_S$ ~7 earthquakes that caused death and destruction in the local town of Gazli in 1976 and 1984 (Section 3.3.1). When this field had been largely depleted, it was used for storage. Gas was cycled in and out as required. Plotnikova *et al.* [1996] report seismicity up to M 5 induced by this process that correlates with the amount of gas stored.

The best-documented case is that of the 2013 Castor project, Spain. This project aimed to use a depleted oilfield in the Gulf of Valencia, the old Amposta Field, ~20 km from the coast of northeastern Spain (Figure 73). It was planned to store 1.3 x $10^9$ $m^3$ of natural gas there, sufficient to meet 25% of Spain's storage requirements. Earthquakes began shortly after the commencement of gas injection, however, the largest of which was $M_W$ 4.3. Public reaction to the earthquakes was negative, not least because the population was sensitized after the 2011 $M_W$ 5.1 Lorca earthquake only two years before, 250 km to the south along the coast (Section 3.1). We understand that as a result the project has been discontinued.

The old Amposta oil reservoir occupies fractured and brecciated Lower Cretaceous dolomitic limestone and is one of several in the region (Figure 74). It produced 56 million barrels (~9 x $10^6$ $m^3$) of an estimated total in-place volume of 140 million barrels of oil (22 x $10^6$ $m^3$) 1973-1989. Secondary injection for enhanced recovery was not needed because of strong natural water drive. After 1989 the depleted field lay dormant.

Installation of the necessary infrastructure for conversion of the reservoir into a gas storage facility commenced in 2009 and included a platform and gas pipeline. Injection of an initial ~$10^8$ $m^3$ (at 25˚C and 0.1 MPa pressure) of cushion gas (i.e. gas intended as permanent inventory in the reservoir) was conducted in 2013 at 1.75 km below sea level.

Three days after injection began, seismicity with events up to M 2.6 occurred (Figure 75 and

Figure 76). Injection was stopped after 12 days but earthquakes continued to occur. The largest, a

$M_W$ 4.3 event, occurred two weeks after injection stopped. In total, over 1000 earthquakes were detected, more than 420 with $M \geq 2$ (

Figure 76). Seismicity was still ongoing in 2016 [Gaite *et al.*, 2016].

Accurate hypocentral locations were difficult to calculate because the project, being offshore, was monitored by a seismic network with limited coverage. The closest station was 26 km from the Castor platform and, since most of the stations were on land, there was restricted azimuthal coverage [Gaite *et al.*, 2016]. As a result, different studies of the hypocentral locations yield different results and even the orientation of the hypocentral distribution as a whole (which might reveal the activated fault structure) and the hypocentral depths (which might show proximity to the injection site) vary significantly between studies. Both NW and NE orientations for the hypocentral zone are reported, along with depths that vary from close to the gas injection depth to several kilometers deeper (Figure 75) [e.g., Cesca *et al.*, 2014; Gaite *et al.*, 2016].

The epicentral area forms part of the dominantly ENE-WSW Catalan-Valencian normal-faulting extensional region [Perea *et al.*, 2012] and focal mechanism studies of the mainshock show motion compatible with slip in this sense [Cesca *et al.*, 2014]. The most significant potentially seismogenic feature near the old Amposta Field is the 51-km-long, NE-SW oriented, Fosa de Amposta fault system [Gaite *et al.*, 2016]. If such a major fault zone were it to rupture in its entirety a M 5-7 earthquake could occur (Figure 77). Combined interpretation of the locations and source mechanisms suggests that this fault was not activated, however.

The seismicity was unusual for the area in both magnitude and seismic rate compared with the preceding two decades (Figure 73). Although earthquake activity occurs along the coast of Spain to the north and south, the Pyrenees mountain chain in Portugal, and the coast of North Africa, no significant historical seismicity was known on the fault system local to the Castor project prior to the gas injection. For this reason, and because of the close spatial and temporal correlation with gas injection, there is little doubt that the earthquakes were induced.

### 4.2.2 $CO_2$ for oil recovery

There are approximately 100 enhanced oil recovery injection sites where $CO_2$ is used, mostly in Texas. *HiQuake* contains two cases where seismicity is postulated to be induced by this process.

These are at the Cogdell Field, Texas [Gan & Frohlich, 2013] and Weyburn Oilfield, Saskatchewan [Maxwell & Fabriol, 2004; Verdon *et al.*, 2013]. The latter is a hybrid project and also classified as a Carbon Capture and Storage (CCS) project (Section 4.2.3).

Early on in its history, the Cogdell Oilfield generated earthquakes surmised to have been induced by water injection [Gan & Frohlich, 2013]. Lately, $CO_2$ has been injected and is associated with earthquakes up to $M_W$ 4.4 (Figure 78).

The Oilfield is a large subsurface limestone reef mound, not a fault-bounded oil trap, and there are no mapped faults nearby. Production began in 1949 and 1957-1983 oil recovery was enhanced by brine injection. This was associated with earthquakes, including a $M_L$ 5.3 event in 1978. This earthquake was only poorly located as a result of the rudimentary nature of seismic monitoring in Texas at the time. Davis and Pennington [1989] suggested that the earthquakes correlated with injection volume and high reservoir pressure gradients.

Gas injection began in 2001 and grew to a constant, high level of ~40 x $10^6$ $m^3$/mo from 2004. It was introduced at ~2.1 km depth, 20 MPa pressure and 75˚C, under which conditions $CO_2$ is supercritical. In 2006, after 23 years of seismic quiescence and following a significant increase in gas injection rate, earthquakes began again. Over the following five years 18 events with M > 3 occurred and in 2011 one of $M_W$ 4.4.

A 21-month period March 2009 - December 2010 could be studied in detail because at this time USArray, a rolling program to cover the entire country with temporary seismic stations[8], swept across Texas. During this period the network recorded 93 locatable events, many within 2 km of wells actively injecting gas. Locations and focal mechanisms showed that the events occurred on previously unknown faults. Although the neighboring Kelly-Snyder and Salt Creek Fields have similar operational histories, seismicity is not induced in them.

### 4.2.3 Carbon Capture and Storage (CCS)

In the case of Carbon Capture and Storage (CCS), in addition to causing a nuisance, induced earthquakes could rupture the impermeable containment caprock that contains the $CO_2$ in the

[8] http://www.usarray.org

storage reservoir, and release it back into the environment. Carbon geostorage is in its infancy, but 20-30 tests are already underway globally, including eight operational commercial-scale plants[9]. Of these, three are seismogenic. An illustrative range of seismic responses is provided by the Sleipner Field, the Weyburn Field (Saskatchewan, Canada) and In Salah (Algeria) [Verdon *et al.*, 2013].

Since 1996 ~$10^6$ tonnes/year of $CO_2$ has been removed from the natural gas produced from the Sleipner Field (Norwegian North Sea) and re-injected into a shallow saline aquifer (the Utsira Formation). This aquifer is large and comprises well-connected, little-faulted sandstone with high porosity and permeability at ~1 km depth beneath North Sea mean sea level. By 2011 the total volume of $CO_2$ injected amounted to only ~0.003% of the available pore space. No pore-pressure increase, mechanical deformation or seismicity has been detected for the entire >20 years of injection. The Sleipner Field is, however, not seismically monitored locally so small earthquakes would go undetected. The nearest earthquakes to the Sleipner Field listed in the British Geological Survey catalogue are a $M_L$ 3.5 event at 1 km distance and a M 2.5 earthquake at 6 km distance. The uncertainties in these locations are large.

The Weyburn Oilfield, Saskatchewan, Canada, has been exploited for 45 years and is somewhat seismogenic. $CO_2$ injections started in 2000 both for enhanced oil production and $CO_2$ sequestration and now ~3 x $10^6$ tonnes/year are injected annually. This is accompanied by minor, low-magnitude earthquake activity (Figure 79). Some earthquakes clustered near injection wells, but there are no clear temporal correlations are apparent.

In contrast, vigorous earthquake activity accompanied $CO_2$ sequestration at the producing In Salah Gasfield, Algeria. There, $CO_2$ was injected into a low-permeability, 13–20% porosity, ~20-m-thick fractured sandstone in a non-producing, water-dominated part of field at 1,850–1,950 m depth. Hundreds of earthquakes accompanied surface uplift.

$CO_2$ injection at In Salah 2004 - 2013 amounted to a total of ~3.85 x $10^6$ tonnes of $CO_2$ which was produced from nearby gas wells and re-injected via horizontal boreholes. There was little pressure communication with the producing part of the field. Pore pressures increased from

[9] http://www.ccsassociation.org/faqs/ccs-globally/

initial conditions of ~18 MPa at the injection points to ~30 MPa whilst reducing in the production parts of the reservoir (Figure 80). Deformation monitoring detected surface-blistering type uplift of up to ~1 cm/year locally around the injection wells.

A nearby borehole seismometer detected over 1000 events in 2010. The data were consistent with locations in the receiving formation beneath the injection well though there was no correlation with $CO_2$ injection (Figure 81). The project was subsequently terminated because of seal integrity concerns.

Verdon *et al.* [2013] conclude that at Sleipner, where the target aquifer is large and pressure increases during injection minimal, little deformation, either seismic or aseismic, results. At Weyburn, deformation and seismicity may be partly mitigated by ongoing oil extraction which serves to offset pressure increase resulting from the $CO_2$ injections. At In Salah, however, the formation into which $CO_2$ is injected had poor pressure communication with the producing parts of the reservoir and natural gas extraction did not compensate for the injections. Pore pressures increased as a consequence leading to both seismic and aseismic deformation.

Another seismogenic CCS demonstration site is at Decatur, Illinois [Kaven *et al.*, 2015]. There, ~$10^6$ tonnes of supercritical $CO_2$ were injected over a period of three years at a depth of 2.1 km into a regionally extensive, 460-m-thick high porosity/permeability sandstone. The $CO_2$ used is a by-product of local ethanol production. Approximately 180 earthquakes up to $M_W$ 1.26 occurred over about two years within a few kilometers of the injection well and at the approximate depth of injection. Kaven *et al.* [2015] concluded that earthquakes nucleated on preexisting faults in the basement well oriented with respect to the regional stress field. Little seismic hazard is posed to the host formation because the earthquakes are distant and small.

All other CCS projects have been shorter in duration and with total volumes no more than 10s or 100s of thousands of tonnes. CCS projects have developed recently in China where eleven projects are reported [Huaman & Jun, 2014]. Limited information is available on these projects and none regarding seismicity induced.

#### 4.2.4 Injection into the subsurface: Summary

Diverse fluids are injected into the ground for various reasons and related seismogenic behavior

is variable. For most projects no earthquakes are reported. For others, small earthquakes occur that are of insufficient general interest to publish details. For a small minority induced seismicity is sufficiently troublesome to hinder operations or result in project abandonment.

Correlations between seismic and operational parameters vary. Earthquakes thought to be induced may be co-located with injections to 10s or 100s of meters or they may occur tens of kilometers away. Earthquakes may begin as soon as operations start or be delayed for decades. Small operations may induce large earthquakes and large operations may be aseismic.

Why is Oklahoma is highly seismogenic while large-scale injection projects are conducted in many states of the USA without nuisance earthquakes occurring? We are not aware of any current theories as to why this is.

## 5 Explosions

Since the first test of a nuclear device, the Trinity explosion of July 16, 1945, approximately 2000 such tests have been conducted by eight nations, 1,352 of them underground. Seismicity was associated with 22 of these, 21 in the USA and one in Russia [Boucher *et al.*, 1969; Engdahl, 1972; Hamilton *et al.*, 1972; McKeown, 1975; McKeown & Dickey, 1969].

American nuclear tests were conducted at the Nevada Test Site for the 48-year-period 1945-1992 (Figure 82). Boucher *et al.* [1969] investigated the possibility of induced seismicity associated with 16 nuclear tests by searching the University of Nevada database of earthquake locations. They reported induced earthquakes after all of the 10 tests where the explosion itself registered $m_b \geq 5.0$. The explosions themselves are not included in the *HiQuake* database. The largest earthquake induced was at least one magnitude unit smaller than the inducting explosion. Earthquakes may have been induced by many, if not all of the tests, but been too small to be clearly recorded.

A test ironically named Faultless (19/1/1968) induced clearly visible surface slip on faults up to 40 km away, even though the test was only one megaton in yield. Ground deformation associated with this, and other nuclear tests, has been captured on film [McKeown & Dickey, 1969][10].

[10] See, for example, https://www.youtube.com/watch?v=6ETHnsKnKiA

Detailed studies of the seismicity induced by large nuclear tests were done for the Benham (19/12/1968), Purse (07/05/1969), Jorum (16/09/1969) and Handley (26/03/1970) tests (Figure 83) [Hamilton *et al.*, 1972; McKeown, 1975]. Earthquakes occurred immediately after the tests, and clustering on Pahute Mesa where a 4-km-thick sequence of volcanic rocks contains both caldera- and basin-range-type normal faults. Most of the earthquakes induced occurred 10-70 days after the tests, at < 5 km depths and closer than ~15 km to ground zero. The locations of the earthquakes were mostly controlled by local geological structure and lay on faults in the caldera ring-fracture zones (Figure 83) [McKeown & Dickey, 1969].

Underground nuclear tests in Amchitka, Alaska, resulted in permanent displacement on faults up to 1 m in the vertical and 15 cm in the horizontal for fault up to 8 km long [McKeown & Dickey, 1969]. Both the Milrow (1969) and Cannikin (1971) tests generated several hundred small earthquakes with M < 4, thought to be related to deterioration of the explosion cavity. The sequences concluded with large, complex events and simultaneous subsidence of the surface resulting from final collapse of the explosion cavity. In the case of the Cannikin test, small events continued up to 13 km from ground zero for several weeks. The earthquakes are thought to have released ambient tectonic stresses. The more modest post-test seismic response from tests in Amchitka compared with those conducted in Nevada may result from the lower level of tectonic stress [Engdahl, 1972]. Tectonic stress is also released simultaneously with the explosions themselves, as shown by blast focal mechanisms involving both shear and explosive components (Figure 22) [Toksöz & Kehrer, 1972; Wallace *et al.*, 1983]. The largest earthquake induced by a nuclear test had a magnitude of $m_b$ 4.9 and was associated with collapse of the cavity of the Cannikin, Amchitka test.

Most large chemical explosions are associated with rocket launching, military research and operations, and accidents in the military, space-program and industrial sectors. Such explosions may be equivalent of several kilotonnes (kt) of TNT. They occur at the surface on land or on ships and are thus poorly coupled to the ground. Tsunamis, but not earthquakes, have been reported in association with some of these.

It has been suggested that deep penetrating bombs may modulate earthquake activity. Balassanian [2005] examined earthquake activity over ~2-year periods spanning bombing

incidents at Kosovo, Yugoslavia (1999), Baghdad, Iraq (1991), Tora Bora, Afghanistan (2001) and Kirkuk, Iraq (2003). It was suggested that the incidence of M ≥ 5 earthquakes increased within 1000 km and one year of the bombings at Kosovo and Tora Bora but not after those at Baghdad and Kirkuk. Arkhipova *et al.* [2012] suggested that the 23 October, 2011 M 7.8 Van earthquake, eastern Turkey, was encouraged by mass bombing associated with the Libyan conflict, 1300-1500 km away.

Deep penetrating bombs explode at depths of a few meters in the ground, improving the coupling by factors of several tens of percent compared with equivalent surface explosions. Nevertheless, deep penetrating bombs are generally not larger than the equivalent of ~1 kt of TNT, much smaller than the megatonne- or multi-megatonne scale typical of nuclear devices reported to have induced earthquakes. In the case of the nuclear tests, earthquakes have been induced out to a maximum of ~40 km away and activity has decayed away over periods of a few days or weeks [Boucher *et al.*, 1969]. Given the relatively small subsurface effects of chemical explosions and the great distances and relatively long time delays of earthquakes postulated to have been induced by them, these suggestions must be considered speculative.

## 6 Summary

Human-induced earthquake are reported from every continent except Antarctica Figure 84. Figure 85 - Figure 90 show regional maps for Europe, the Middle East, central- and east Asia, India and vicinity, southern Africa, North-, central- and South America, Australia and New Zealand. Induced seismicity correlates with industrial activity and not with tectonic plate boundaries.

The magnitudes of the largest earthquakes associated with projects of different types varies widely. The largest have been reported for water reservoirs, conventional oil and gas exploitation, and geothermal operations. Median magnitudes also vary between project types but the most commonly reported are $3 \leq M < 4$ which apply to water reservoirs, construction, conventional oil and gas, hydrofracturing, mining, and research projects. For some types of project the number of cases reported is small. For all project types it is essentially certain that large numbers of smaller induced earthquake sequences have not been reported.

Relationships between seismic and operational parameters have been suggested for a number of projects. For example, seismic moment released and volume injected correlate in shale gas hydrofracturing operations at the Etsho area, Horn River Basin, British Columbia (Figure 67) [Farahbod *et al.*, 2015]. Of interest for future projects is what correlations might exist for all projects of the same kind.

From the point of view of nuisance, the magnitudes of the largest earthquakes induced are the most important. Seismic rate and total number of earthquakes are of secondary importance because the fractal nature of earthquakes means that most are small. Because a large and systematic part of the true dataset is missing (i.e. the unreported cases) correlations with operational parameters cannot convey any information on average $M_{MAX}$. Of interest is whether *the largest* $M_{MAX}$ correlates with operational parameters.

Figure 91 shows a plot of $M_{MAX}$ vs. water reservoir volume for 126 cases. The magnitude of *the largest* $M_{MAX}$ (i.e., the apparent $M_{MAX}$ ceiling) increases with reservoir volume. However, there is no correlation between $M_{MAX}$ and reservoir volume for the dataset as a whole. If reporting were complete, the region of the plot beneath the $M_{MAX}$ upper bound would be entirely populated with points. Because the reported data are biased in this way we have not calculated correlation coefficients between all values of $M_{MAX}$ and other parameters.

Relationships observed include:

- *Water reservoir volume* (Figure 91): Volumes plotted range from 0.004 $km^3$ to 164 $km^3$. There is a nearly linear boundary to the upper left of the cloud of points which suggests a relationship between reservoir volume and largest possible $M_{MAX}$. The 2008 $M_W$ ~8 Wenchuan, China, event, which is disputed because of its seemingly disproportionately large size, also plots on this alignment.
- *Water reservoir mass per unit area* (Figure 92): The largest $M_{MAX}$ (i.e. the upper bound of $M_{MAX}$) increases with reservoir water mass per unit area.
- *Volume added or removed in surface operations* (Figure 93): The largest $M_{MAX}$ increases with this parameter.

- *Volume of material removed from the subsurface* (Figure 94): We combined conventional oil and gas, geothermal, and mining-produced volumes. The largest reported $M_{MAX}$ increases with volume produced. The relationship for $M_{MAX}$ for injection volumes proposed by McGarr [2014] on the basis of theoretical considerations fits these data well (Figure 95).
- *Shale-gas hydrofracturing – injection pressure, rate and volume* (Figure 96): The largest $M_{MAX}$ increases with all these parameters, in agreement with the relationship proposed by McGarr [2014].
- *Injected volume for all projects* (Figure 97): Data from 69 cases provide data to study this parameter. The largest earthquake plotted is the 2011 $M_W$ 5.7 Prague, Oklahoma, event. This and a small number of additional earthquakes, mostly postulated to be induced by waste fluid injection, slightly exceed the upper-bound magnitude limit proposed by McGarr [2014].
- *Injection pressure* (Figure 98): Data are available for 79 cases. Pressures range from atmospheric to 89 MPa. There is a tendency for the largest $M_{MAX}$ to reduce with maximum injection pressure.

*Volume or proxy volume removed from or added to the subsurface* (Figure 99): We calculated volume or proxy volume (mass converted to volume using an appropriate density) for 218 cases. There is a clear upper bound to $M_{MAX}$. The relationship proposed by McGarr [2014] for injection volumes fits this wider dataset well with a few exceptions.

*Mass removed from or added to the subsurface* (Figure 100): As for volume, there is a clear linear observed upper bound to $M_{MAX}$.

- *Yield of nuclear devices* (Figure 101): $M_{MAX}$ for induced earthquakes correlates with explosion size for the seven cases for which data are available. This finding is in agreement with the correlation between the activated-fault length and explosive yield at Pahute Mesa, Nevada Test Site [McKeown & Dickey, 1969].
- *Project scale* (Figure 102): We updated the plot of McGarr *et al.* [2002] with 20 additional cases. The data generally confirm the earlier observations. Two cases exceed the empirical upper bound of McGarr *et al.* [2002]–the 1979 $M_L$ 6.6 Imperial Valley,

California, earthquake (linked to the Cerro Prieto geothermal field; Section 3.4) and the 2008 $M_W$ ~8 Wenchuan, China, earthquake (Section 2.1.1).

- *Project type* (Figure 103): The largest earthquakes postulated to have been induced, in order of decreasing magnitude, are associated with water reservoirs, groundwater extraction and conventional oil and gas operations. These have all been linked to earthquakes with M >7. Only relatively small earthquakes have been postulated to be associated with CCS, research experiments, construction and hydrofracturing. The number of projects in each category varies.
- *Distance of epicenter from the inducing project* (Figure 104): There is a slight tendency for the largest reported $M_{MAX}$ to decrease with distance from the project.

A relationship is not observed for:

- *Dam height* (Figure 105): Data are available for 159 cases, many from Brazil, China, and the USA.
- *Water reservoir area* (Figure 106): Areas of seismogenic reservoirs range from 1.6 $km^2$ to 53,600 $km^2$. The result that there is no significant tendency for the largest $M_{MAX}$ to increase with reservoir area is perhaps unsurprising because large parts of reservoirs may be shallow.
- *Pressure change in subsurface reservoirs* (Figure 107): No correlation was found for the 55 cases where data are available.
- *Injection rate for all projects* (Figure 108): Although some individual projects report correlations there is no clear correlation for projects as a whole.

Figure 109 shows the distribution of induced earthquakes by tectonic regime. The most numerous cases are from intraplate areas (79% of all cases) with the next largest category (13%) located in convergent plate-boundary zones. Most large industrial projects are conducted on land and most land is in the interior of plates with plate boundaries comprising relatively (though not absolutely) narrow zones. Most spreading plate boundaries are in the oceans and currently beyond reach of industrial development. Because induced earthquakes are mostly in intraplate regions they affect regions not traditionally associated with seismicity nor accustomed to it.

The lack of a relationship between $M_{MAX}$ and operational parameters such as injection rate, coupled with the difficulty of predicting which projects will be seismogenetic and which not, suggests that non-operational parameters are important. The pre-existing stress state is the most obvious such parameter. Several lines of research indicate that most faults in the crust are nearly critically stressed, though they may not be optimally oriented to slip under ambient conditions. The local geology, in particular pre-existing faults and fractures, must be important for understanding the extreme variations in seismogenesis between apparently similar projects in different locations. In order for large earthquakes to occur, faults that are suitably orientated and stressed must pre-exist.

The empirical results of this study have implications for individual projects. For example, at The Geysers geothermal field, California, net production (i.e. total production minus re-injection) since 1960 has been ~1.7 x $10^9$ $m^3$. The relationship of McGarr [2014], which links fluid-injection volume to the largest $M_{MAX}$ (Figure 97) fits well data from all volumetric projects. This relationship predicts that the upper bound to induced earthquakes associated with The Geysers volume change is M 7.0. This geothermal field has a maximum NW-SE long dimension of ~21 km. The largest induced earthquake reported from projects of this scale is ~M 6.6 (Figure 102). Figure 110 shows a histogram of numbers of seismogenic geothermal power-producing fields ranked by size [data from Bertani, 2010]. The larger the geothermal operation the more likely it is that induced earthquakes are reported.

The largest earthquake that has occurred to date at The Geysers is the 2014 $M_W$ 4.5 event. There is no evidence that a fault long enough to sustain a M 6.6 or 7.0 earthquake exists in the reservoir. However, The Geysers lies between the regional Mercuryville fault to the southwest and the Collayomi fault zone to the northeast, within the active Pacific/North America transform plate boundary zone. There is no evidence that the Mercuryville fault zone is active, but the Collayomi fault zone contains at least one active fault [Lofgren, 1981].

## 7 Discussion and conclusions

### *7.1 How common are induced earthquakes?*

The total number of industrial projects in various categories, along with the number reported to be seismogenic are given in Table 3. Without doubt under-reporting is severe. Seismicity at projects remote from settlements is likely to escape notice. Known cases may not be publicized unless they are large and of nuisance or unusual interest. For example, ~2.5 million shale-gas hydrofracture jobs have now been completed world-wide. All successful hydrofracturing projects induce small earthquakes but only 21 cases have been reported (Table 3; Section 4.1.6). The absence of reports of seismicity does not correspond to an absence of seismicity. Statements such as "no seismicity is reported" does not equate to no induced earthquakes. Some earthquakes may also have been reported by national seismic networks without their induced nature being recognized.

$M_{MAX}$ for the 562 seismogenic projects where this parameter is reported is shown as a plot of cumulative number of cases vs. $M_{MAX}$ in Figure 111. The linearity of the distribution at the high-magnitude end suggests that reporting is complete for $M_{MAX}$ 5 and above, and that underreporting becomes progressively greater for projects smaller than $M_{MAX}$ 4. Downward extrapolation of the linear, $M_{MAX}$ 5 - 7 part of the plot suggests that ~30% of M ~4 induced earthquakes have gone unrecognized or unreported, 60% of M ~3 events and ~90% of those with M ~2 (Table 4).

The hydrocarbon fields around Britain provide a regional example of this problem. Comparison of the UK earthquake database of the British Geological Survey with maps of hydrocarbon fields in the North Sea suggests correlations between fields and earthquake locations (Figure 112). Expanded maps of several fields are shown in Figure 113. Epicenters cluster near the Beatrice Oilfield (Moray Firth), the Britannia Gasfield, the Southern North Sea Gas Province and the Leman Gasfield.

Most of the recorded earthquakes in the southern North Sea occur in or near fields developed in Permian Rotliegend reservoirs. There, gas is produced using simple pressure depletion from the original hydrostatic pressure. Water is not injected to support production. Many of the poorer-

quality wells used to explore and appraise this gas province were prop-fracked to obtain initial gas flow and a few fields [e.g., Clipper South, Gluyas & Swarbrick, in press, 2016; Purvis *et al.*, 2010] used hydrofracturing in development wells. The Viking Graben contains mostly oilfields that were developed by allowing natural pressure decline to deliver the first oil and then injecting water to support continued production. The water used is seawater at typical North Sea temperatures of ~4˚C, while the reservoirs are at 90-140˚C. The central North Sea and Moray Firth contain a heterogeneous mix of oil and gas fields produced by a combination of pressure depletion and water injection. When discovered some fields were naturally at high pressure and close to the fracture gradient.

Many of these activities are potentially seismogenic. Nevertheless, there are no reports of induced seismicity from these fields. Comparison of seismicity with hydrocarbon production information available from DECC for 1975-2008 shows no temporal correlations and, because the North Sea was seismogenic before hydrocarbon production started, it cannot be ruled out that the seismicity is natural. Detailed work on individual events and their possible connection to operations in individual oil and gas fields is required to resolve this ambiguity [Wilson *et al.*, 2015].

### *7.2 Hydraulics*

Groundwater influences earthquake occurrence. Overwhelming, observational data show that pore pressure in fault zones strongly influences seismicity (Section 1.3). The suggestions that large-scale extraction of groundwater influences seismicity imply an unfortunate association between earthquakes and human need to manage water for utilization and flood control.

The five cases we found of earthquakes suggested to be linked to groundwater extraction raise the question of whether other earthquakes that were both shallow and where major water table changes have occurred were induced. An example is the 2011 M 7.1 Christchurch, New Zealand, earthquake (Figure 114). The city of Christchurch is built on what was once an extensive swamp fed by the rivers Avon and Heathcote and numerous smaller streams. Major engineering works have changed the hydrology there over the last century.

The 1811-1812 New Madrid earthquakes occurred in the central Mississippi river valley. This

renowned sequence included three M ~7 earthquakes and about seven with M > ~6.5. These earthquakes are remarkable for having been felt at distances of up to 1700 km as a result of efficient transmission of seismic waves through the eastern USA lithosphere. They are also remarkable in occurring in an intraplate area. They are a paradox in any paradigm that expects large earthquakes to occur in plate boundary zones.

The New Madrid earthquakes occurred at and just south of the confluence of the 6,000 $m^3/s$ Middle Mississippi and the 8,000 $m^3/s$ Ohio rivers which forms the Lower Mississippi River. The possibility that the earthquake activity is linked to local hydraulics has been suggested previously but not seriously entertained. In view of the growing evidence that hydraulic changes can modulate the seismic behavior of faults it may be timely to revisit this possibility with investigation into pre-earthquake hydraulic activity and numerical modeling.

Hydraulic effects may explain why both mass addition and removal can induce earthquakes. This is illustrated by the fact that the commonest earthquake-induction process is mining (i.e. mass removal–38% of cases; Figure 115) and the second most common is water reservoir impoundment (i.e. mass addition–24%). Hydraulic changes induced by mass redistribution may result in migration of fluid into fault zones, increasing pore pressure. This process may explain the possible induction of earthquakes by erecting the Taipei 101 building (Section 2.1.2). It may also explain earthquake induction by hydrocarbon extraction in the absence of fluid injections, since natural groundwater recharge may occur.

Global earthquake databases show that moderate earthquakes are fairly common near large lakes and reservoirs, *e.g.*, in east Africa, even though induction has not been proposed. Intraplate earthquakes in the UK are not currently understood. At least 21% of UK earthquakes in the British Geological Survey catalog are thought to be related to mines, but many others are probably natural. The seismic rate in the UK is ~one $M_L$ 3.6 event per year [Wilson *et al.*, 2015]. A possible link with hydraulics is under investigation [Graham *et al.*, 2017].

### *7.3 How much stress loading is required to induce earthquakes?*

Earthquakes occur naturally, without any human intervention at all. The minimum amount of added anthropogenic stress needed for an earthquake to start is thus zero.

Many natural processes contribute to stress build-up on faults. These include tectonic deformation, volcanism, natural heat loss, isostatic uplift following deglaciation or oceanic unloading, Earth tides, intraplate deformation resulting from distant plate boundary events, remote large earthquakes, erosion, dissolution, the natural migration of groundwater and weather. To these are added industrial activities. It is an ill-posed question to ask the origin of the final stress increment that "broke the camel's back" and precipitated an earthquake. In the case of large earthquakes this question may be asking whether a particular skier was responsible for an avalanche.

Instead of viewing industrial activity as inducing earthquakes, it could instead be viewed as modulating the timescale on which inevitable earthquakes occur. Unfortunately it cannot be known what events would have occurred had the industrial activity not been done because history cannot be re-run with a change of circumstance. Furthermore, had an equivalent earthquake occurred at a different time, it cannot be known if it would have affected people and infrastructure to the same extent. Nevertheless, in the cases of many industrial projects, the association between earthquakes and the project is undeniable. The clear induction of some earthquakes by very small incremental stresses means that objections to induced status on the grounds that the stress perturbation was too small may be moot.

Anthropogenic stress changes proposed to have induced earthquakes range from a fraction of a MPa [e.g., Keranen *et al.*, 2014], the equivalent of about a meter of rock overburden, to several tens of MPa (Table 5) (Figure 116). For example, both the 2007 $M_L$ 4.2 Folkestone, UK, earthquake and the 2008 $M_W$ ~8 Wenchuan, China, earthquake have been attributed to anthropogenic stress changes of only a few kPa.

The minimum amount of stress loading that might plausibly induce an earthquake is of interest. The question "How much stress change is needed to induce earthquakes?" may be unanswerable. However, it may be possible to address the question "What is the smallest stress change observed induce earthquakes?" This can be attempted using natural stress changes known to correlate with earthquakes, as follows (Table 6).

### 7.3.1 Earth tides

The spatial non-uniformity of the gravitational fields of the Sun and Moon (and to a much smaller extent, other celestial bodies) produces differential stresses in the solid body of Earth approaching 0.005 MPa. Loading of the solid Earth by ocean tides produces additional stresses that can be about an order of magnitude larger but depend strongly on geographic location. The stress drops of most earthquakes are 1 - 10 MPa so tides might sometimes have a detectable effect on earthquake occurrence.

Most early studies of earthquakes and tides failed to find any significant correlation. The main cause of this failure was probably over-simplification of the problem. Both stresses and earthquake mechanisms are tensors, but many studies looked, for example, for correlations between seismicity and tidal amplitude ranges, effectively treating both stress and earthquake mechanism as scalars. Another difficulty with such analyses was the difficulty of computing ocean tides from the complicated shapes of ocean basins.

There were, however, two exceptions to this failure. First, deep moonquakes, detected by seismometers placed by Apollo astronauts, correlate strongly with tides [Latham *et al.*, 1973]. Second, earthquakes at volcanic and geothermal areas show a tidal effect that is easily detected [e.g., McNutt & Beavan, 1981]. This suggests interactions between fluid pressure and the volumetric components of earthquake mechanisms are important. Recently, studies that account for earthquake focal mechanisms and compute ocean loading accurately have found that shallow thrust-faulting earthquakes correlate significantly with tidal stresses [Cochran *et al.*, 2004].

### 7.3.2 Static stress changes resulting from large earthquakes

The 1989 $M_W$ 6.9 Loma Prieta, California, earthquake modulated seismicity from around the epicenter out to distances where the coseismic stress changes were no more than 0.01 MPa (equivalent to ~0.4 m of overburden) [Reasenberg & Simpson, 1992]. The 1992 $M_W$ 7.3 Landers, California, earthquake also modulated nearby seismicity. Aftershocks were abundant up to about two source dimensions from the mainshock (a few tens of km), where the Coulomb stress on optimally orientated faults was increased by > 0.05 MPa. They were sparse where stress was reduced by this amount (Figure 117). The 1992 $M_W$ 6.5 Big Bear aftershock occurred in a region

where stress was increased by 0.3 MPa [King *et al.*, 1994]. The effect of static stress changes on neighboring faults has also been expressed in terms of the number of years by which the next large earthquake has been advanced in time [e.g., King *et al.*, 1994; Reasenberg & Simpson, 1992].

#### 7.3.3 Remote triggering

The 1992 $M_W$ 7.3 Landers, California, earthquake is remarkable because it precipitated earthquake activity up to 17 source dimensions distant from the mainshock (1,250 km). Most of this activity occurred at volcanic or geothermal areas such as Yellowstone. Static stress changes are vanishingly small at such distances. These remote earthquakes are thought to have been triggered by dynamic stress changes of a few tenths of a MPa in the propagating shear- and surface elastic waves interacting with fluids in hydrothermal and magmatic systems [Hill *et al.*, 1993]. This phenomenon of "remote triggering" has subsequently been observd elsewhere. When first unambiguously recognized following the Landers earthquake, it was thought only volcanic and geothermal areas were affected and the process might reveal the locations of geothermal areas previously unknown. However, remote triggering has now been reported in other environments, *e.g.*, the hydrocarbon region of Oklahoma (Figure 58) [van der Elst *et al.*, 2013].

#### 7.3.4 Weather

A number of studies have postulated that earthquakes were induced by heavy rainfall [*e.g.*, Husen *et al.*, 2007; Roth *et al.*, 1992]. Correlations have also been suggested between “slow earthquakes” (accelerated creep on faults) and atmospheric pressure changes accompanying typhoons in Taiwan [Liu *et al.*, 2009]. Such pressure changes alter stress on land areas but not beneath the ocean because seawater flow maintains pressure equilibrium offshore. The effect contributes a stress change of ~0.003 MPa that encourages slip on coast-parallel thrust faults.

### *7.4 How large are induced earthquakes?*

Stress changes postulated induce earthquakes do not correlate with stress drops brought about by the earthquakes or magnitudes. Counter-intuitively, $M_{MAX}$ reported for induced sequences *decreases* with increasing calculated stress perturbation (Figure 116). The final size of an earthquake is determined by how much of a fault was sufficiently to move once activation began.

If slip on a fault reduces to zero before the next event on the same fault starts, a series of discrete events is recognized. If slip does not stop, the event may grow and all the strain release is considered to have occurred in a single event. Great earthquakes that rupture much of the lithosphere typically comprise a cascading chain of M ~7 sub-events, each triggered by the stress changes resulting from the previous ones. Although likely very rare, it cannot be ruled out that industrial activity could contribute to the onset of an initial sub-event. It is also not uncommon for foreshocks to occur immediately preceding the onset of a mainshock several magnitude units higher. An initial $M_W$ 5 earthquake in Oklahoma may have triggered successive earthquakes, including the $M_W$ 5.7 event the following day [Keranen *et al.*, 2013]. In the case of the great 2008 $M_W$ ~8 Wenchuan earthquake (Section 2.1.1), once the first sub-event began slip on the fault did not stop until several large fault segments had failed.

This view is consistent with the findings of McGarr [2014]. He derived a relationship that related volume injected to the size of injection-induced earthquakes and showed that it fit well observations of 18 of the largest-magnitude earthquakes (Figure 95). However, he also pointed out that this upper bound only applies to induced earthquakes whose source regions were confined to the volumes directly affected by the injection, and that if fault slip propagated outside of this volume then larger earthquakes could occur.

### *7.5 Natural or induced?*

The strength of evidence for earthquake induction varies greatly between cases. For some examples the association with an industrial activity is beyond reasonable doubt. For example, over 250,000 earthquakes have been located in a tight cluster in The Geysers geothermal area, California, by the U.S. Geological Survey during the last half century. At the other end of the spectrum, induction has been suggested for cases where only one earthquake occurred and the calculated stress changes were smaller than those induced by Earth tides, *e.g.*, for the 2007 $M_L$ 4.2 Folkestone, UK, earthquake [Klose, 2007b]. For those cases, mere coincidence cannot be ruled out (Section 2.1.3 and Section 7.3). Induction of earthquakes over 1,000 km away and over a year later by bombing of cities with non-nuclear weapons is not strongly supported (Section 5).

The number postulated induced cases is increasing rapidly and with it the urgency for management strategies. It is desirable, not only to know *a posteriori* whether an earthquake was

natural or induced, but also to forecast which projects may be seismogenic and how great the hazard is likely to be. In the past, schemes have been proposed to address the question whether earthquakes are natural or induced. For example, Davis and Frohlich [1993] list seven questions to profile a seismic sequence and judge whether it was induced or not (Table 7). In the light of the large number of case histories now available, some these parameters can be re-examined:

1. *Whether the region had a previous history of seismicity*. Induced earthquakes have now been postulated to occur in both historically seismic and aseismic areas. Evidence from research in boreholes suggests that faults everywhere are close to failure, regardless of the known history of seismicity.
2. *Close temporal association with the induction activity*. Reported delays in the onset of postulated inducted seismicity vary from essentially zero to several decades.
3. *In the case of injection-related earthquakes, proximity of a few kilometers*. Distances of up to 25 km have now been reported (Figure 104; Section 4.1.2).
4. *Known geological structures that can channel flow*. Many earthquakes postulated to be induced have been attributed to previously unknown faults.
5. *Substantial stress changes*. Stress changes as small as a few kPa have been postulated to induce earthquakes (Section 2.1.3).

Simple criteria for deciding whether an earthquake is induced or not are elusive. There is extreme diversity in the circumstances of cases. Postulated induction activities may take place over time periods from a few minutes to decades. The volumes of material added or removed vary over many orders of magnitude and the maximum magnitude of events postulated to be induced vary from $M < 0$ to $M \sim 8$.

Several unusual characteristics are commonly reported for earthquakes suspected of having been induced. These include:

1. Unusually shallow nucleation depths (*e.g.*, the 2011 $M_W$ 5.1 Lorca, Spain, earthquake, Section 3.1);

2. Occurrence on previously unknown faults ("blind faults"; *e.g.*, in the Cogdell oilfield, Texas, Section 4.2.2);
3. Release of stress in the same sense as the regional on suitably orientated structures (*e.g.*, in Oklahoma, Section 4.1.2);
4. The largest earthquake in a sequence occurring after the induction activity has ceased, suggesting that fluid diffusion is important (*e.g.*, the 1962-1968 Denver earthquakes, Section 4.1.1);
5. Faults in the basement beneath water and hydrocarbon reservoirs being reactivated, sometimes transecting the sedimentary formations above (*e.g.*, the Coalinga, California, earthquake; Section 3.3.2).

These observations raise a number of questions. For example, if induced seismicity commonly occurs on previously unknown faults, could hazard be reduced by extensive subsurface mapping prior to operations? Since the crust is thought to be pervasively faulted and near to failure essentially everywhere, it is not clear this would be the case–perhaps everywhere should be considered potentially seismogenic. Also, if large earthquakes occur after operations have stopped, for how long should seismic hazard mitigation measures be continued after the end of a project?

More reliable, but less universally applicable ways of discriminating include:

1. Simple spatial and temporal associations, *e.g.*, earthquakes beginning to occur as soon as injection starts and close to the injection point;
2. Earthquakes occurring in previously aseismic regions;
3. Visual observation, *e.g.*, gallery collapses in mines or ground rupture when a nuclear test is conducted;
4. Earthquake focal mechanisms, *e.g.*, discriminating between natural, shear-faulting earthquakes and volumetric mining collapses, as was done by McGarr [1992a; b] for well-recorded earthquakes in South African gold mines and Dreger *et al.* [2008] for a mining collapse in Utah.

Work is currently ongoing to develop additional ways of discriminating induced from natural earthquakes. These include using statistical features of background earthquakes and clustered

sub-populations. For example, Zaliapin and Ben-Zion [2016] have suggested several statistical features that may distinguish induced seismicity from natural tectonic activity including a higher rate of background events and more rapid aftershock decay.

### *7.6 Why are earthquakes induced by some industrial projects and not others?*

In addition to needing an explanation for why earthquakes occur at particular projects, any theory for induced earthquakes must also explain why they do not occur at most projects. This endeavor is hampered by under-reporting (Section 7.1; Table 3). A necessary pre-requisite to explaining induced seismicity as a whole or in different categories is to know its true extent.

For industrial activity as a whole, reports of induced earthquakes are extraordinarily rare (Table 3). Induced nuisance earthquakes are even rarer. Only ~2% of mines, water reservoirs, and CCS projects are reported to be seismogenic. All other categories of project for which we found data were < 2% seismogenic.

Individual cases are diverse and site-specific and the lack of similarities is perhaps a stronger feature than common factors. With the exception of large geothermal projects and hydrofracturing (where almost all are probably seismogenic but only 0.001% are reported to be so) it is seemingly unpredictable which projects will report induced earthquakes. Many if not most induced earthquakes, except at hydrofracturing projects, were unexpected. On the other hand, a research experiment that specifically aimed to induce seismicity, by injecting water into an active fault zone, failed to do so (Section 4.1.8) [Prioul *et al.*, 2000].

A majority of induced earthquakes occur in intraplate areas (Figure 109). This is not surprising in view of the fact that rocks are close to failure everywhere so the potential for inducing earthquakes in intraplate and plate-boundary regions may be similar (Section 1.1). This, coupled with many earthquake sequences being unexpected and in areas previously aseismic, means that populations may be unprepared. To add to this, pre-industrial seismic risk assessments may be difficult if there is no history of seismicity or seismic monitoring. Wilson *et al.* [2015] recently tried to rectify this problem for the UK in advance of possible expansion of the shale-gas industry by estimating a baseline for UK seismicity.

For most non-research purposes the parameter of importance is not whether seismicity is induced

but whether nuisance seismicity is induced (Section 1.2). $M_{MAX}$ is thus critical. Section 6 describes an initial examination of *HiQuake* for correlations. The currently observed upper limit to $M_{MAX}$ correlates with water reservoir volume and mass per unit area, volume added or removed at the surface, volume extracted or added to the subsurface, injection pressure (negative correlation), rate and volume, the yield of nuclear tests and scale of project. Most of these are basically measures of project size. Factors such as reservoir pressure change and injection/extraction rate do not correlate with the observed $M_{MAX}$ ceiling.

Suggestions for what operational parameters might be adjusted to mitigate induced seismicity include injecting into formations that are sealed from the basement, and avoiding known faults. There has, however, yet to be a demonstration of an approach that works in general for projects of a particular type. It is also not clear how we would we recognize success since there can be no evidence for the earthquake that did not occur. More complete reporting would be beneficial.

### *7.7 Future trends*

#### 7.7.1 Earthquake prediction

There is presently no reliable method to predict earthquakes. Current approaches to reducing hazard comprise long-term forecasting based on the history of past earthquakes including instrumental data, historical information, and paleoseismology using methods such as trenching [e.g., Obermeier, 1996]. This approach assumes that patterns of seismicity persist in local areas. It cannot make predictions, even in plate boundary zones [Lindh, 2005], and may work even more poorly in intraplate areas (Section 1.1) [Brooks *et al.*, 2017; Stein *et al.*, 2015]. In regions with little history of seismicity it may not be possible to implement.

Nicol *et al.* [2011] reviewed this issue from the point of view of CCS. Focus tends to be on reservoir-scale pressure increases and the effect of crustal loading on local faults is not routinely considered. Modeling crustal loading or unloading, along with the likely effects on groundwater, might be fruitful avenues of approach. Another useful approach could be to study jointly surface deformation and seismicity. The technology to measure surface deformation is well developed. Both satellite and ground based methods are available but rarely have integrated studies with ground truthing been reported. InSAR and GPS were applied to the depleted Alkmaar Gas Field

in the Netherlands [Gee *et al.*, 2016], and Intermittent SBAS satellite data were used to confirm the deformation from earlier GPS work. These results could potentially be integrated with legacy earthquake data.

The two types of data have been jointly interpreted in the case of several projects [e.g., Goertz-Allmann *et al.*, 2014; Keiding *et al.*, 2010]. However, systematic relationships have not been explored for induced earthquakes as a whole.

### 7.7.2 Monitoring recommendations

Good industrial practice first and foremost requires high-quality information. Projects that have the potential to induce earthquakes should be monitored seismically and geodetically. Joint interpretation of these two types of data is more powerful than either in isolation. In addition to the nuisance of seismic deformations (i.e. earthquakes), aseismic deformations can deform the surface and cause nuisance such as infrastructure damage, flooding, and other changes to groundwater circulation.

Geophysical monitoring need not necessarily be elaborate and can be tailored to the circumstances. Unless there is evidence or compelling expectations for earthquakes or surface deformation, minimal instrumentation will suffice. Data should be publically available to all stakeholders.

The current paper contributes a full review of what type of projects have been reported to induce earthquakes in the past. This is currently the best guide identifying what projects will induce earthquakes in future.

### 7.7.3 Earthquake management

The largest reported induced earthquake has increased with time from M 6.3 in 1933 to ~M 8 in 2008 (Figure 118). The number of reported cases has also increased greatly, probably because of the increasing number of large-scale industrial projects. The lower magnitude threshold of reporting is reducing, probably partly because of improved monitoring.

There is a growing need to manage the problem of industrially induced earthquakes and this is

well-illustrated by coal mining in China (Section 3.2.1). The expanding Chinese economy is founded on coal as an energy source but at the same time shallow resources are being rapidly depleted (Figure 119). The future trend is thus to go deeper [Li *et al.*, 2007]. In the two decades from 1980-2000 the average mining depth increased from 288 m to 500 m. Now, over 75% of the coal has been removed from the top 1000 m and the recent increase in mine seismicity there results largely from increases in mining depth and the size of galleries. Super-deep mines (>1200 m in depth), as have induced seismicity in South Africa for decades, are planned in China for the future. Fluid injection for waste disposal, enhanced oil recovery, hydrofracturing and geothermal energy, are also expanding rapidly and have resulted in some of the most significant increases in induced seismicity in recent years [Ellsworth, 2013]. Other industries such as building dams and CCS may expand over the coming years.

Management of the problem is moving forward rapidly as additional stakeholders become involved [e.g., Wang *et al.*, 2016]. For example, the issue of induced earthquakes is now of concern to the US Army Corps of Engineers because of the threat to critical federal infrastructure, *e.g.*, levees and dams. No societal benefit comes without price–there is no such thing as a free lunch. However, public policy, engineering, preparation, and outreach can enable economically and societally beneficial projects to go ahead under appropriate health-and-safety conditions and in contexts that are understood and acceptable to stakeholders.

*Acknowledgments*

This work benefitted from discussions with Julian Bommer, Bruce Julian, Kosuke Heki, Tianhui Ma, Steve Spottiswoode, Michelle Grobbelaar and Deborah Weiser. Ang Li assisted with locating Chinese cases. The project was funded by the Nederlandse Aardolie Maatschappij BV (NAM), Schepersmaat 2, 9405 TA Assen, The Netherlands. This paper is based on a report submitted to Jan van Elk and Dirk Doornhof (NAM).

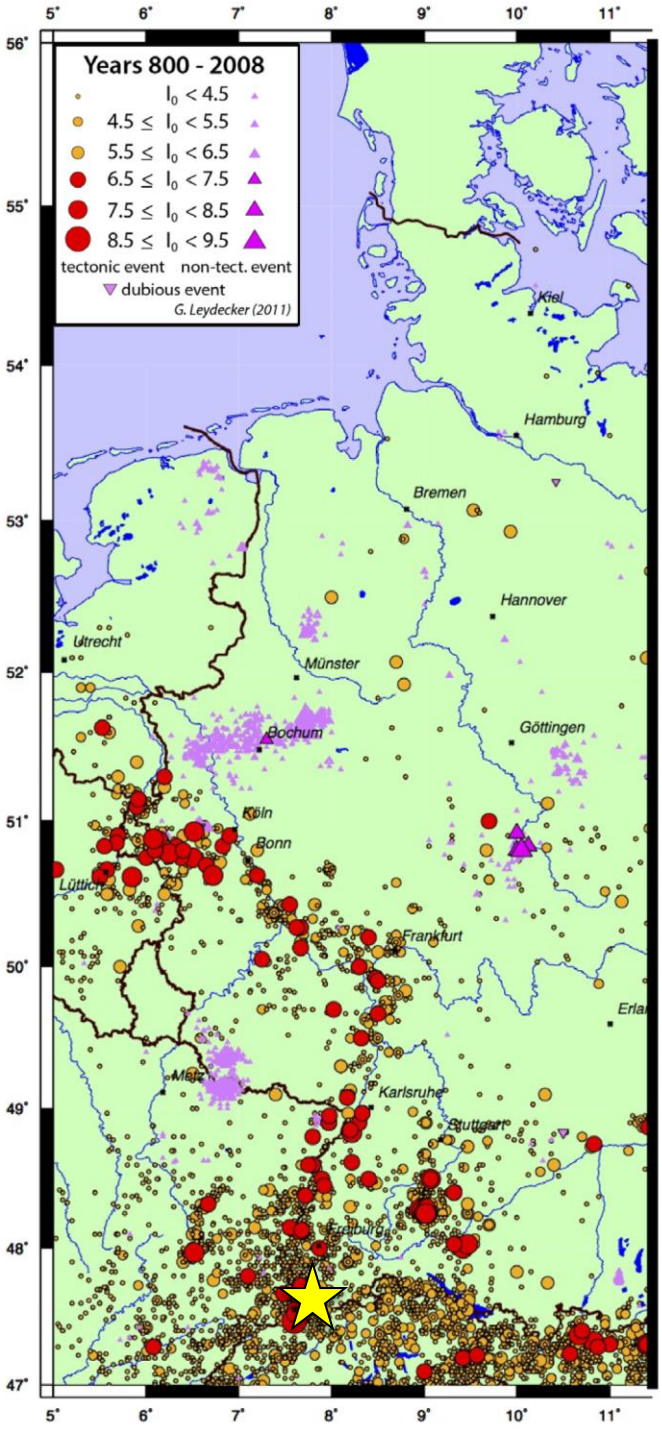


Figure 1: Map of central Europe showing historical earthquakes with different epicentral intensities from 800 AD [from Stein *et al.*, 2015]. Yellow star: city of Basel, Switzerland.

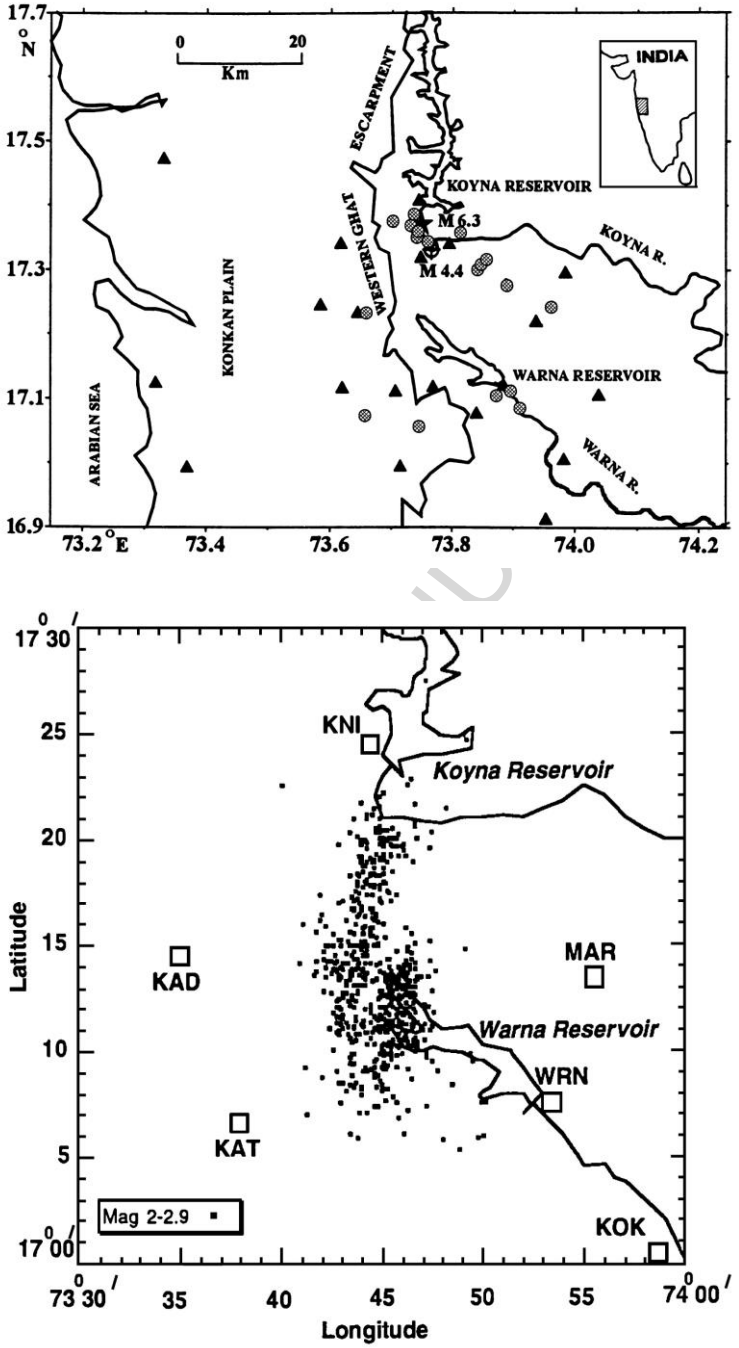


Figure 2: Top: Map of Koyna area, India, showing the dam, reservoir, seismic stations and boreholes. Bottom: Same area showing earthquakes with M 2-2.9 for the period October 1993 to December 1994 [from Gupta, 2002].

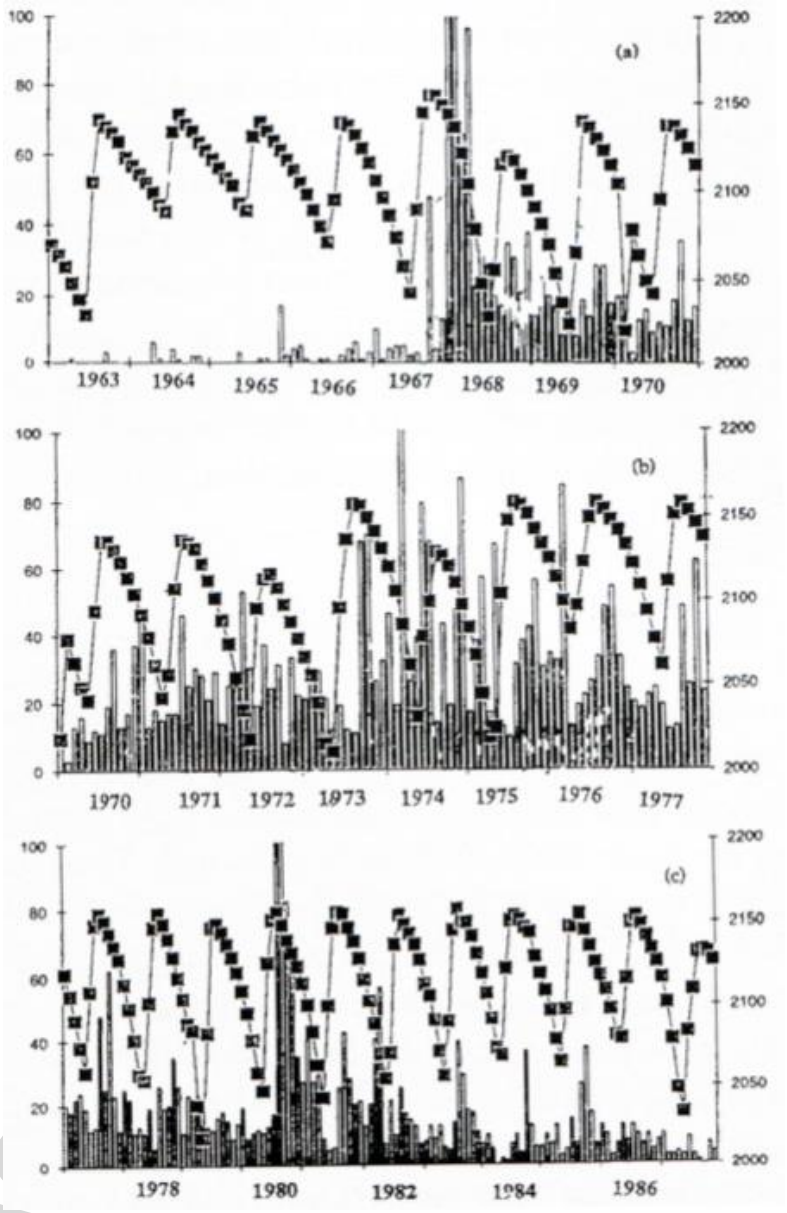


Figure 3: Number of earthquakes in the region of the Koyna dam, India, for the period 1963-1986 (left axis), along with reservoir water level (right axis, in m) [from Talwani, 1995].

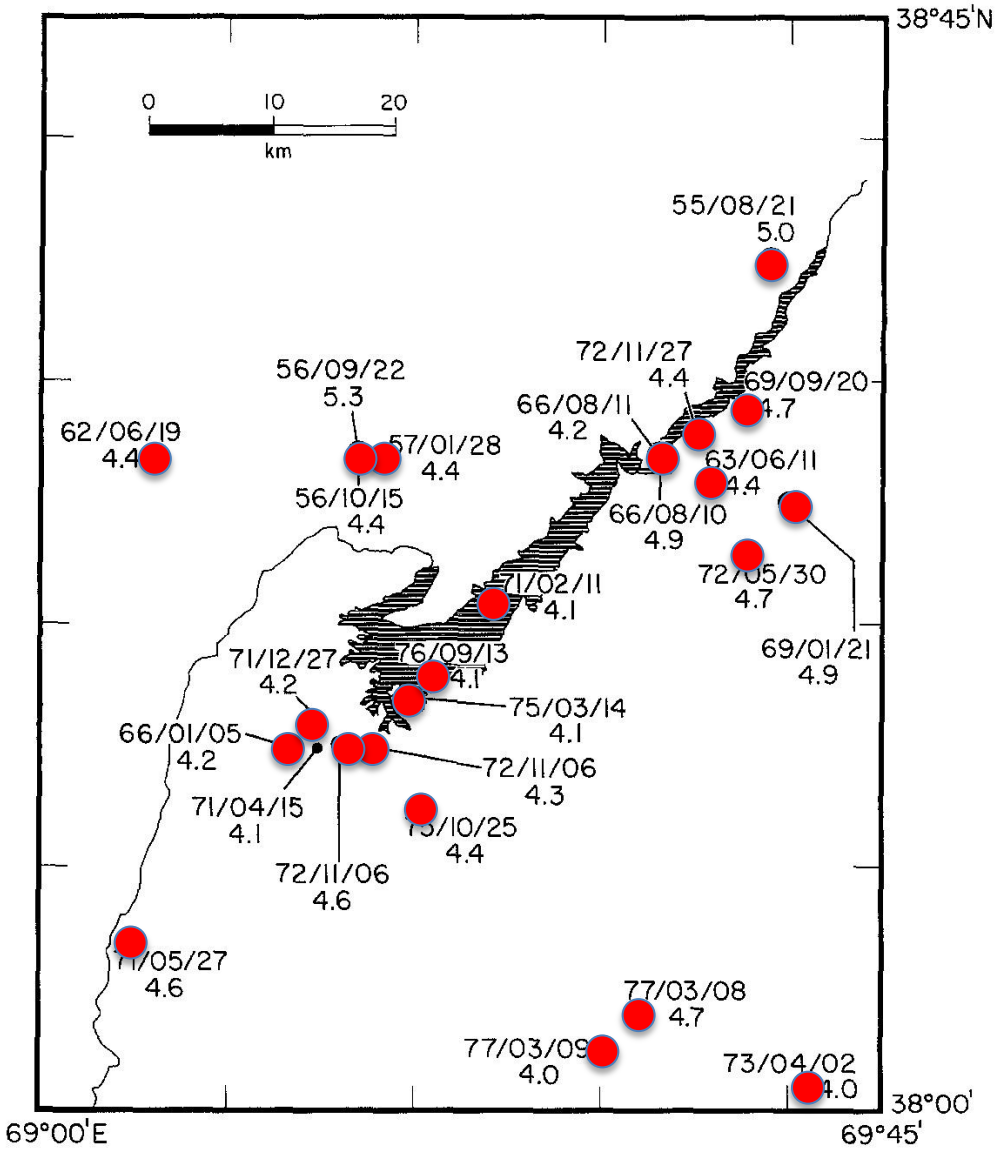


Figure 4: Map of Nurek dam and reservoir, Tadjikistan, showing earthquakes with M $\geq$ 4.0 for 1955-1979 [from Simpson & Negmatullaev, 1981].

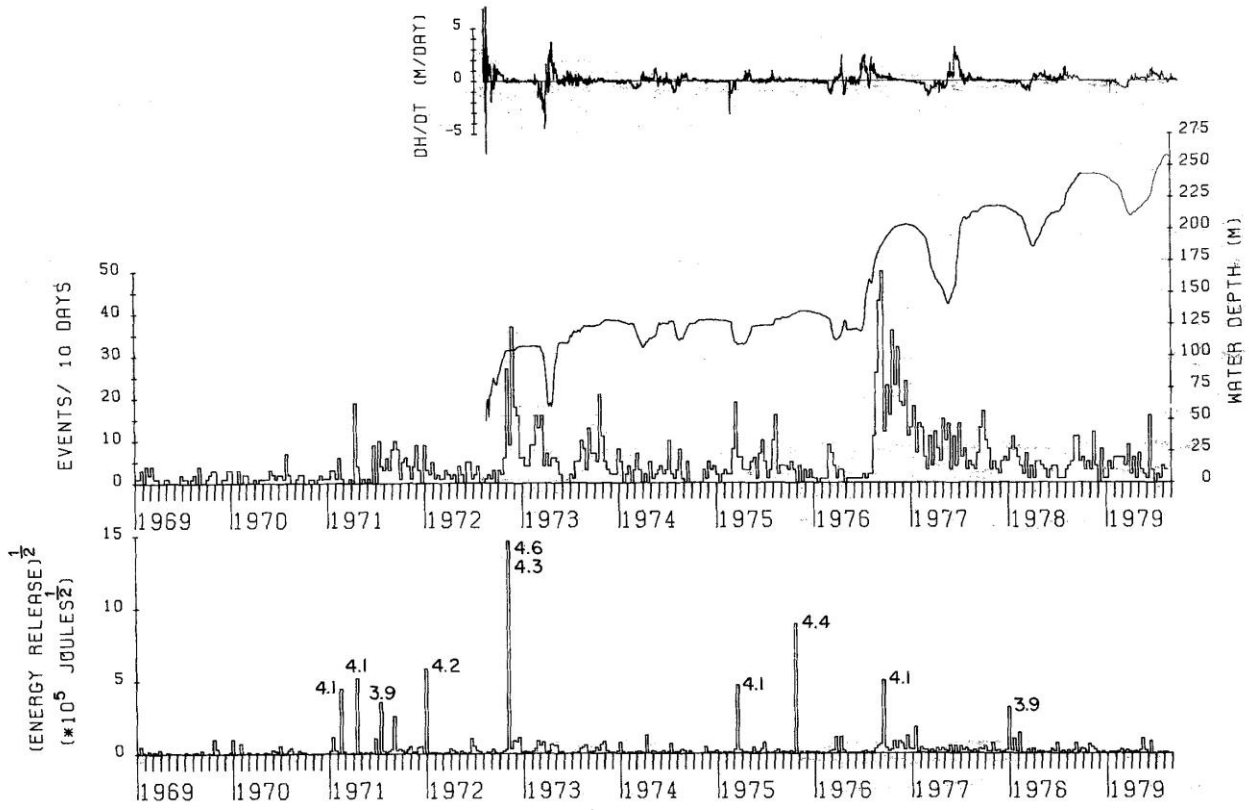


Figure 5: Water depth and seismicity for 1969-1979 in the vicinity of Nurek dam, Tadjikistan [from Simpson & Negmatullaev, 1981].

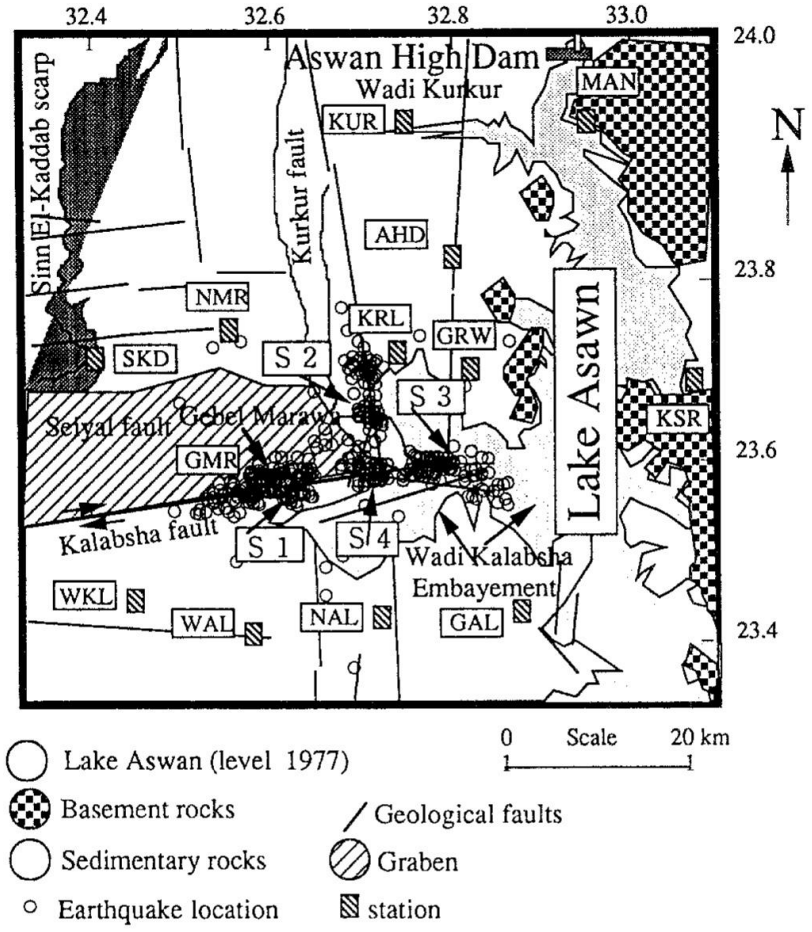


Figure 6: Map showing Lake Aswan, Egypt, and epicenters of induced earthquakes [from Awad & Mizoue, 1995].

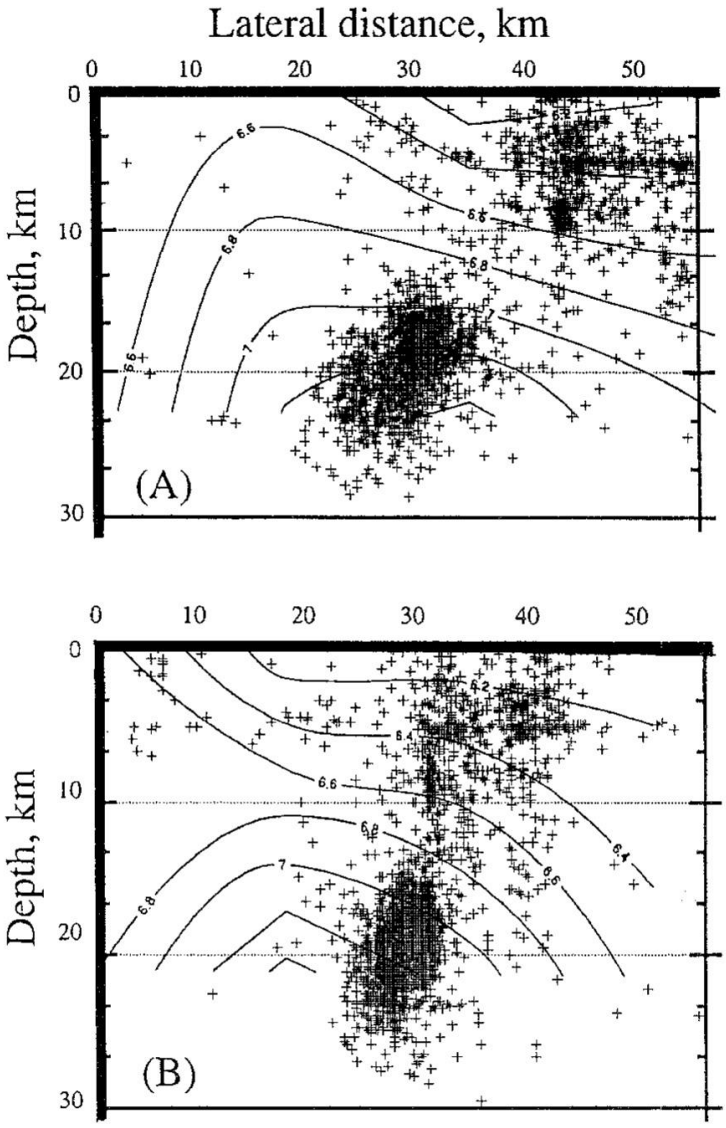


Figure 7: Cross sections showing hypocentral distribution of earthquakes postulated to have been induced by impoundment of Lake Aswan [from Awad & Mizoue, 1995].

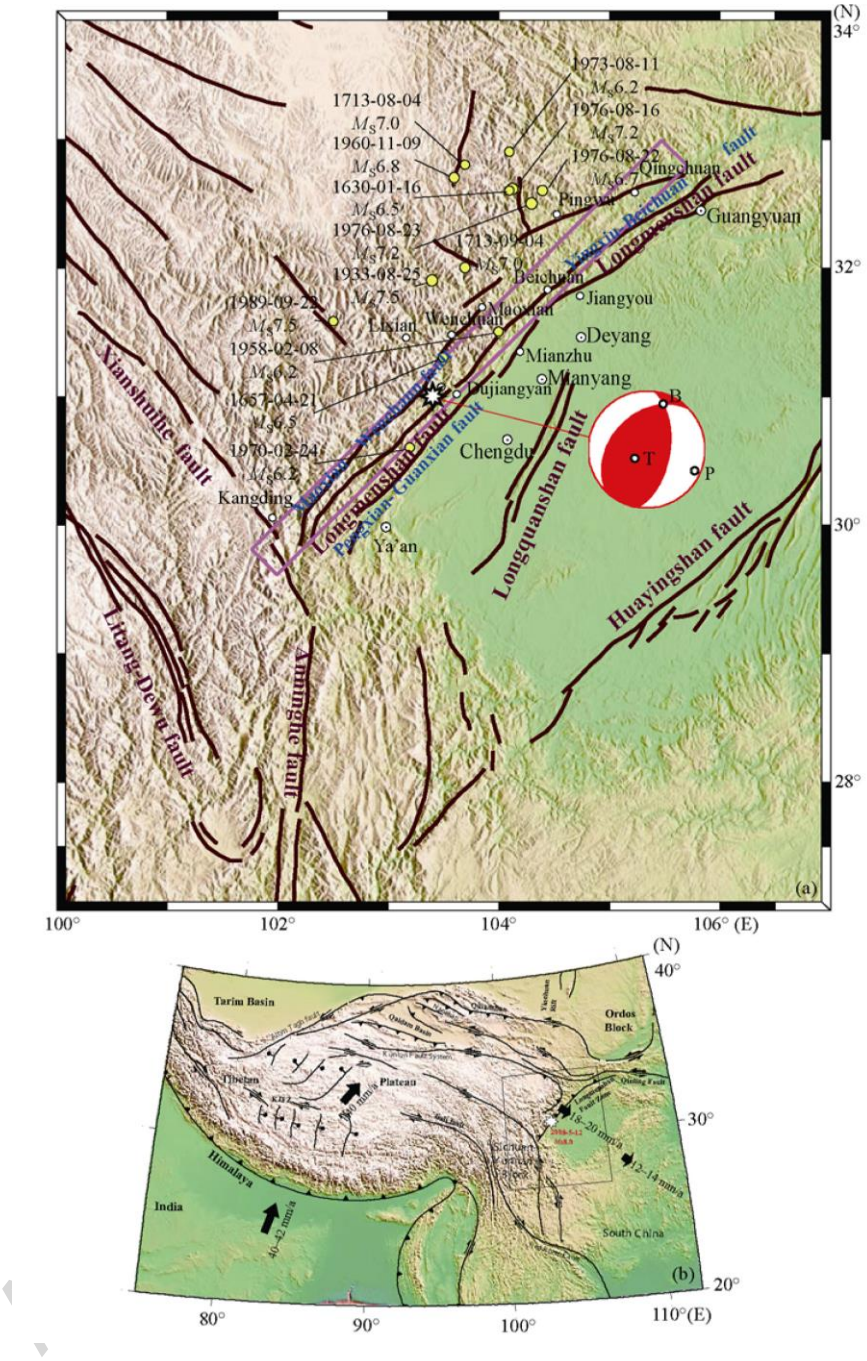


Figure 8: Top: Star: location of the 2008 $M_W$ ~8 Wenchuan, China, earthquake; lines: main faults of the Longmenshan fault zone; yellow circles: historical earthquakes; white circles: main cities; lilac rectangle: projection of the fault plane that slipped; beach ball: lower hemisphere projection of the focal mechanism of the mainshock. Bottom: regional tectonic setting [from Zhang *et al.*, 2008].

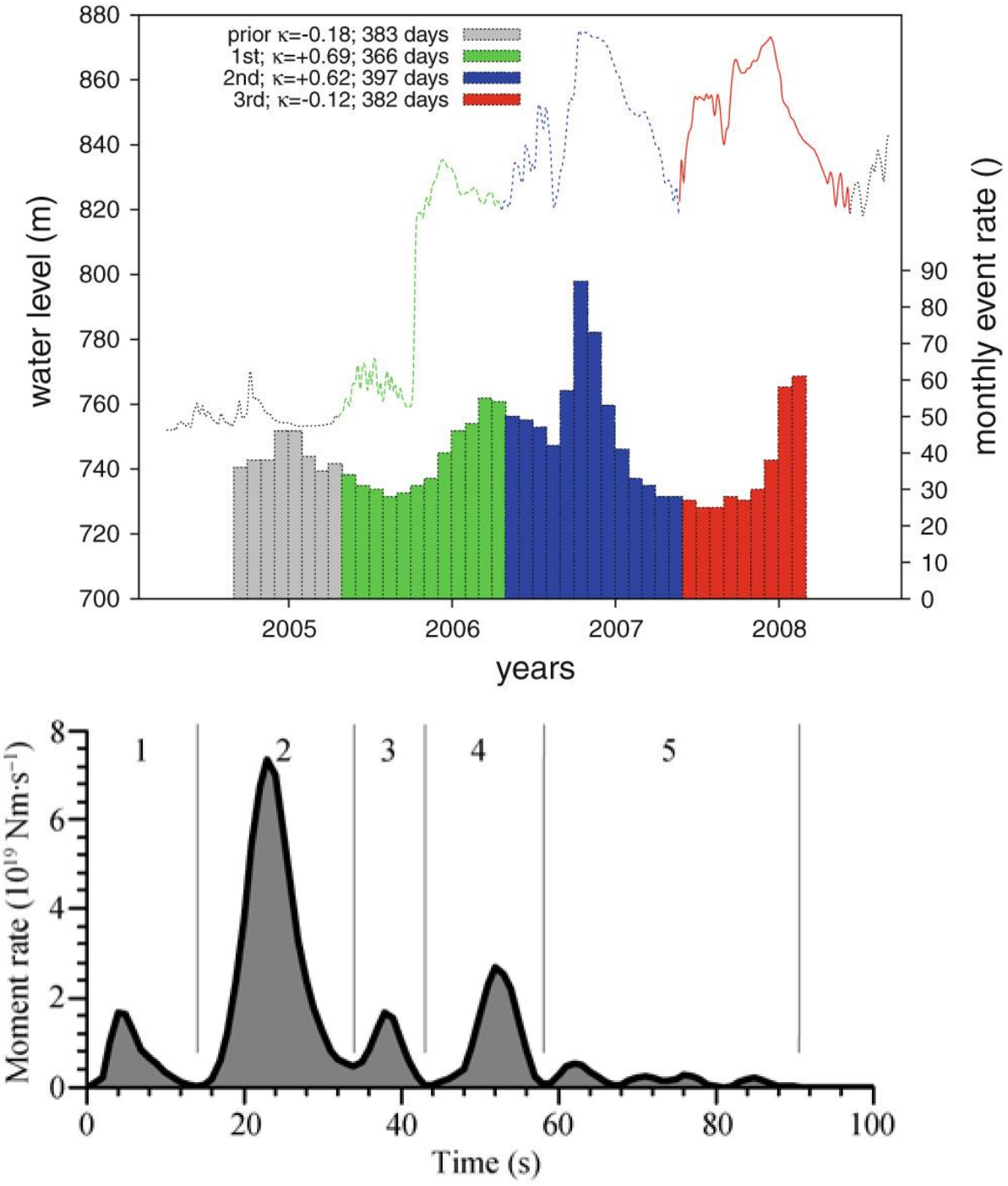


Figure 9: Top: Water level change in the Zipingpu, China, water reservoir and earthquake event rate in the vicinity prior to the May 2008 $M_W$ ~8 Wenchuan earthquake [from Klose, 2012]. Bottom: Source time function of the 2008 great Wenchuan, China earthquake [from Zhang *et al.*, 2008].

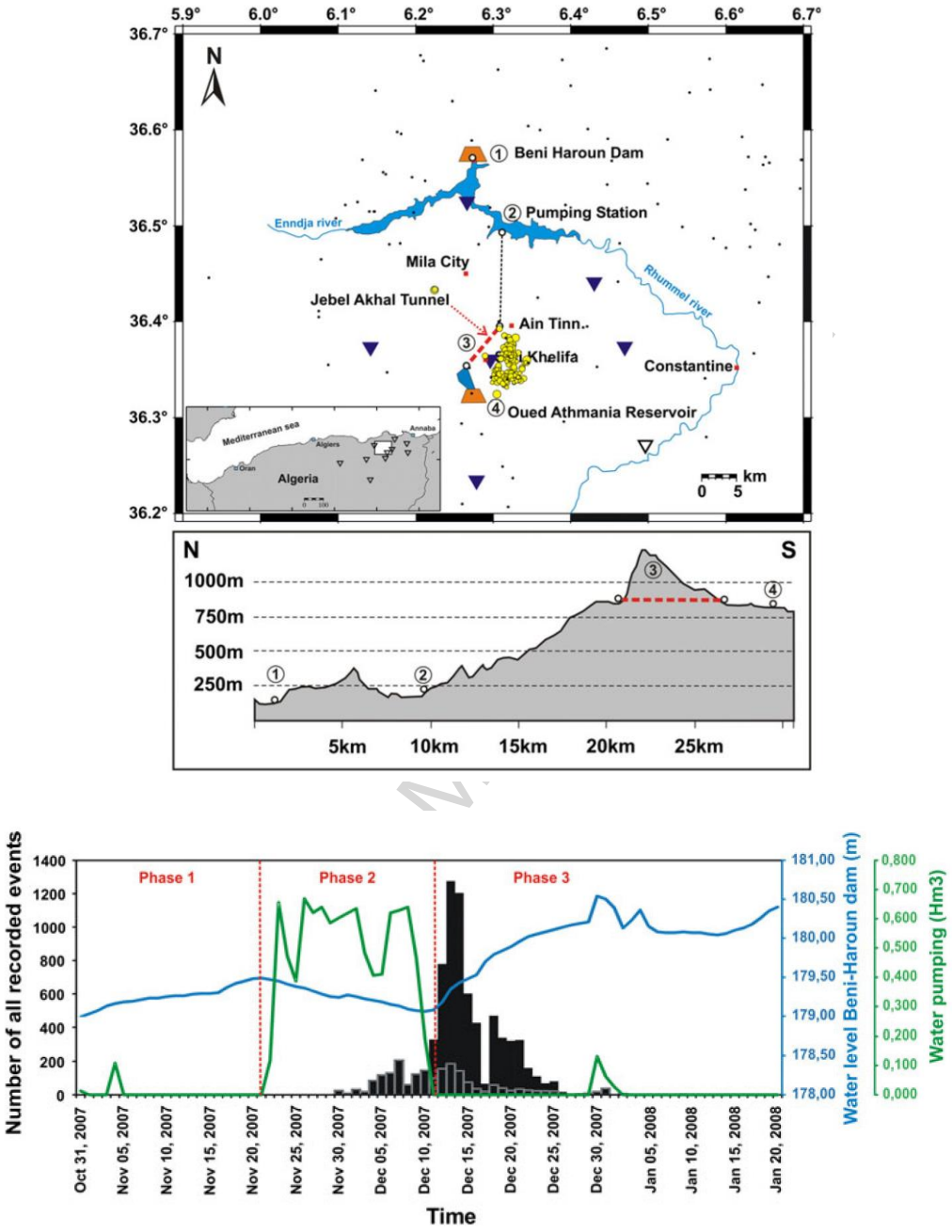


Figure 10: Map of hydraulic system in Mila region, Algeria. Top: Water transport system (dashed lines) from Beni Haroun dam to Oued Athmania reservoir. Red dashed line: tunnel through Mt. Jebel Akhal; black dots: seismicity for 2006–2007; triangles: seismic stations; yellow dots: epicenters of earthquakes. Middle: topographic profile of hydraulic system. Bottom: Number of earthquakes recorded, water level in Beni Haroun dam, and volumes of water pumped vs. time around the seismogenic period. Black histogram: events recorded; gray histogram: events recorded by the network, discarding a temporary station deployed in the epicentral area for 17 days during the swarm. This exemplified the effect of varying the number of seismic stations [from Semmane *et al.*, 2012].

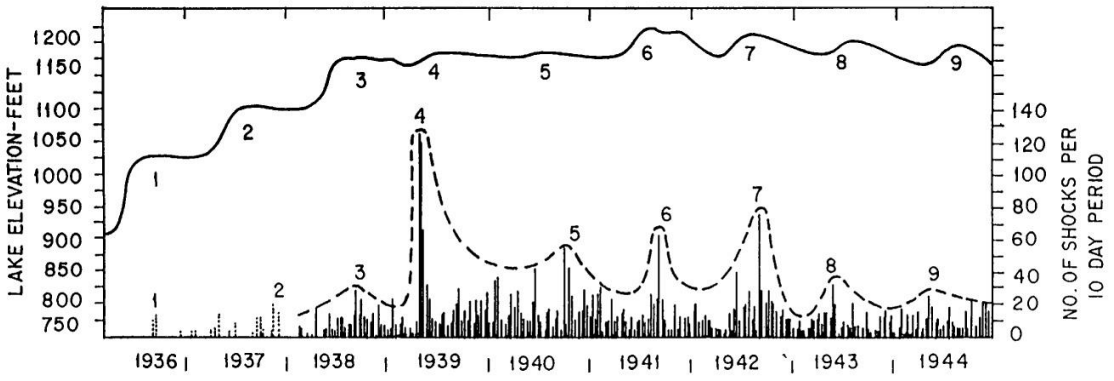


Figure 11: Earthquakes and water level at Lake Mead, Arizona, which is impounded behind Hoover dam [from Gupta, 2002].

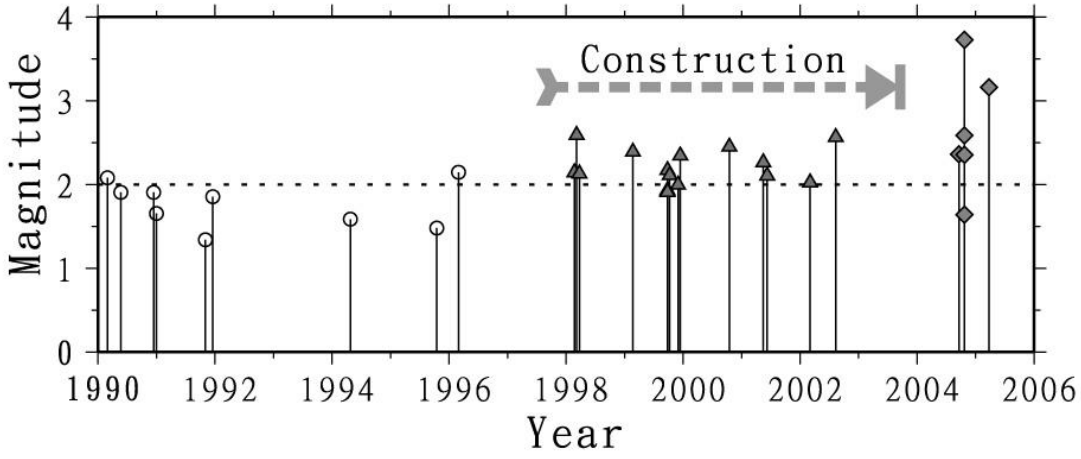


Figure 12: Top: The Taipei 101 building[11]. Bottom: Earthquake history for a 16-year period spanning the construction of the Taipei 101 building, Taiwan [from Lin, 2005].

[11] http://inhabitat.com/taipei-101-worlds-tallest-green-building/green-taipei-101-1

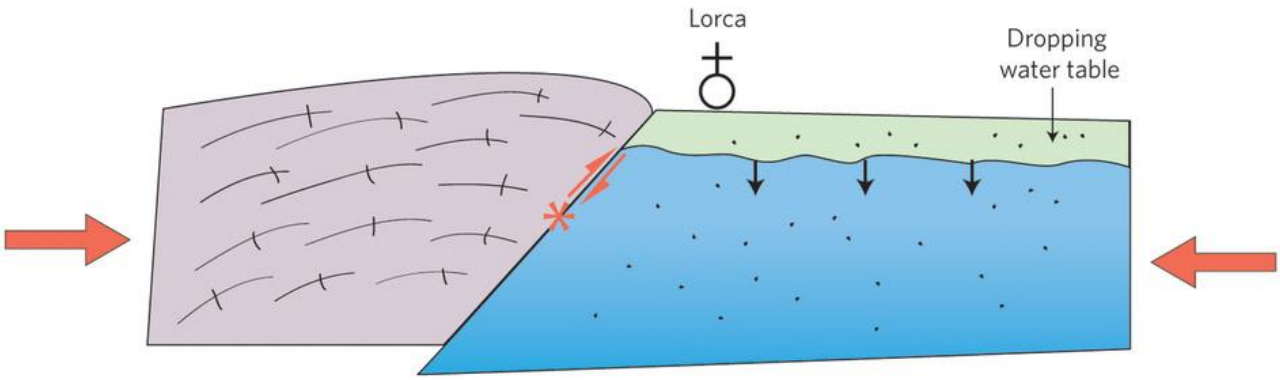


Figure 13: Schematic figure showing the mechanism proposed by Gonzalez *et al.* [2012] for inducing the 2011 $M_W$ 5.1 Lorca, Spain, earthquake [from Avouac, 2012].

Figure 14: Destruction in the church of Santiago resulting from the 2011 $M_W$ 5.1 Lorca, Spain, earthquake [12].



[12] https://en.wikipedia.org/wiki/2011_Lorca_earthquake

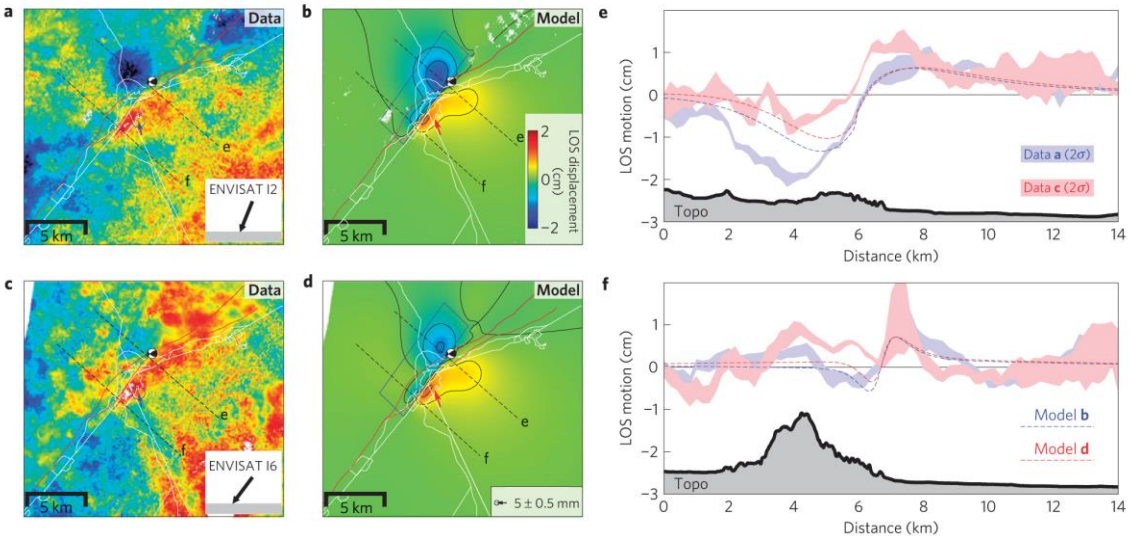


Figure 15: (a–d): ground deformation data and model for the 2011 $M_W$ 5.1 Lorca, Spain, earthquake. (a and c): descending line-of-sight (LOS) displacement map and horizontal GPS vector; (b and d): distributed slip model predictions. Insets in a and c indicate LOS angle, positive values away from the satellite. Blue rectangle: fault surface projection; dashed lines: profile locations; (e and f): observed and simulated data along two profiles, and local topography [from González *et al.*, 2012].

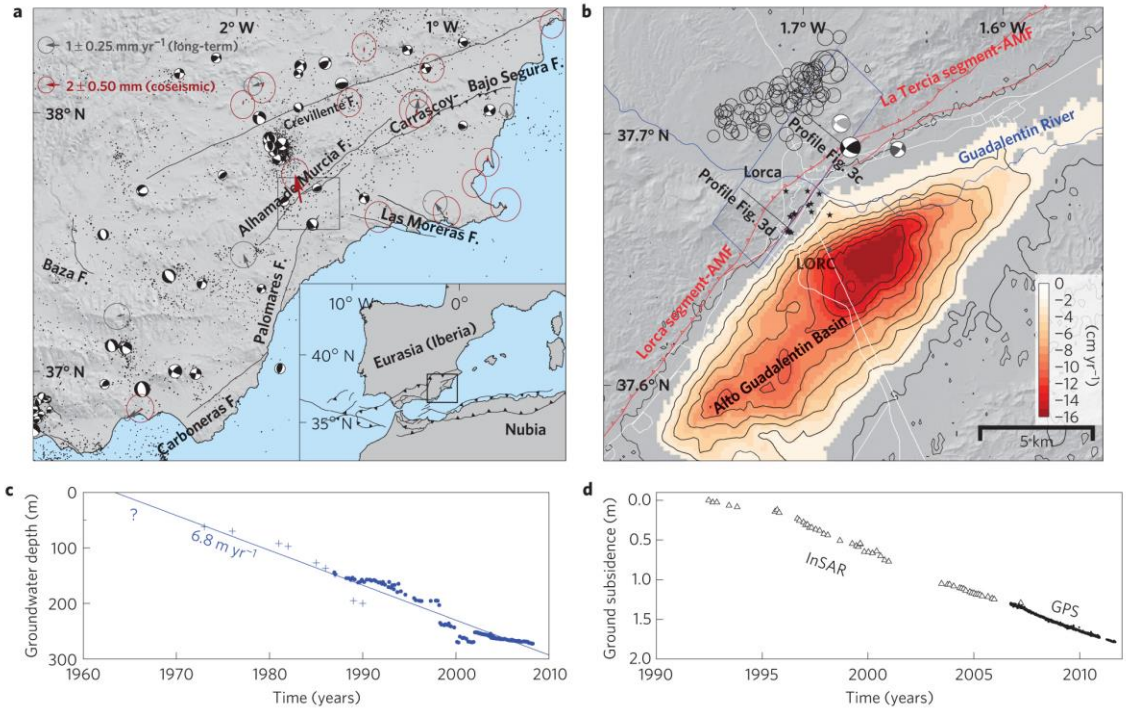


Figure 16: Location and kinematics of the Lorca earthquake. a: southwest Spain seismicity (2000–2010), focal mechanisms (1970–2010), long-term GPS velocity (2006–2011, gray) and coseismic vectors (red). Major mapped faults are labeled. b: Lorca city and Alto Guadalentin Basin. Mainshock focal mechanisms (black), pre-shock (light gray), largest aftershock (dark gray), and relocated seismic sequence. Black stars are damage locations, red lines are faults. Contour lines indicate 2 cm/a InSAR subsidence due to groundwater pumping. Blue rectangle: fault surface projection. AMF, Alhama de Murcia Fault. c, Groundwater depth. d, InSAR (triangles) and line-of-sight (LOS)-projected GPS ground-surface subsidence at station LORC [from González *et al.*, 2012].

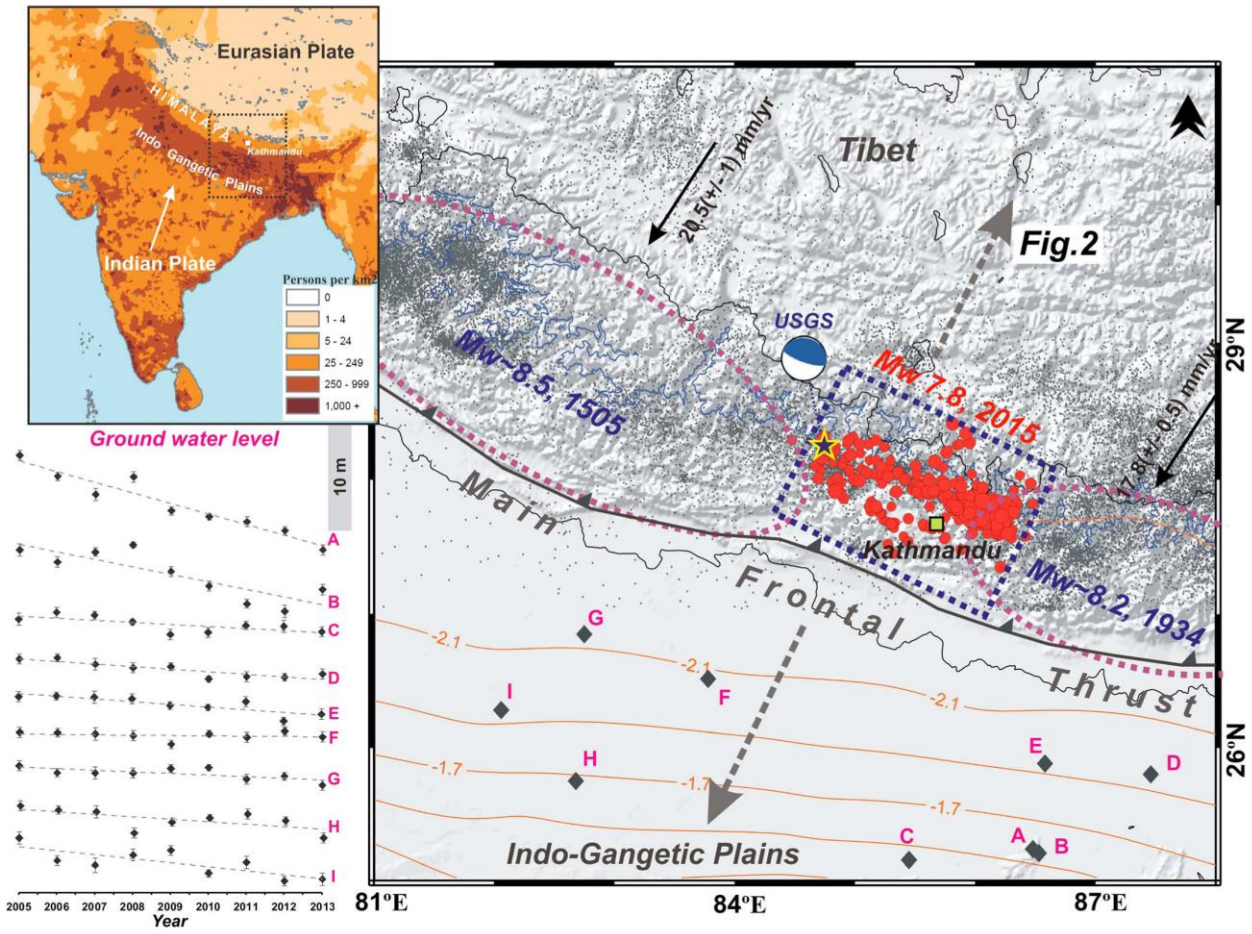


Figure 17: Seismotectonic context of the 2015 $M_W$ 7.8 Gorkha, Nepal earthquake. Black star: epicenter of the mainshock; red circles: aftershocks; black arrows: convergence rate; gray dots: mid-crustal seismicity 1995-2008; blue contour: 3500-m elevation; ellipses: approximate rupture locations of historic events since 1505; orange contours: anthropogenic groundwater loss in cm/a water thickness for the period 2002-2008 (multiply by 5 to get drop in water table); black diamonds: sampling sites; inset at left: site depletion trends; inset top left: population density (people/km$^2$) [from Kundu *et al.*, 2015].

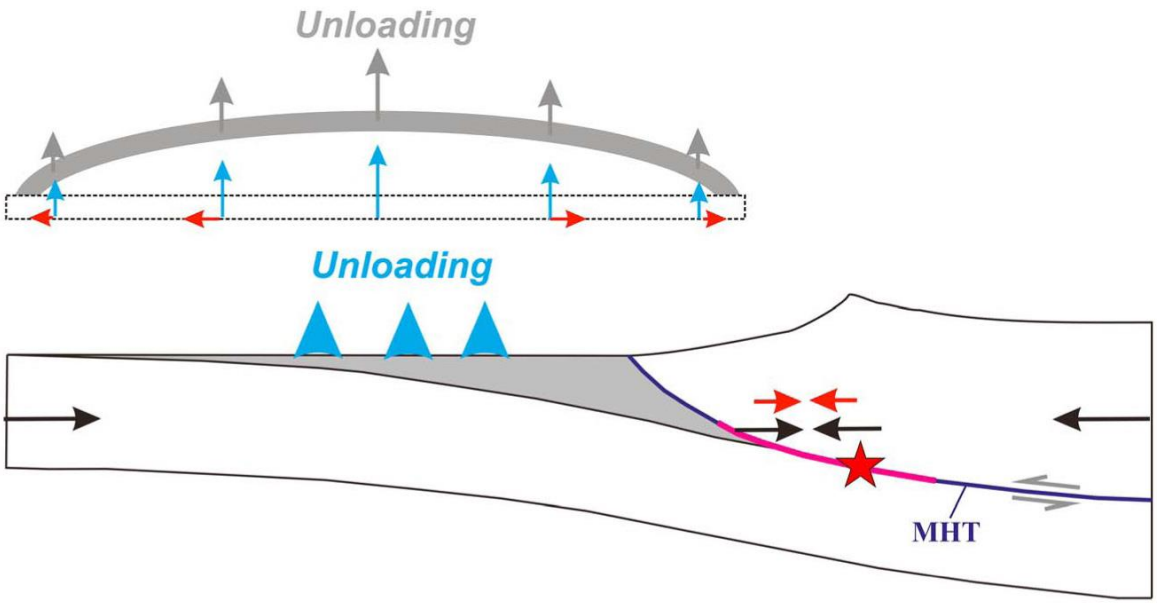


Figure 18: Schematic diagram showing the effect of unloading by anthropogenic groundwater loss on the Main Himalayan Thrust. Dewatering induces a component of horizontal compression (red arrows) that adds to the secular interseismic contraction (black arrows) at seismogenic depths. Red star: the 2015 Gorkha, Nepal earthquake; pink line: the associated rupture [from Kundu *et al.*, 2015, after ].

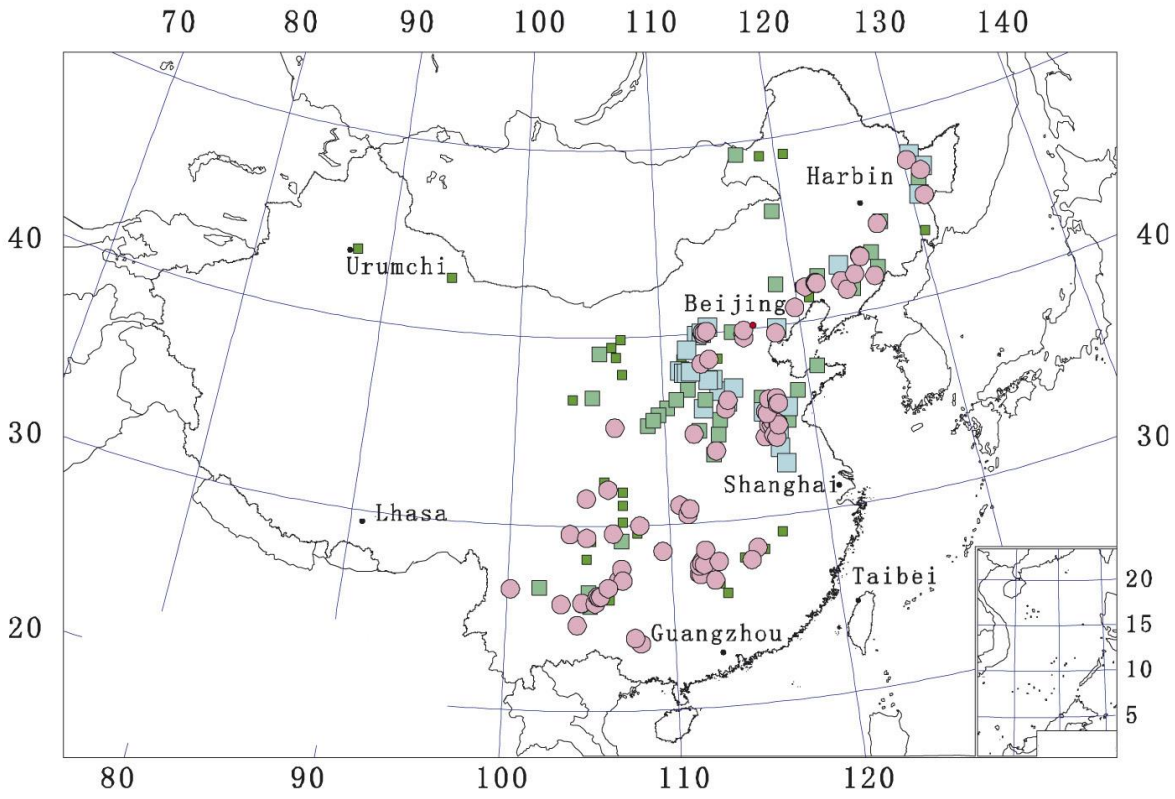


Figure 19: Map of China. Green squares: Small, medium and large state-owned coal mines. Pink dots: Coal mines where mining-induced seismicity occurs [from Li *et al.*, 2007].

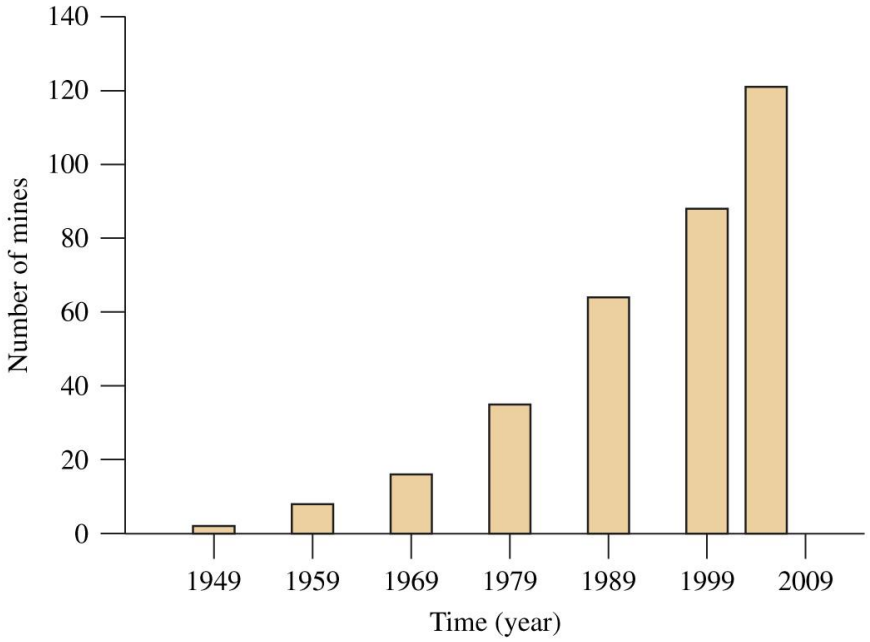


Figure 20: Number of mines in China with rockburst hazard vs. time [from Li *et al.*, 2007].

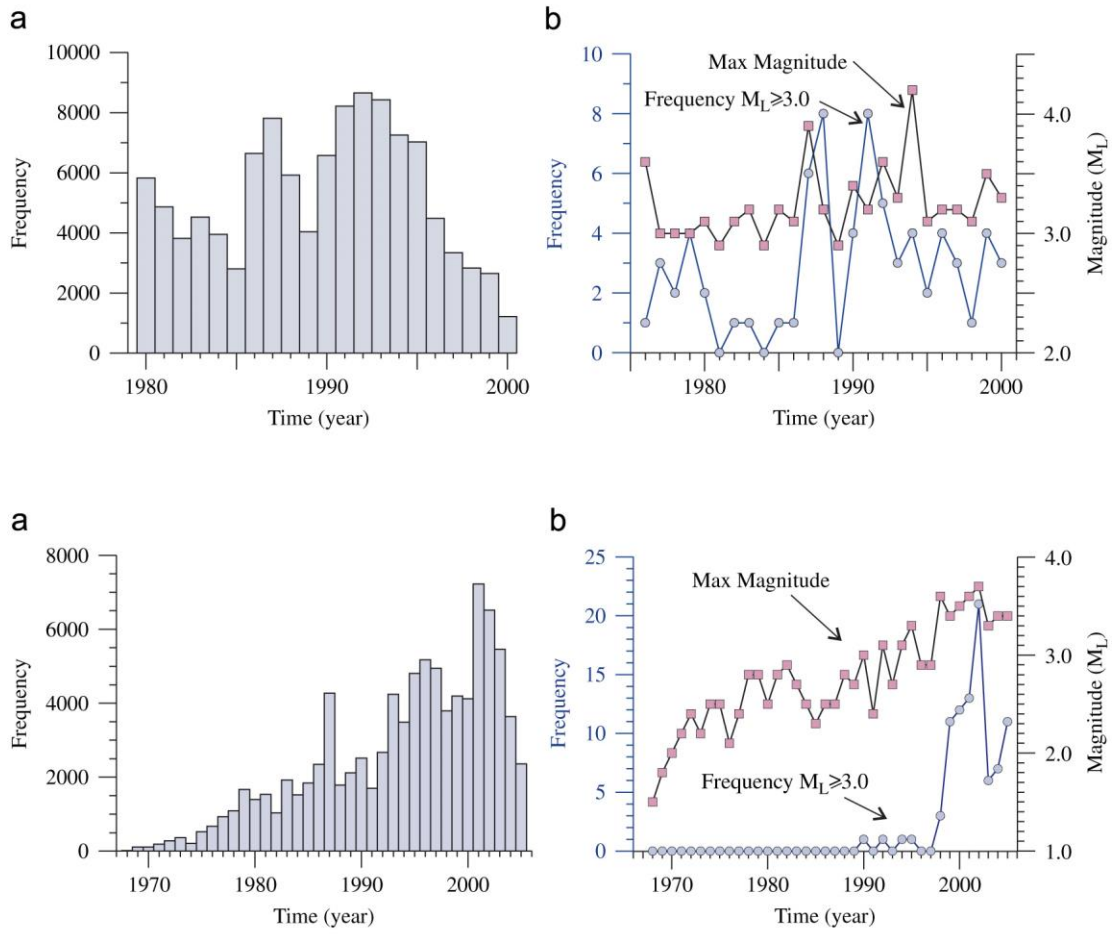


Figure 21: Top panels: Mining-induced earthquakes at Mentougou coal mine, Beijing, (a) events M > 1.0, (b) events M > 3.0 and the maximum event magnitudes. Bottom panels: same as top panels except for the Fushun coal mine field in Liaoning Province [from Li *et al.*, 2007].

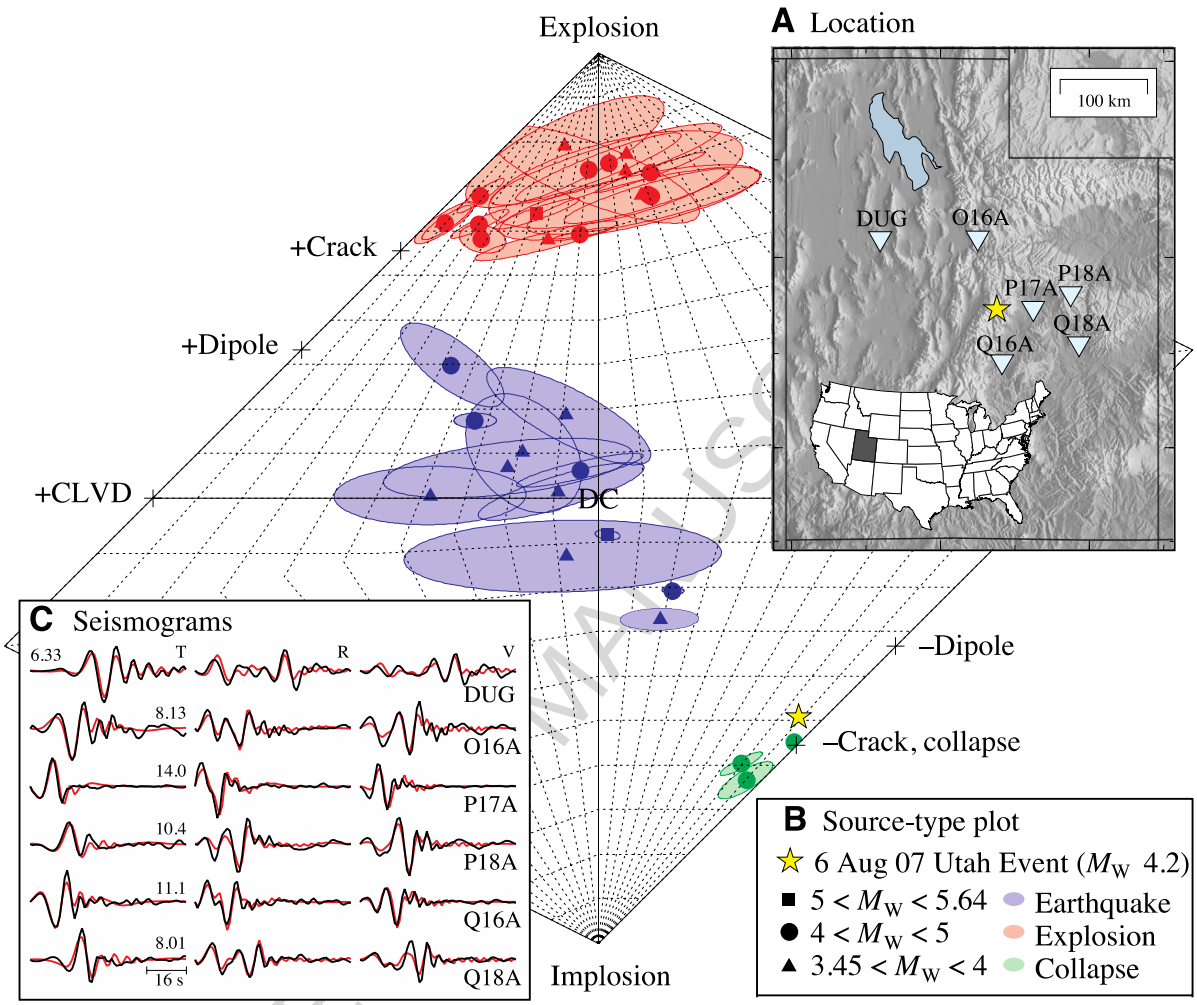


Figure 22: (A) Locations of the 6 August 2007 Crandall mine, Utah, earthquake and six of the closest USArray and Advanced National Seismic System (ANSS) seismic stations. (B) Source-type plot showing separation of populations of earthquakes, explosions, and collapses. Yellow star shows the focal mechanisms solution. (C) Observed seismograms (black) compared to synthetics (red) for the solution, which is similar to a horizontal closing crack (B). The maximum displacement (10-7 m) of each set of tangential (T), radial (R), and vertical (V) observations is given [from Dreger *et al.*, 2008].

Figure 23: Surface imprints of Neolithic flint mining at Grimes Graves, Suffolk, England[13].



[13] www.english-heritage.org.uk

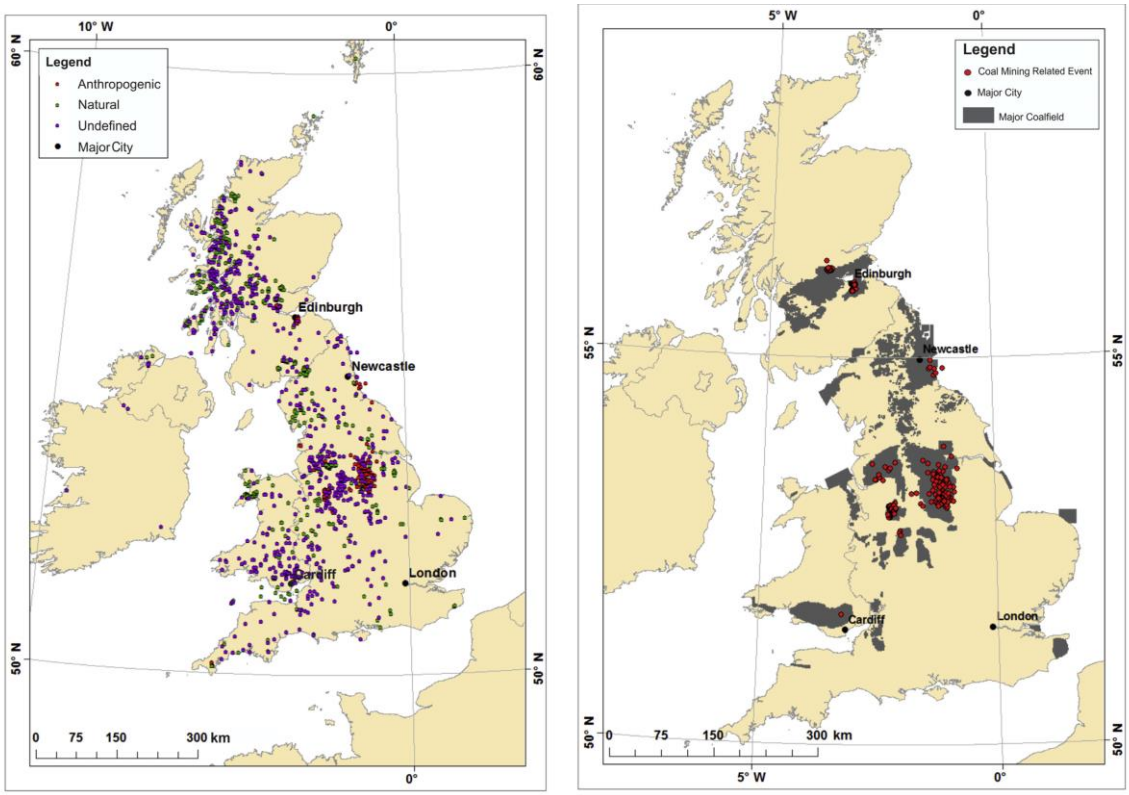


Figure 24: For earthquakes with $M_L \geq 1.5$ for the period 1970-2012, left: map of the UK showing 1769 onshore seismic events categorized as anthropogenic (red), natural (green) and undefined (purple). Right: 369 events postulated to be induced by coal mining. These correlate spatially with major coalfields (dark gray) [from Wilson *et al.*, 2015].

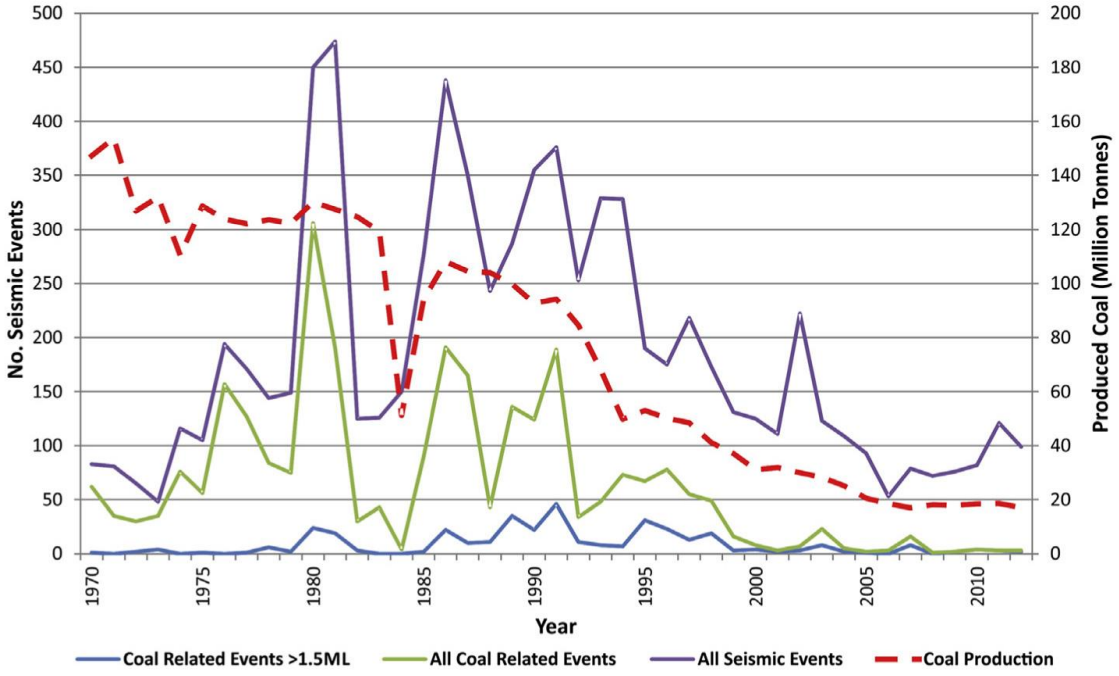


Figure 25: UK coal production (dotted red line) vs. numbers of earthquakes postulated to be induced (blue line: $M_L \geq 1.5$, green line: all located earthquakes in the British Geological Survey database) for the period 1970-2012. The effect of the miners' strike of 1984 can be seen clearly in the drop in production and seismicity [from Wilson *et al.*, 2015].

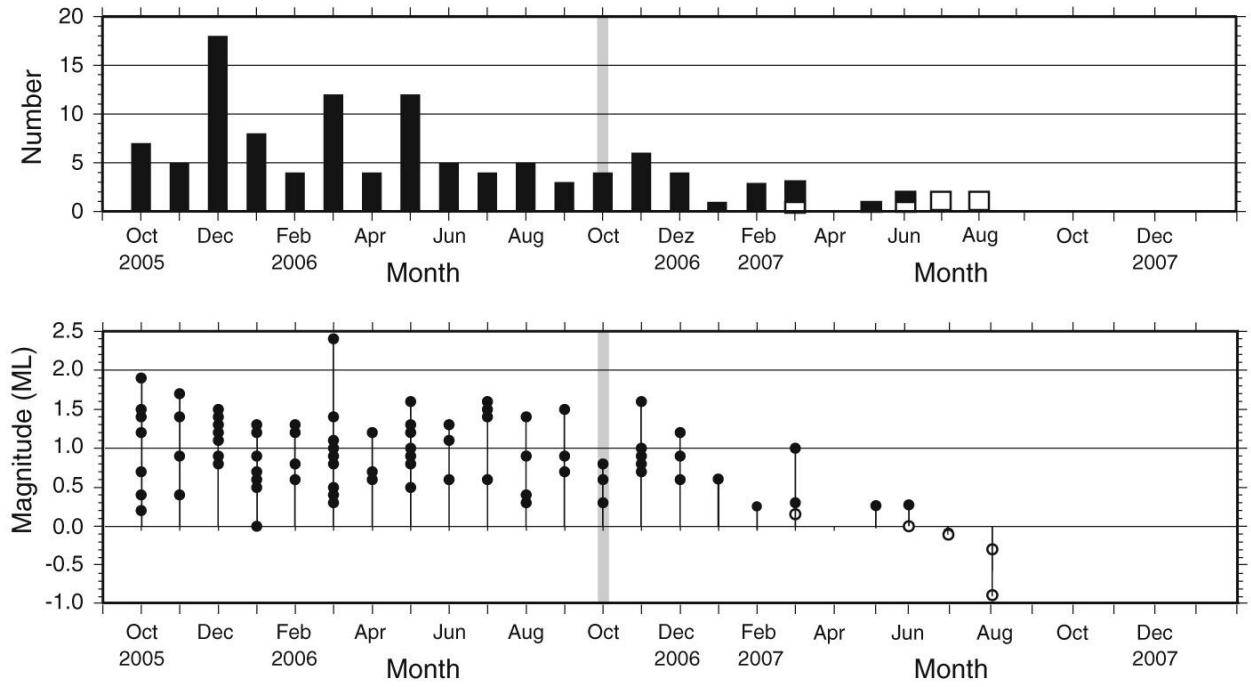


Figure 26: Temporal evolution of the seismicity observed in the vicinity of the multi-function station Faido, Switzerland, October 2005 - December 2007. Top: number of events per month. Bottom: local magnitudes. Open circles: earthquakes for which magnitude could only be computed using data from one station. Gray band marks the end of the excavation work [from Husen *et al.*, 2012].

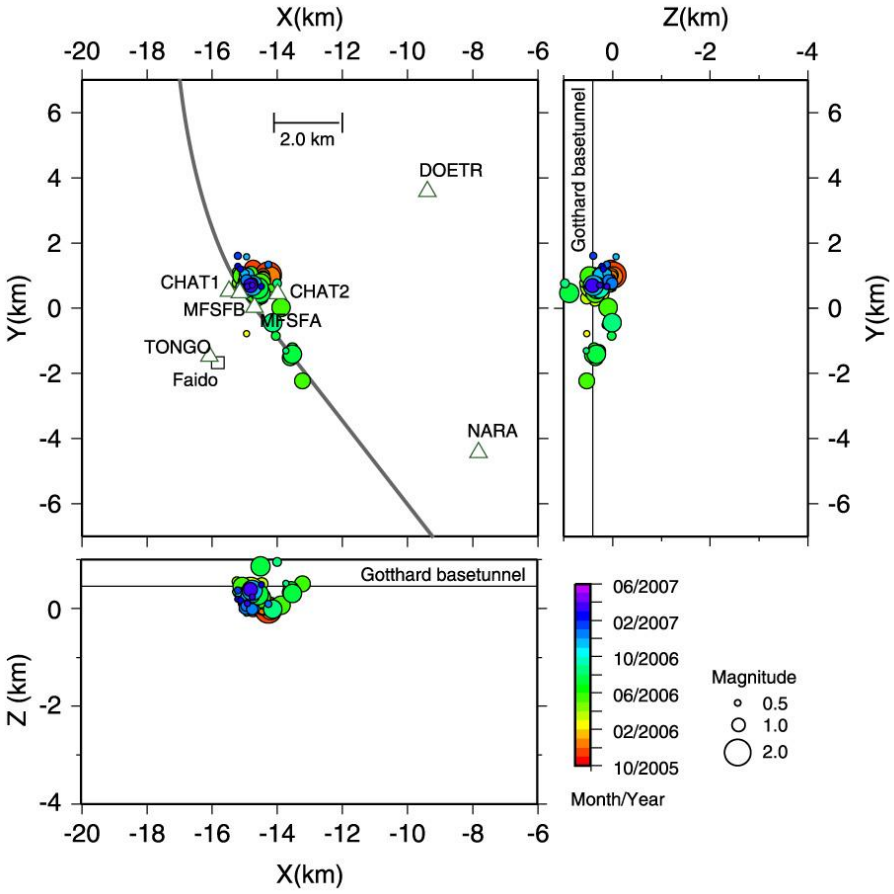


Figure 27: Hypocenter locations of earthquakes in the vicinity of the multi-function station Faido, Switzerland, October 2005 - June 2007 [from Husen *et al.*, 2012].

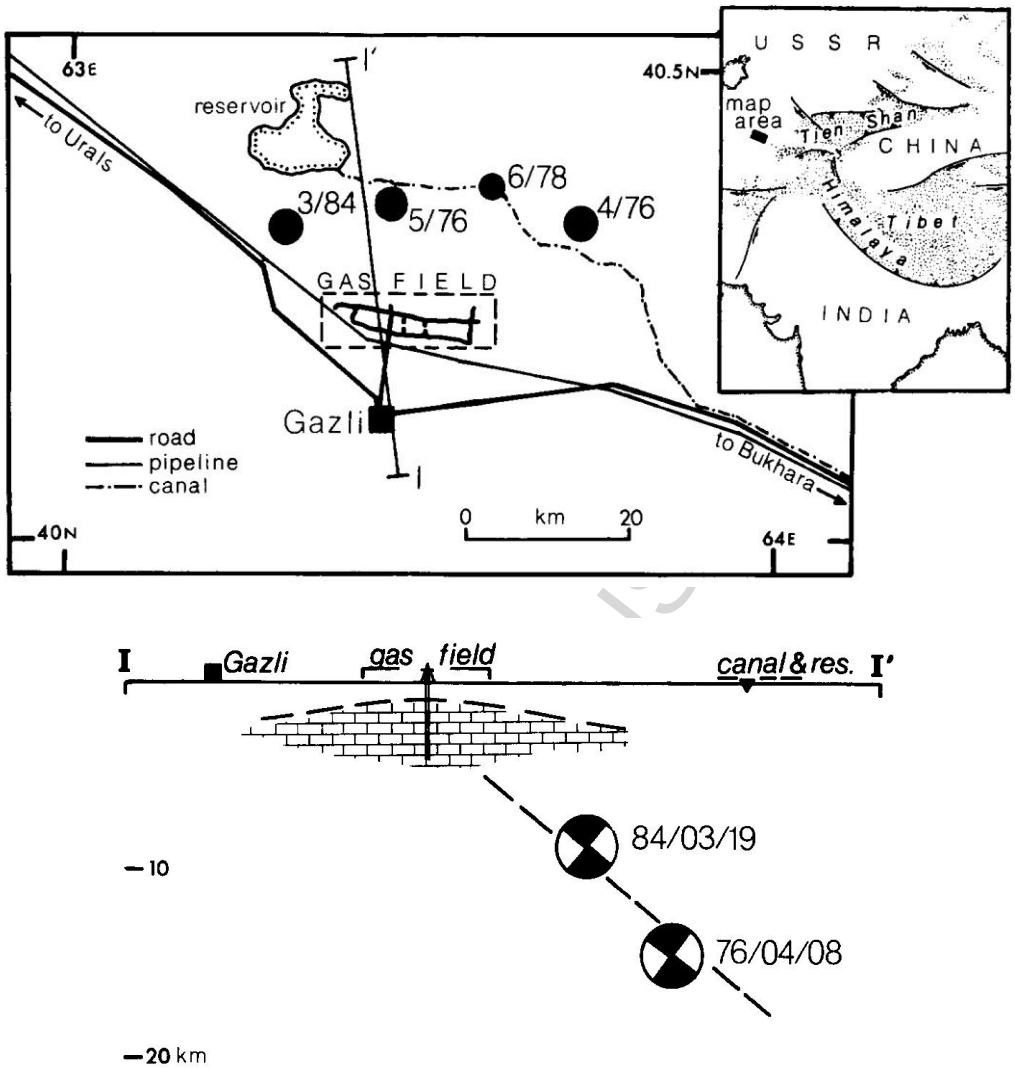


Figure 28: Top: Map of the Gazli, Uzbekistan, area showing epicenters of the three M ~7 earthquakes in 1976 and 1984, and the M 5.7 earthquake in 1978. Bottom: Cross-section with hypocenters projected at their distance from the town of Gazli, with focal mechanisms of the $M_S$ 7.0 events of 8 April 1976 and 19 March 1984. The fault plane (dashed line) is deduced from geodetic data [from Simpson & Leith, 1985].

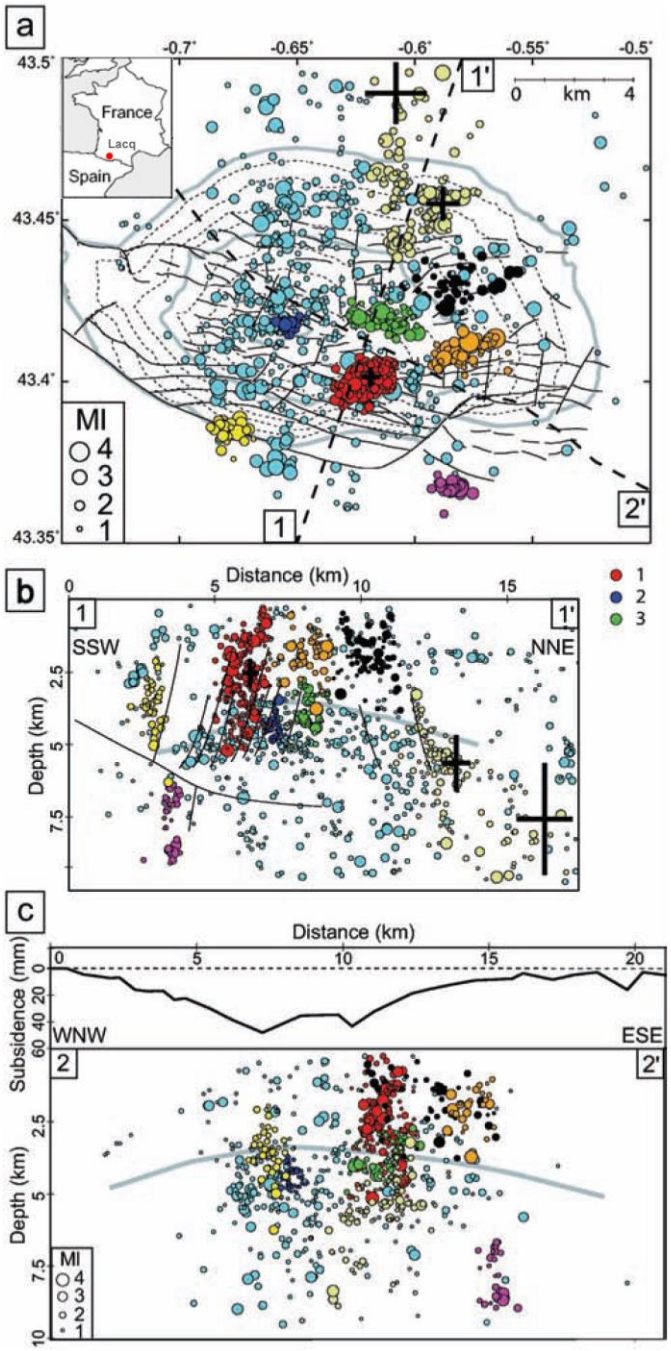


Figure 29: Seismicity in the Lacq Gasfield, France. (a) Map view and location of cross-sections. Inset shows location in the region. (b) SSW-NNE cross-section and (c) WNW-ESE cross section. Colors: different earthquake clusters; dashed and solid gray lines: isobaths of the gasfield; black lines: faults; crosses: location uncertainties for three swarms [from Bardainne *et al.*, 2008].

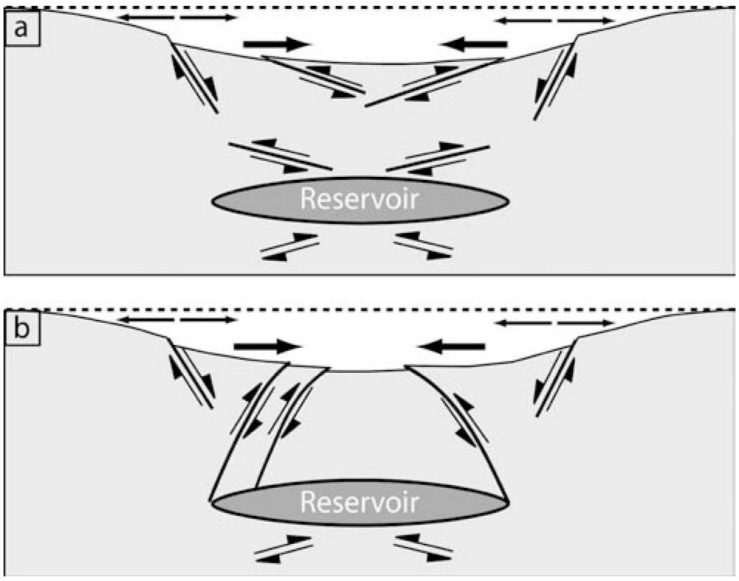


Figure 30: Deformation models of (a) Segall [1989], and (b) Odonne *et al.* [1999] for a depleting subsurface reservoir. Both models predict extensional deformation on the flanks and compressional deformation centrally in the field [from Bardainne *et al.*, 2008].

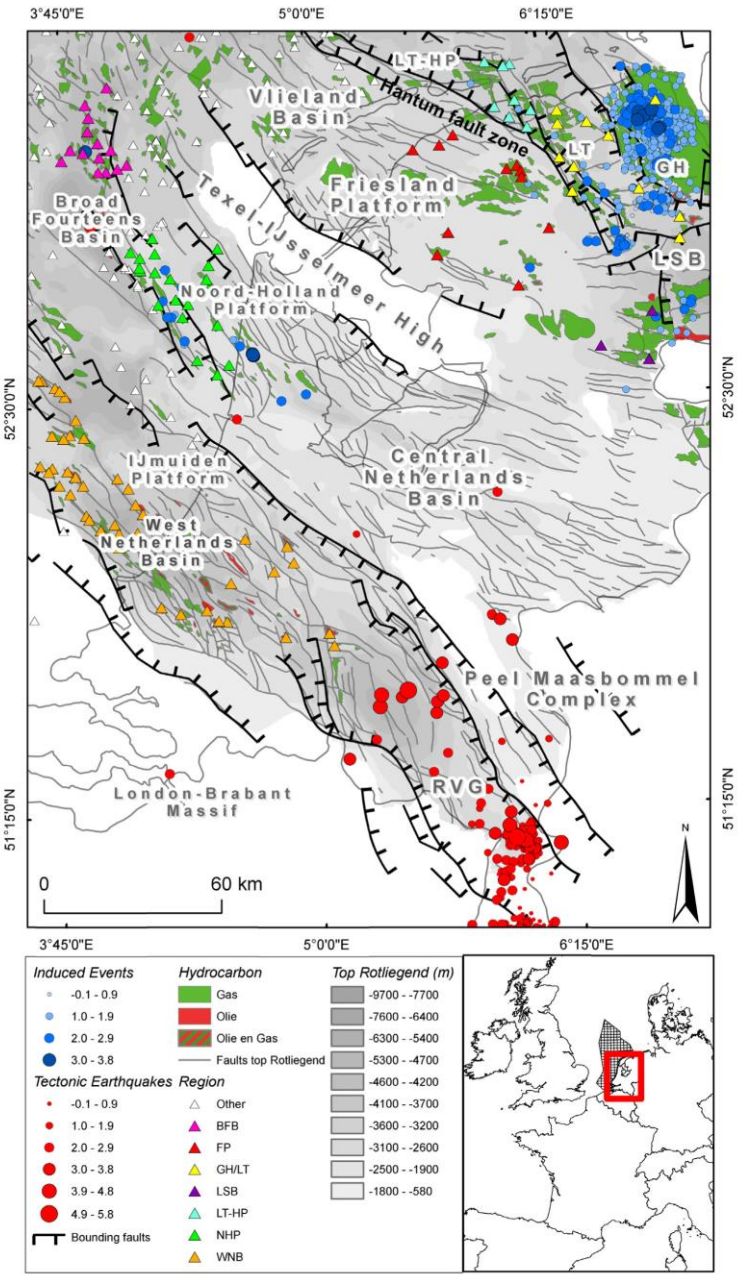


Figure 31: Tectonic map, seismicity, and hydrocarbon reservoirs in the Netherlands. Red circles: natural seismicity; blue circles: induced seismicity; green: gas reservoirs; red: oil reservoirs; solid lines: major fault zones; triangles: where leak-off tests have been performed. BFB=Broad Fourteen Basin, FP=Friesland Platform, GH/LT=Groningen High/Lauwerszee Trough, LSB=Lower Saxony Basin, LT-HP=Lauwerszee trough-Hantum Platform, NHP=Noord Holland Platform, WNB=West Netherlands Basin, RVG=Roer Valley Graben, PB=Peelrand Block, EL=Ems Low [from Van Wees *et al.*, 2014].

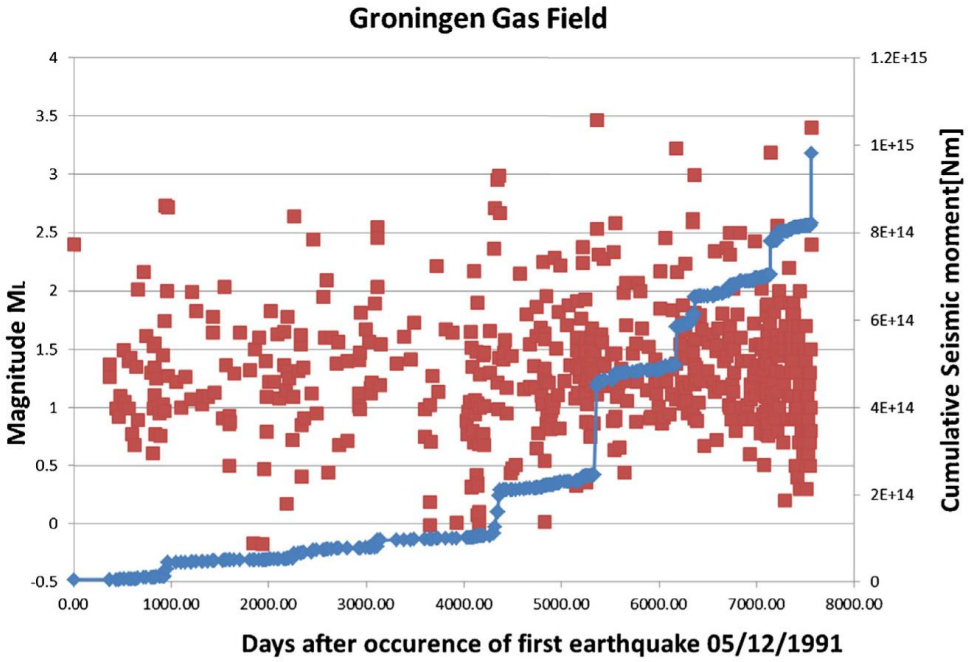


Figure 32: Magnitude of induced events in the Groningen Gasfield, Netherlands, 5 December, 1991 - 16 August, 2012, and cumulative seismic moment in Nm [from Van Wees *et al.*, 2014].

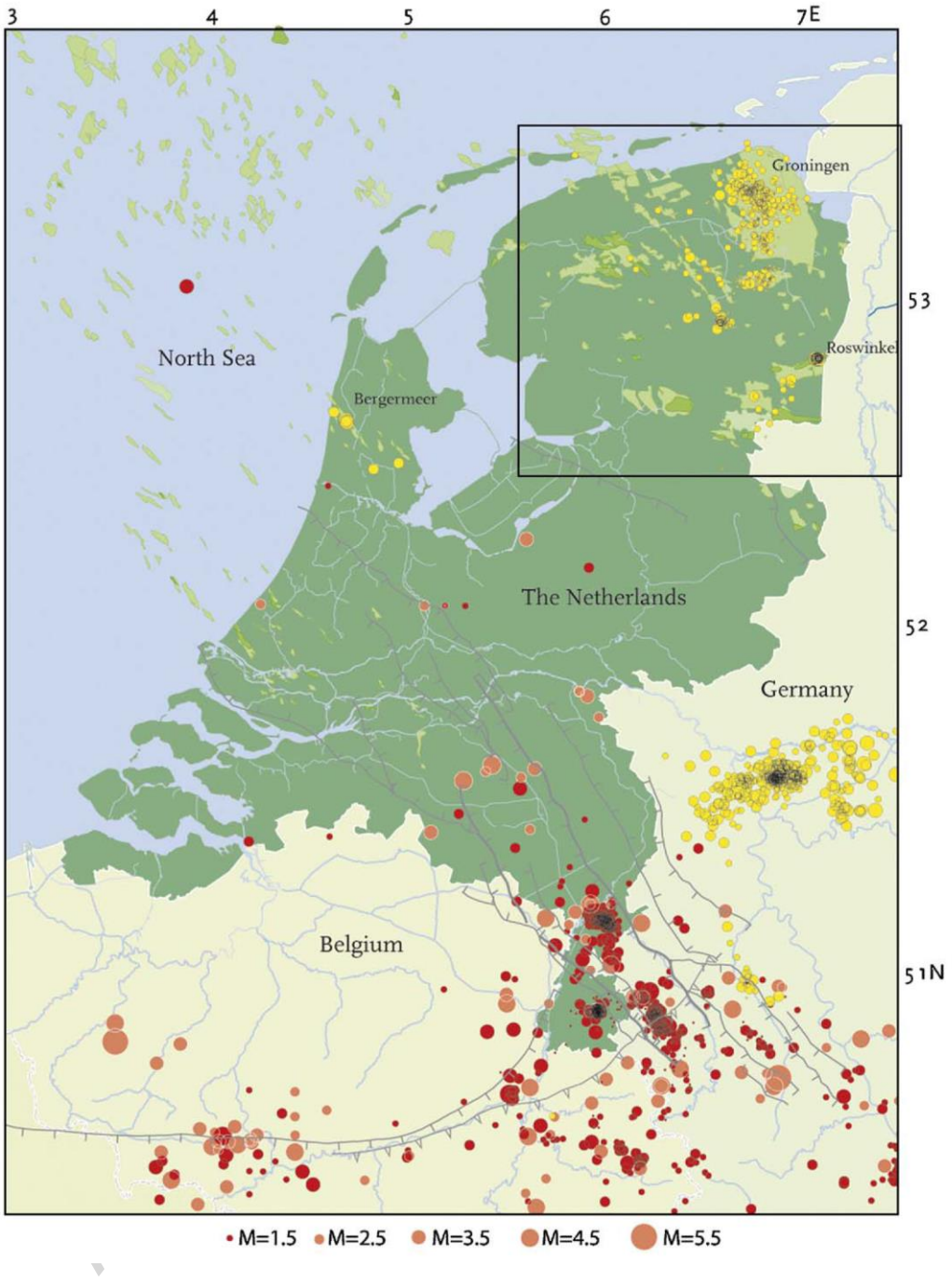


Figure 33: Seismicity in the Netherlands and surrounding region since 1900. Red circles: natural tectonic earthquakes; yellow circles: suspected induced earthquakes (usually mining or gas exploitation); gray solid lines: mapped faults in the upper-North-Sea formation; light green: approximate contours of gasfield. Detail of boxed region shown in Figure 34 [from van Eck *et al.*, 2006].

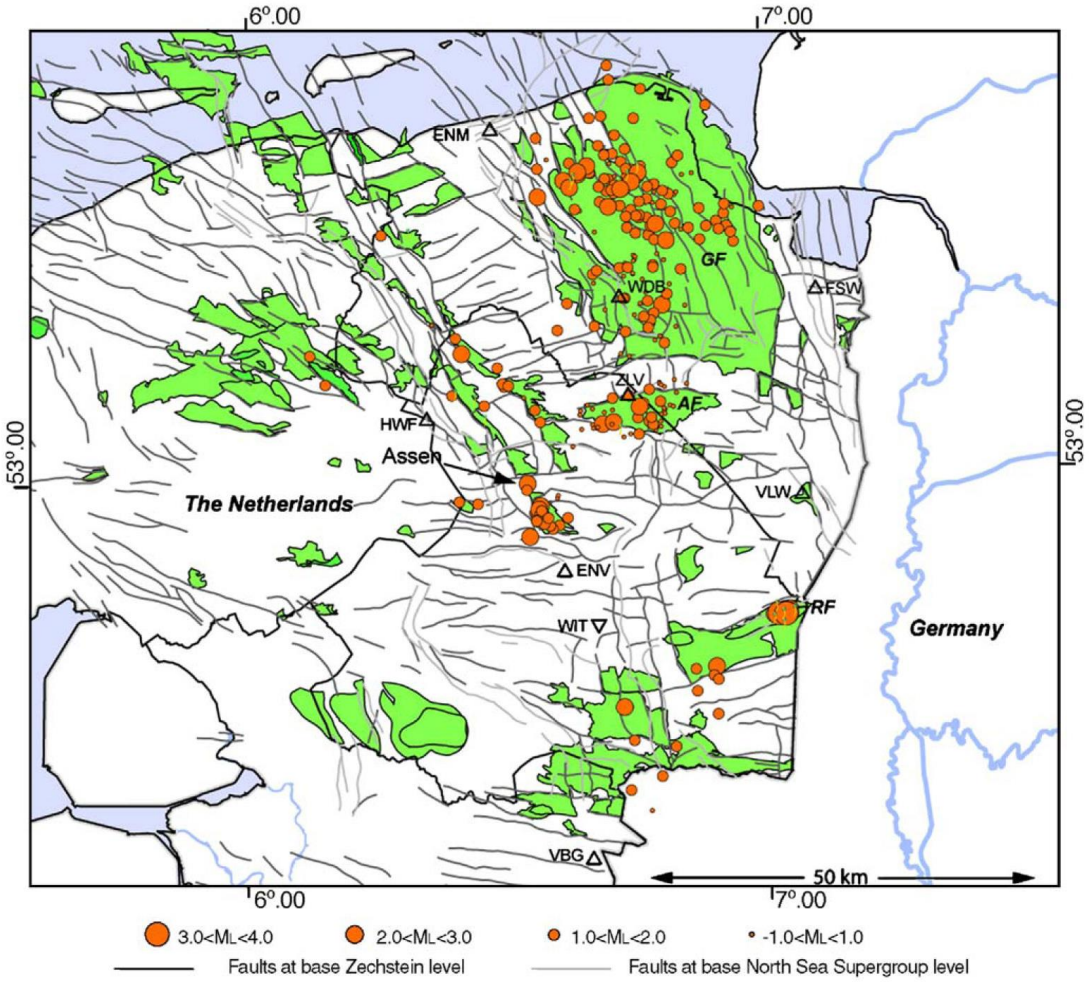


Figure 34: Map showing produced gasfields (green), major fault structures and seismicity (orange dots) in the northeast Netherlands (boxed region of Figure 33). RF: Roswinkel Field; GF: Groningen Field; EF: Eleveld Field; AF: Annerveen Field [from van Eck *et al.*, 2006].

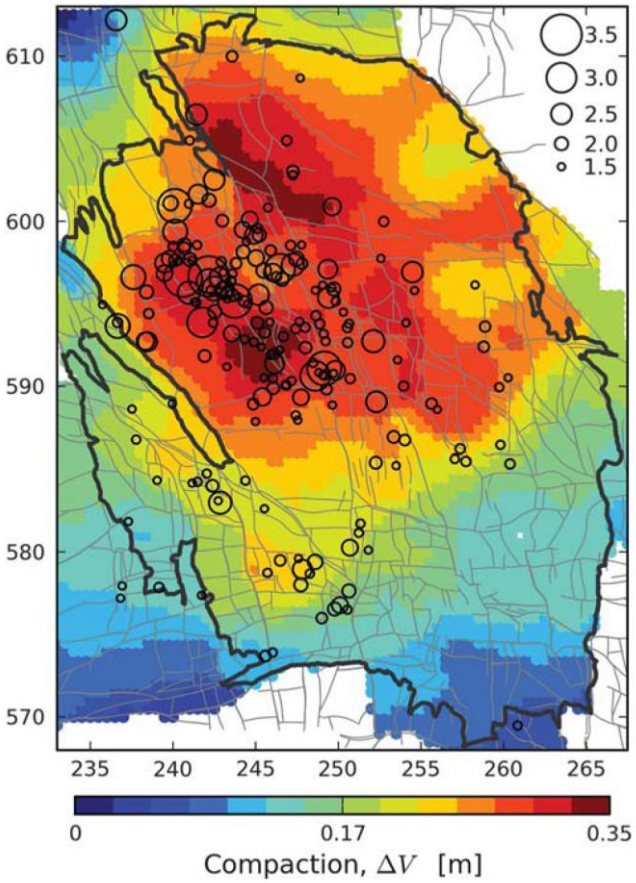


Figure 35: Earthquake epicenters for events with M ≥ 1.5 for the period 1995-2012, superimposed on a model of reservoir compaction for 1960-2012. Black line: perimeter of the Groningen Gasfield; thin gray lines: faults close to the reservoir level. Map coordinates are kilometers in the Dutch national triangulation coordinate system (Rijksdriehoek) [from Bourne *et al.*, 2015].

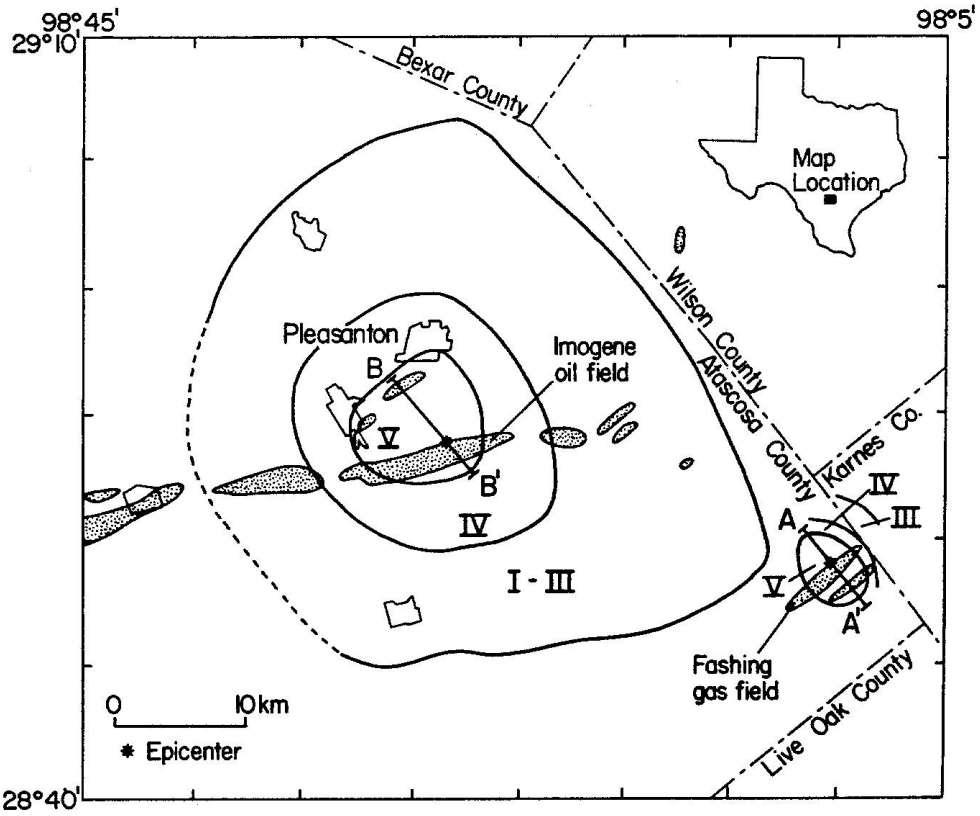


Figure 36: Oilfields and gasfields in the Imogene/Fashing area, south Texas, where earthquakes are postulated to have been induced. Shaded regions are more prominent fields. Isoseismals for the largest events on the Modified Mercalli intensity scale are shown [from Pennington *et al.*, 1986].

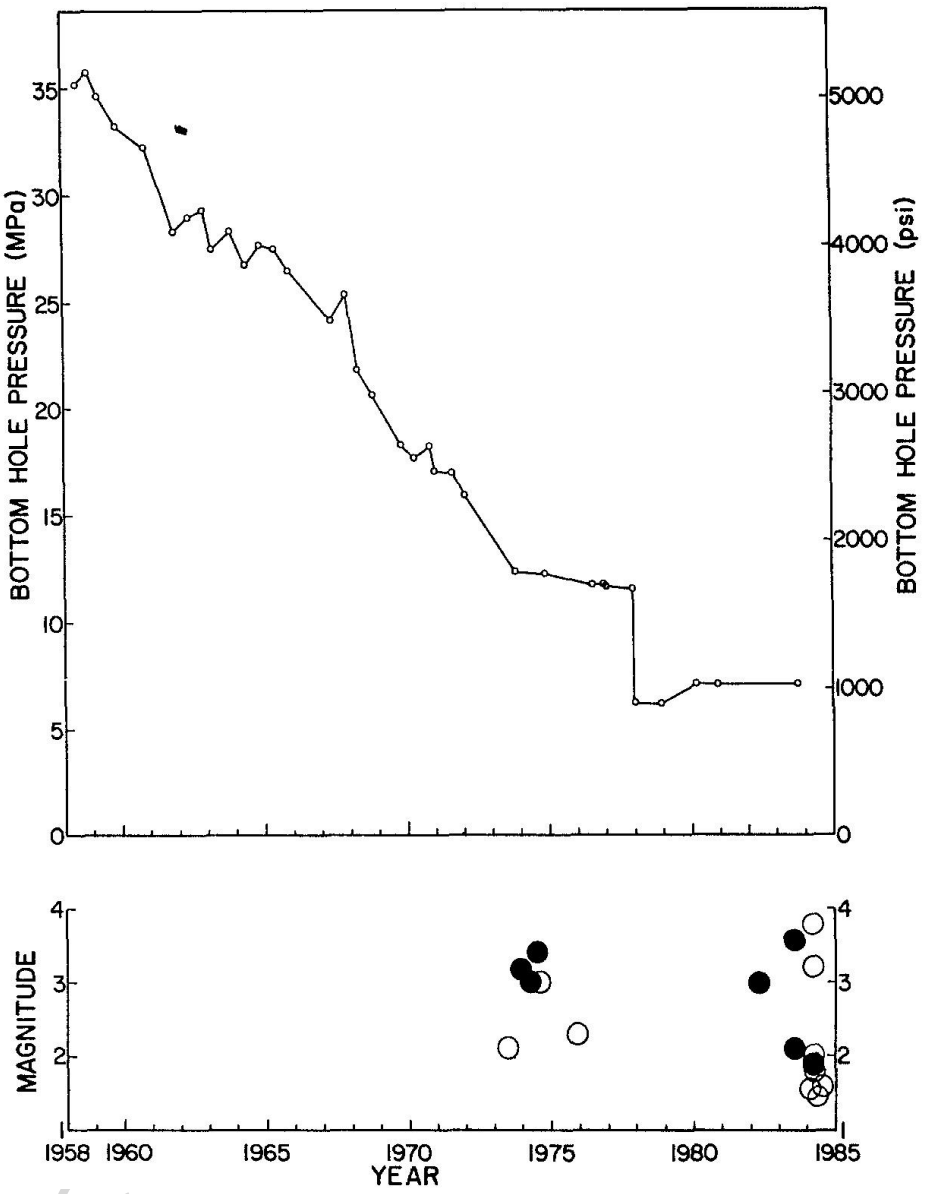


Figure 37: Pressure history of a well near the fault in the Fashing Gasfield along with known earthquakes in the Fashing-Pleasanton area. Black dots: earthquakes from the Fashing area; open circles: earthquakes from the Pleasanton (Imogene) area [from Pennington *et al.*, 1986].

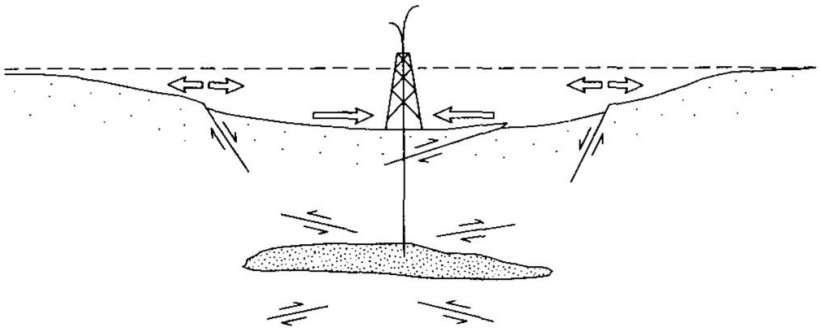

Figure 38: Schematic cross section summarizing surface deformation and faulting associated with fluid withdrawal. Normal faults develop on the flanks of the field, as observed at the Goose Creek, Texas, Oilfield. Reverse faults develop above reservoirs as observed at Wilmington, Buena Vista Hills, the Pau Basin and beneath the Strachan Field [from Segall, 1989].

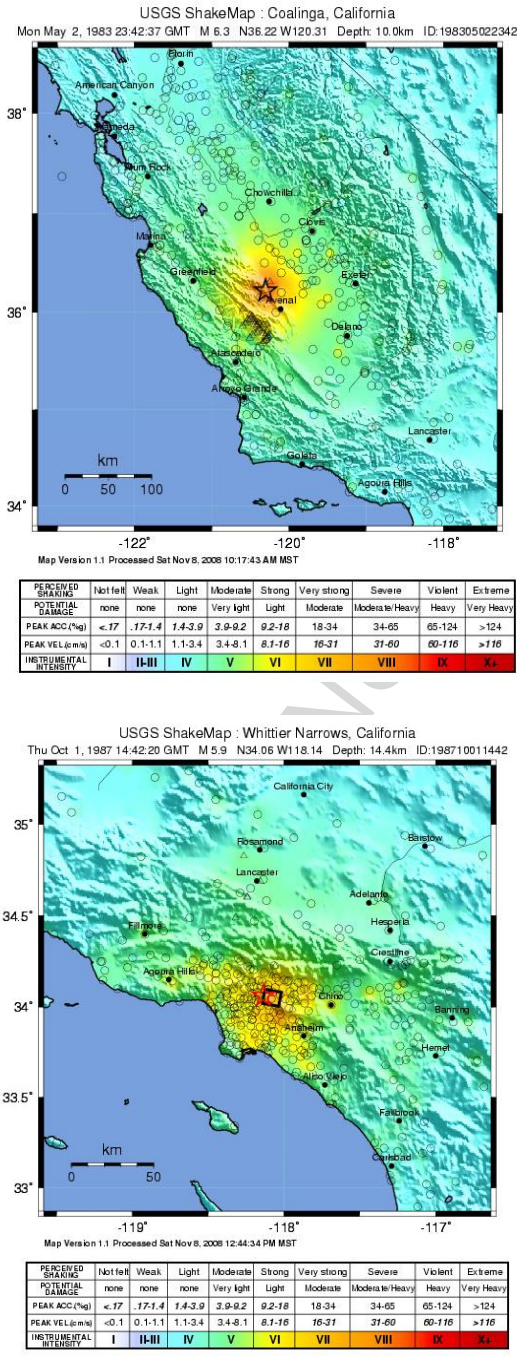


Figure 39: U.S. Geological Survey shake maps[14]. Top: 1983 $M_W$ 6.2 Coalinga, California earthquake, which injured 94 people and was felt throughout half the state. Bottom: 1987 $M_L$ 5.9 Whittier Narrows, California earthquake, which killed six people.

[14] http://earthquake.usgs.gov/earthquakes/shakemap/

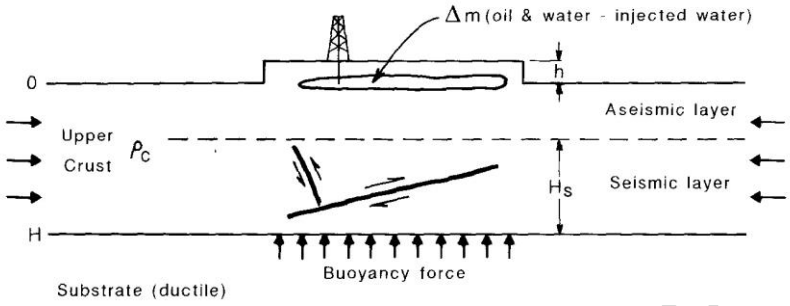


Figure 40: Schematic cross section showing proposed crustal response mechanism to oil production. Mass removal results in a vertical force imbalance causing seismic deformation in the seismogenic layer. This deformation, together with aseismic deformation in the shallow crust, restores isostatic balance [from McGarr, 1991].

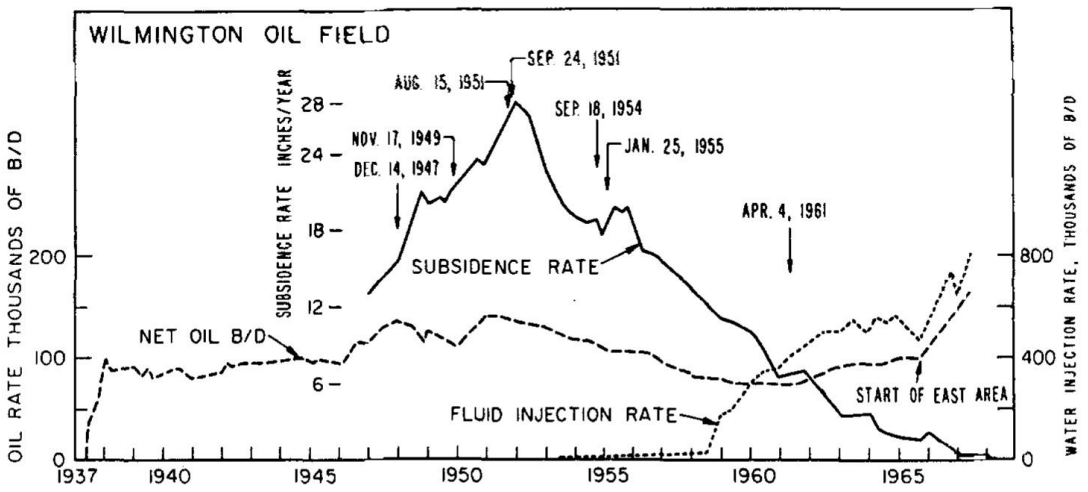


Figure 41: For the Wilmington Oilfield, California, subsidence rate in the center of the field, oil production and water injection rates. Arrows show dates of major damaging earthquakes [from Kovach, 1974].

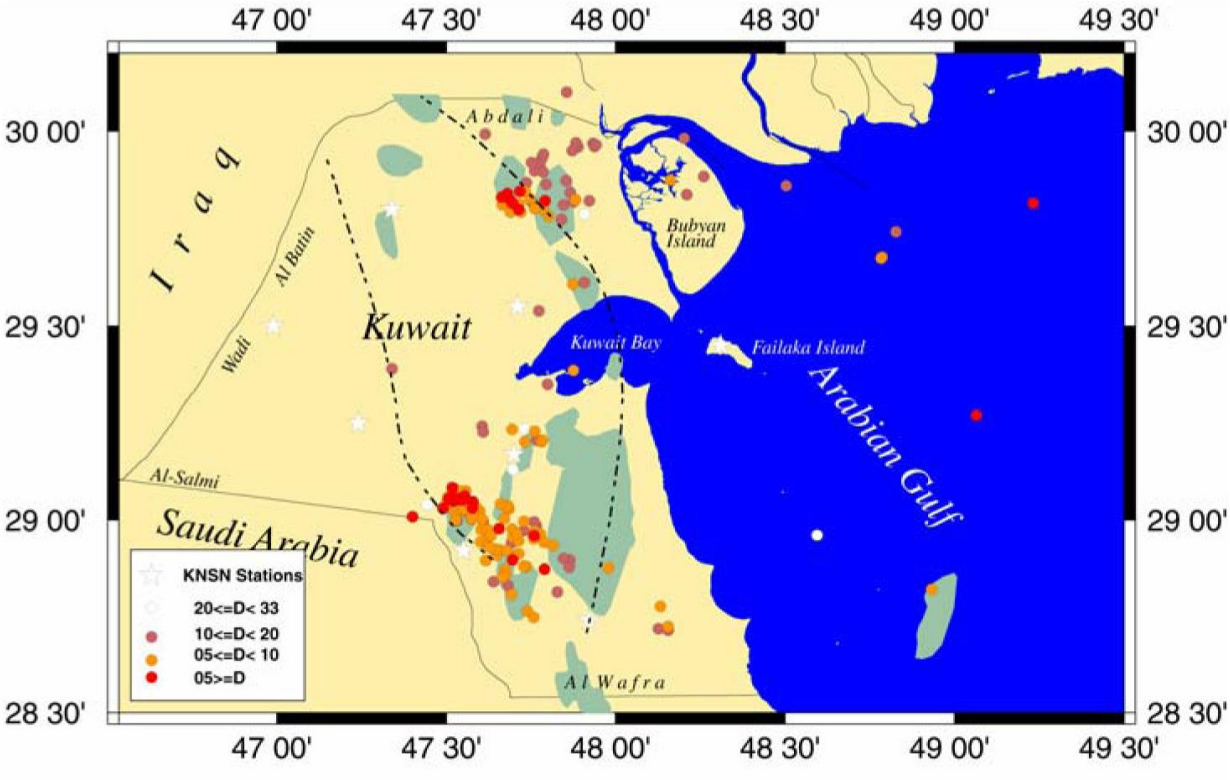


Figure 42: Seismicity of Kuwait for the period March 1997 - October 2007 [from Al-Enezi *et al.*, 2008].

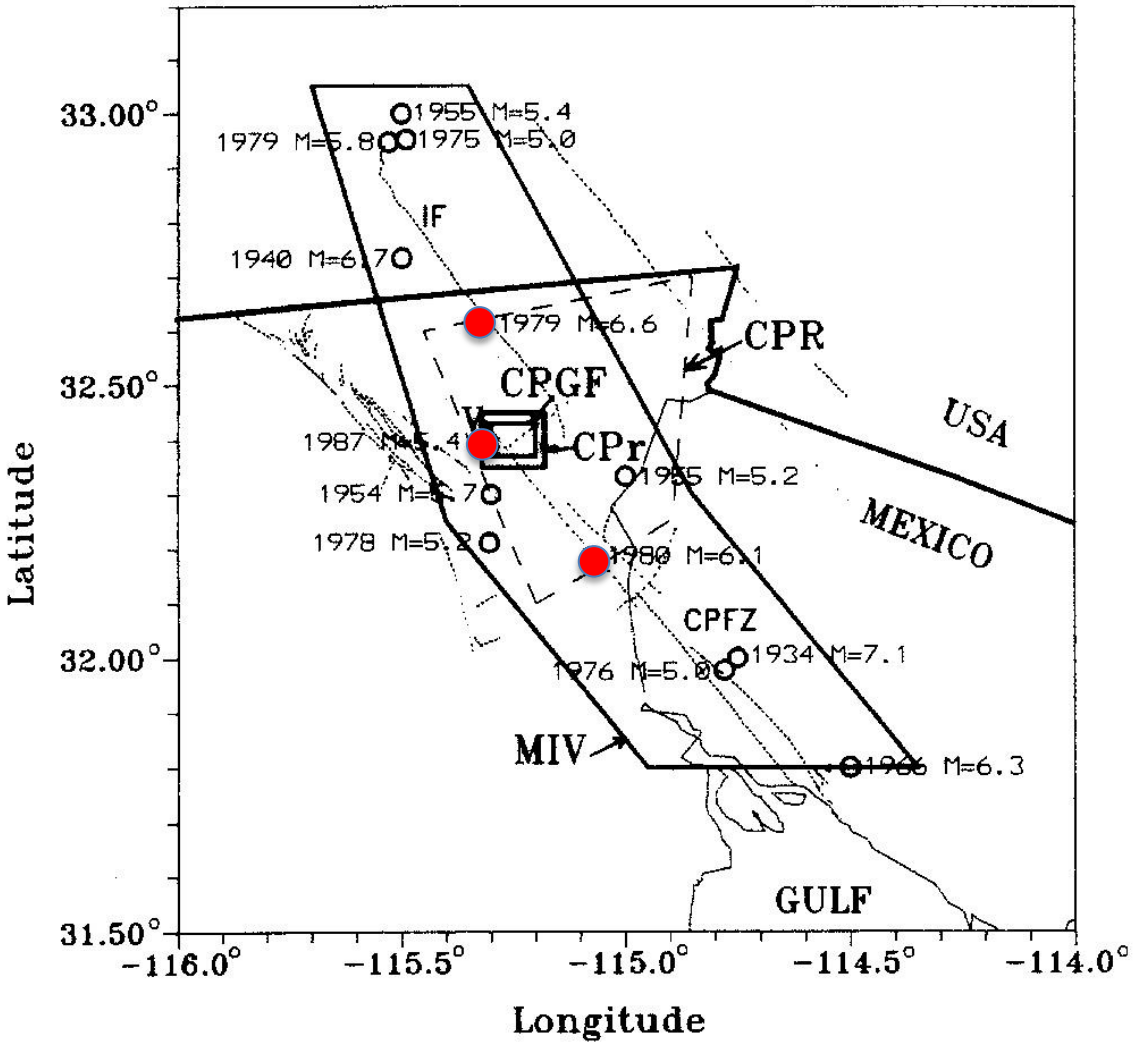


Figure 43: The Cerro Prieto geothermal field. Circles: earthquakes with M ≥ 5; red dots: earthquakes with M > 6; dotted lines: faults; IF: the Imperial fault; CPFZ: Cerro Prieto fault zone; V: the Cerro Prieto volcano [from Glowacka & Nava, 1996].

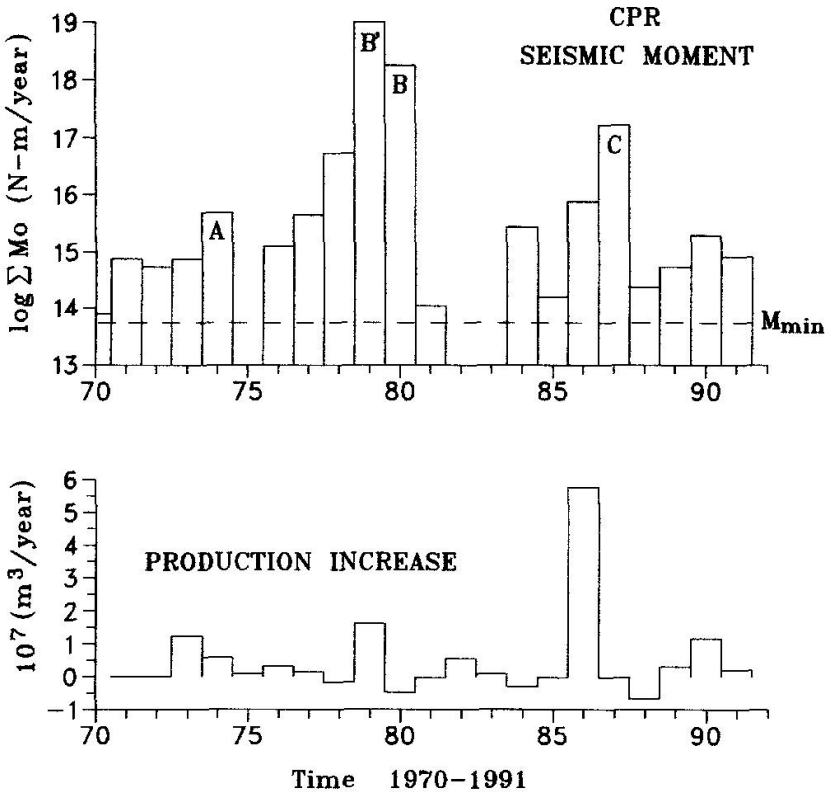


Figure 44: For the Cerro Prieto geothermal field, Mexico, top: annual seismic moment release; bottom: production rate [from Glowacka & Nava, 1996].

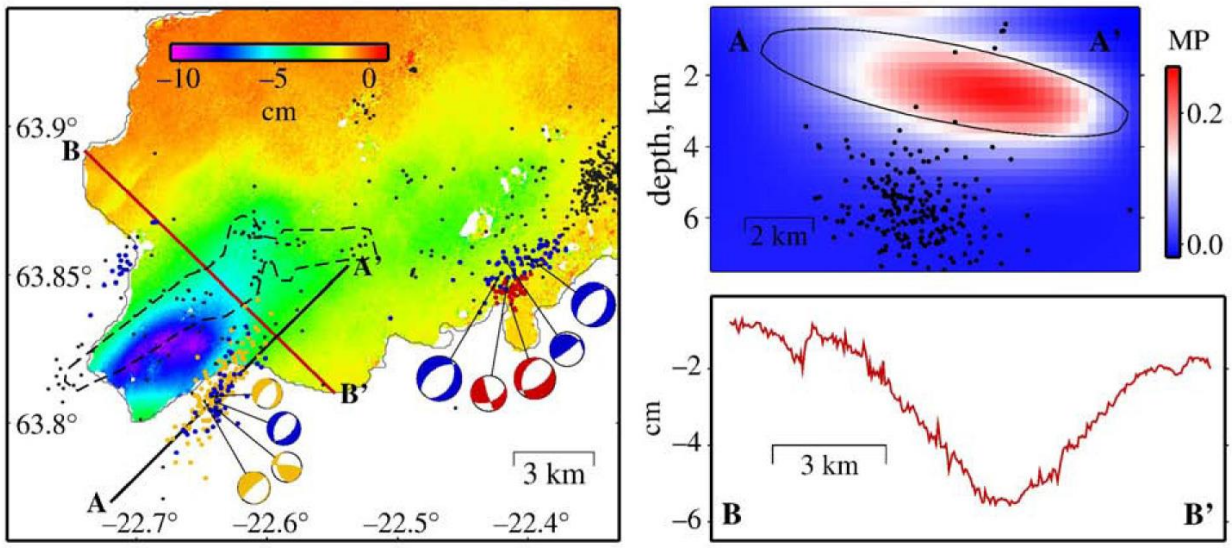


Figure 45: For the Reykjanes and Svartsengi geothermal fields, southwest Iceland, left: the near-vertical radar displacement field June 2005 - May 2008, earthquake locations and focal mechanisms. Black dots: background events. Distinct swarm events are shown for 2006 (orange), 2007 (red) and 2008 (blue). Stippled outline: location of the 1972 swarm activity from Klein *et al.* [1977]. Top right: profile AA′ shows the predicted change in Coulomb failure stress for normal slip on NE-SW-trending fault planes, computed using an elastic half-space ellipsoidal source model for subsidence around the Reykjanes geothermal field. Bottom right: profile BB′ shows the observed near-vertical radar displacement across the Reykjanes subsidence bowl [from Keiding *et al.*, 2010].

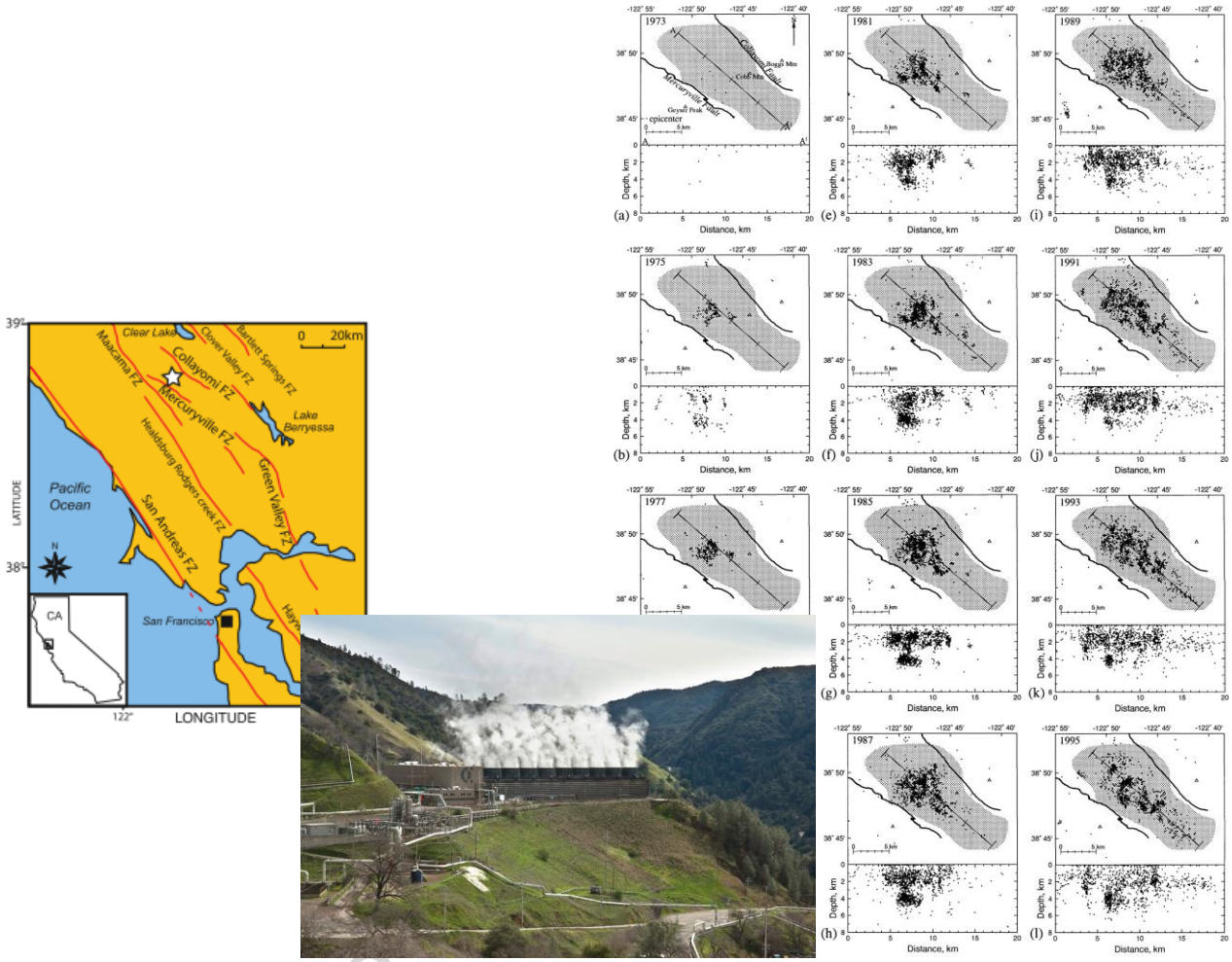


Figure 46: The Geysers geothermal field, California. Left: regional map showing location of the field. Middle: McCabe Units 5 and 6 at The Geysers[15]. Right: maps of seismicity at The Geysers at biannual intervals from 1973 to 1995. Locations are from the Northern California Seismic Network catalogue for earthquakes with M > 1.2. Gray area: steam field. Line shows line-of-section for depth sections below each map [from Ross *et al.*, 1999].

[15] http://www.energy.ca.gov/tour/geysers/

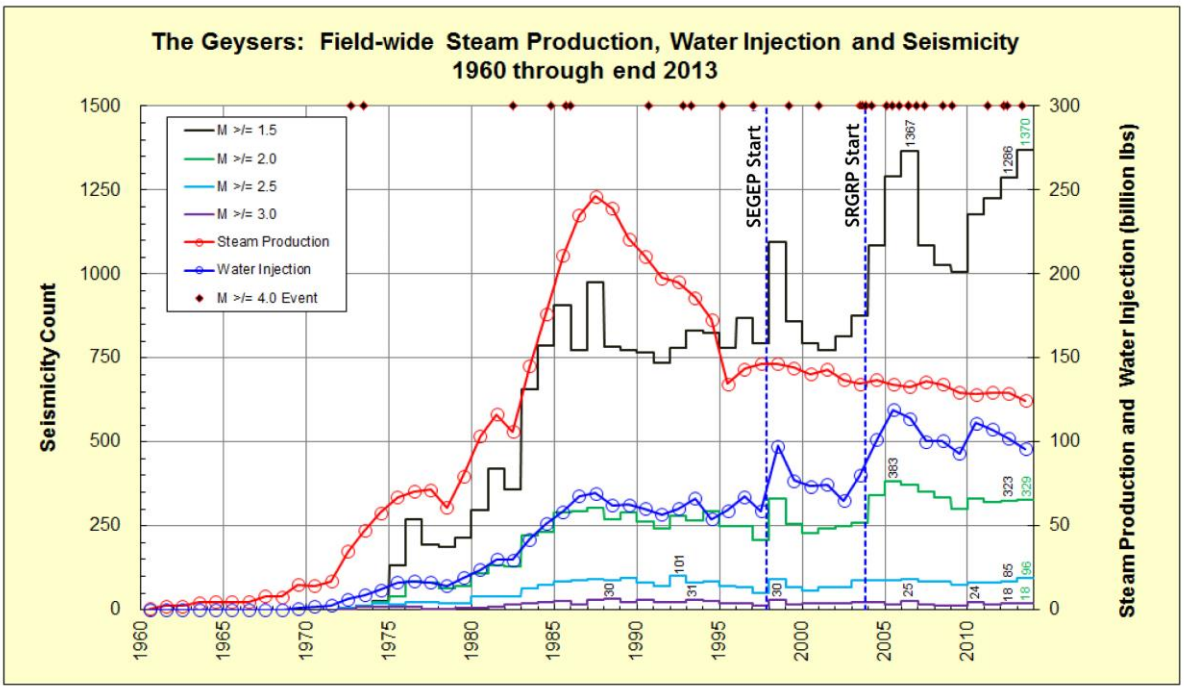


Figure 47: Yearly field-wide steam production, water injection and seismicity 1960-2013. Earthquakes with M ≥ 4 are indicated as red diamonds along the top boundary of the graph [from Hartline, 2014].

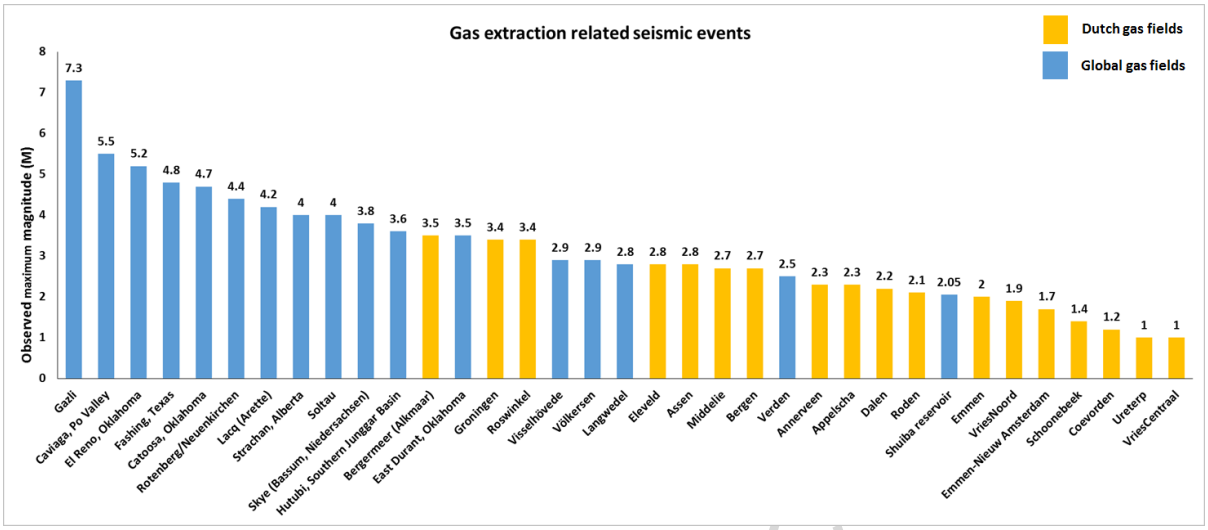


Figure 48: $M_{MAX}$ for seismicity postulated to be induced by the extraction of natural gas at the 35 fields where this parameter is reported. The Hutubi, northwest China case is associated with both extraction and storage [Tang *et al.*, 2015].

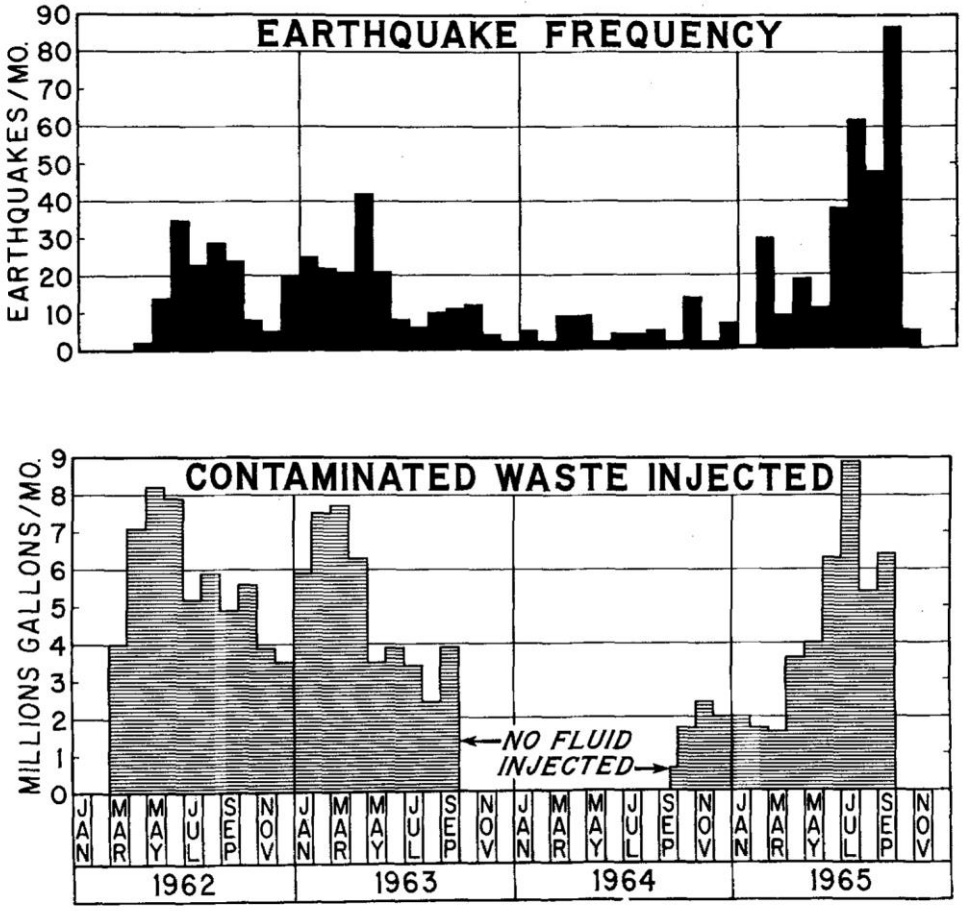


Figure 49: Top: Earthquake frequency. Bottom: injection rate at the Rocky Mountain Arsenal well, Colorado [Healy *et al.*, 1968].

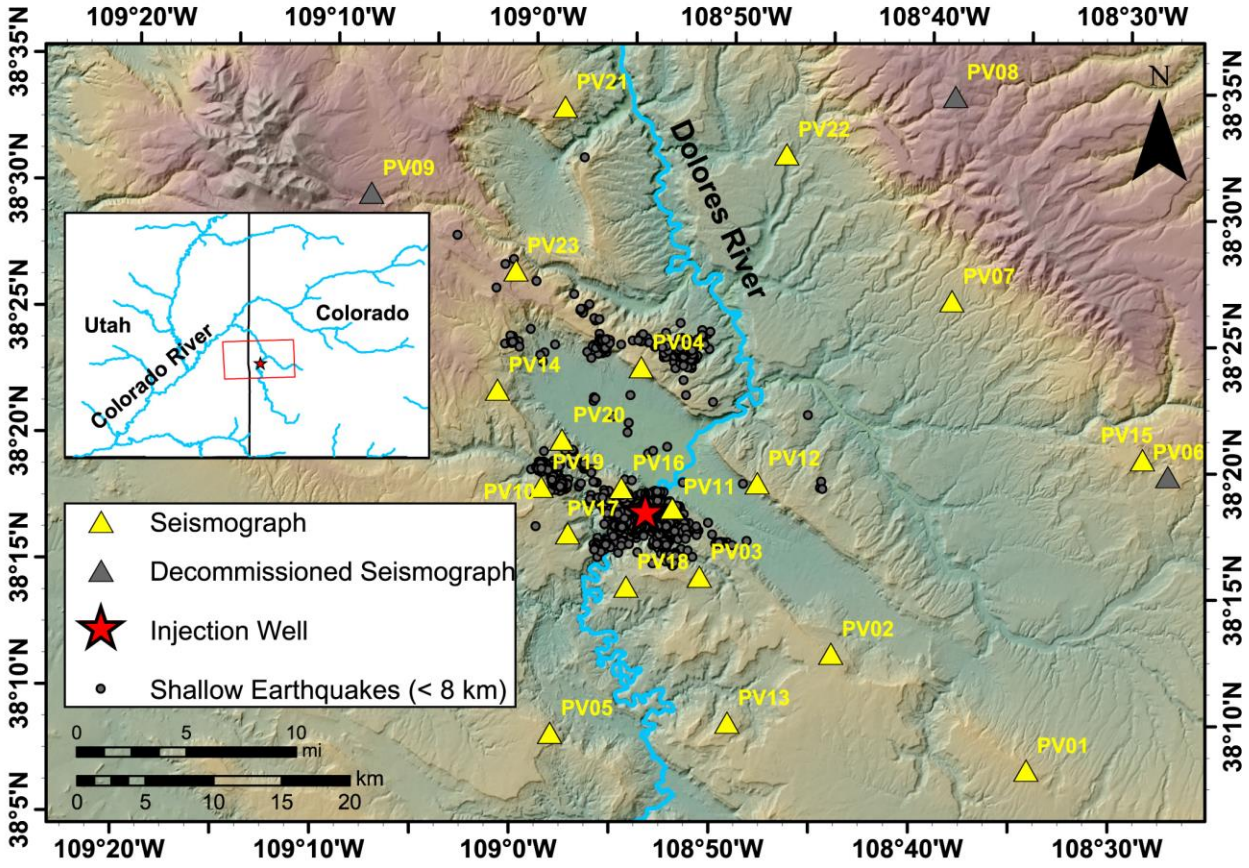


Figure 50: The region around Paradox Valley, Colorado (the northwest-oriented depression). Yellow triangles: seismic stations; gray circles: earthquakes thought to be induced by brine injections [from Yeck *et al.*, 2015].

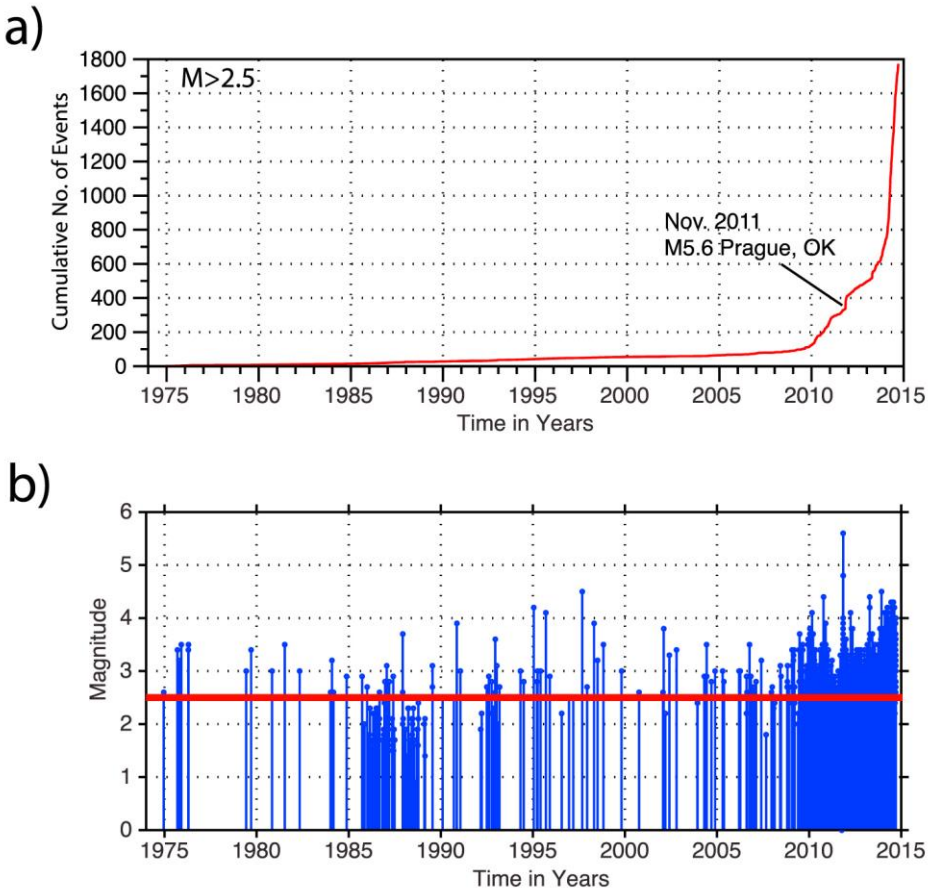


Figure 51: Earthquakes recorded on the National Earthquake Information Center (NEIC)[16] system for the period 1975 through 2014. a) Cumulative seismicity in Oklahoma with M > 2.5. b) Earthquake magnitudes [from McNamara *et al.*, 2015].

[16] http://earthquake.usgs.gov/contactus/golden/neic.php

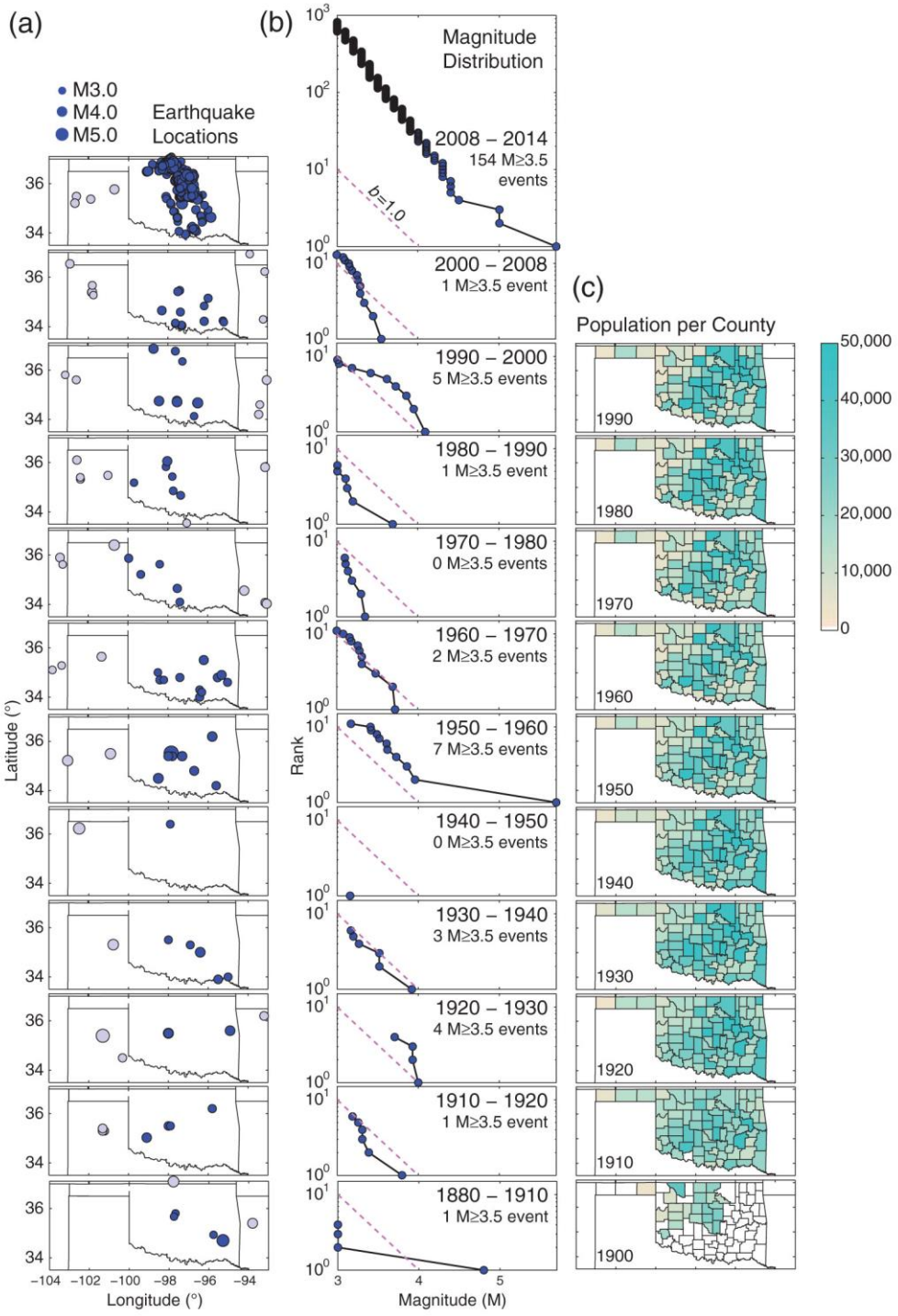


Figure 52: Oklahoma seismicity. Left panels: Earthquake locations: blue–Oklahoma, gray–neighboring states. Centre panels: magnitudes plotted cumulatively 1880 - 2014. Right panels: human population by county [from Hough & Page, 2015].

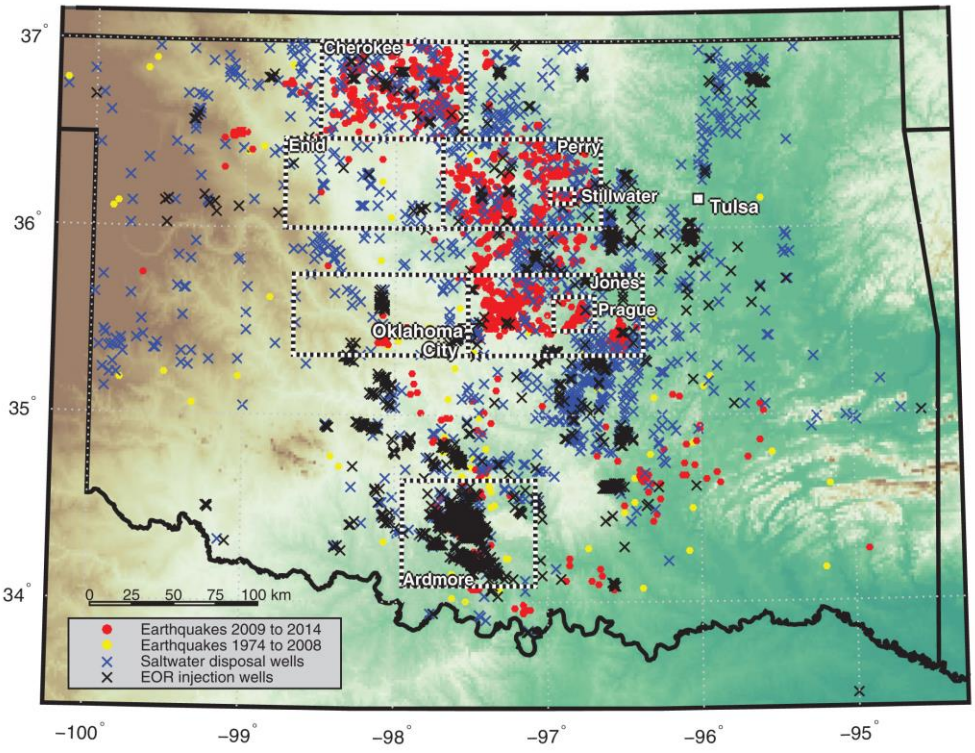


Figure 53: Earthquakes and injection wells in Oklahoma. Red dots: locations of earthquakes 2009–2014; yellow dots: historical earthquakes 1974–2008; black crosses: enhanced oil recovery wells; blue crosses: salt water disposal wells that injected more than 30,000 barrels (~4800 $m^3$) in any month in the most recent three years of data; boxes: areas of detailed study [from Walsh & Zoback, 2015].

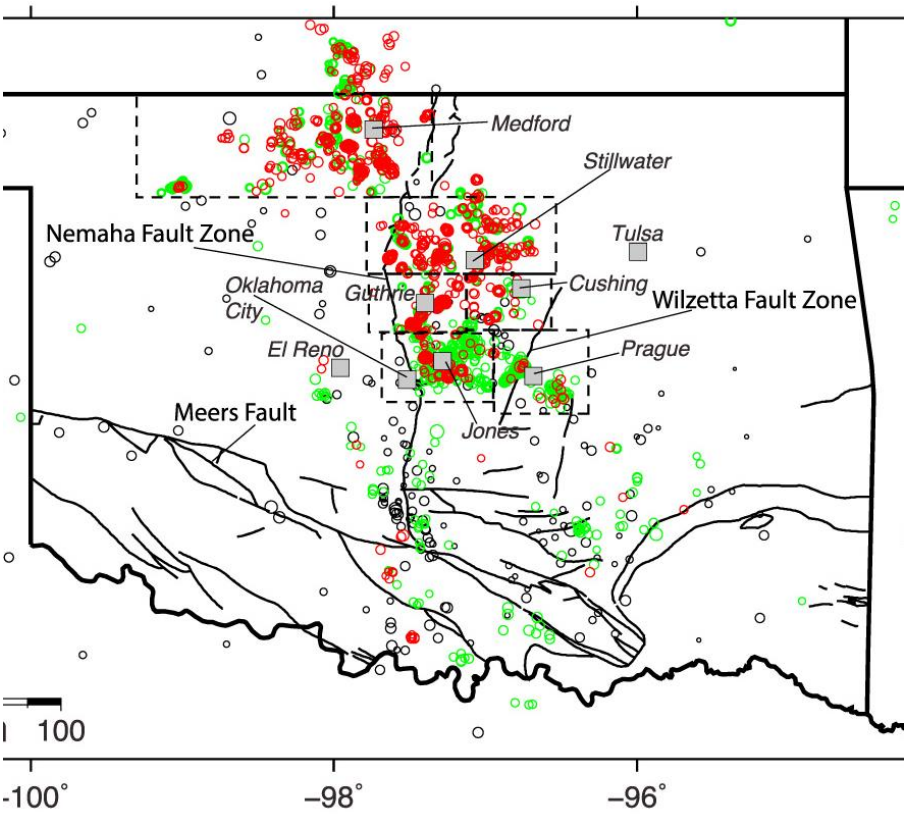


Figure 54: U.S. Geological Survey earthquake epicenters from the National Earthquake Information Center (NEIC) database[17], 1974 - 2014. Black lines: subsurface and surface faults; dashed black lines: detailed study regions; Meers fault: the only known active fault in Oklahoma prior to the recent increase in seismicity [from McNamara *et al.*, 2015].



[17] http://earthquake.usgs.gov/contactus/golden/neic.php

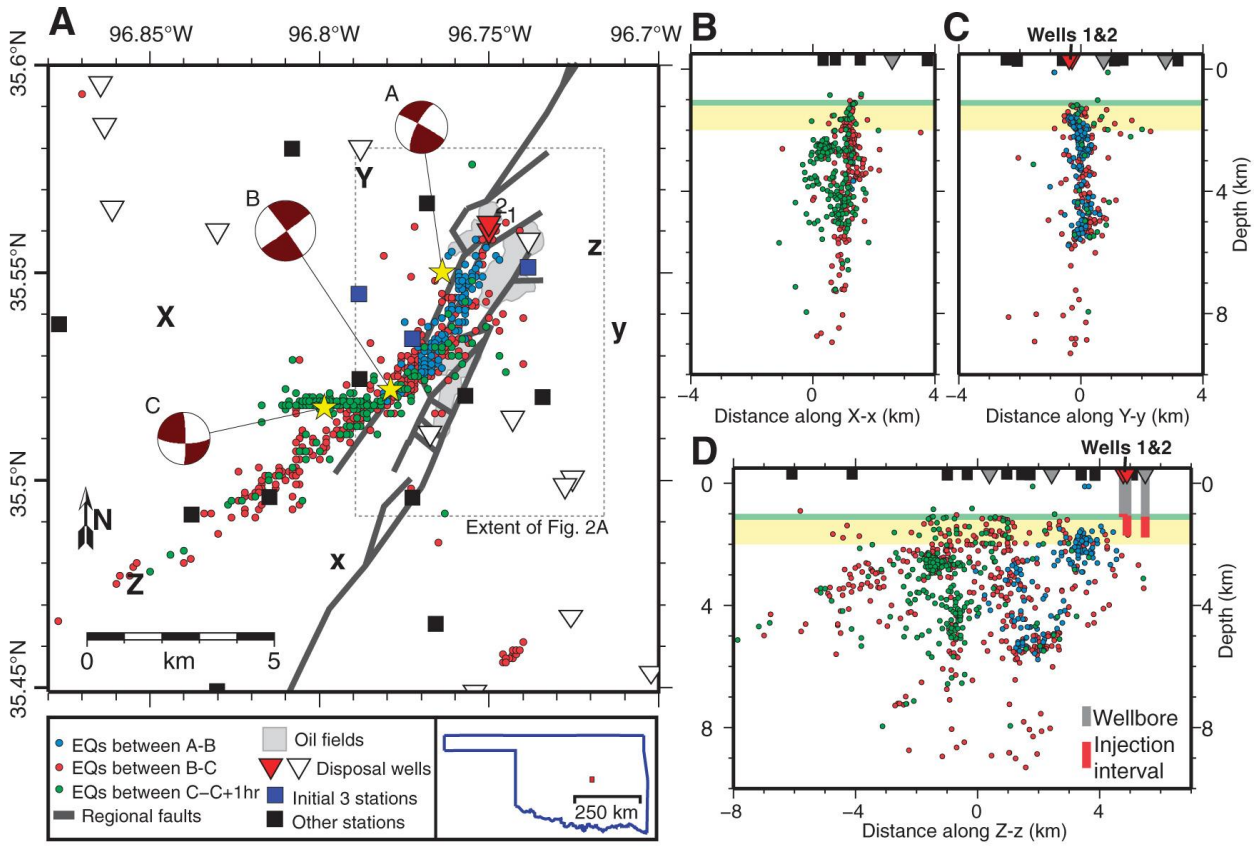


Figure 55: Seismicity, focal mechanisms, seismic stations, active disposal wells, and oilfields in the neighborhood of the 2011 Prague, Oklahoma, seismic sequence. Stars: major earthquakes in the sequence. B–D: Cross sections showing seismicity projected from up to 4 km out of plane. Vertical lines: wellbores, red where perforated or open; green bands: the Hunton and Simpson Groups; yellow bands: Arbuckle Group which overlies basement. Inset: Oklahoma and location of map area [from Keranen *et al.*, 2013].

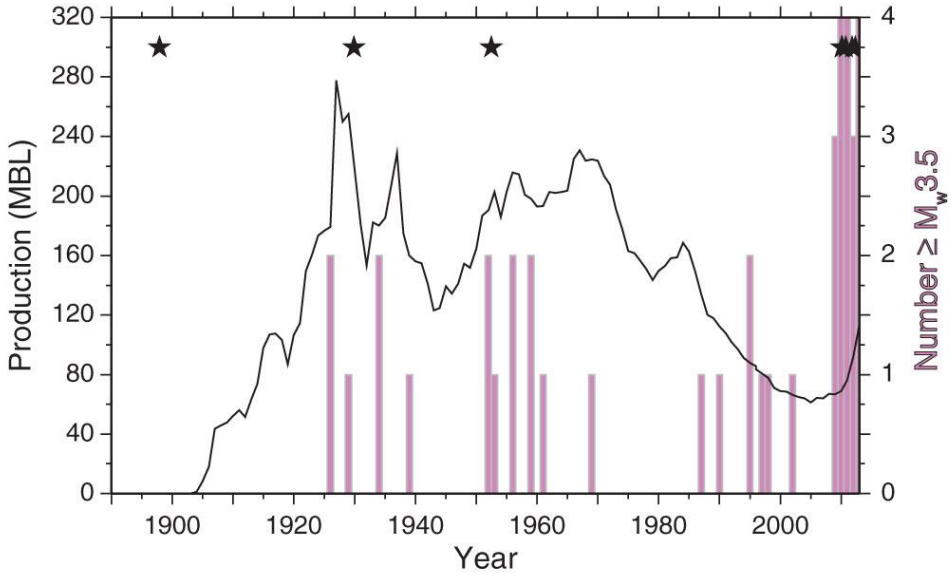


Figure 56: Oklahoma seismicity rates compared with oil production in millions of barrels (multiply by 0.159 to convert to $m^3$). Bars: number of earthquakes with $M \geq 3.5$ in a given year; black stars: $M \geq 4$ events [from Hough & Page, 2015].

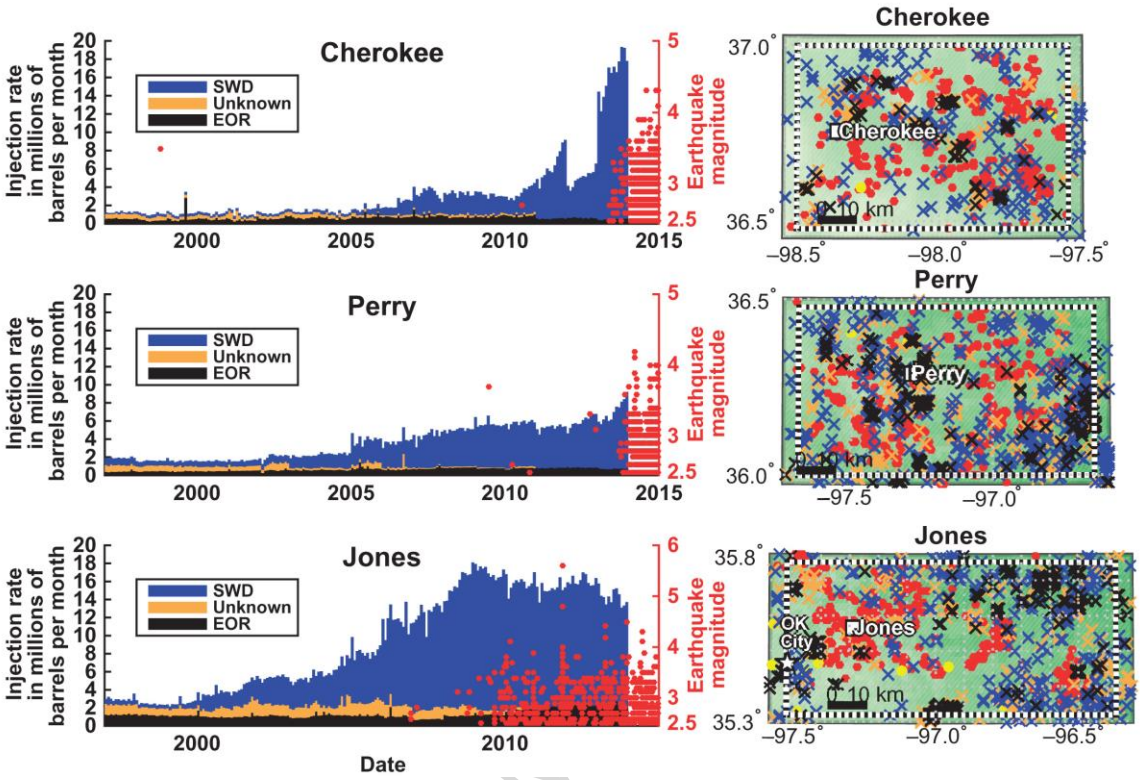


Figure 57: Injection from enhanced oil recovery, brine disposal, and unknown wells, and earthquakes in the Cherokee, Perry, and Jones study areas (boxes in Figure 53). Symbols are the same as in Figure 53. Each study area is 5000 km$^2$ in size [from Walsh & Zoback, 2015].

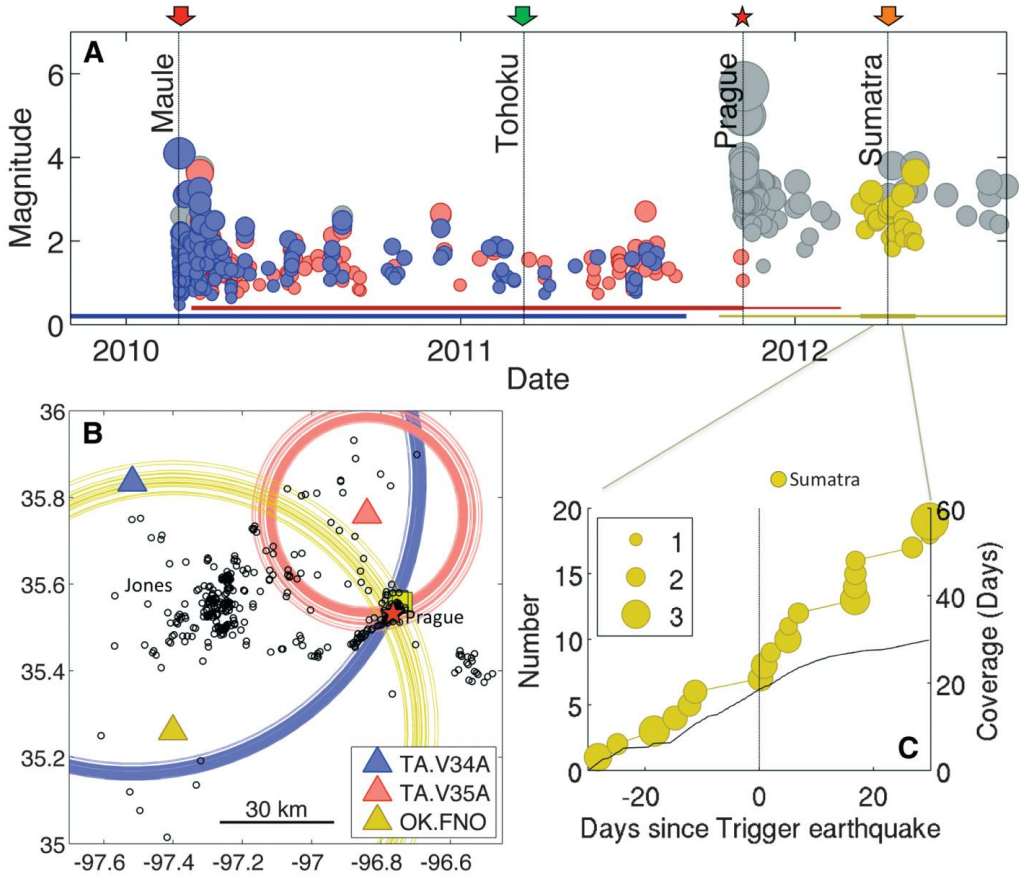


Figure 58: Earthquakes in the Prague, Oklahoma, area. (A) Detected events, showing triggering by the 2010 Maule, Chile earthquake. Red star: the 6 November 2011 $M_W$ 5.7 mainshock. (B) Distances to detected events. (C) Cumulative number of events in the time period surrounding the 11 April 2012 $M_W$ 8.6 and 8.2 Sumatra earthquakes [from van der Elst *et al.*, 2013].

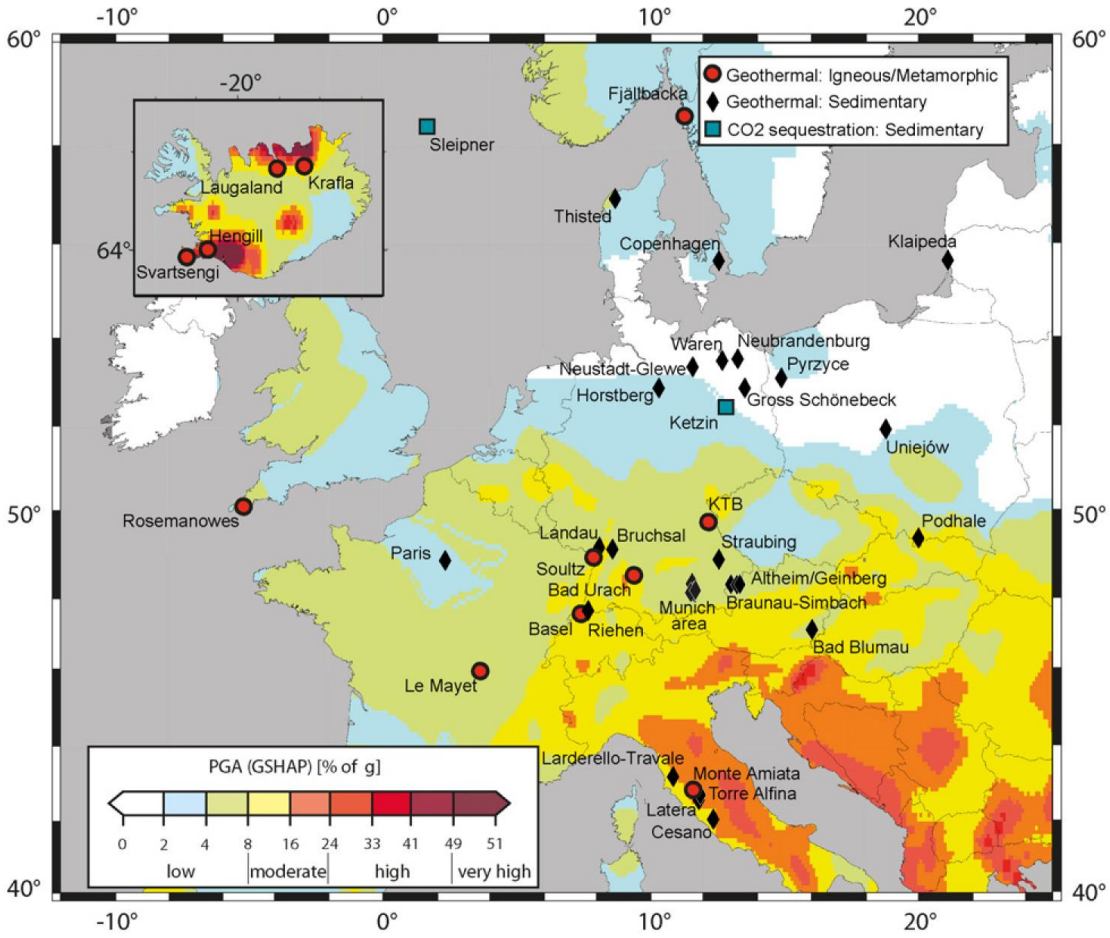


Figure 59: Location of geothermal and $CO_2$ injection sites in Europe, superimposed on a seismic hazard map from the Global Seismic Hazard Assessment Program (GSHAP[18]). Color scale denotes GSHAP index of local seismic hazard from natural earthquakes defined as peak ground acceleration in percent of the acceleration due to gravity (*g*) on stiff soil that has a 10% probability of being exceeded in 50 years [equivalent to a recurrence period of 475 years; from Evans *et al.*, 2012].

[18] http://www.seismo.ethz.ch/static/GSHAP

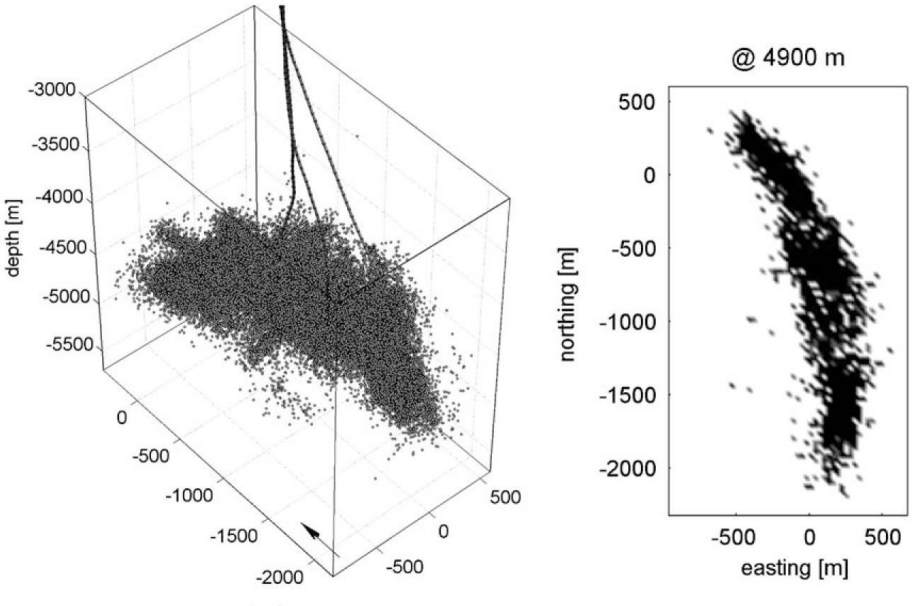


Figure 60: Top left: Distribution of earthquake hypocenters at the Soultz-sous-Forêts EGS project in perspective view. Solid lines: wells GPK2, GPK3 and GPK4. Top right: Depth slice of the hypocenter density distribution at 4900 m depth. Dark shading: regions of high density [from Baisch *et al.*, 2010].

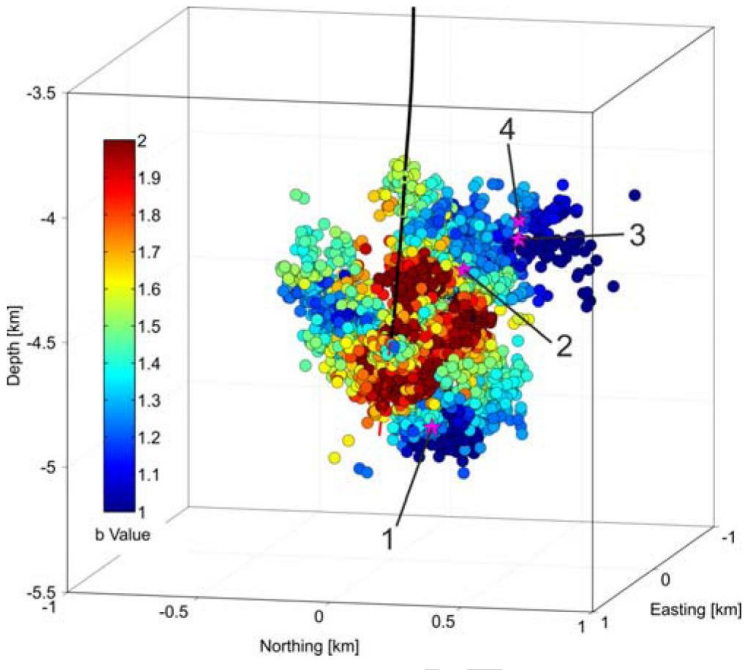


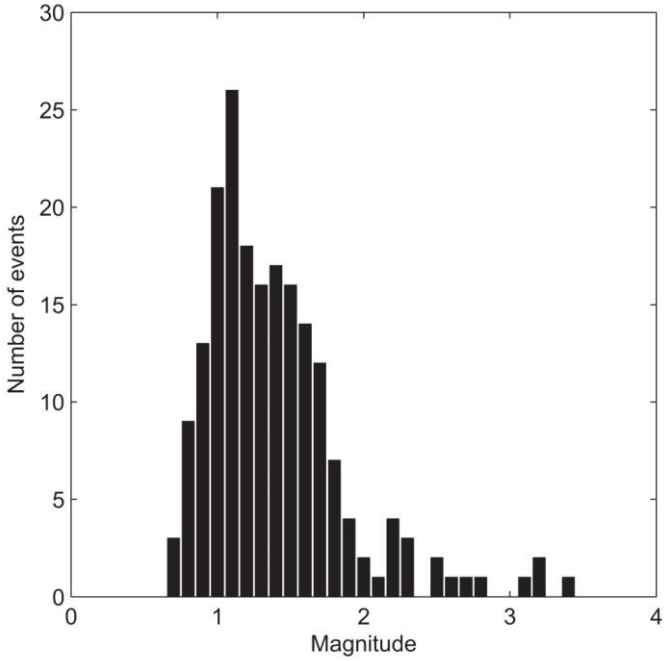


Figure 61: Top: Earthquakes induced by hydraulic stimulation of the Basel, Switzerland, EGS injection well in 2006 and 2007. Hypocenters are color coded according to *b*-values calculated for the volume in which they occurred. Stars: large earthquakes [from Zang *et al.*, 2014b]. Bottom: Magnitude histogram of the induced seismicity recorded by the Swiss Seismological Service 3 December, 2006 - 30 November, 2007 [from Deichmann & Ernst, 2009].

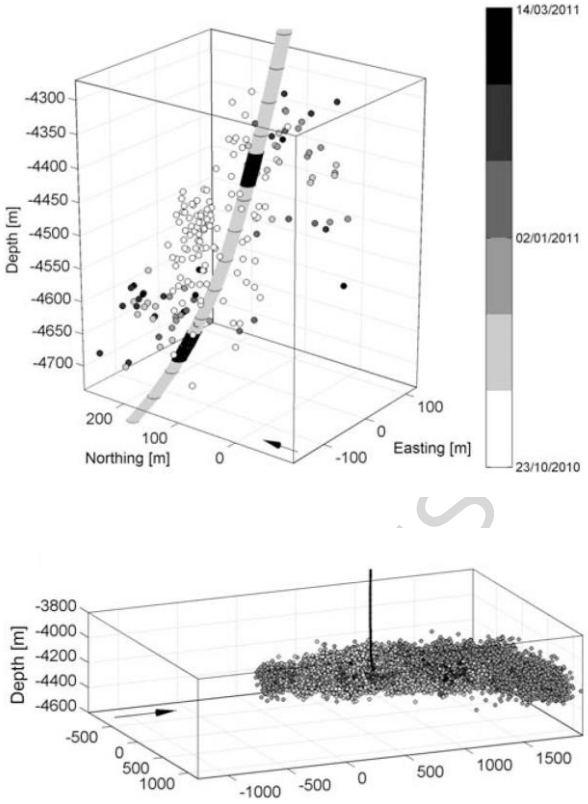


Figure 62: EGS-induced earthquakes at Cooper Basin, Australia. Top: the Jolokia Field–hypocenters of earthquakes induced by hydraulic stimulation of well 1 in in 2010. Known fracture intersections with the wellbore are shown in black. Bottom: the Habanero field–hypocetnres of earthquakes induced by stimulation of well 4 (vertical line) in 2012 [from Baisch *et al.*, 2015].

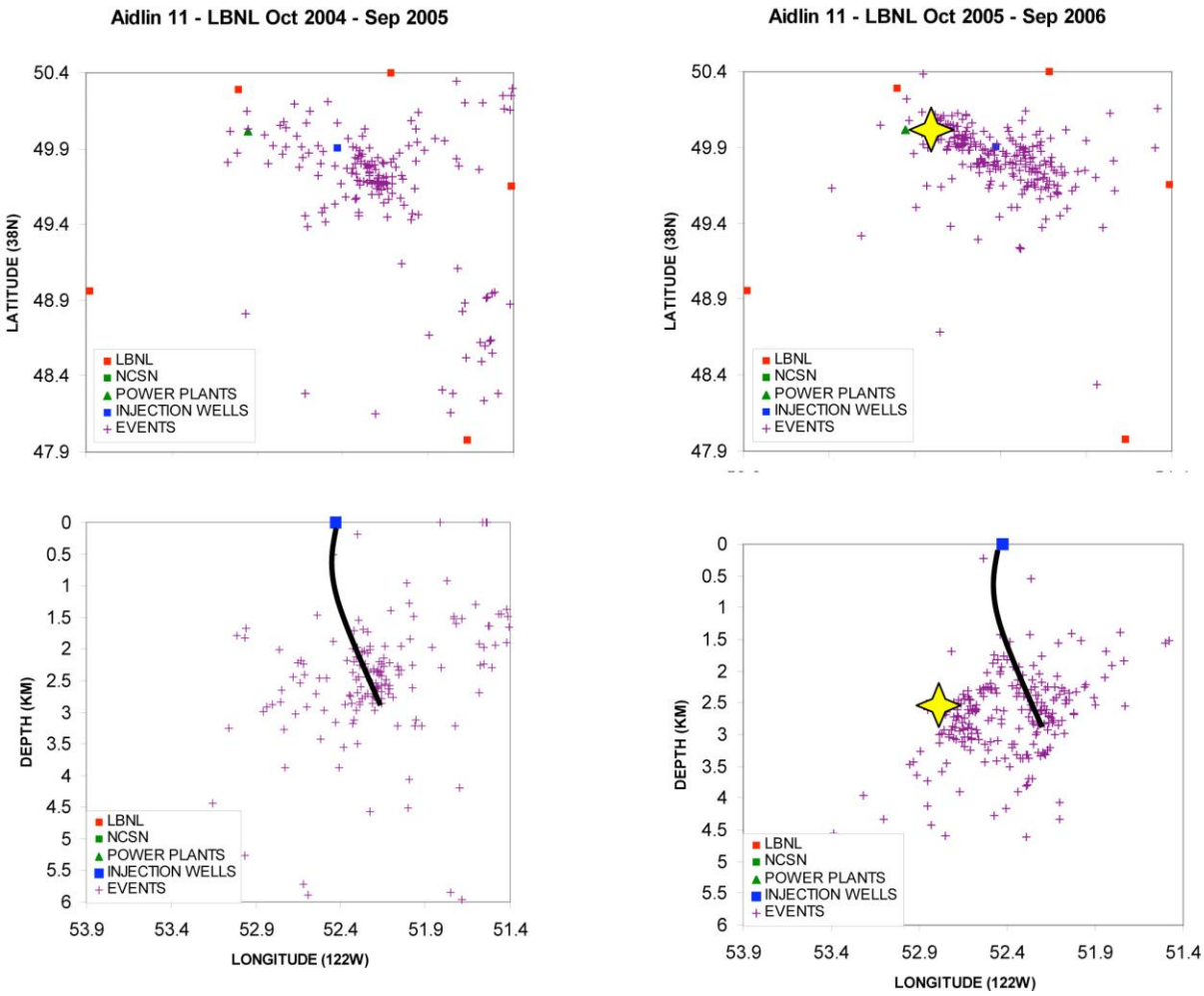


Figure 63: Earthquakes surmised to be injection-related at the northwest Geysers geothermal area. Maps and east-west cross sections show earthquakes in the Aidlin area. Blue square and black line: Injection well; yellow star: a M 4 event that occurred October 2005 [from Majer & Peterson, 2007].


Figure 64: States of the USA where shale-gas hydrofracturing is currently ongoing.

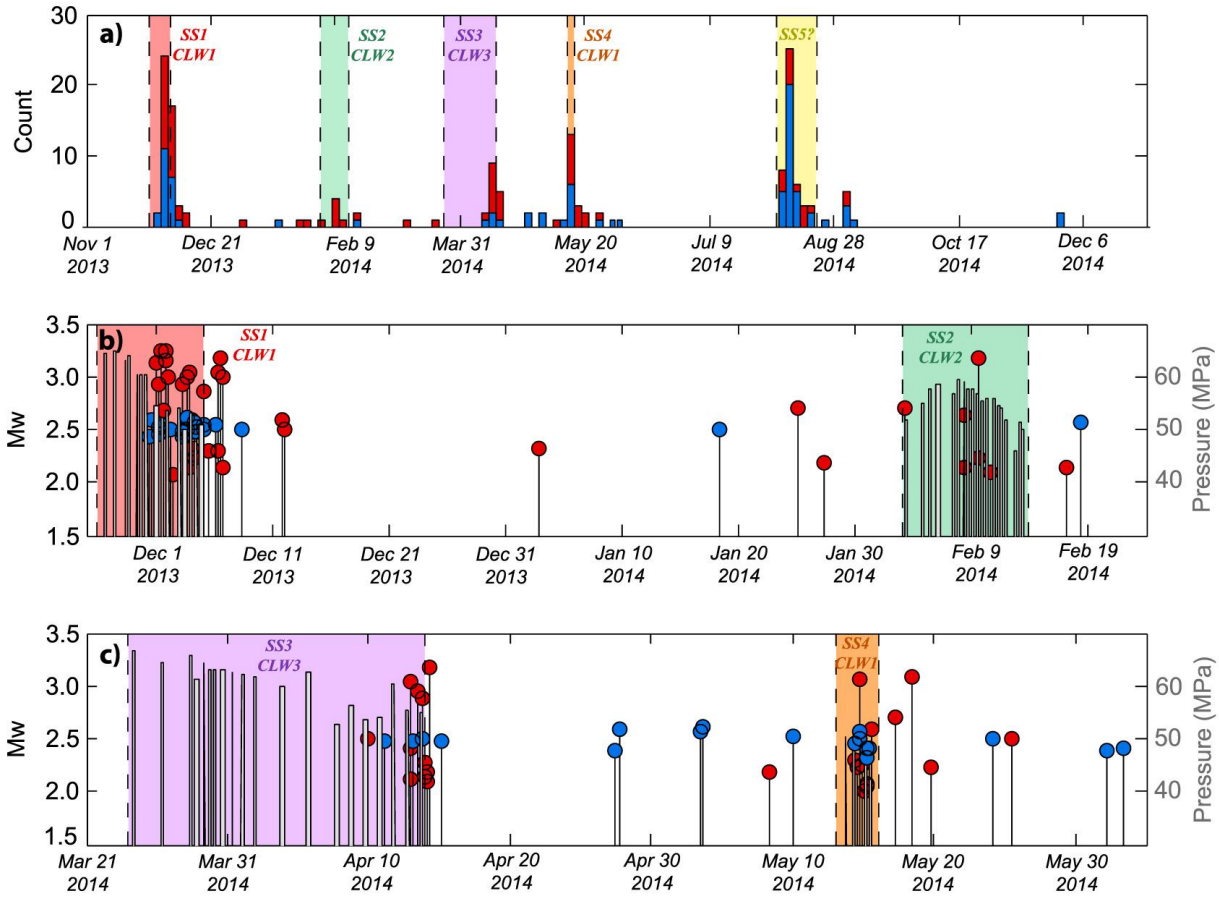


Figure 65: Comparison of earthquakes and hydraulic fracturing completions at Crooked Lake, Alberta, Canada. (a) Histogram of located seismicity (red bars), with number of earthquakes increased using waveform cross correlation (blue bars). Hydrofracture schedules are bounded by colored boxes and labeled with respective sub-sequence and borehole. (b) Magnitudes of located (red circles), detected (blue circles) earthquakes and average injection pressure during hydrofracture stages (gray bars). (c) Same as (b) for later borehole completions [from Schultz *et al.*, 2015].

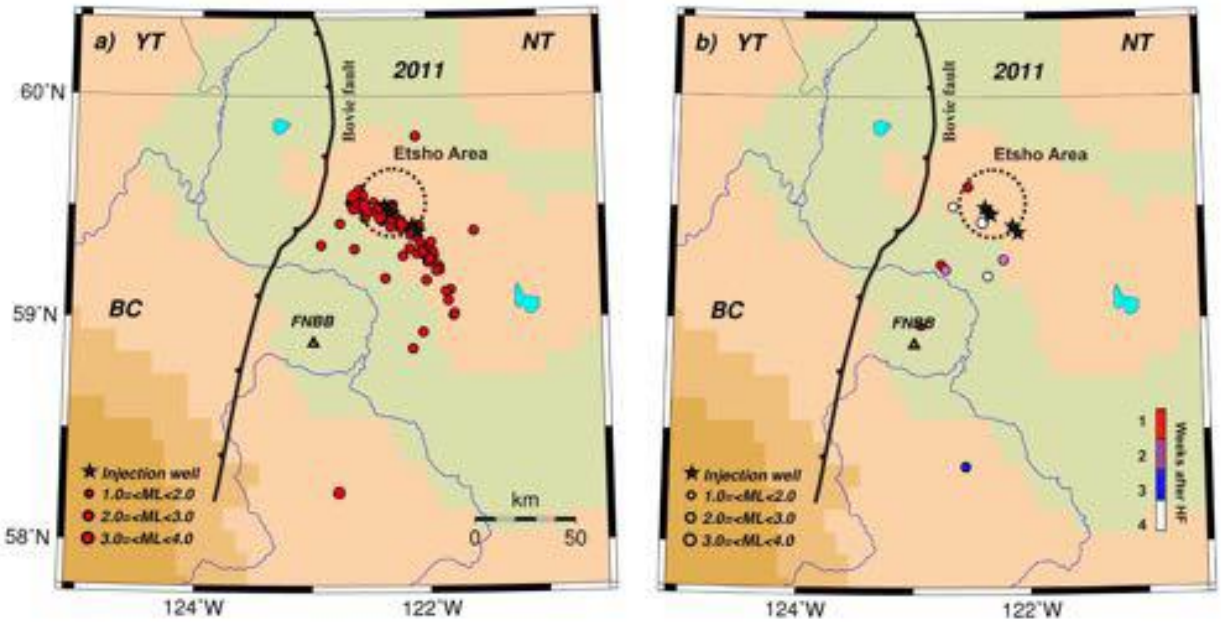


Figure 66: Map of the Horn River Basin, British Columbia, Canada. Left: seismicity on days when hydrofracturing took place. Right: days when it did not occur [from Farahbod *et al.*, 2015].

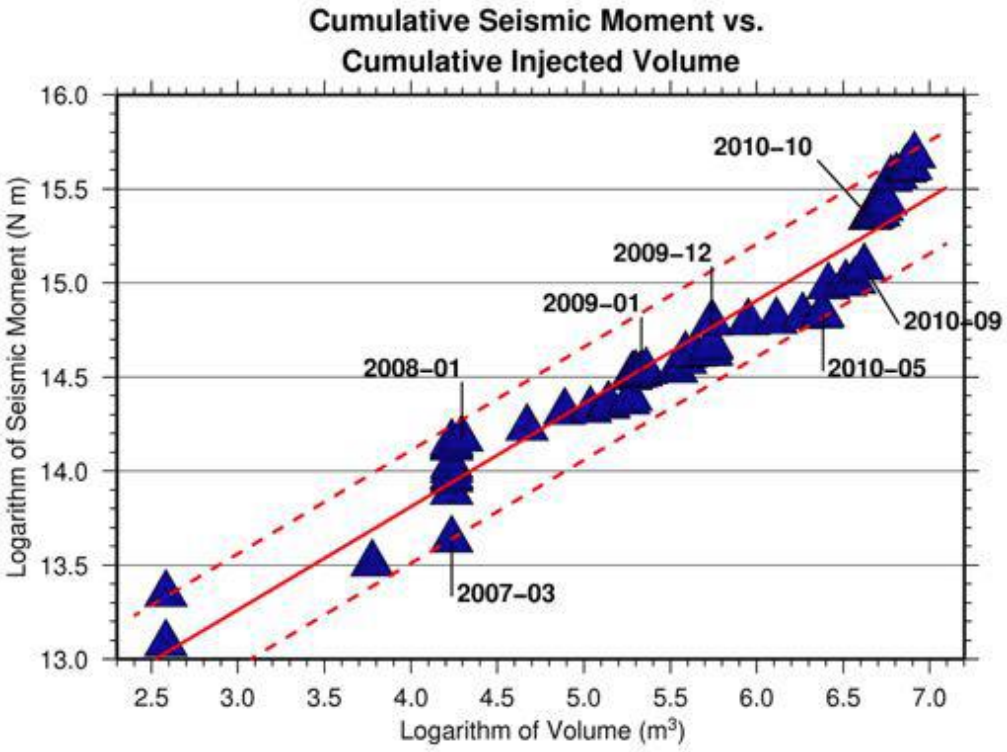


Figure 67: Logarithm of seismic moment vs. logarithm of volume injected in shale gas hydrofracturing operations in the Etsho area, Horn River Basin, British Columbia, Canada [from Farahbod *et al.*, 2015].

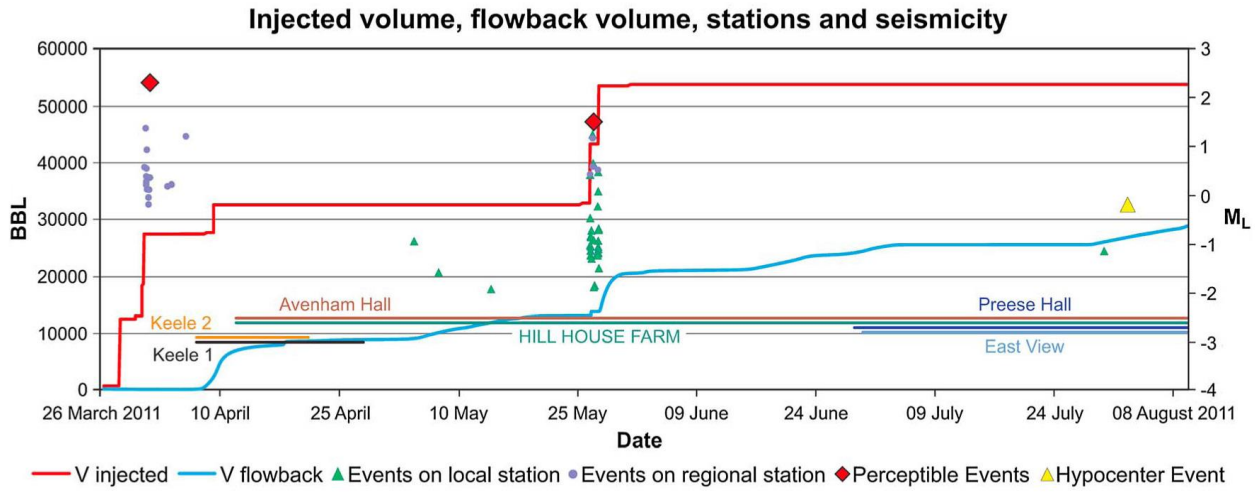


Figure 68: Injection activity and seismicity associated with shale-gas hydrofracturing at Preese Hall, Lancashire, UK. Red line: injected volume; blue line: flow-back volume from the well-head in US barrels (0.159 $m^3$); violet dots: earthquakes detected on seismic stations at distances of > 80 km; green triangles: earthquakes detected on two local stations; yellow triangle: event for which source mechanism and reliable hypocenter were obtained [from Clarke *et al.*, 2014b].


Figure 69: Site of the former Cacoosing Valley, Pennsylvania, quarry. Red oval: approximate boundary of the old quarry. Satellite image from Google Maps.

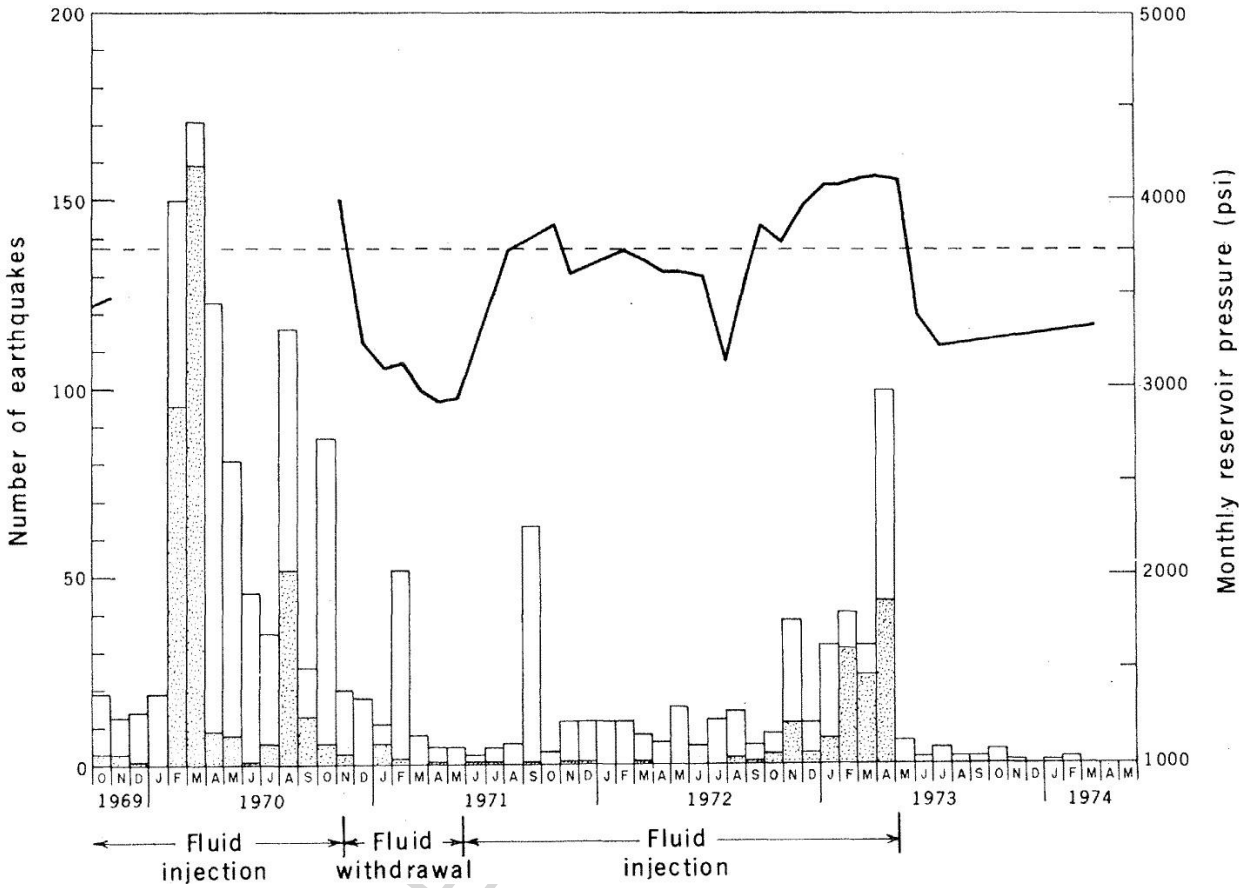


Figure 70: Frequency of earthquakes at the Rangely Oilfield, Colorado, and reservoir pressures during fluid injection and fluid withdrawal. Stippled bars: earthquakes within 1 km of injection wells; black line: pressure history in injection well Fee 69; dashed line: predicted critical reservoir pressure [from Raleigh *et al.*, 1976].

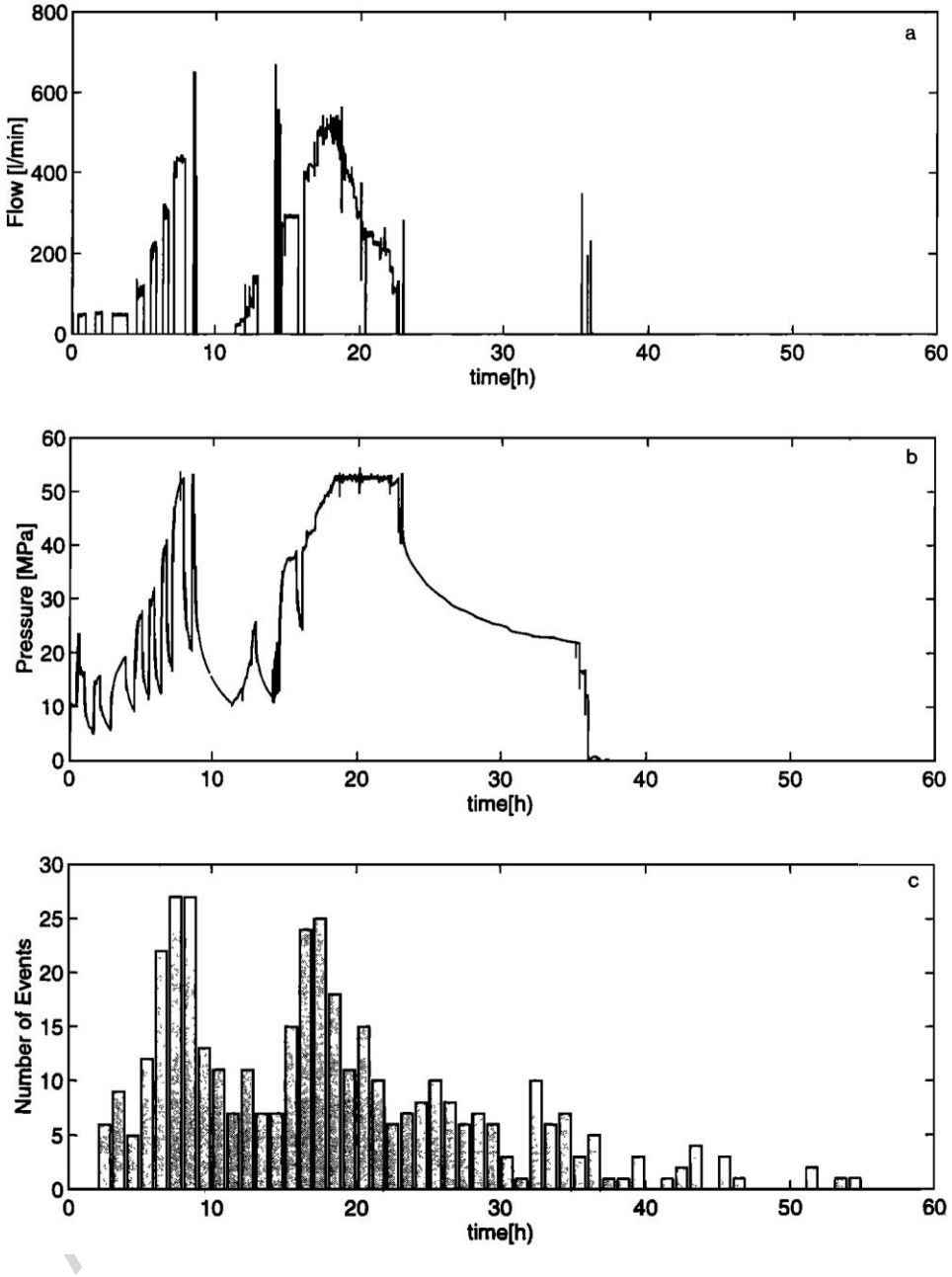


Figure 71: Flow rates, pressure and number of earthquakes induced by brine injection into the Kontinentales Tiefbohrprogramm der Bundesrepublik Deutschland (KTB–the German Continental Deep Drilling Program) borehole during a 60-hour period [from Zoback & Harjes, 1997].

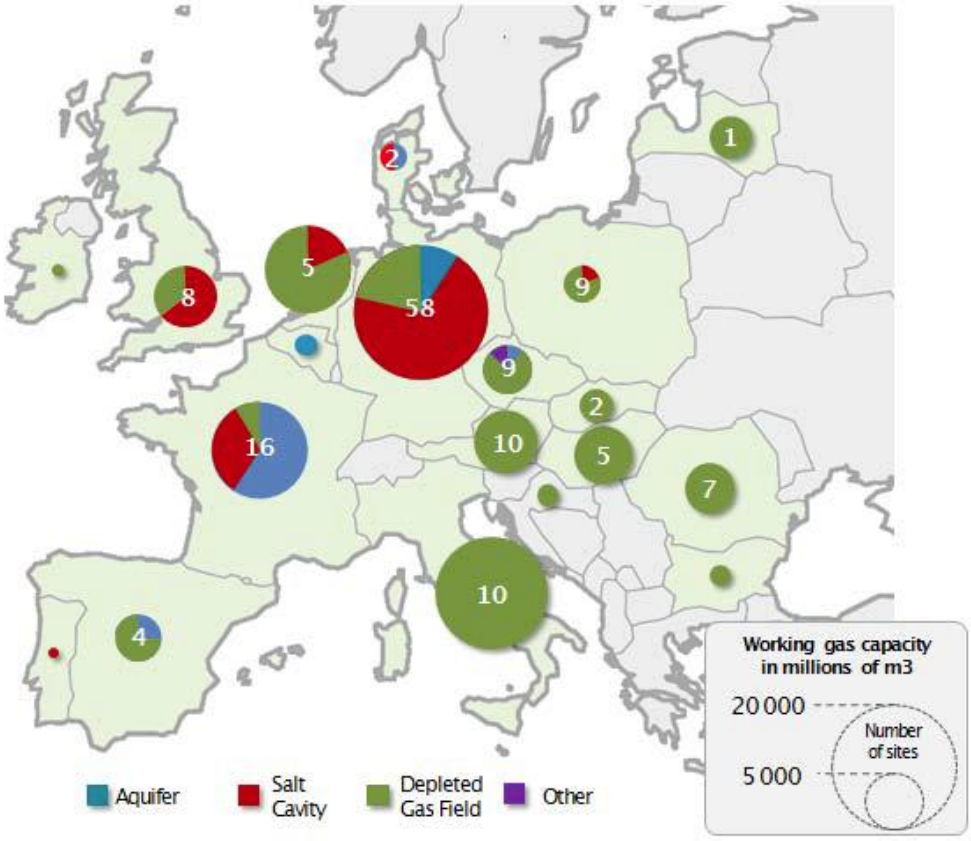


Figure 72: Working gas capacities of underground storage sites in Europe[19].

[19] http://www.gasinfocus.com/en/ ; http://www.gie.eu/index.php/maps-data/gse-storage-map

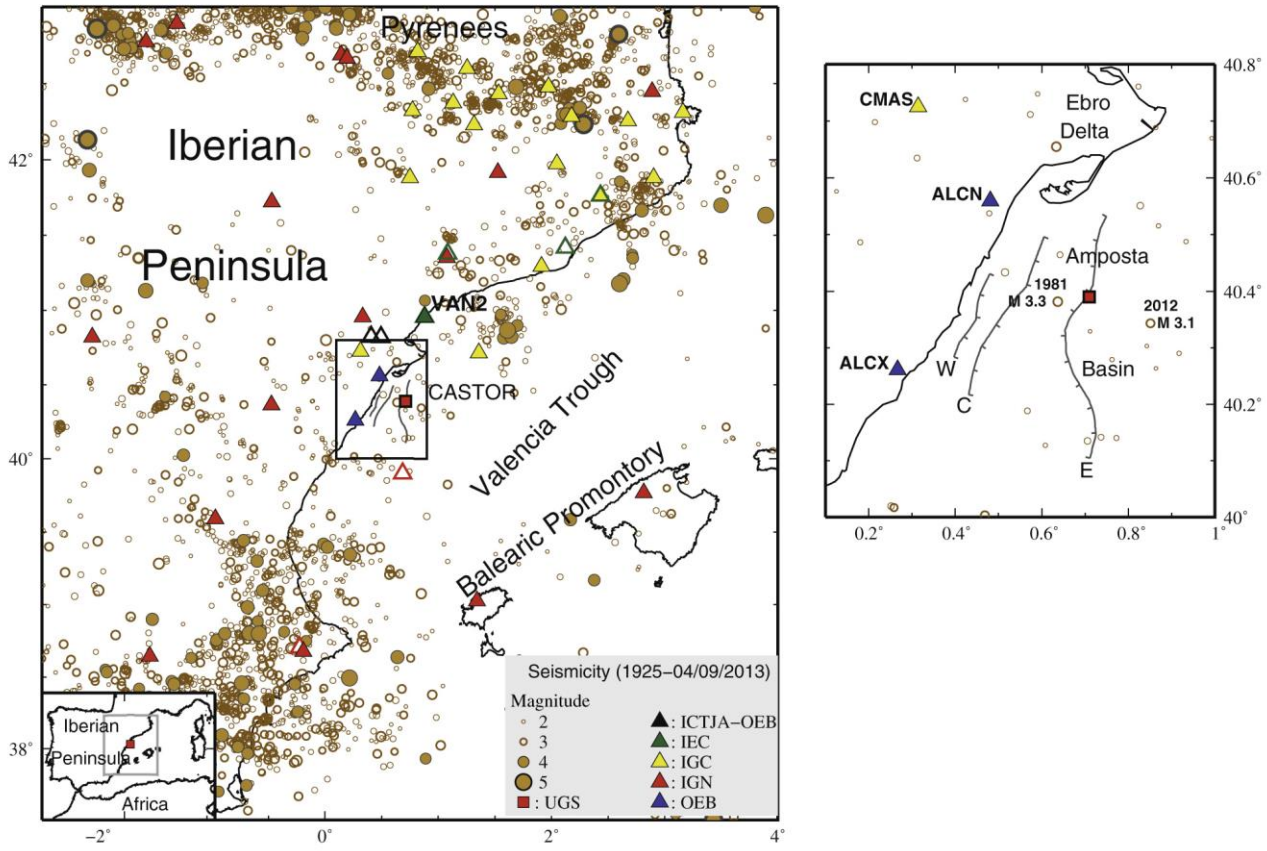


Figure 73: Seismicity of the eastern Iberian Peninsula, Spain. Triangles: seismic stations; red square: location of the Castor underground gas storage reservoir. W, C and E denote the Western, Central and Eastern Amposta faults [from Gaite *et al.*, 2016].

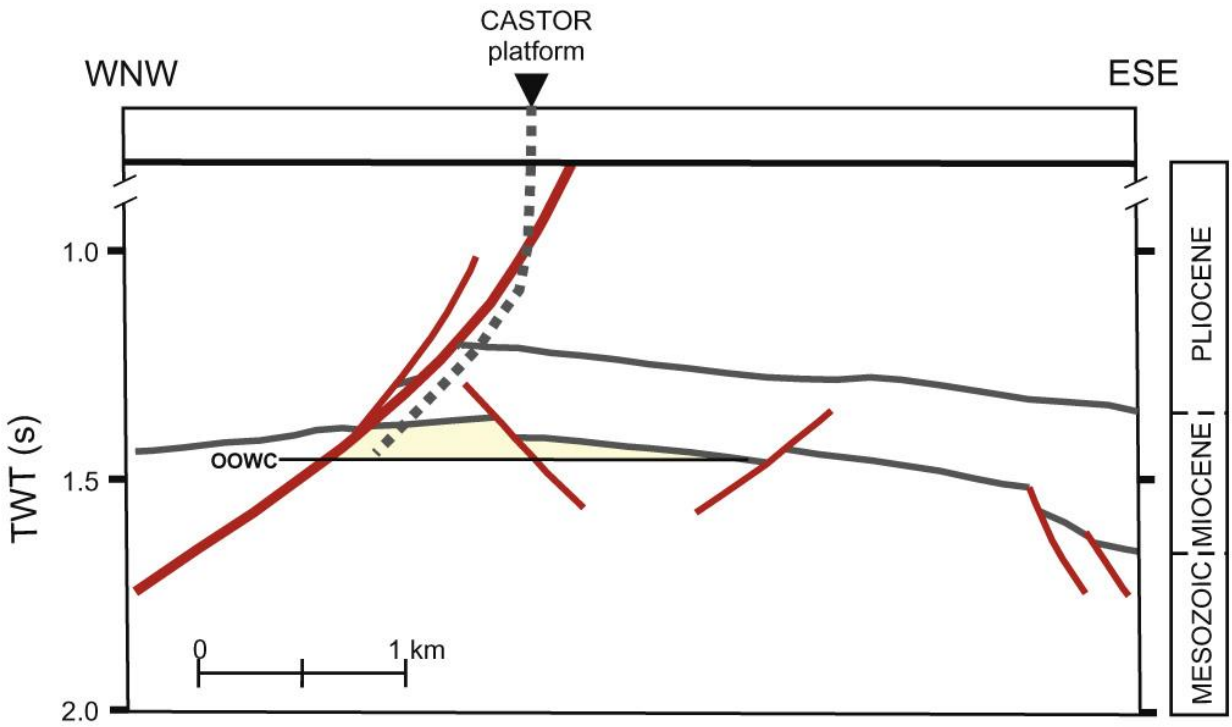


Figure 74: Schematic diagram of the old Amposta Oilfield, Spain, in WNW-ESE section. TWT: two-way traveltime; dashed line: approximate location of the Castor injection well: OOWC: original oil-water contact at 1940 m depth; yellow area: approximate location of the gas reservoir [from Gaite *et al.*, 2016].

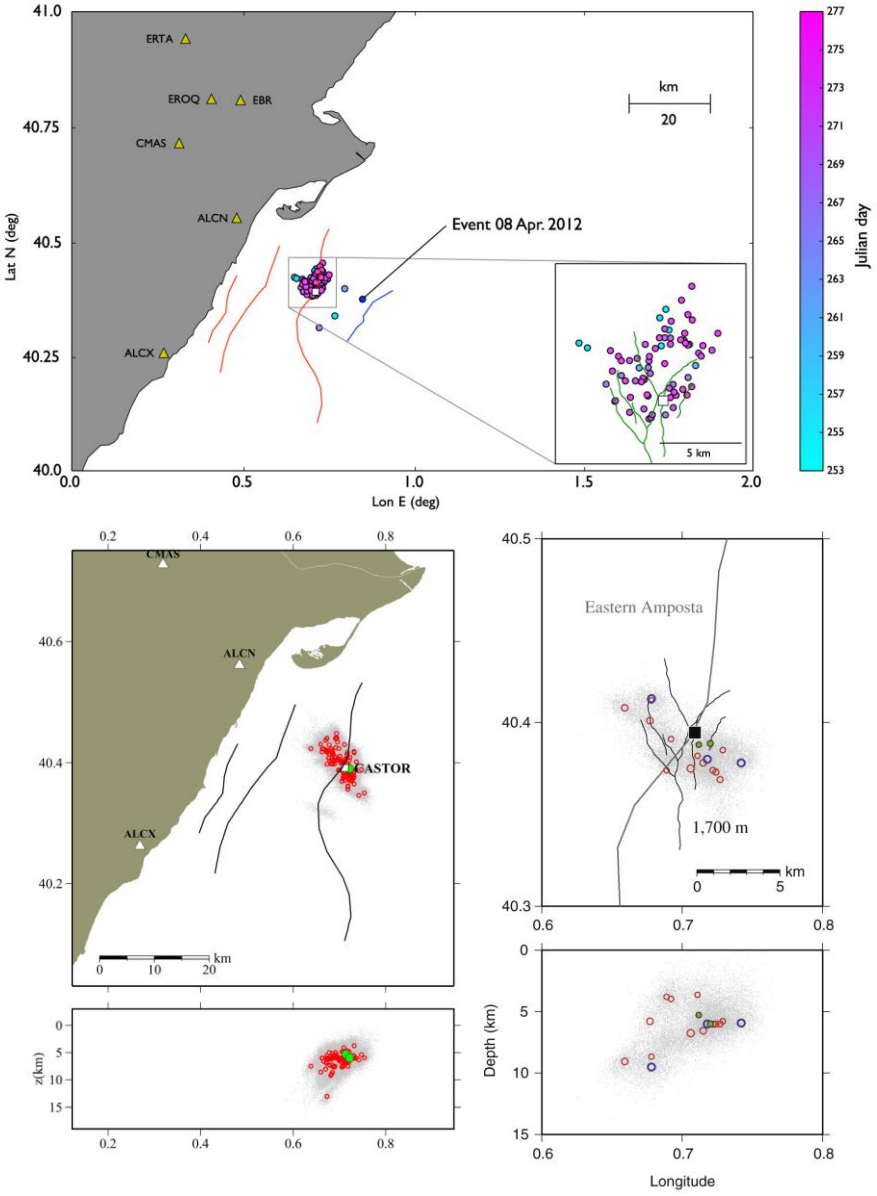


Figure 75: Top: Faults and epicenters for the largest events in the 2013 earthquake sequence in the "old Amposta Field". White square: Castor platform; colored lines: faults near the injection site; red lines: the Amposta faults; blue and green lines: additional faults [from Cesca *et al.*, 2014]. Bottom left: map and cross-section showing 116 earthquakes associated as a multiplet; triangles: seismic stations; white square: injection well; green dots: two events with M 3.0 and 3.2. Bottom right: map and cross-section of earthquakes with M > 3; black square: injection well [from Gaite *et al.*, 2016].

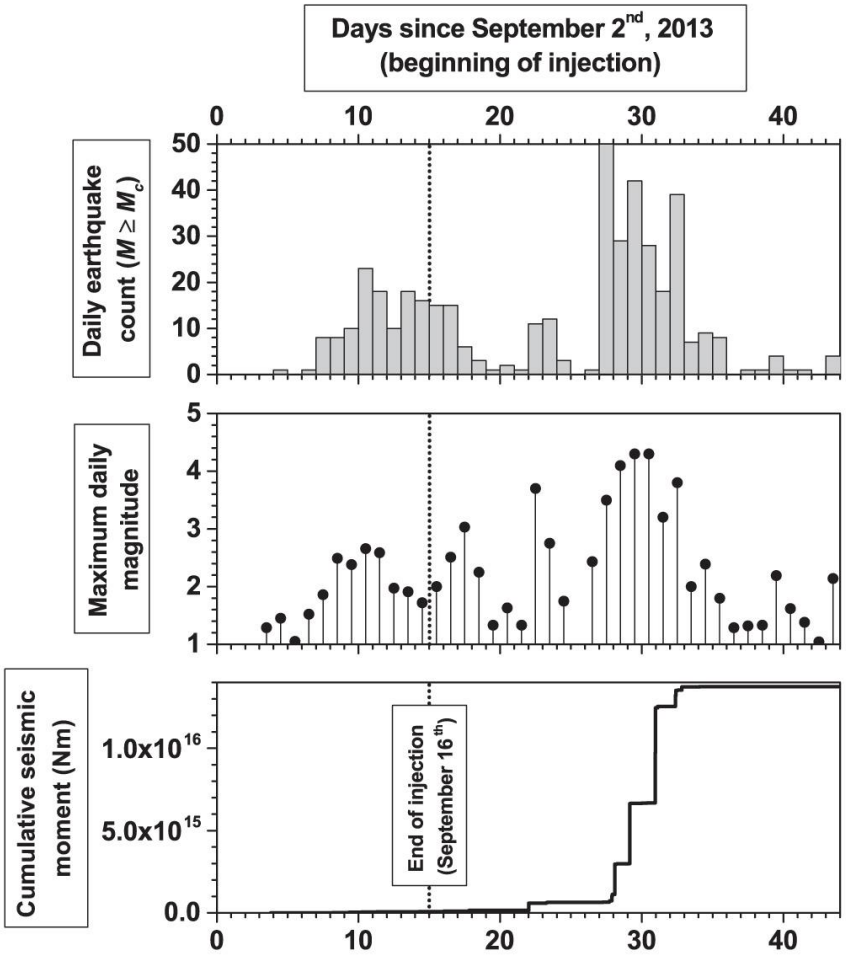


Figure 76: Temporal evolution of seismicity with M > 2 associated with the Castor project, Spain, for 44 days from the beginning of gas injection, 2 September, 2013. Top: daily number of events. Centre: maximum daily magnitude. Bottom: cumulative seismic moment [from Cesca *et al.*, 2014].

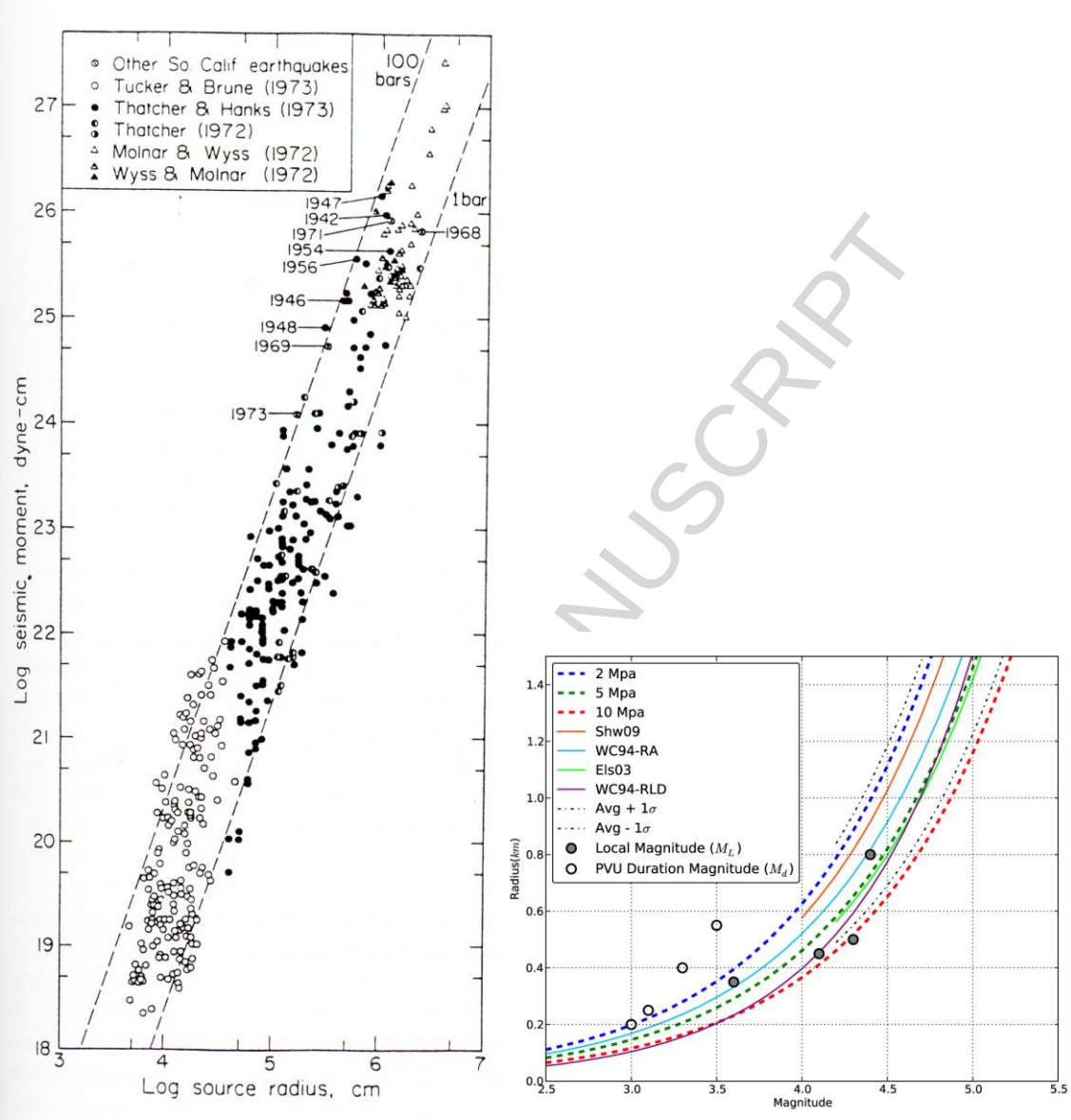


Figure 77: Left: Set of data for small earthquakes showing the relationship between seismic moment and source radius. Dashed lines are of constant stress drop [Hanks, 1977]. Right: Rupture radius vs. duration earthquake magnitude for several models. Black dotted lines: average of these relationships ±1σ; blue, green and red dashed lines: relationships derived from the moment-magnitude relation of Hanks and Kanamori [1979] for stress drops of 2, 5 and 10 MPa respectively, and estimated fault radius using half the rupture-length-at-depth parameter; gray and white circles: values for individual earthquakes induced at Paradox Valley, Colorado [from Yeck *et al.*, 2015].

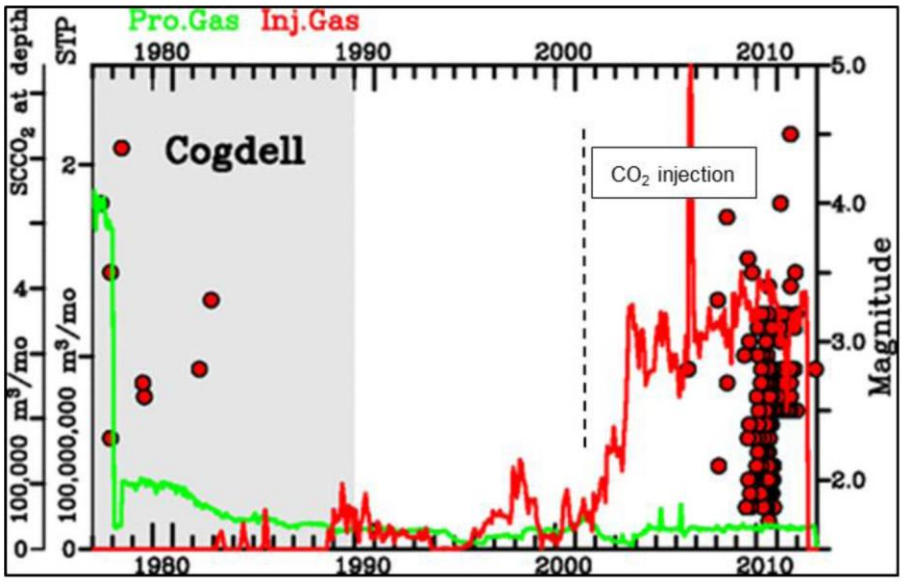


Figure 78: Operations and seismicity at the Cogdell Oilfield, Texas. Green: monthly volumes of natural gas produced; red: gas injected; red dots: earthquakes detected 1977-2012. There was a clear increase in seismic activity from 2006, five years after the start of $CO_2$ injection [from Gan & Frohlich, 2013].

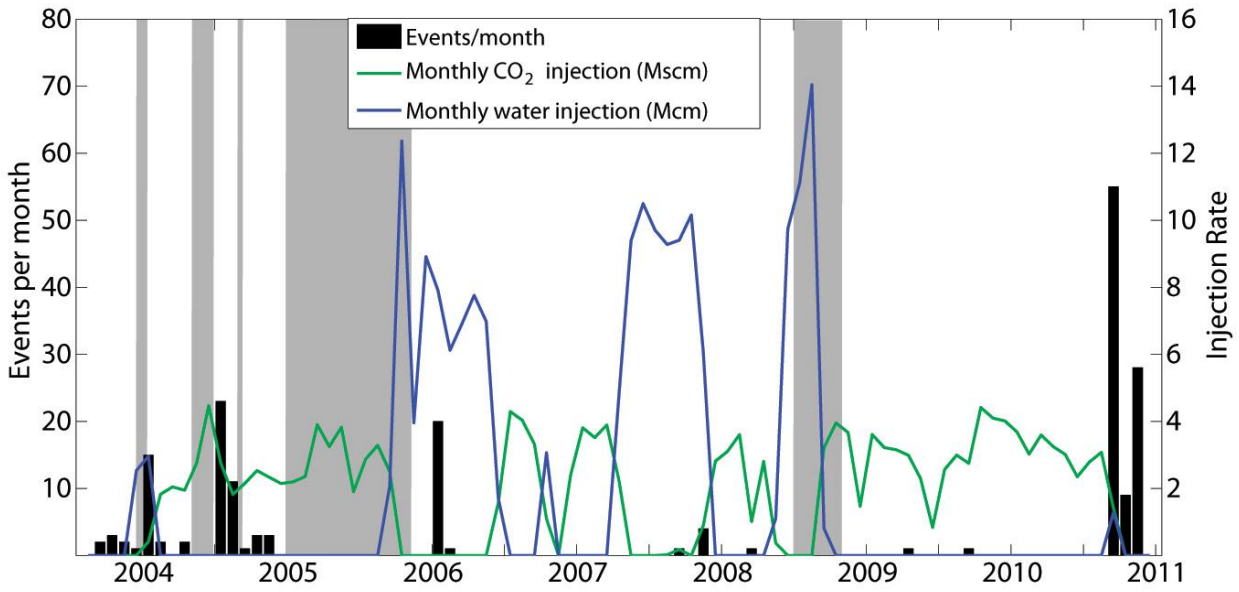


Figure 79: $CO_2$, water injection, and associated earthquakes at the Weyburn Oilfield, Saskatchewan, Canada. Shaded periods: monitoring array was inoperative [from Verdon *et al.*, 2013].

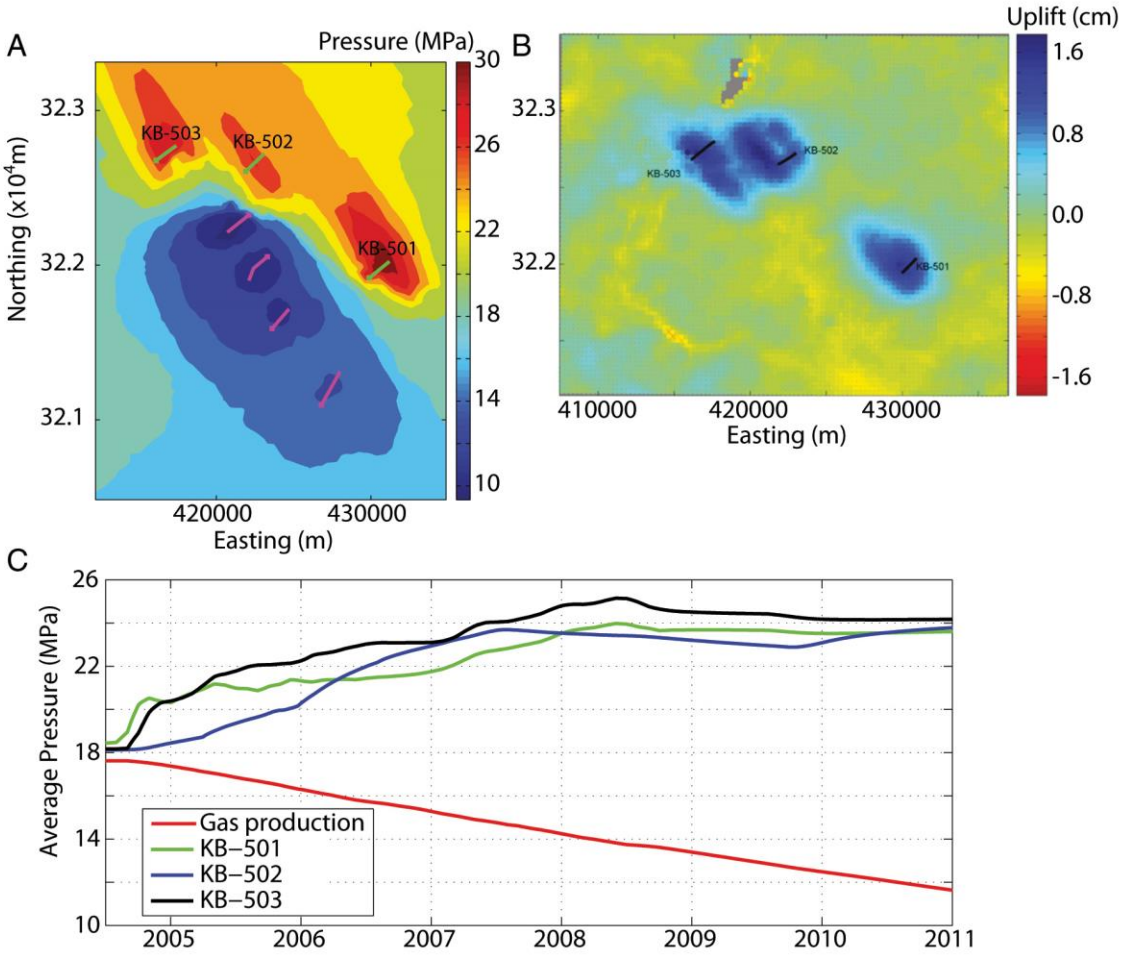


Figure 80: Modelled pore pressure and geo-mechanical deformation at In Salah, Algeria. A: Map of pore pressure after three years of injection. B: Surface uplift measured by InSAR. C: Modelled pressure at the three injection wells and in the producing part of the reservoir [from Verdon *et al.*, 2013].

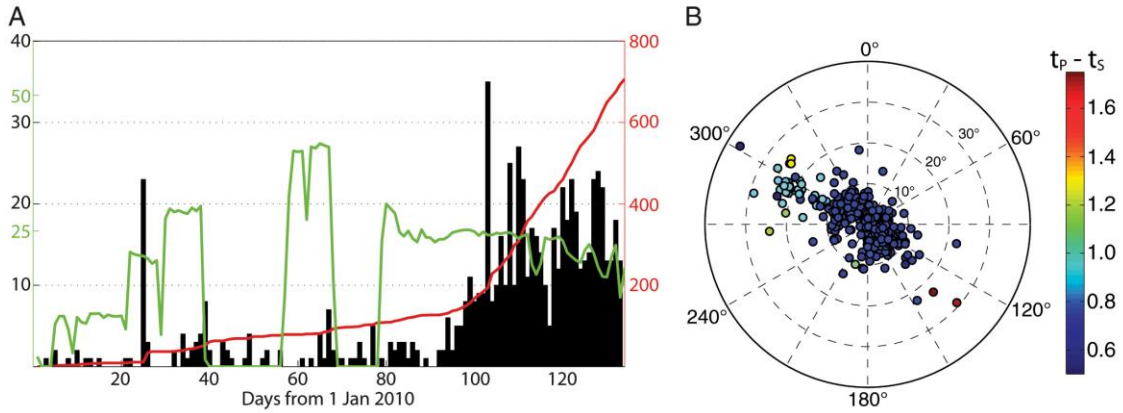


Figure 81: Microseismicity at In Salah, Algeria. A: Black: daily seismicity rate; red: cumulative number of events January-April 2010; green: $CO_2$ injection rate in millions of standard cubic feet per day[20]. B. Event arrival angles in polar projection, colored by differential *S*- and *P*-wave arrival times [from Verdon *et al.*, 2013].

[20] 1 million standard cubic feet of gas per day at 15˚C = 28,252.14 $m^3$/day

Figure 82: Aerial photograph of the Nevada test site, USA. View of Yucca Flat looking south-southeast. Center of ring road is at 37˚N 9.57', 116˚W 4.63', elevation 4,400 m[21].



[21] https://en.wikipedia.org/wiki/Nevada_Test_Site

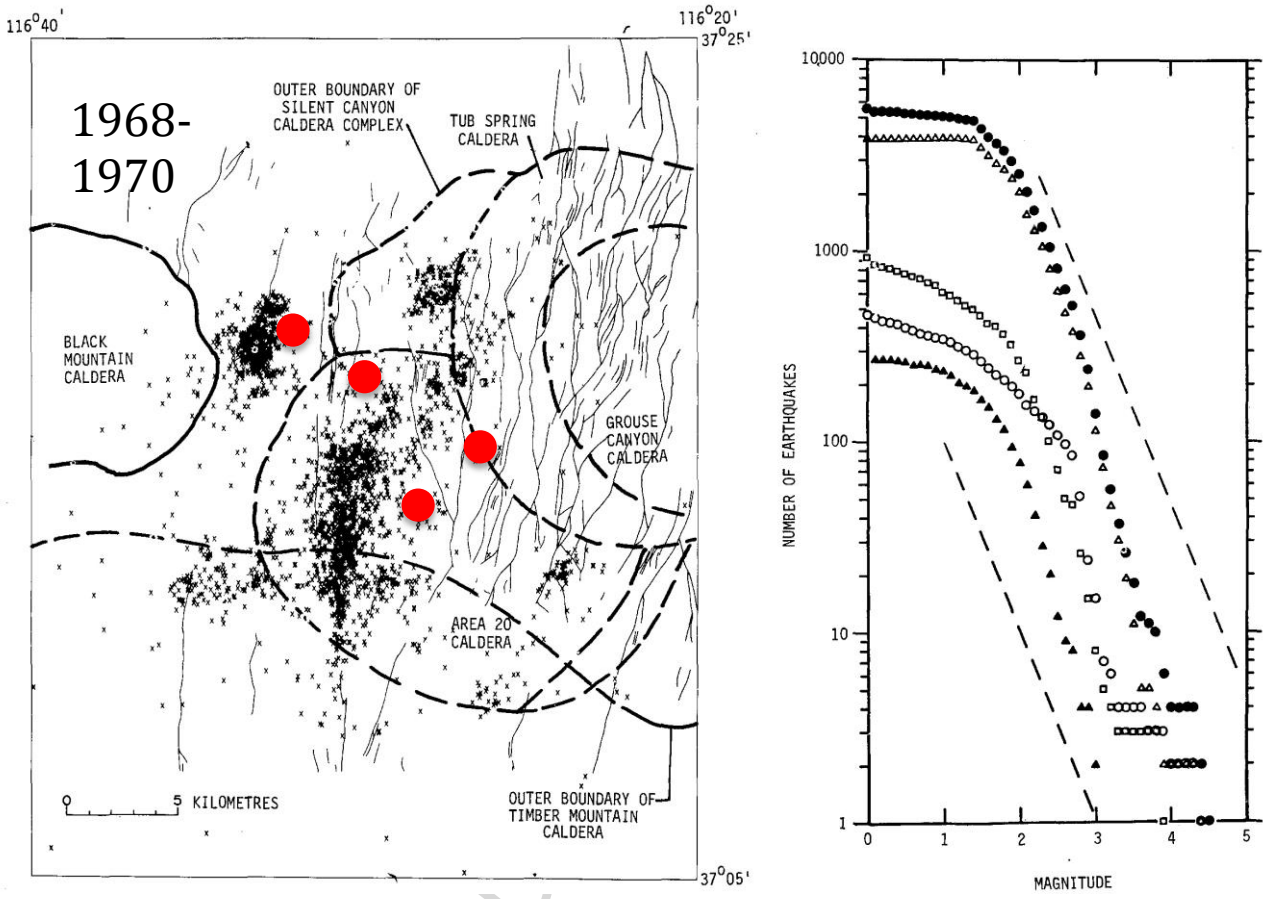


Figure 83: Left: Epicenters of aftershocks of the Benham (1968), Jorum (1969), Purse (1969), and Handley (1970) nuclear explosions at the Nevada Test Site. Heavy lines: caldera boundaries; light lines: basin-range faults; red dots: locations of nuclear explosions. Right: Frequency-magnitude distribution for aftershocks in Pahute Mesa [from Hamilton *et al.*, 1972]. Dots: entire recording period; open triangles: the period Benham to Purse; solid triangles: Purse to Jorum; circles: Jorum to Handley; squares: Handley to the end. Dashed lines have a slope of -1; the data above M 2 define "*b*-slopes" of about -1.4 [from McKeown, 1975].

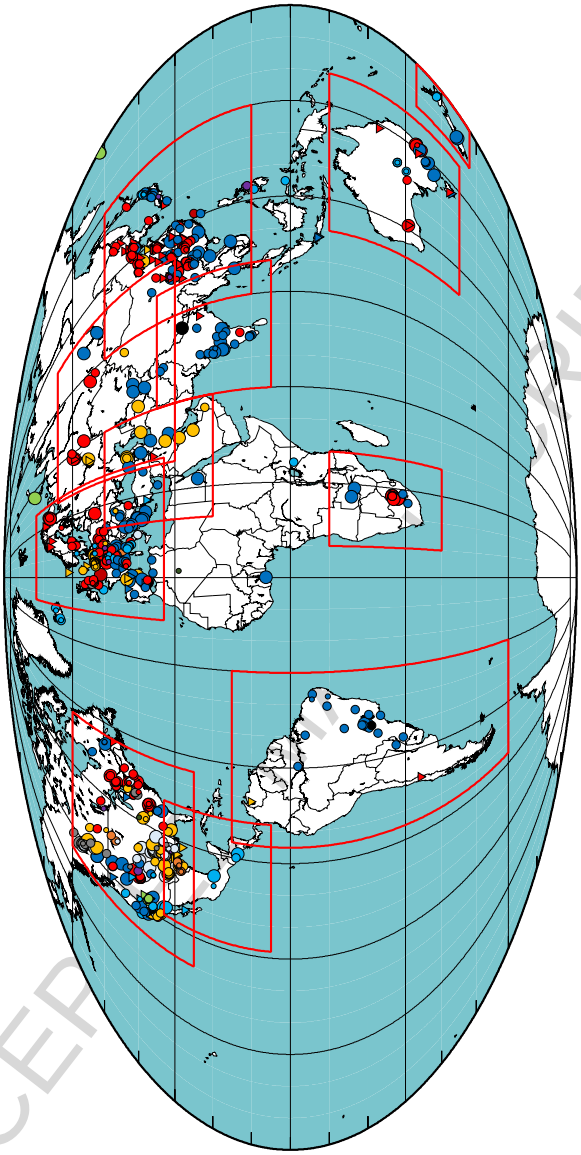

Figure 84: Cases of human-induced seismicity world-wide, in Mollweide projection, centered on the Greenwich meridian. Colors of symbols indicate different categories of seismogenic activity. Circle sizes indicate the magnitudes of the largest reported induced earthquakes in each category, and inverted triangles indicate cases for which this magnitude was not reported. Red boxes show the locations of the regional maps.

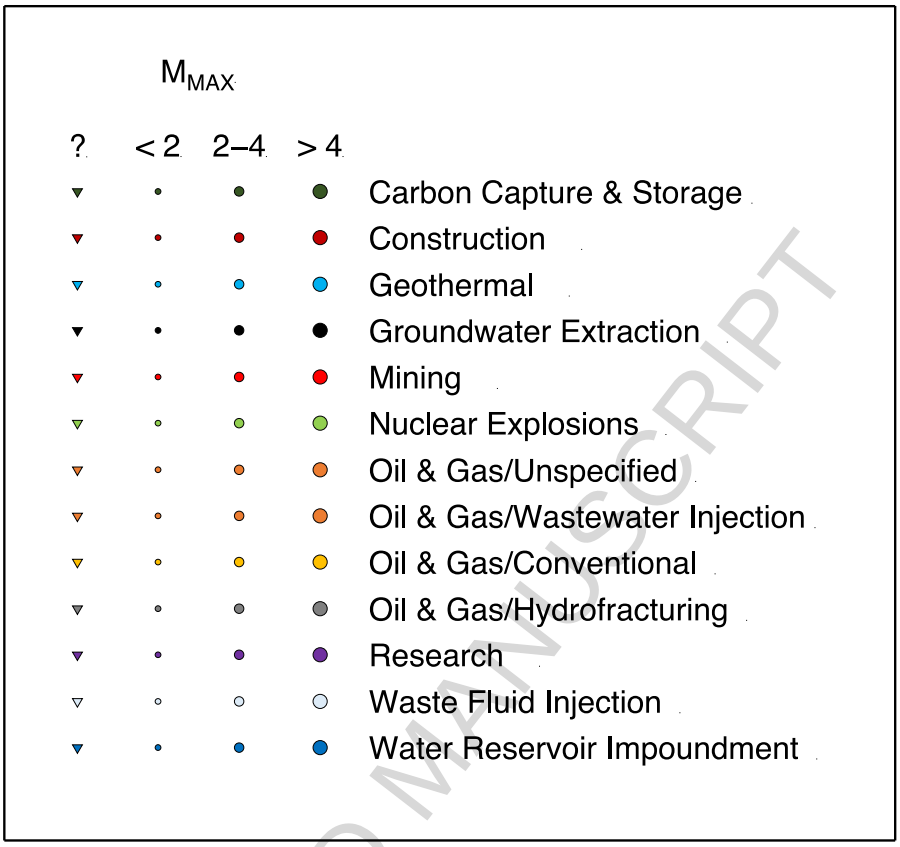


(Legend for Figure 84.)

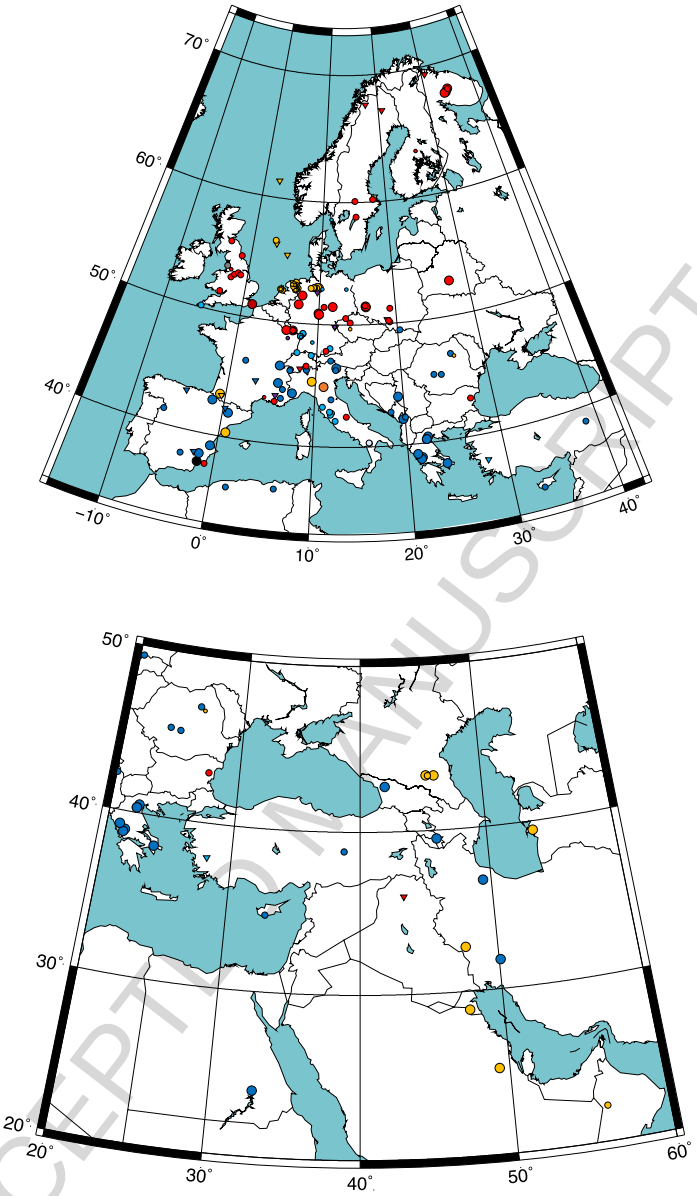


Figure 85: Same as Figure 84 except for (top) Europe, and (bottom) Middle East.

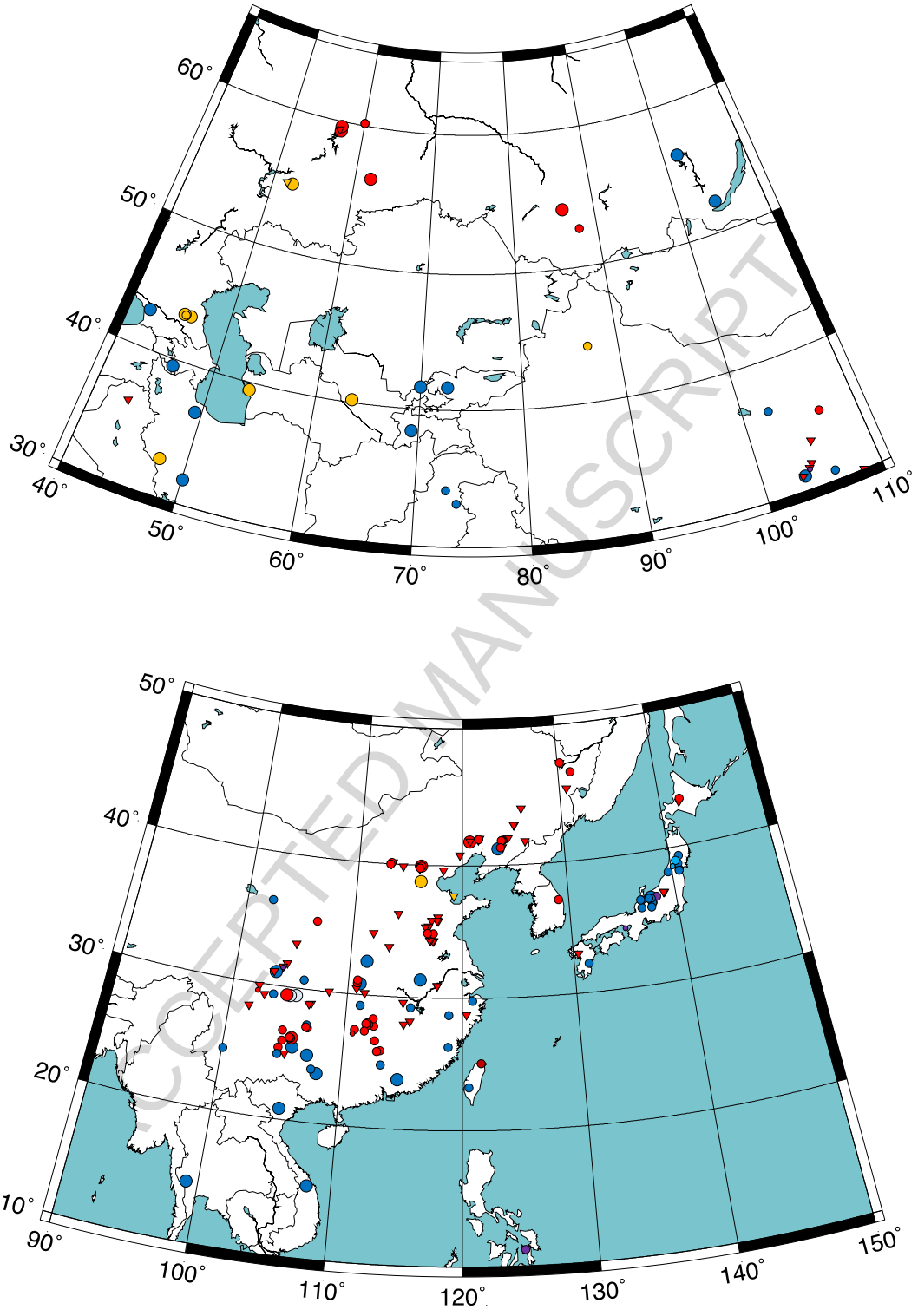


Figure 86: Same as Figure 84 except for (top) central Asia, and (bottom) east Asia.

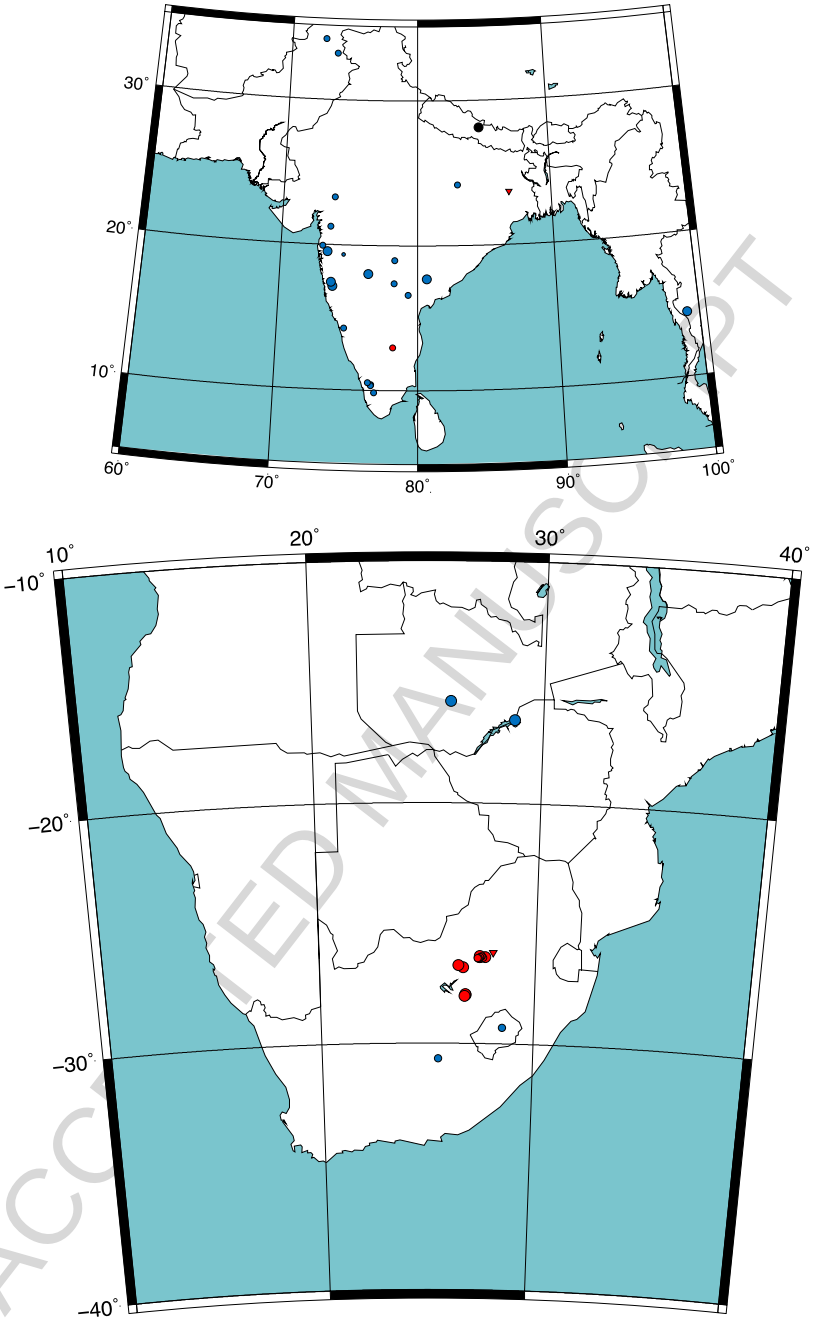


Figure 87: Same as Figure 84 except for (top) India and vicinity, and (bottom) southern Africa.

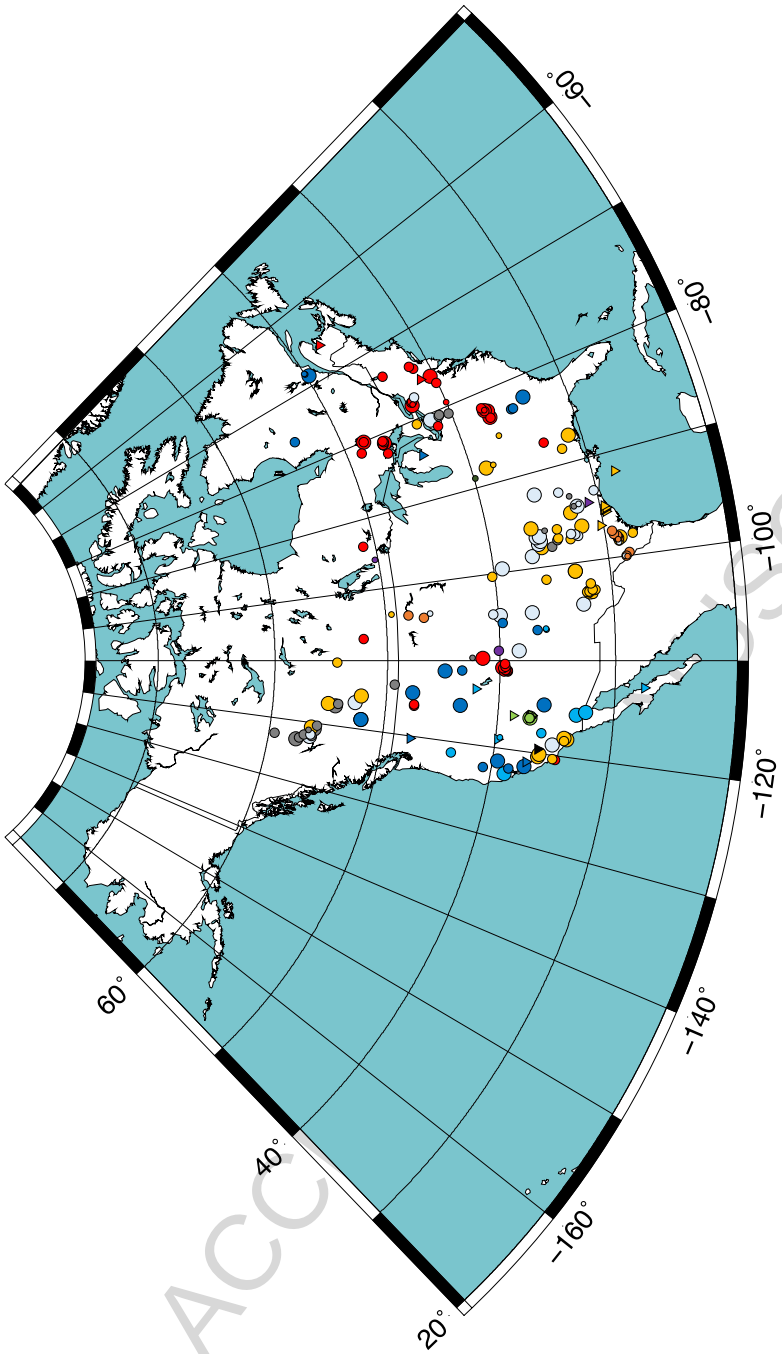

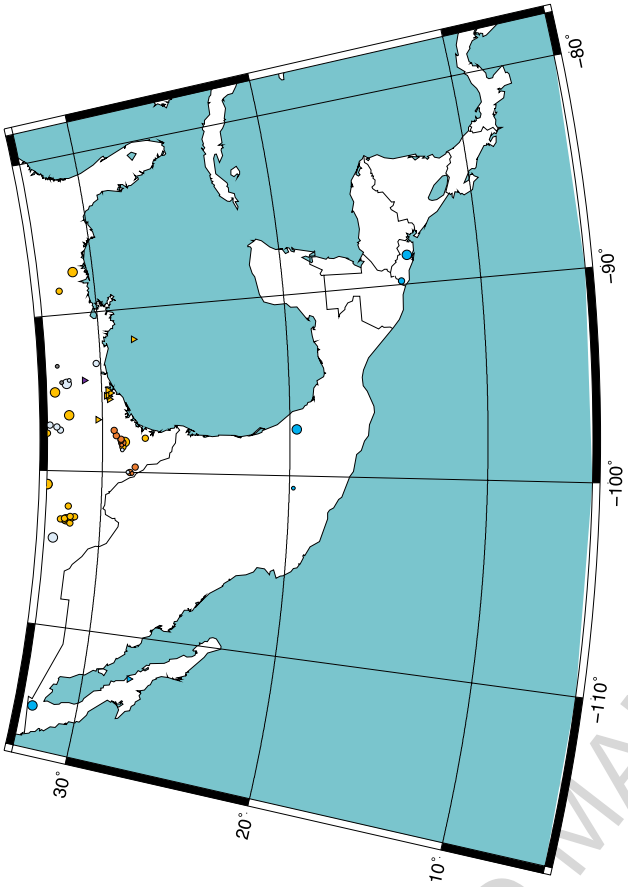


Figure 88: Same as Figure 84 except for (top) North America, and (bottom) central America.

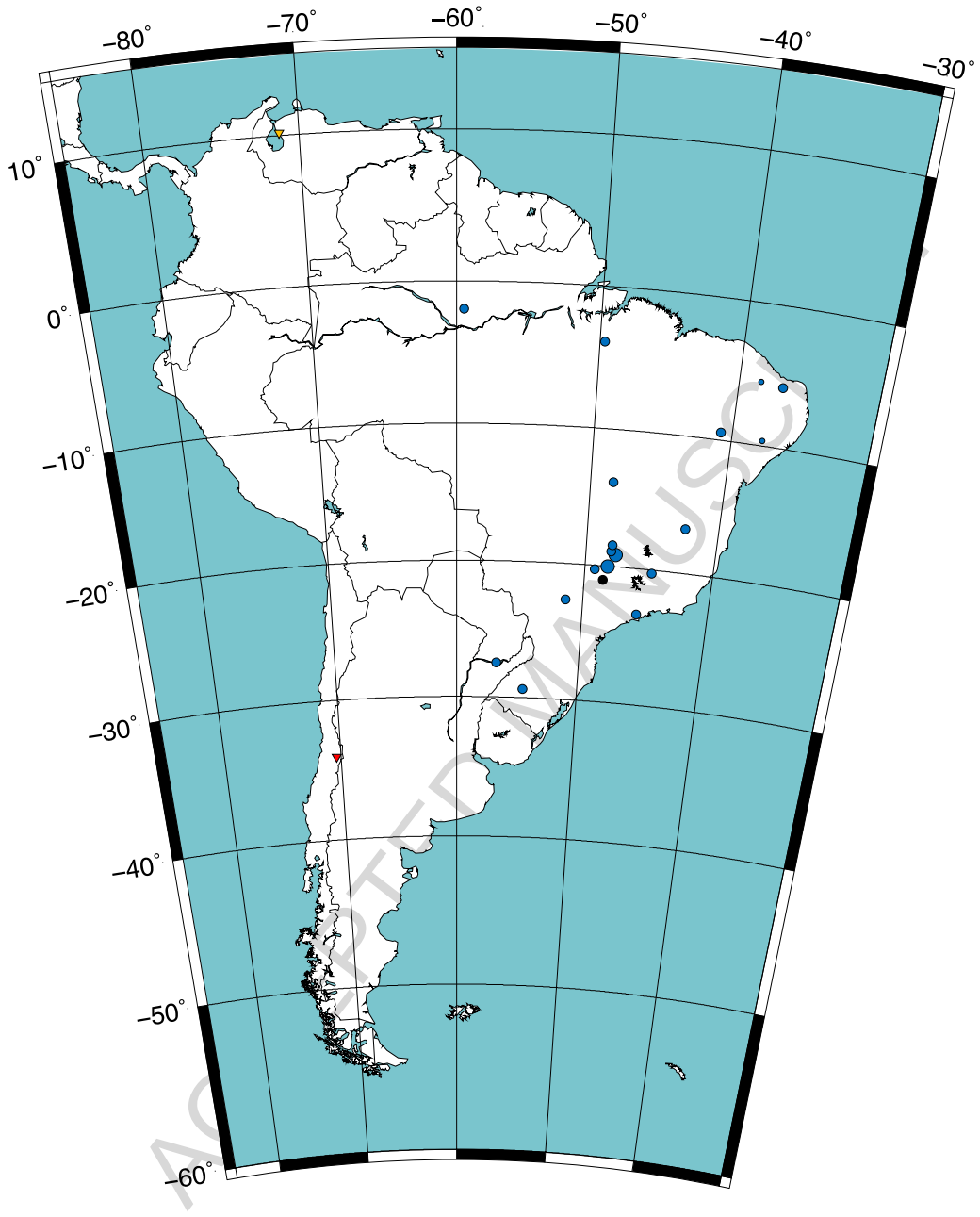


Figure 89: Same as Figure 84 except for South America.

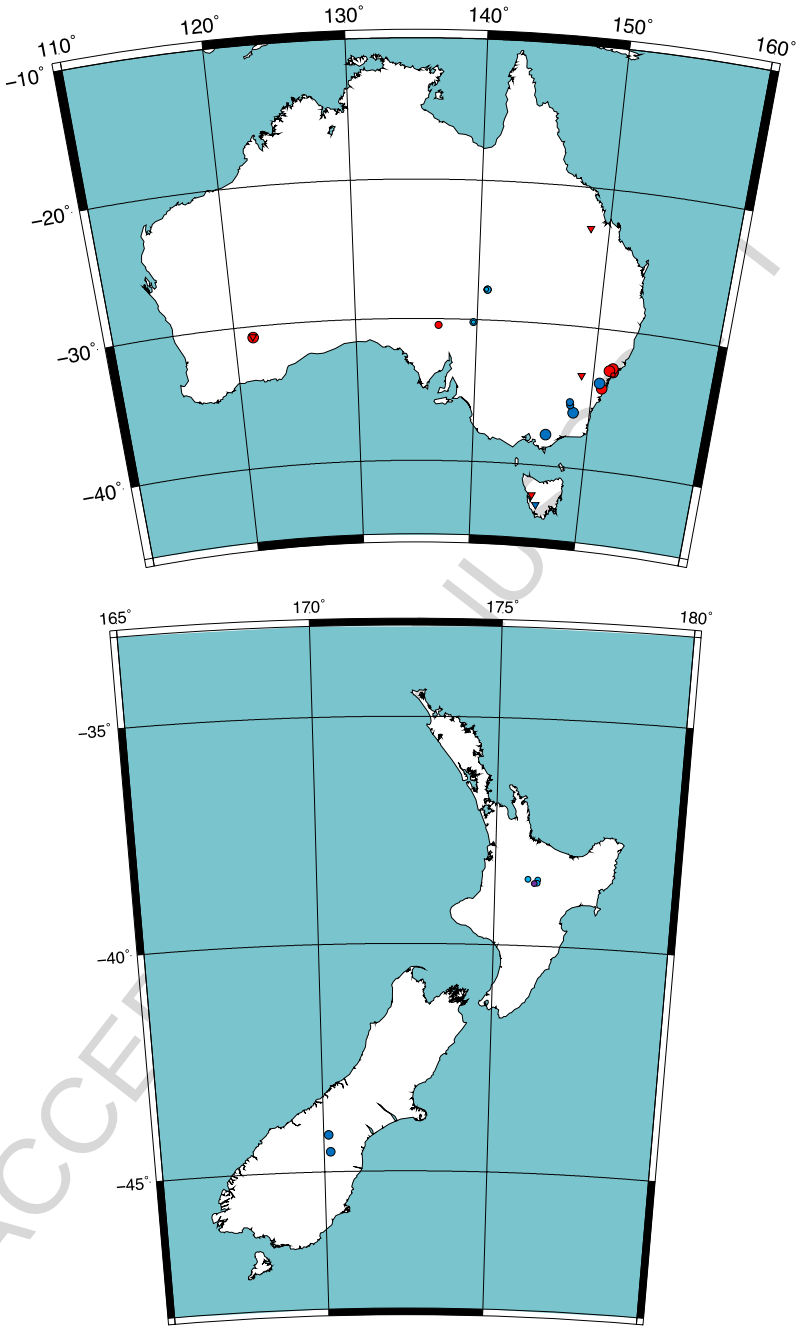


Figure 90: Same as Figure 84 except for (top) Australia, and (bottom) New Zealand.

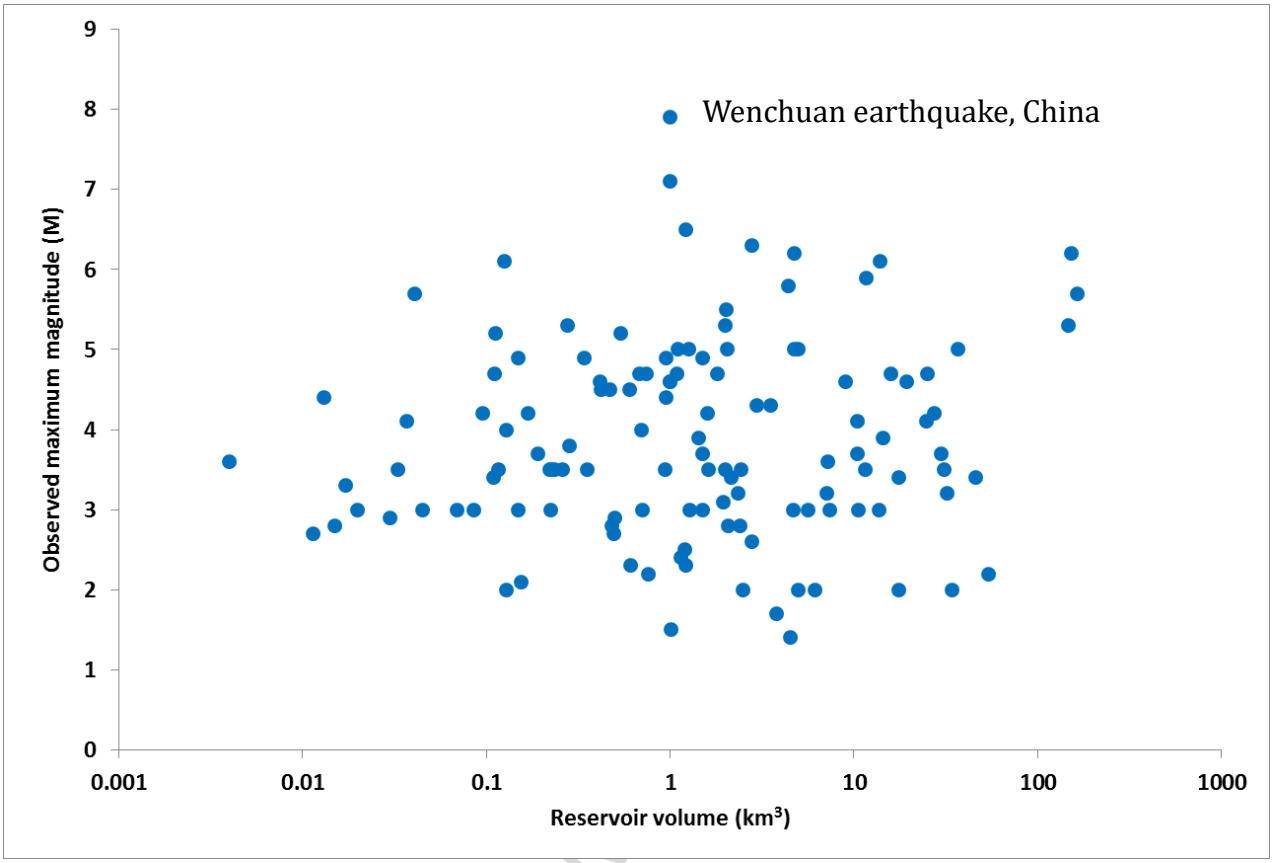


Figure 91: Plot of $M_{MAX}$ vs. water reservoir volume for the 126 cases for which data are available.

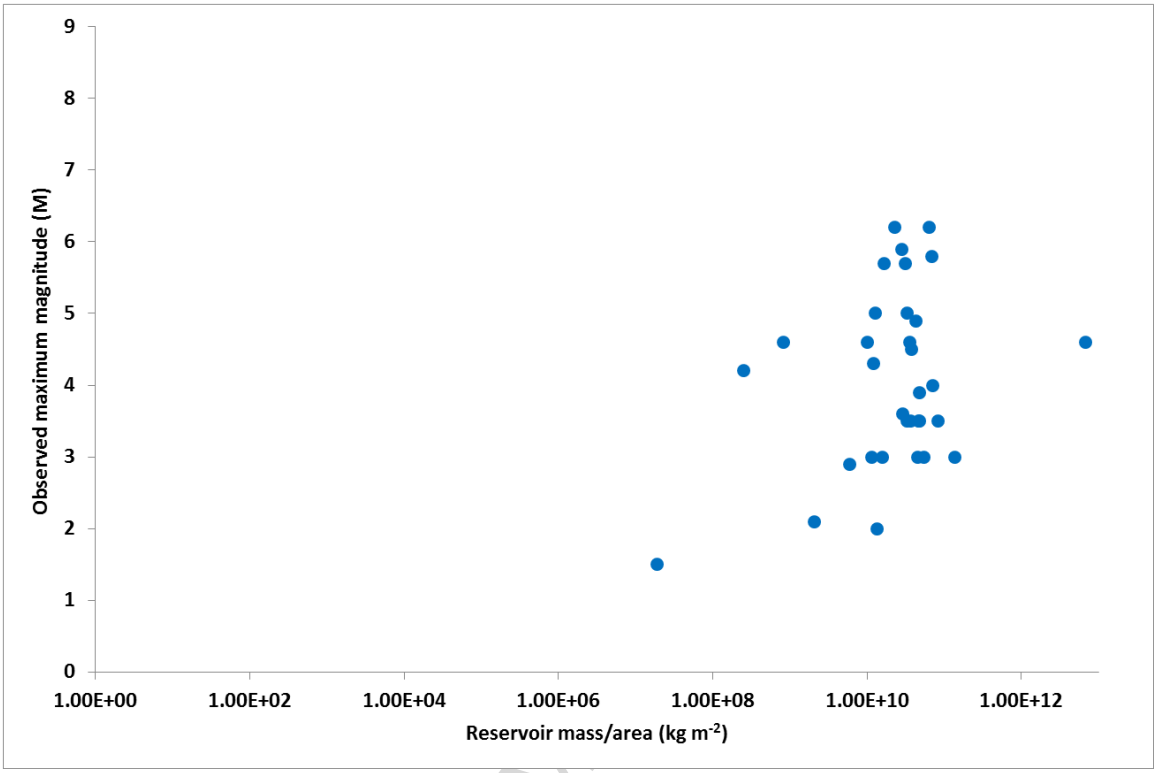


Figure 92: Plot of $M_{MAX}$ vs. water reservoir mass per unit area for the 33 cases for which data are available.

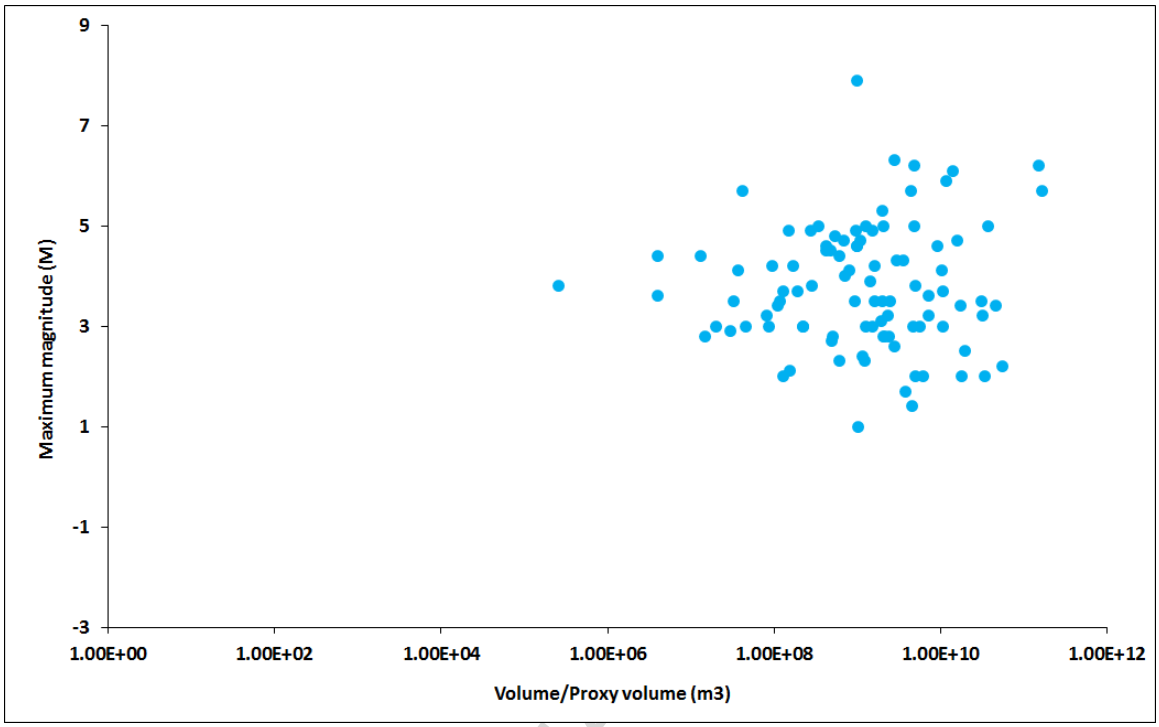


Figure 93: Plot of $M_{MAX}$ vs. volume added or removed by surface operations.

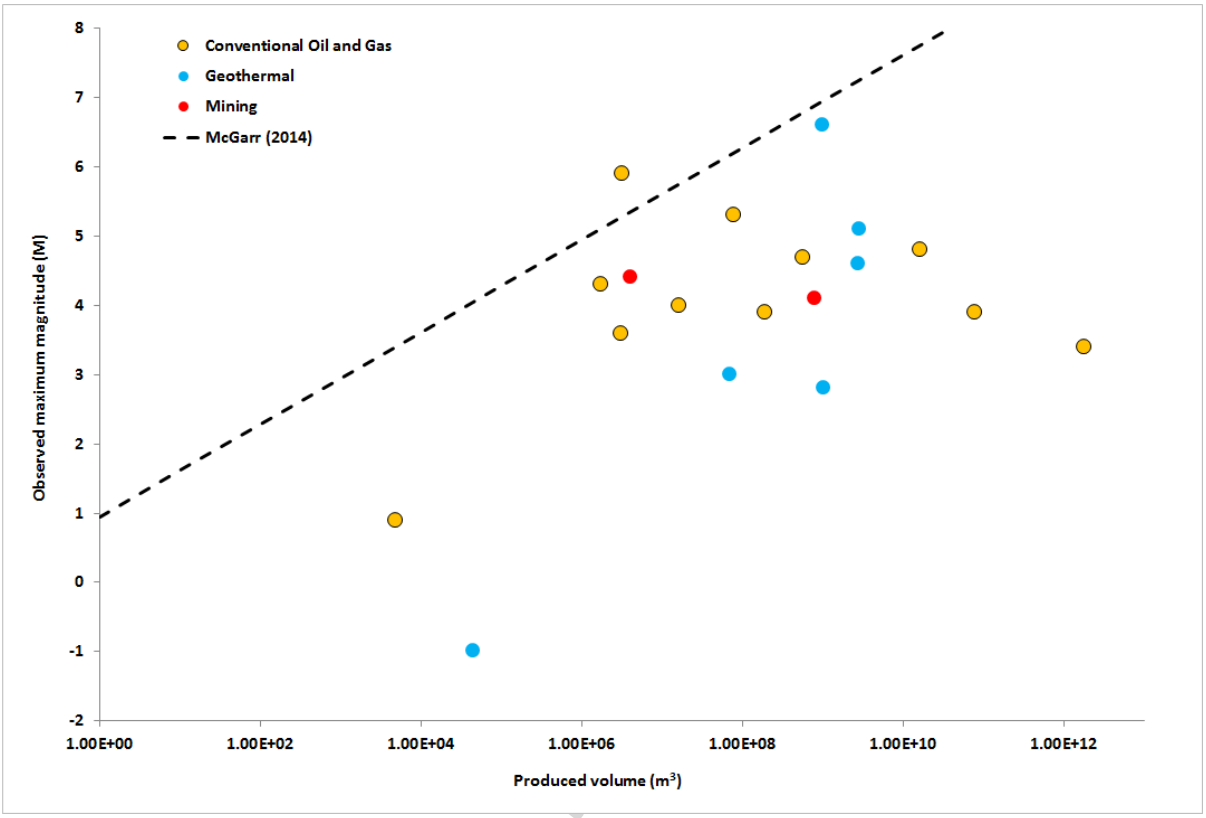


Figure 94: $M_{MAX}$ vs. produced volume ($m^3$) for 23 projects that involved extraction of mass from the subsurface. Some of these projects also involved injection, so their association with projection is not certain. The upper limit to $M_{MAX}$ proposed by McGarr [2014] on the basis of theoretical considerations is also plotted.

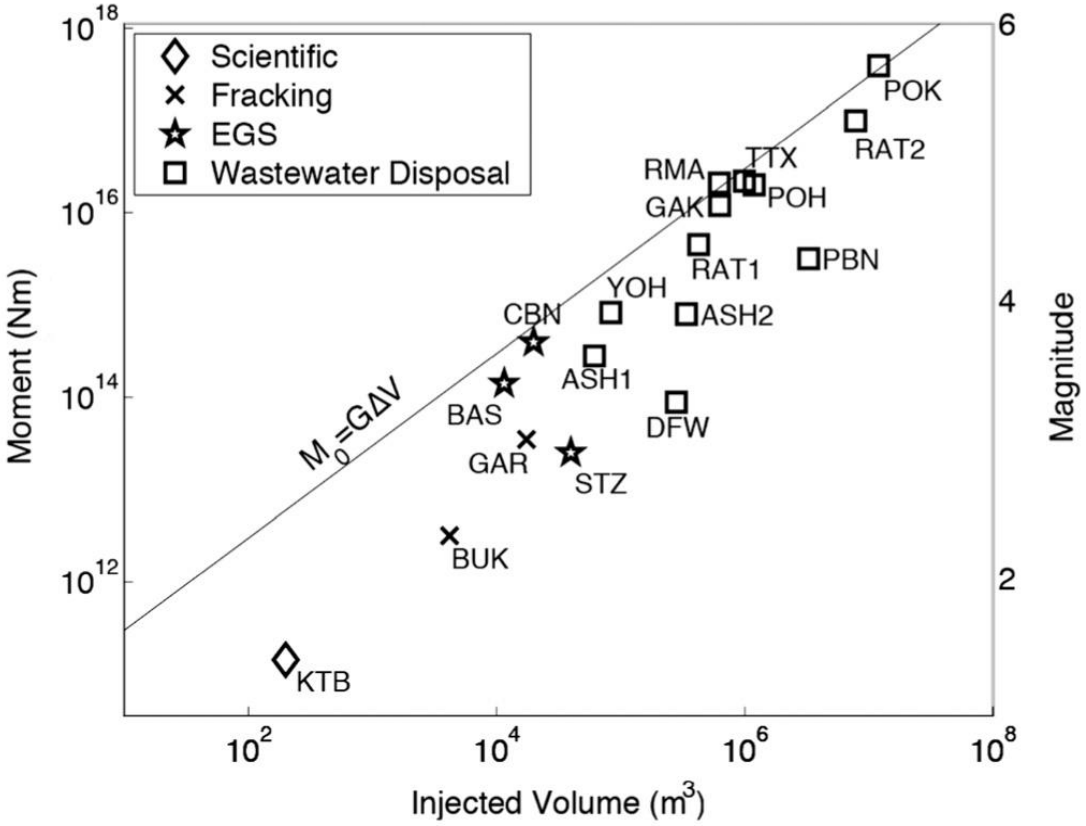


Figure 95: Maximum seismic moment and magnitude vs. total volume of injected fluid from the start of injection until the time of the largest induced earthquake. The line relates the theoretical upper bound seismic moment to the product of the modulus of rigidity and the total volume of injected fluid, and fits the data well [from McGarr, 2014].

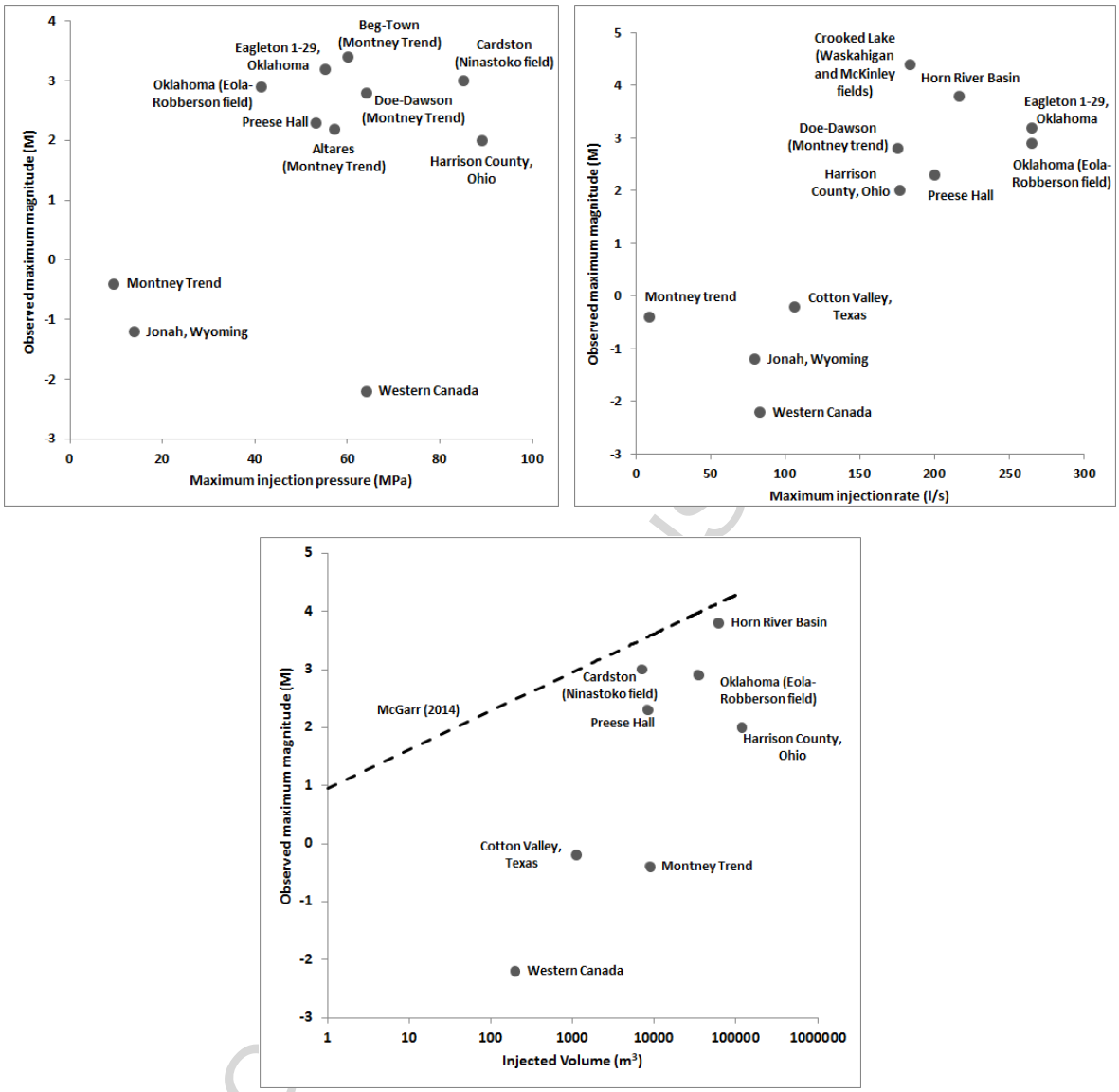


Figure 96: For all cases of shale-gas hydrofracturing-induced earthquakes in our database where data are available, top left: $M_{MAX}$ vs. maximum injection pressure, top right: $M_{MAX}$ vs. maximum injection rate, and bottom: $M_{MAX}$ vs. injected volume.

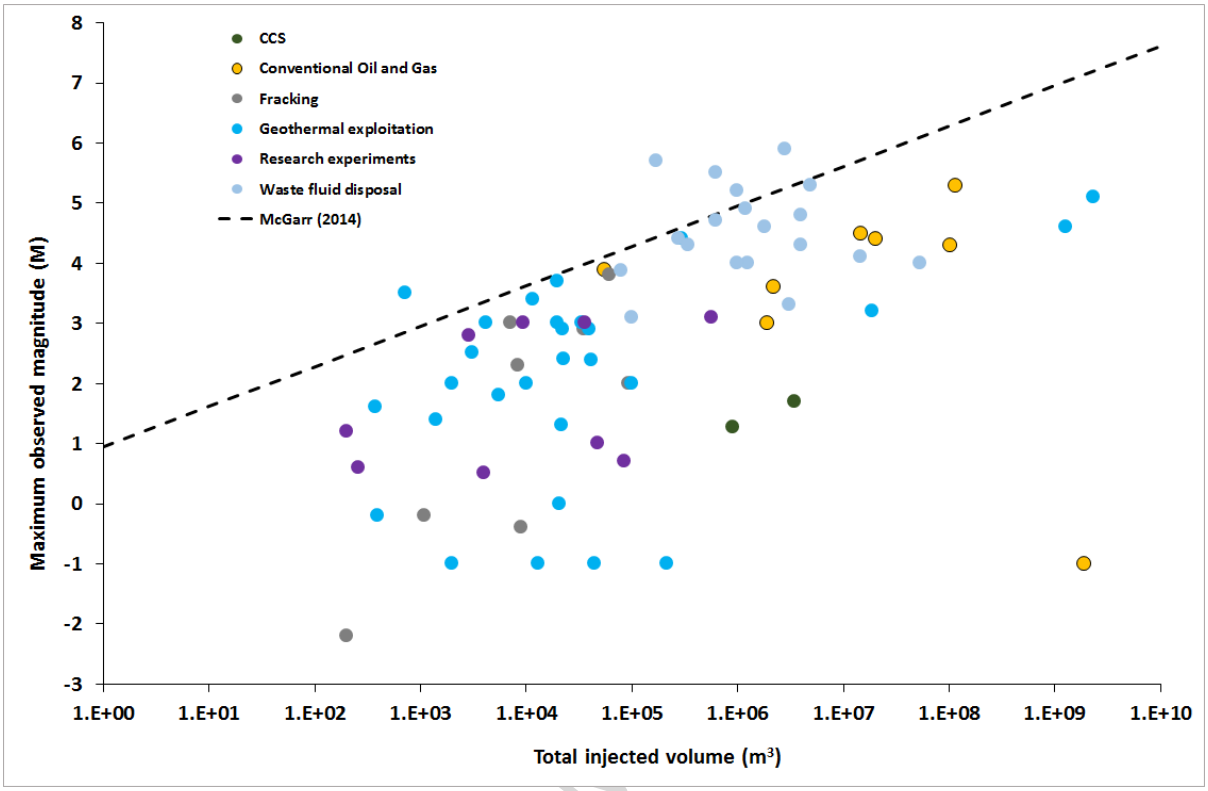


Figure 97: $M_{MAX}$ vs. total injected volume for the 69 cases of induced seismicity for which data are available. The upper-bound magnitude limit proposed by McGarr [2014] on the basis of theoretical considerations is also plotted.

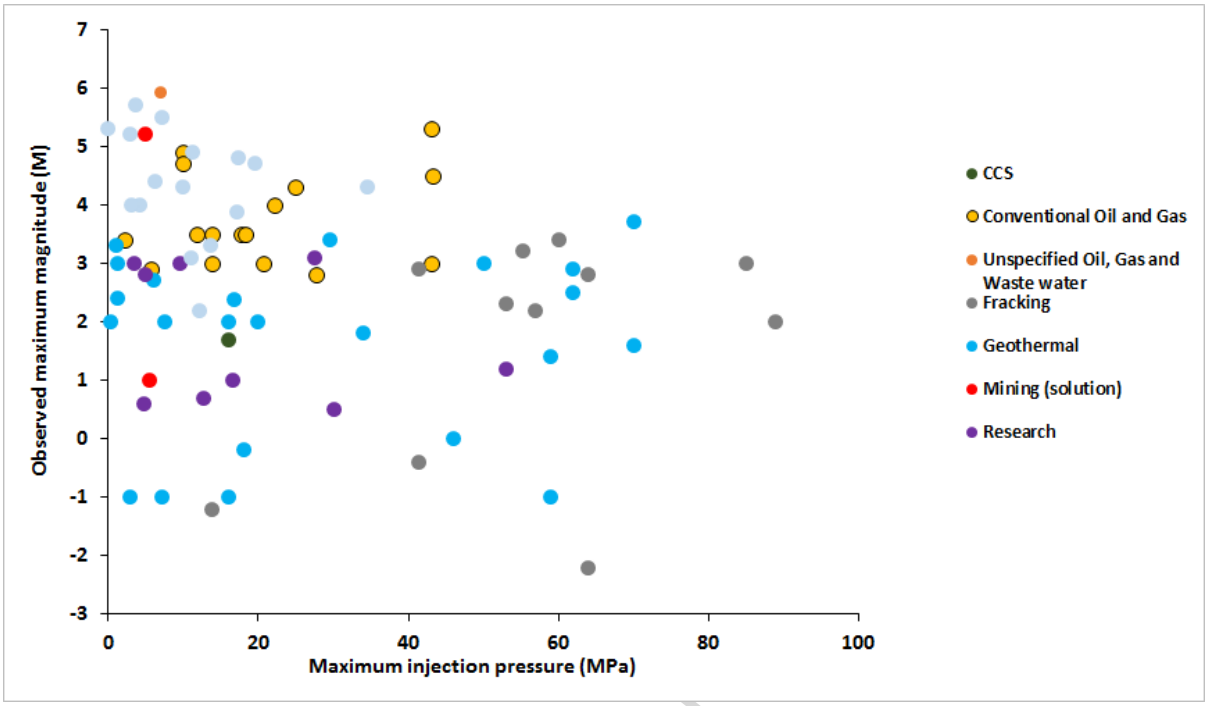


Figure 98: $M_{MAX}$ vs. maximum wellhead injection pressure for the 79 cases where data are reported.

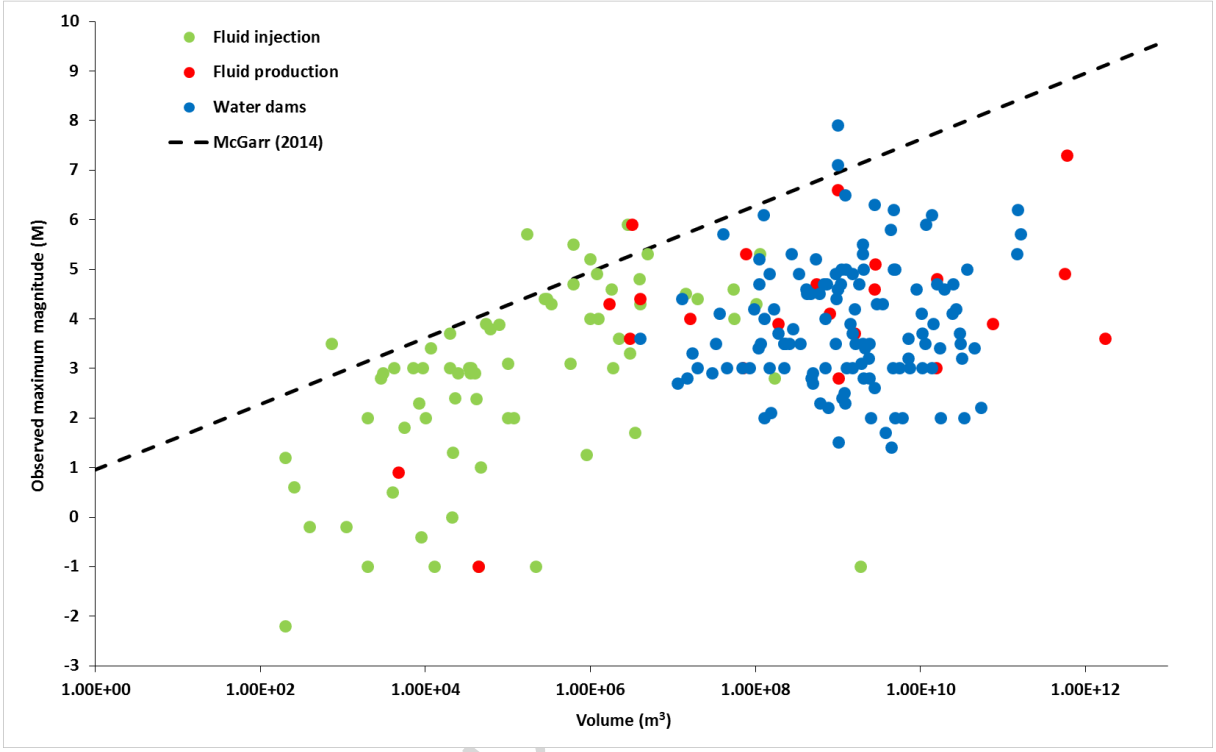


Figure 99: $M_{MAX}$ vs volume or proxy volume of material removed or added for the 218 cases for which data are available, along with the relationship proposed by McGarr [2014] on the basis of theoretical considerations. Volumes and proxy volumes were estimated as follows: Water dams–the volume of the impounded reservoir; fluid injection or extraction–fluid volume injected into or extracted from the subsurface; mining–mass of material excavated, converted to volume using an appropriate density; construction–relevant mass converted to volume using an appropriate density for the building materials; CCS–mass of injected $CO_2$ converted to volume using a density of liquid $CO_2$ of 1100 kg/m$^3$.

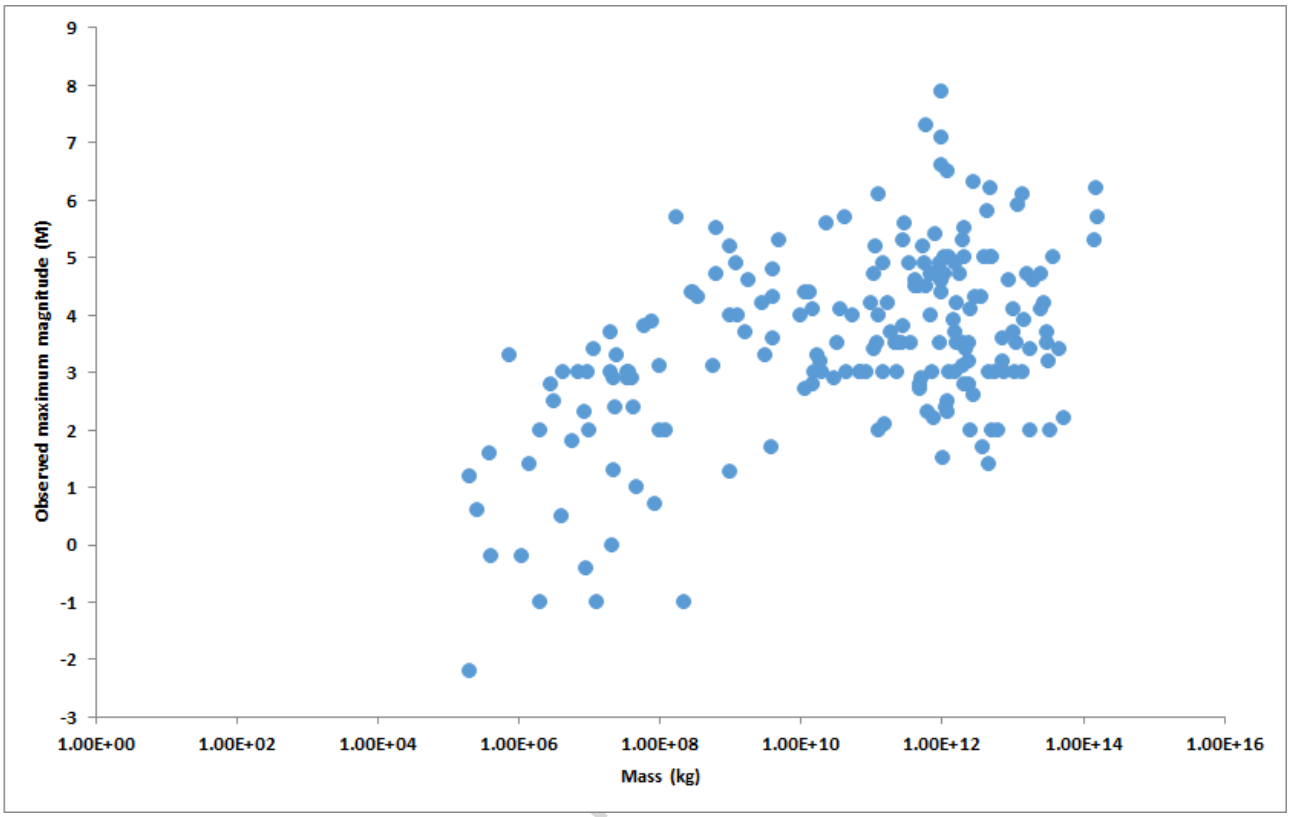


Figure 100: $M_{MAX}$ vs. mass of material removed or added for the 203 cases where data are available. Water volumes were converted to mass using a density 1000 kg/m$^3$. Oil and gas are not included in this plot except where quantity was reported in units of mass. Project types plotted include CCS, construction, conventional oil and gas, shale-gas hydrofracturing, geothermal, mining, research experiments, waste fluid injection and water reservoirs.

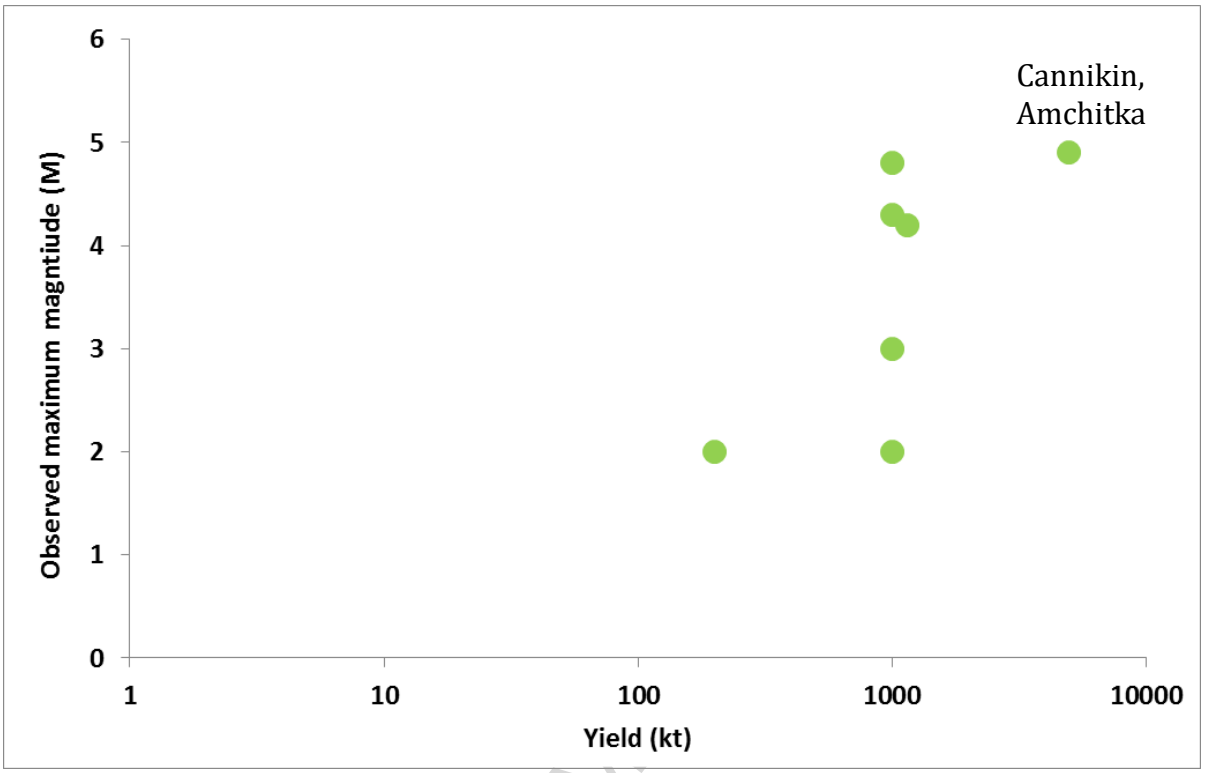


Figure 101: $M_{MAX}$ vs. yield in kilotonnes for nuclear tests that activated faults for the seven cases reported. Only one of these (Benham) is in common with the dataset of McKeown and Dickey [1969] ().

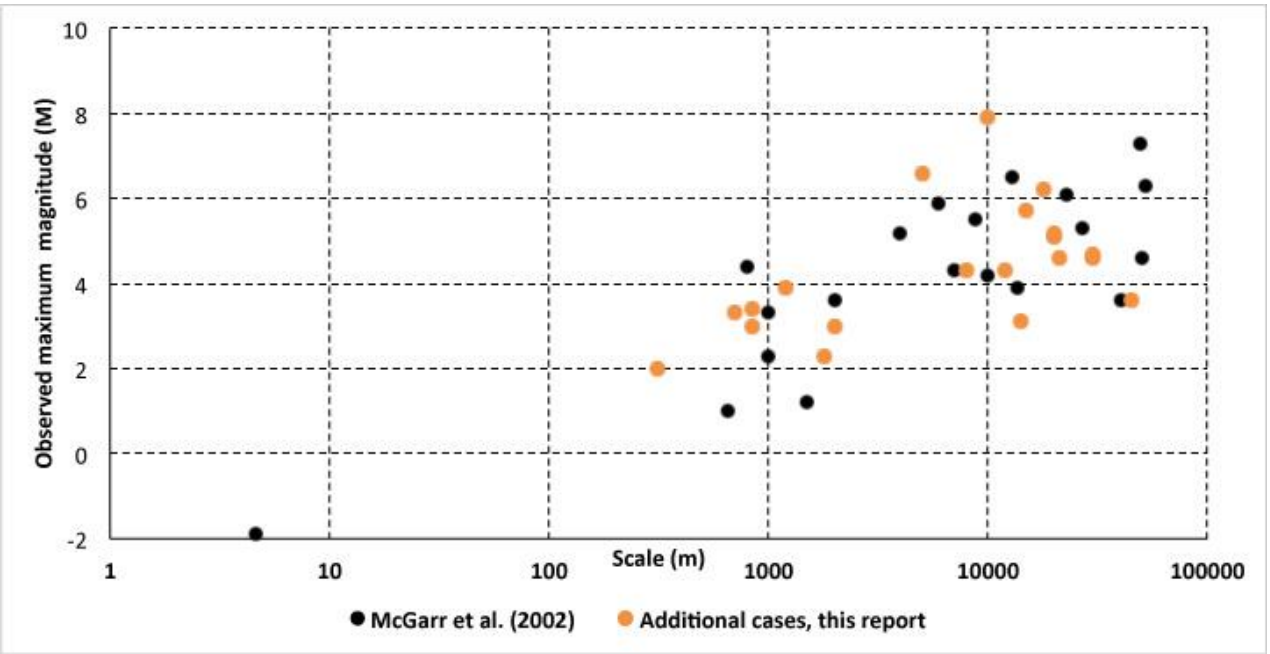


Figure 102: $M_{MAX}$ vs. project scale in meters. Black dots: cases studied by McGarr *et al.* [2002]; orange dots: 20 additional cases from our database. Project scale was estimated using the longest dimension of the project, *e.g.*, the length of a water reservoir.

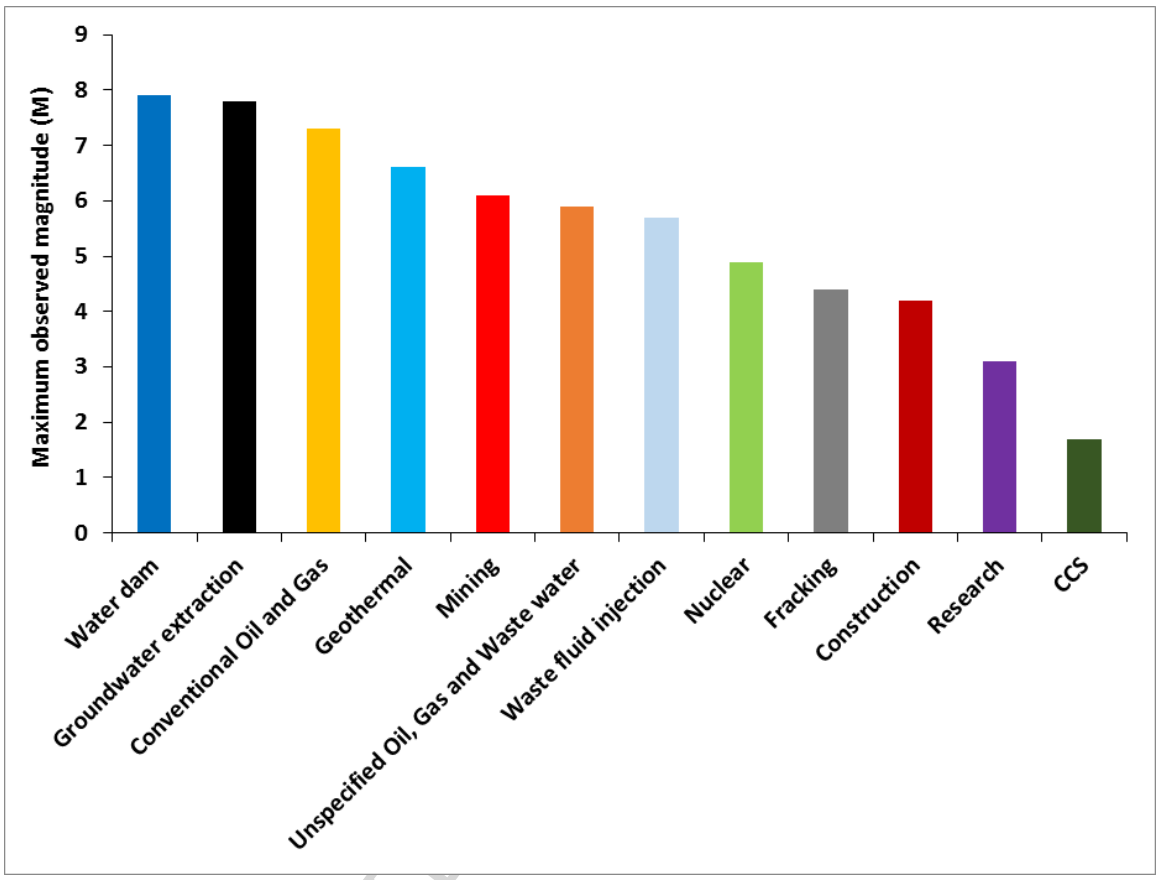


Figure 103: Histogram of $M_{MAX}$ for different categories of project.

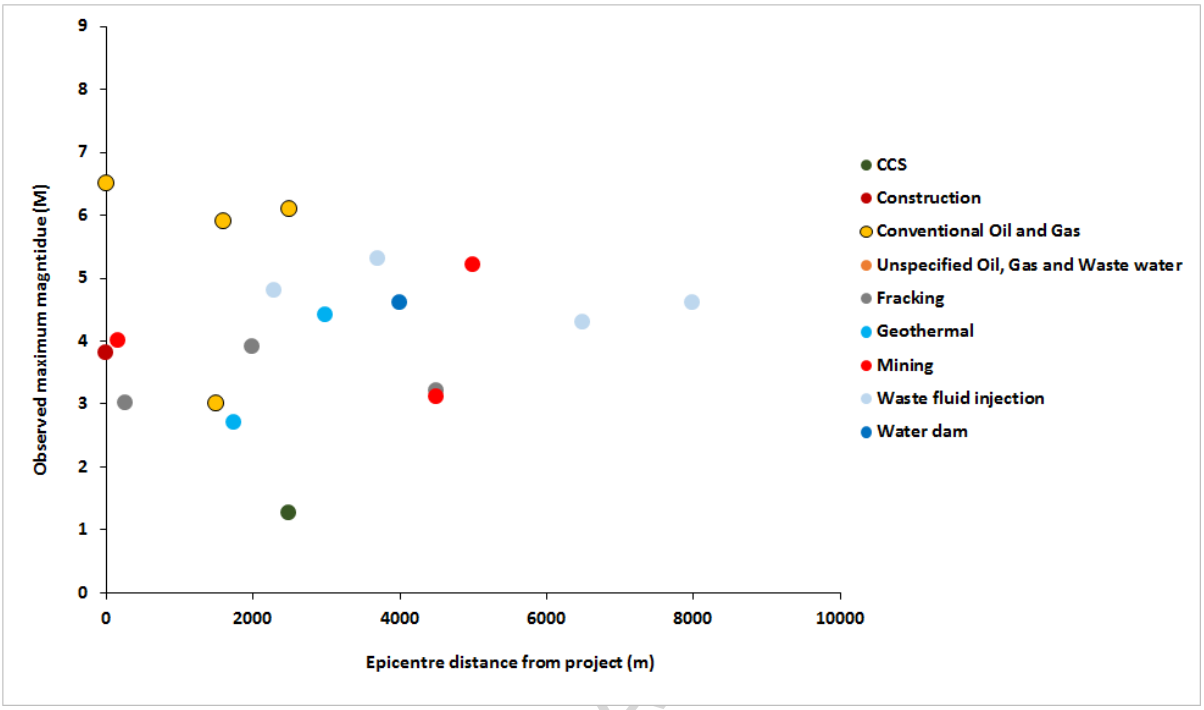


Figure 104: $M_{MAX}$ vs. distance from project for postulated induced earthquakes up to 10 km away for the 19 cases where data are available.

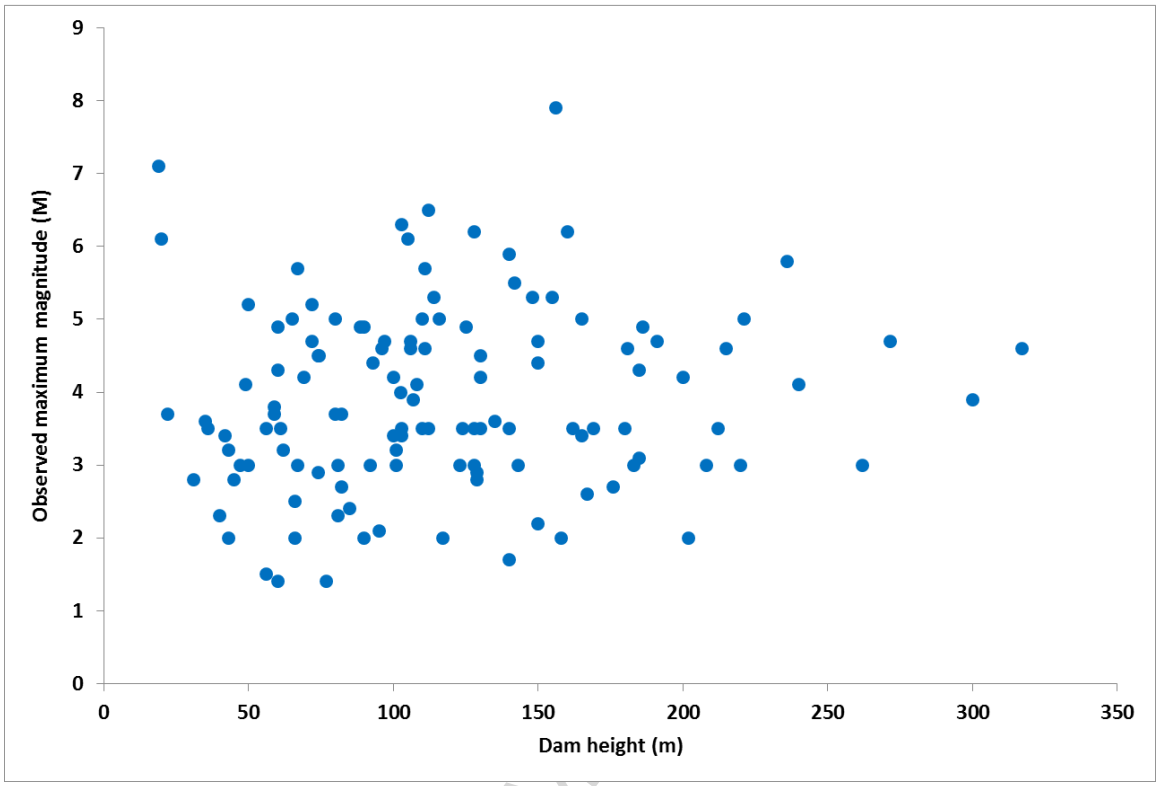


Figure 105: Plot of $M_{MAX}$ vs. dam height for the 159 cases of seismogenic water reservoirs for which data are available.

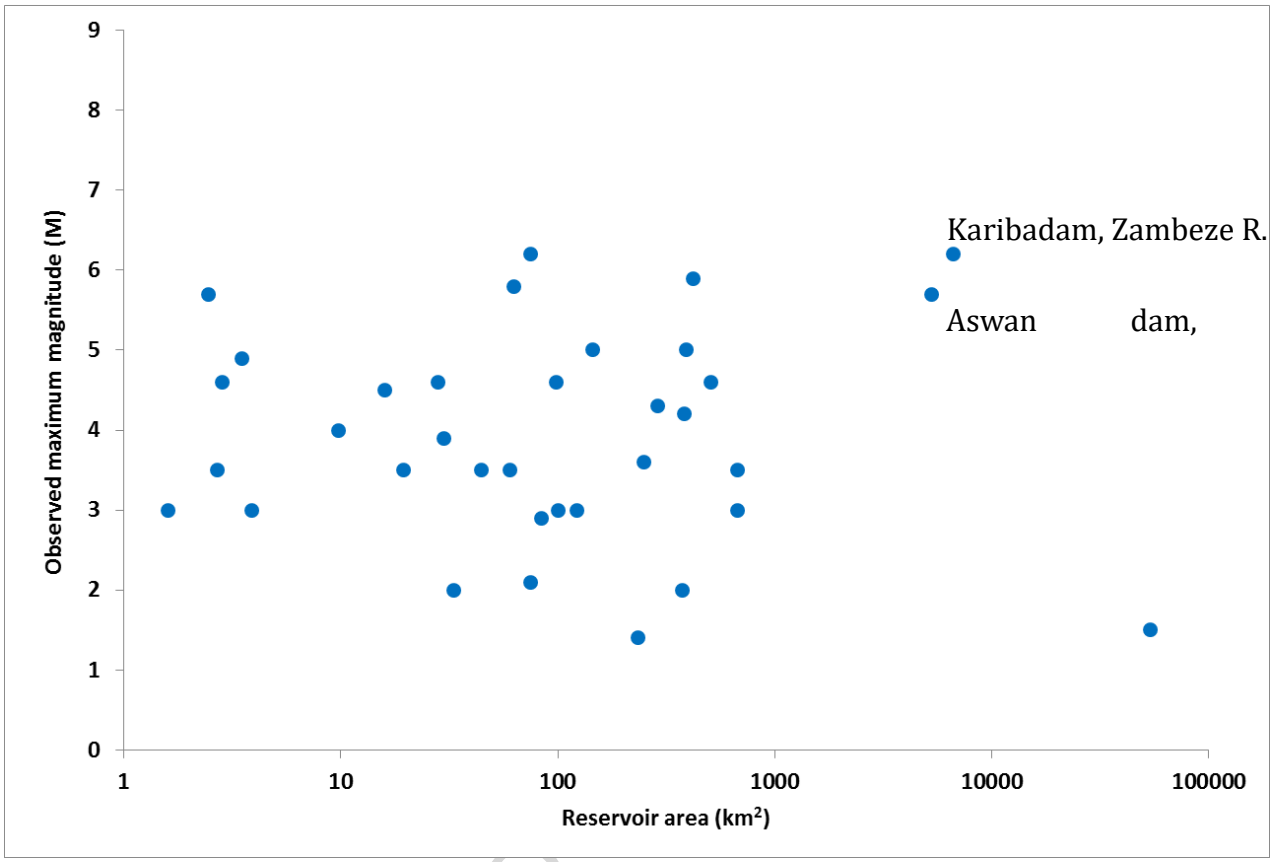


Figure 106: Plot of $M_{MAX}$ vs. water reservoir area for the 35 cases for which data are available.

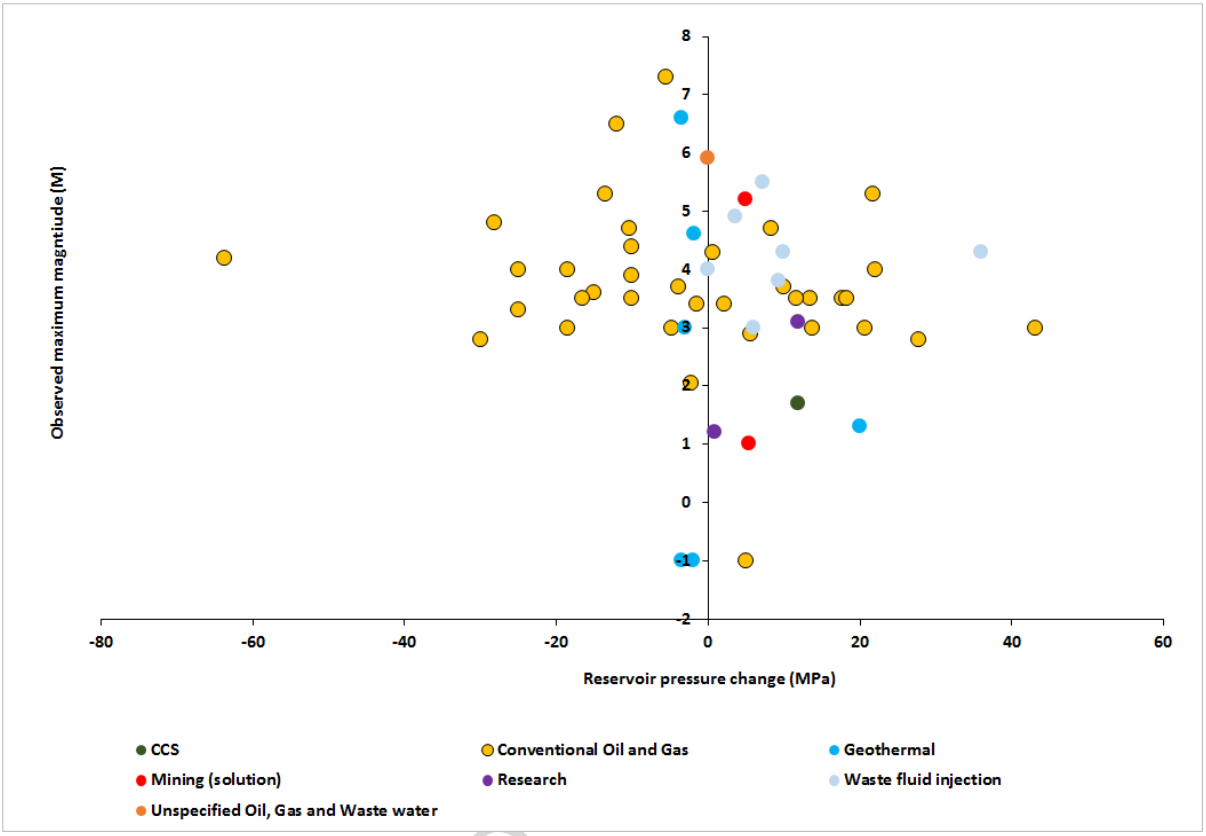


Figure 107: $M_{MAX}$ vs. change in reservoir fluid pressure resulting from production/injection for the 55 cases where data are available. We include 9 cases of conventional oil and gas where the pressure change results from both injection and production.

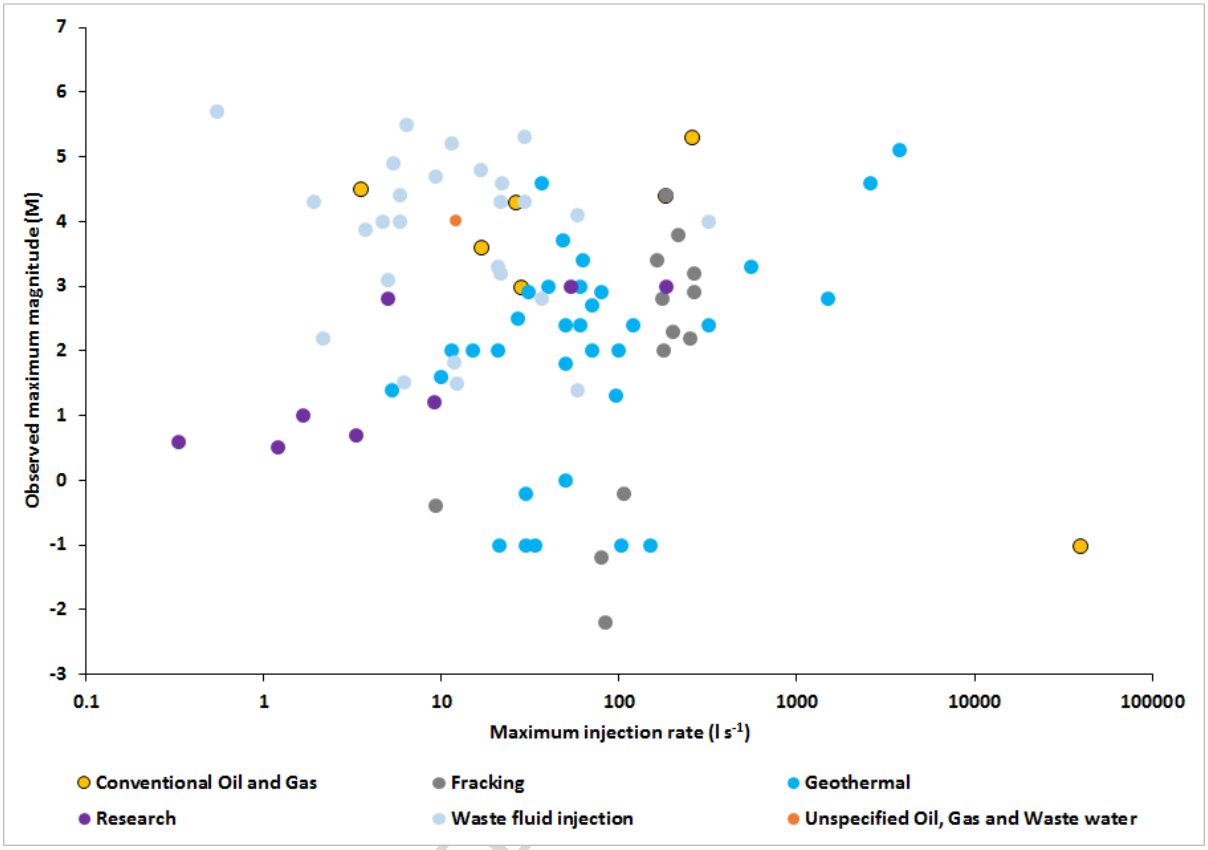


Figure 108: $M_{MAX}$ vs. maximum injection rate for the 88 cases for which data are reported. Rates of injection varied from 0.33 to ~40,000 l/s. At rates greater than ~1000 l $s^{-1}$, values apply to entire fields rather than individual wells.

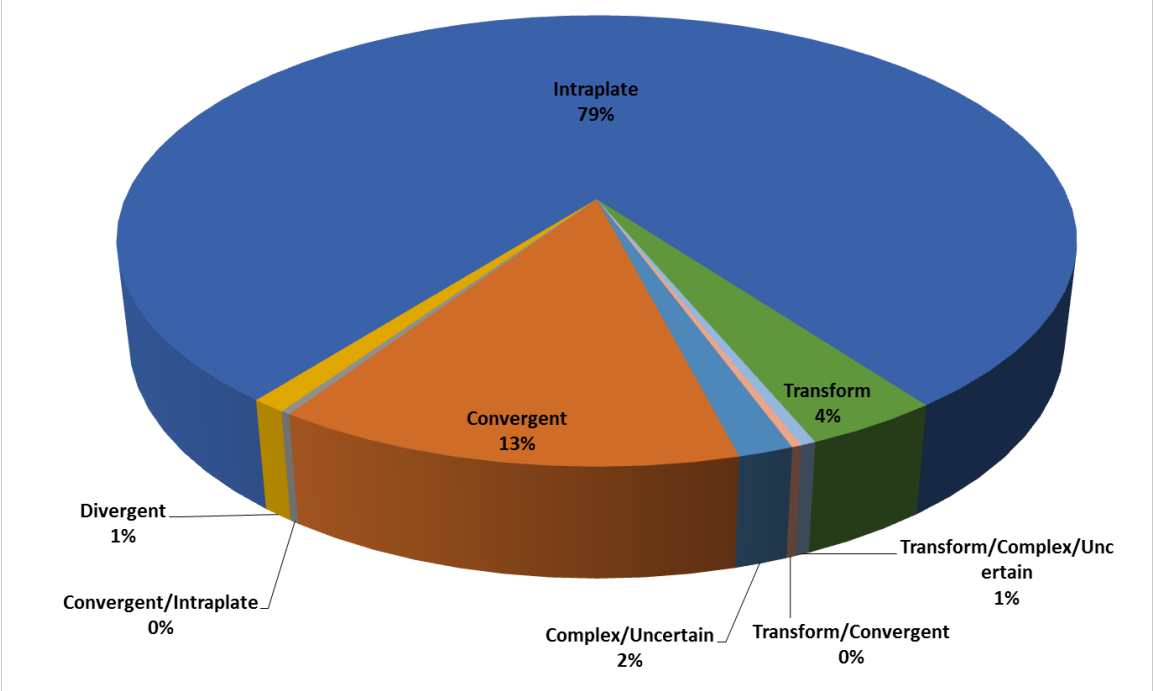


Figure 109: Tectonic settings of cases of human-induced earthquake activity.

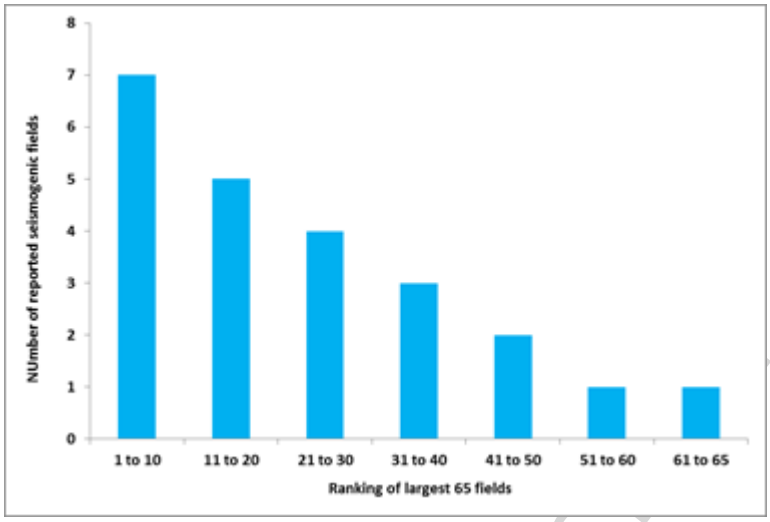


Figure 110: Number of reports of induced seismicity vs. size of field for the 65 largest global power-producing geothermal fields in groups of 10.

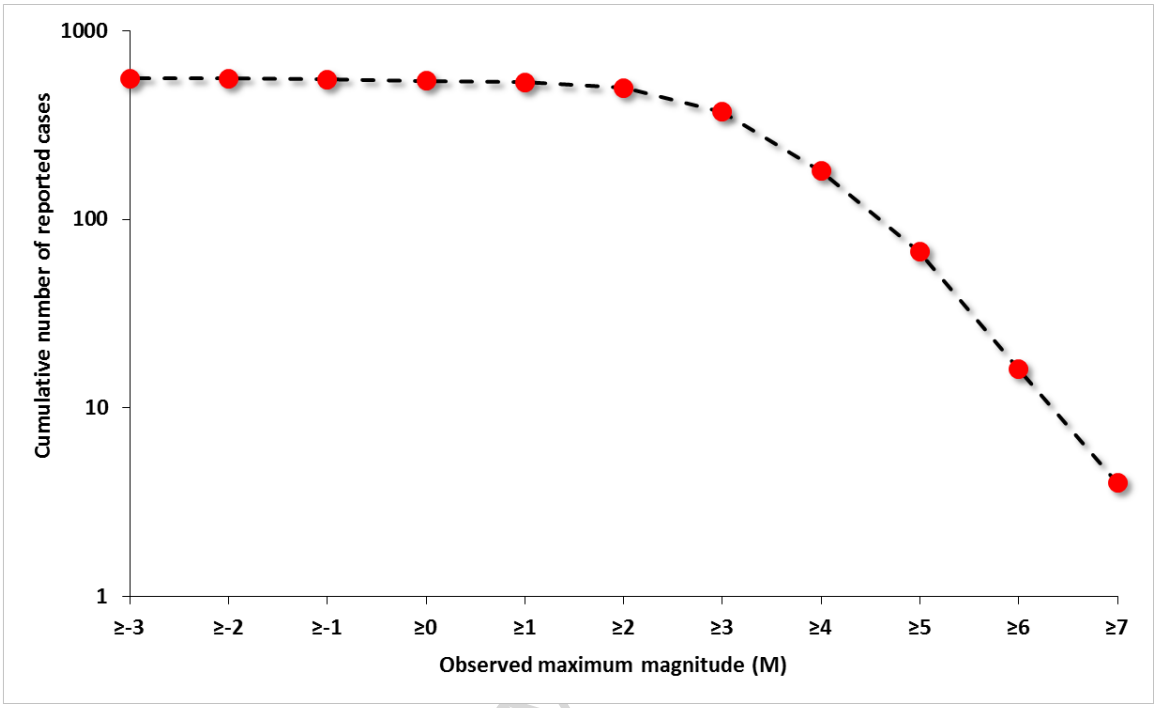


Figure 111: Cumulative number of reported cases of induced seismicity vs. $M_{MAX}$ for the 562 cases for which data are available.

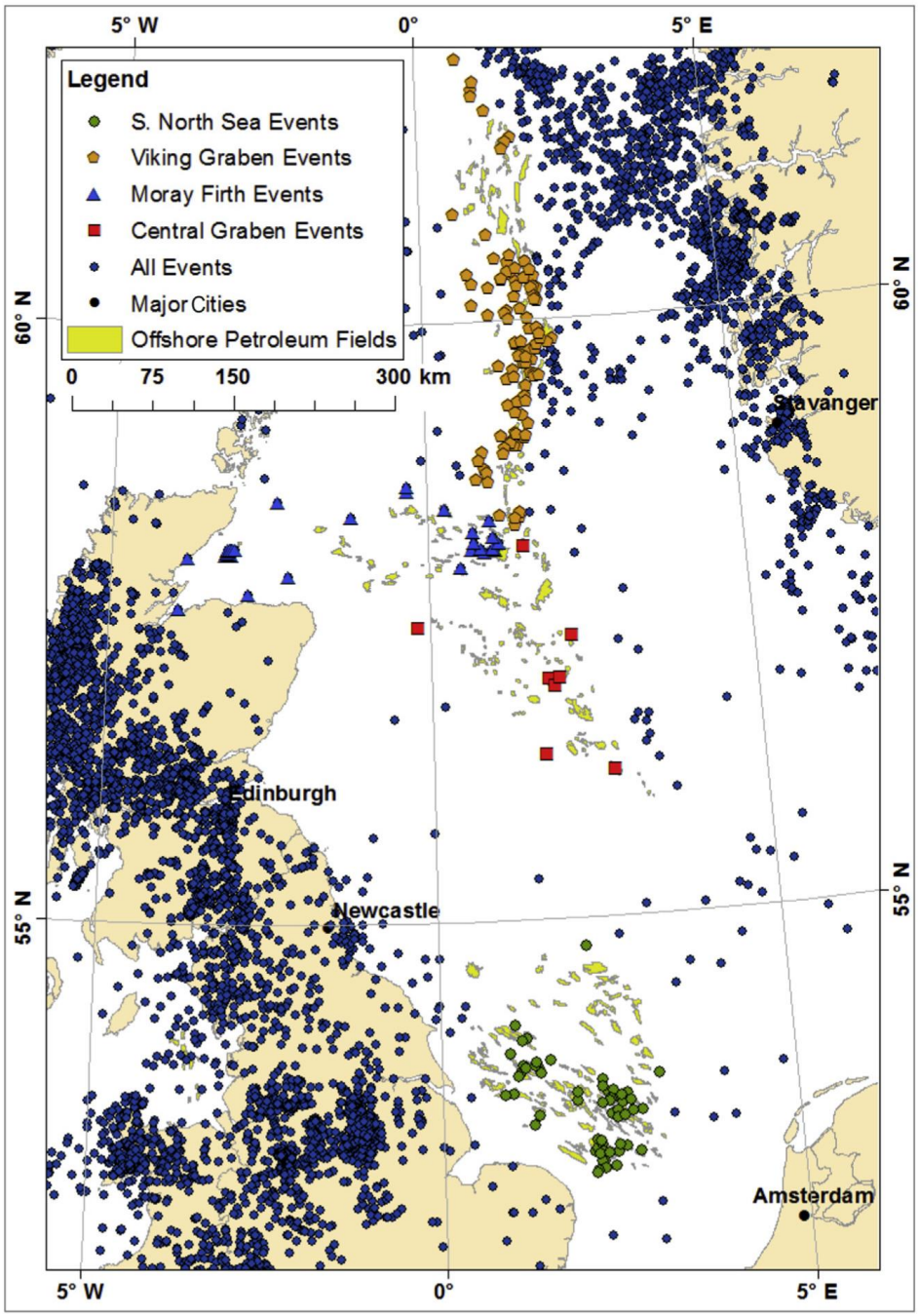


Figure 112: Epicenters from the UK earthquake catalog of the British Geological Survey. Orange circles: Viking Graben events; blue triangles: Moray Firth events; red squares: Central Graben events; green circles Southern North Sea Gas Province events; yellow shading: offshore hydrocarbon fields [from Wilson *et al.*, 2015].

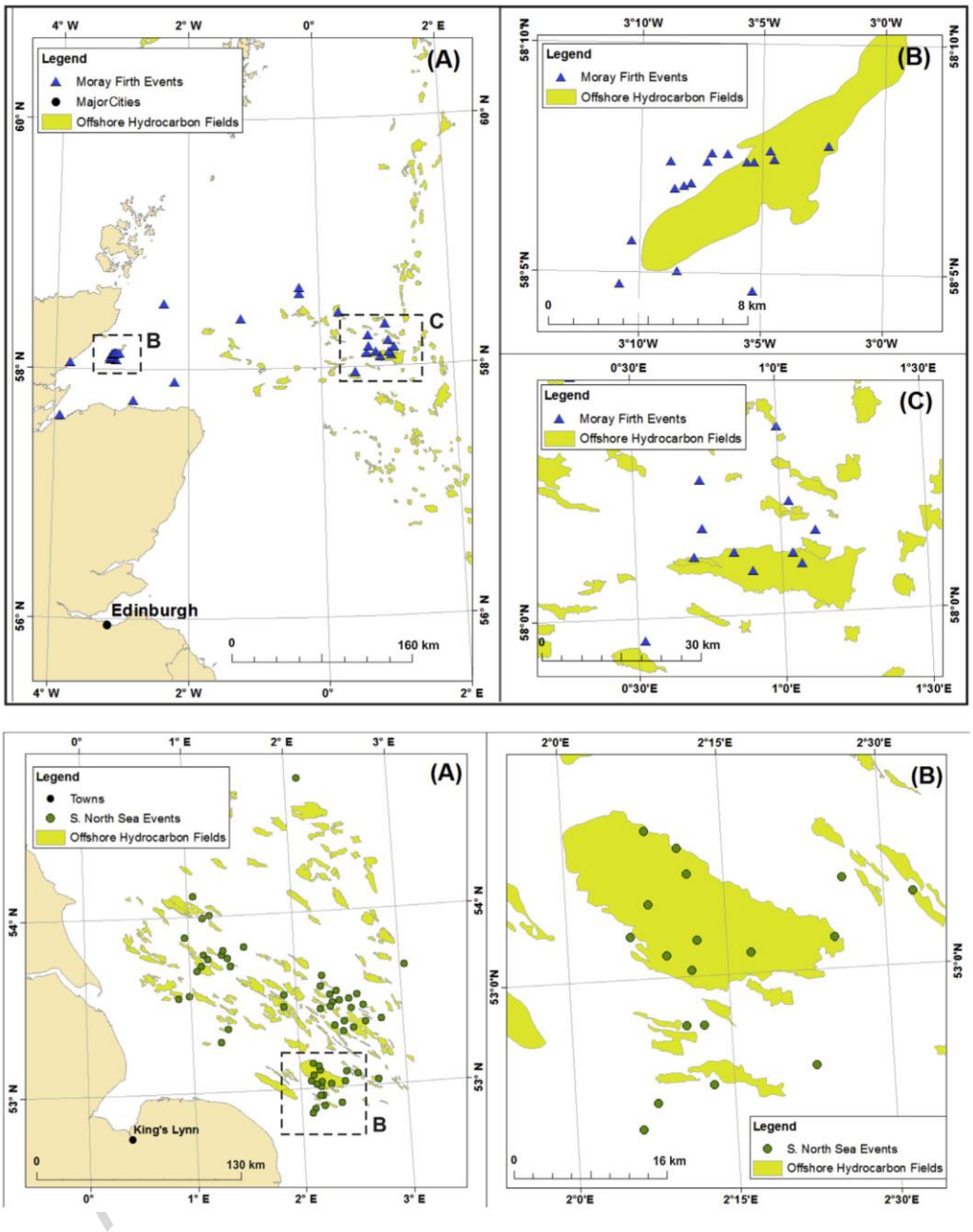


Figure 113: Expanded view of some parts of Figure 112. Top row: A–the Moray Firth. Yellow: hydrocarbon fields; blue triangles: earthquakes. B–the Beatrice Oilfield. C–the Britannia Gasfield. Bottom row: A–the Southern North Sea Gas Province. Green dots: earthquakes. Bottom row: B–the Leman Gasfield [from Wilson *et al.*, 2015].

Figure 114: Damage done to the cathedral in Canterbury, New Zealand, by the 2010 M 7.1 earthquake[22].



[22] http://www.npr.org/sections/parallels/2015/04/05/397093510/will-new-zealand-rebuild-the-cathedral-my-forefather-erected

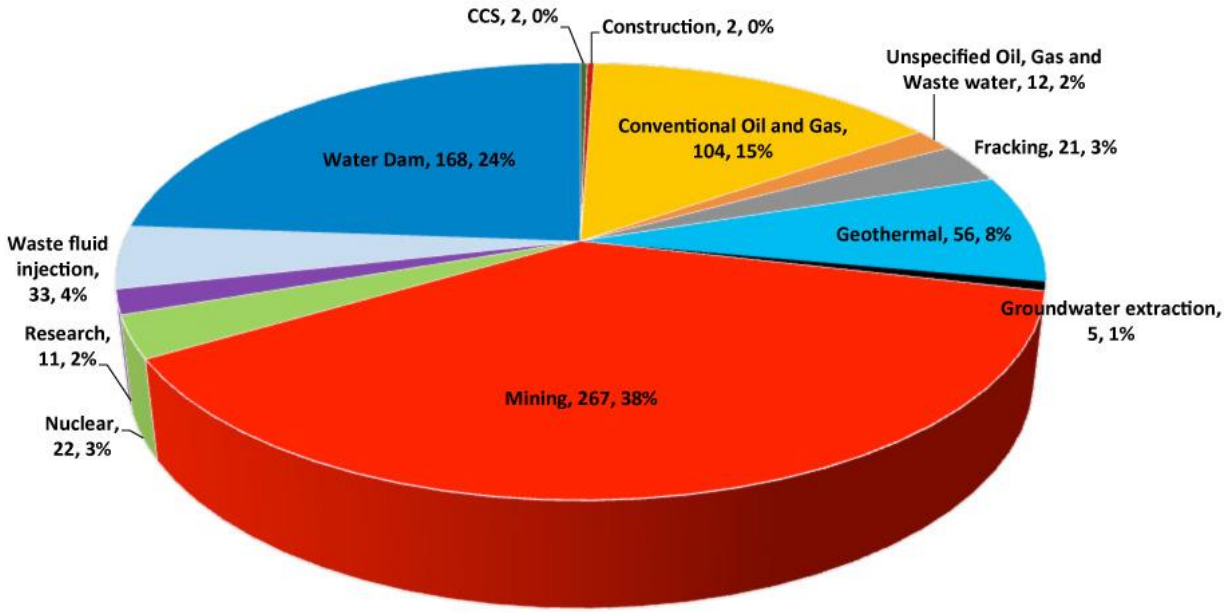


Figure 115: Percentage of total cases for each project category in the database.

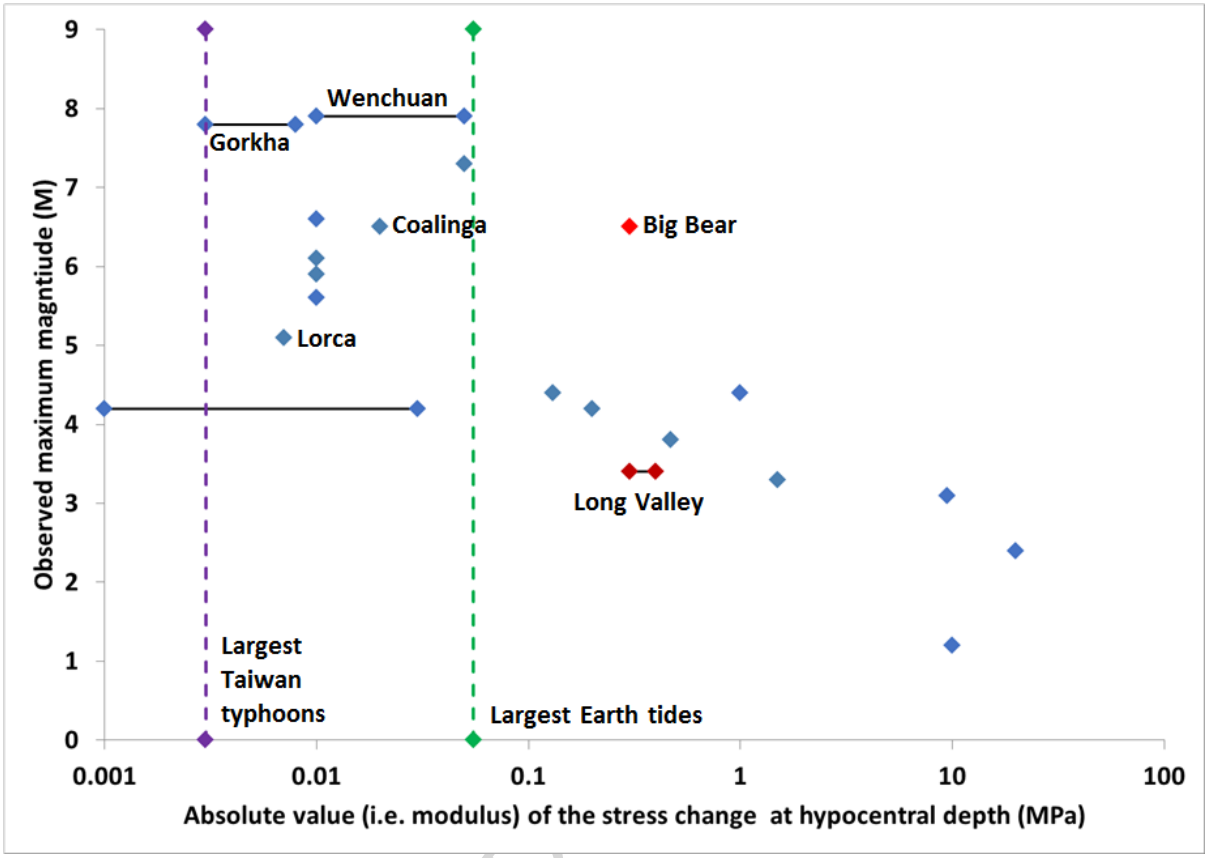


Figure 116: $M_{MAX}$ vs. absolute value of stress changes calculated by various authors to have occurred at the hypocentral depths of possibly induced earthquakes. Vertical dashed green line: largest Earth tides; vertical dashed purple line: largest Taiwan typhoons. Blue diamonds: earthquakes proposed to have been human-induced, diamonds connected by solid black lines: ranges of stress changes calculated. Some example earthquakes are labeled. Red diamonds: natural earthquakes that followed the 28th June 1992 $M_W$ 7.3 Landers, California, earthquake [data from Hill *et al.*, 1993]. The Big Bear earthquake is proposed to have been induced by static stress changes, and the Long Valley earthquakes by remote triggering by the dynamic stresses from surface waves.

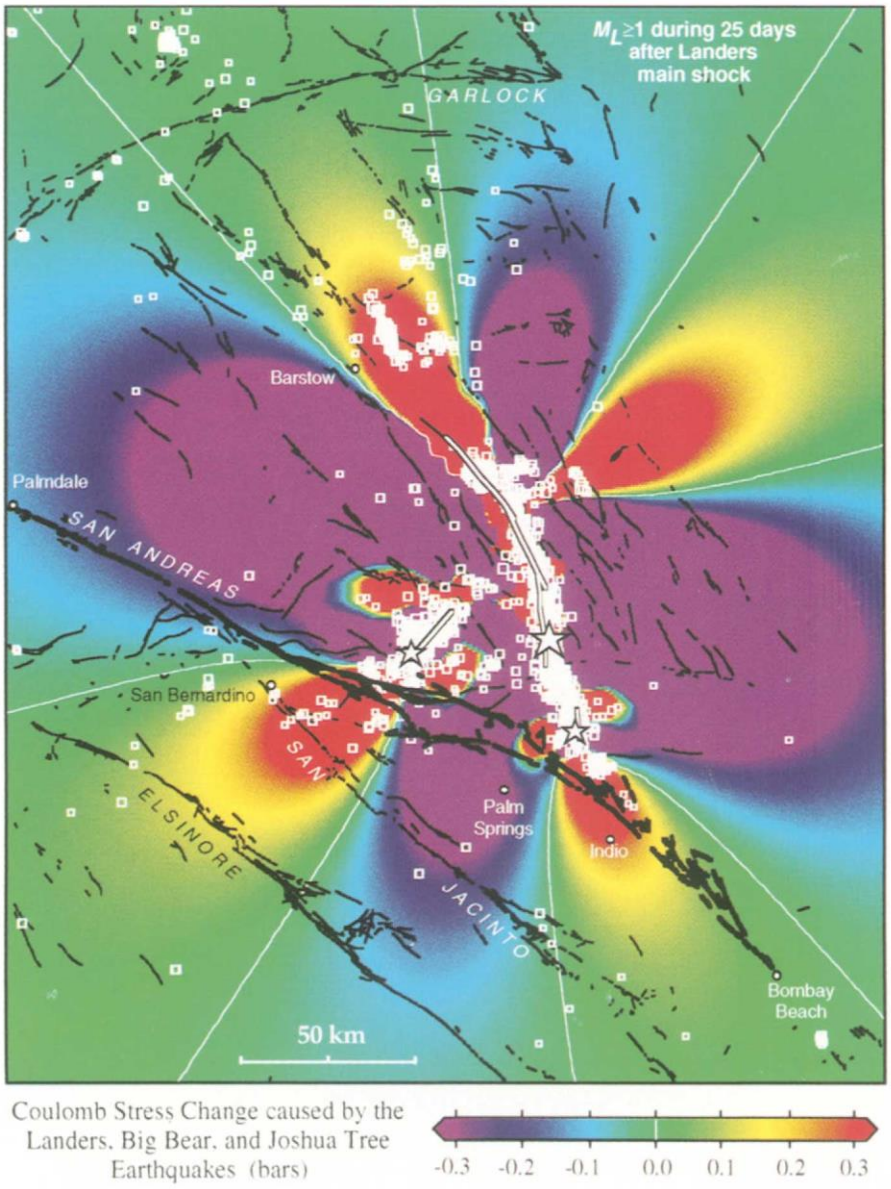


Figure 117: Coulomb stress changes at a depth of 6.25 km caused by the $M_W$ 7.3 Landers, California, earthquake and large aftershocks [from King *et al.*, 1994].

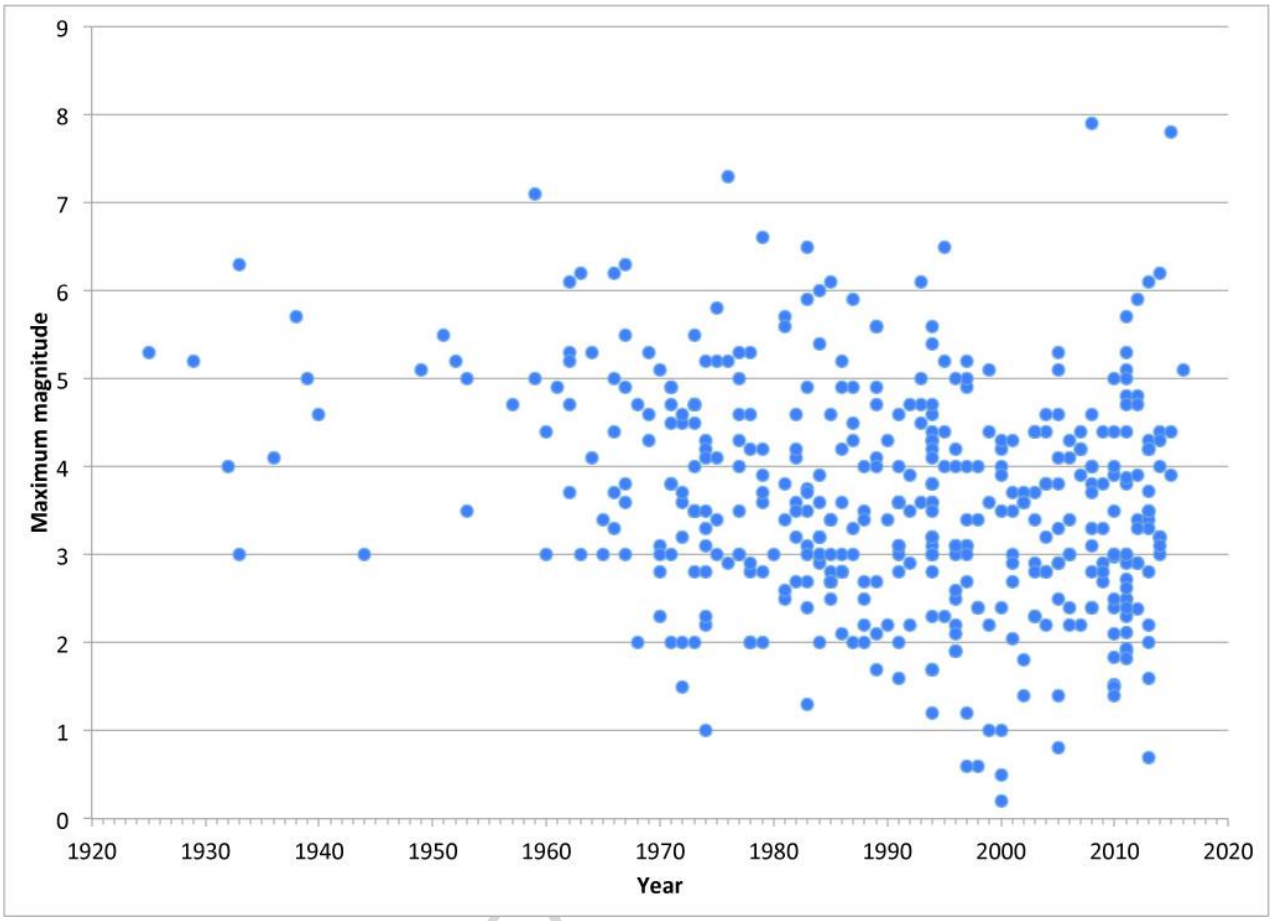


Figure 118: $M_{MAX}$ vs. year for the 419 cases where data are available.

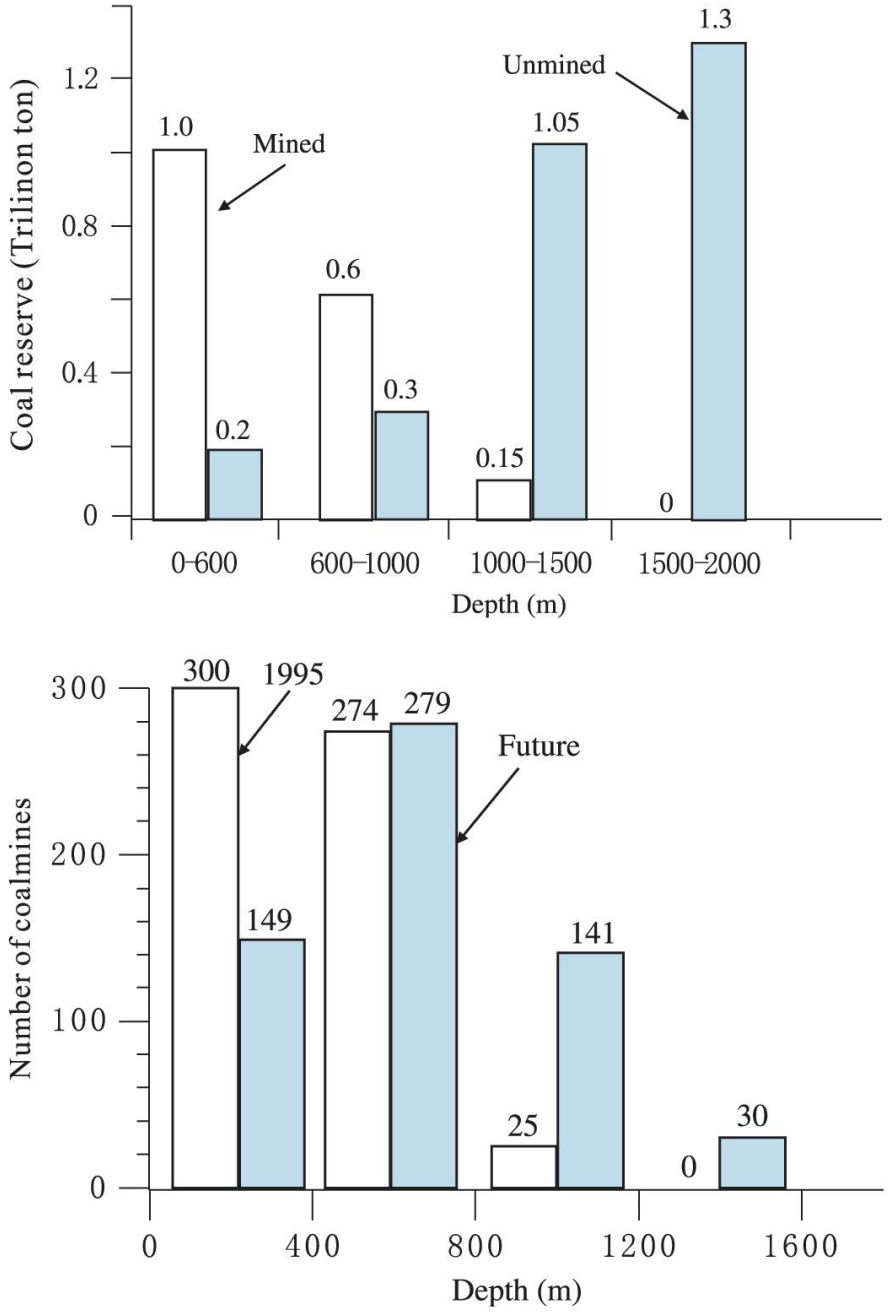


Figure 119: Top: Depth distribution of Chinese coal reserves (1995 statistics). Bottom: Depth distribution of 599 state-owned Chinese coal mines [from Li *et al.*, 2007].

*References*

Ahmad, M. U., and J. A. Smith (1988), Earthquakes, injection wells, and the Perry Nuclear Power Plant, Cleveland, Ohio, Geology, 16, 739-742.

Ake, J., K. Mahrer, D. O'Connell, and L. Block (2005), Deep-injection and closely monitored induced seismicity at Paradox Valley, Colorado, Bull. seismol. Soc. Am., 95, 664-683, doi:10.1785/0120040072.

Al-Enezi, A., L. Petrat, R. Abdel-Fattah, and G. D. M. Technologie (2008), Induced seismicity and surface deformation within Kuwait's oil fields, Proceedings of the Proc. Int. Conf. Geol. Seismol, pp. 177-183.

Allis, R. G., S. A. Currie, J. D. Leaver, and S. Sherburn (1985), Results of injection testing at Wairakei geothermal field, New Zealand, Geothermal Resources Council International Symposium on Geothermal Energy: International Volume, 289-294.

Amidzic, D., S. K. Murphy, and G. Van Aswegen (1999), Case study of a large seismic event at a South African gold mine, Proceedings of the 9th ISRM Congress.

Amos, C. B., P. Audet, W. C. Hammond, R. Bürgmann, I. A. Johanson, and G. Blewitt (2014), Uplift and seismicity driven by groundwater depletion in central California, Nature, 509, 483-486.

Anonymous (2014), Literature review on injection-related induced seismicity and its relevance to nitrogen injection, pp 46, Earth, Environmental and Life Sciences, Utrecht, Netherlands Report TNO 2014 R11761.

Arkhipova, E. V., A. D. Zhigalin, L. I. Morozova, and A. V. Nikolaev (2012), The Van earthquake on October 23, 2011: Natural and technogenic causes, Proceedings of the Doklady Earth Sciences Conference, pp. 1176-1179.

Asanuma, H., N. Soma, H. Kaieda, Y. Kumano, T. Izumi, K. Tezuka, H. Niitsuma, and D. Wyborn (2005), Microseismic monitoring of hydraulic stimulation at the Australian HDR project in Cooper Basin, Proceedings of the Proceedings World Geothermal Congress, pp. 24-29.

Avouac, J.-P. (2012), Earthquakes: Human-induced shaking, Nature Geoscience, 5, 763–764, doi:doi:10.1038/ngeo1609.

Awad, M., and M. Mizoue (1995), Earthquake activity in the Aswan region, Egypt, Pure Appl. Geophys., 145, 69-86, doi:10.1007/bf00879484.

Baisch, S., and H. P. Harjes (2003), A model for fluid-injection-induced seismicity at the KTB, Germany, Geophys. J. Int., 152, 160-170, doi:10.1046/j.1365-246X.2003.01837.x.

Baisch, S., and R. Vörös (2011), Geomechanical study of Blackpool seismicity, pp 58, Report prepared for Cuadrilla Ltd. by Q-con GmbH.

Baisch, S., R. Vörös, R. Weidler, and D. Wyborn (2009), Investigation of fault mechanisms during geothermal reservoir stimulation experiments in the Cooper Basin, Australia, Bull. seismol. Soc. Am., 99, 148-158, doi:doi:10.1785/0120080055.

Baisch, S., M. Bohnhoff, L. Ceranna, Y. Tu, and H. P. Harjes (2002), Probing the crust to 9-km depth: Fluid-injection experiments and induced seismicity at the KTB superdeep drilling hole, Germany, Bull. seismol. Soc. Am., 92, 2369-2380, doi:10.1785/0120010236.

Baisch, S., R. Weidler, R. Voros, D. Wyborn, and L. de Graaf (2006a), Induced seismicity during the stimulation of a geothermal HFR reservoir in the Cooper Basin, Australia, Bull. seismol. Soc. Am., 96, 2242-2256, doi:10.1785/0120050255.

Baisch, S., R. Weidler, R. Vörös, D. Wyborn, and L. de Graaf (2006b), Induced seismicity during the stimulation of a geothermal HFR reservoir in the Cooper Basin, Australia, Bull. seismol. Soc. Am., 96, 2242-2256.

Baisch, S., R. Voeroes, E. Rothert, H. Stang, R. Jung, and R. Schellschmidt (2010), A numerical model for fluid injection induced seismicity at Soultz-sous-Forets, International Journal of Rock Mechanics and Mining Sciences, 47, 405-413, doi:10.1016/j.ijrmms.2009.10.001.

Baisch, S., E. Rothert, H. Stang, R. Voeroes, C. Koch, and A. McMahon (2015), Continued geothermal reservoir stimulation experiments in the Cooper Basin (Australia), Bull. seismol. Soc. Am., 105, 198-209, doi:10.1785/0120140208.

Balassanian, S. Y. (2005), Earthquakes induced by deep penetrating bombing?, Acta Seismologica Sinica, 18, 741-745.

Bardainne, T., N. Dubos-Sallee, G. Senechal, P. Gaillot, and H. Perroud (2008), Analysis of the induced seismicity of the Lacq gas field (southwestern France) and model of deformation, Geophys. J. Int., 172, 1151-1162, doi:10.1111/j.1365-246X.2007.03705.x.

Batini, F., R. Console, and G. Luongo (1985), Seismological study of Larderello-Travale geothermal area, Geothermics, 14, 255–272.

Batini, F., C. Bufe, G. M. Cameli, R. Console, and A. Fiordelisi (1980), Seismic monitoring in Italian geothermal areas I: seismic activity in the Larderello-Travale region, Proceedings of the Second DOE-ENEL Workshop on Cooperative Research in Geothermal Energy, Lawrence Berkeley Laboratory, Berkeley, CA, USA, October 20–22, pp. 20–47.

Bella, F., P. F. Biagi, M. Caputo, E. Cozzi, G. Della Monica, A. Ermini, W. Plastino, and V. Sgrigna (1998), Aquifer-induced seismicity in the Central Apennines (Italy), Pure Appl. Geophys., 153, 179-194, doi:10.1007/s000240050191.

Benetatos, C., J. Malek, and F. Verga (2013), Moment tensor inversion for two micro-earthquakes occurring inside the Haje gas storage facilities, Czech Republic, Journal of Seismology, 17, 557-577, doi:10.1007/s10950-012-9337-0.

Bennett, T. J., M. E. Marshall, B. W. Barker, and J. R. Murphy (1994), Characteristics of rockbursts for use in seismic discrimination, Maxwell Labs Inc, San Diego, California SSS-FR-93-14382.

Bertani, R. (2010), Geothermal power generation in the world: 2005–2010 update report, Proceedings of the World Geothermal Congress 2010, Bali, Indonesia, 25-29 April 2010.

Block, L. V., C. K. Wood, W. L. Yeck, and V. M. King (2015), Induced seismicity constraints on subsurface geological structure, Paradox Valley, Colorado, Geophys. J. Int., 200, 1170-1193, doi:10.1093/gji/ggu459.

Boettcher, M. S., D. L. Kane, A. McGarr, M. J. S. Johnston, and Z. Reches (2015), Moment tensors and other source parameters of mining-induced earthquakes in TauTona Mine, South Africa, Bull. seismol. Soc. Am., 105, 1576-1593, doi:10.1785/0120140300.

Bohnhoff, M., S. Baisch, and H. P. Harjes (2004), Fault mechanisms of induced seismicity at the superdeep German Continental Deep Drilling Program (KTB) borehole and their relation to fault structure and stress field, J. Geophys. Res., 109, doi:10.1029/2003jb002528.

Bossu, R., J. R. Grasso, L. M. Plotnikova, B. Nurtaev, J. Frechet, and M. Moisy (1996), Complexity of intracontinental seismic faultings: The Gazli, Uzbekistan, sequence, Bull. seismol. Soc. Am., 86, 959–971.

Bou-Rabee, F., and A. Nur (2002), The 1993 M 4. 7 Kuwait earthquake: Induced by the burning of the oil fields, Kuwait Journal of Science and Engineering, 29, 155-163.

Boucher, G., A. Ryall, and A. E. Jones (1969), Earthquakes associated with underground nuclear explosions, J. Geophys. Res., 74, 3808-3820.

Bourne, S. J., S. J. Oates, J. J. Bommer, B. Dost, J. van Elk, and D. Doornhof (2015), Monte Carlo method for probabilistic hazard assessment of induced seismicity due to conventional natural gas production, Bull. seismol. Soc. Am., 105, 1721-1738, doi:10.1785/0120140302.

Brooks, E. M., S. Stein, B. D. Spencer, L. Salditch, M. D. Peterson, and D. E. McNamara (2017), Assessing earthquake hazard map performance for natural and induced seismicity in the central and eastern United States, Seismol. Res. Lett.

Brudy, M., M. D. Zoback, K. Fuchs, F. Rummel, and J. Baumgartner (1997), Estimation of the complete stress tensor to 8 km depth in the KTB scientific drill holes: Implications for crustal strength, J. Geophys. Res., 102, 18453-18475.

Calo, M., C. Dorbath, and M. Frogneux (2014), Injection tests at the EGS reservoir of Soultz-sous-Forets. Seismic response of the GPK4 stimulations, Geothermics, 52, 50-58, doi:10.1016/j.geothermics.2013.10.007.

Caloi, P., M. De Panfilis, D. Di Filippo, L. Marcelli, and M. C. Spadea (1956), Terremoti della Val Padana del 15-16 maggio 1951, Annals of Geophysics, 9, 63-105.

Carder, D. S. (1945), Seismic investigations in the Boulder Dam area, 1940-1944, and the influence of reservoir loading on local earthquake activity, Bull. seismol. Soc. Am., 35, 175-192.

Cartlidge, E. (2014), Human activity may have triggered fatal Italian earthquakes, panel says, Science, 344, 141.

Castle, R. O., and R. F. Yerkes (1976), Recent surface movements in the Baldwin Hills, Los Angeles county, California, U.S. Geological Survey Professional Paper 882, pp viii+125, U.S. Geological Survey, Washington, D.C.

Cesca, S., F. Grigoli, S. Heimann, A. Gonzalez, E. Buforn, S. Maghsoudi, E. Blanch, and T. Dahm (2014), The 2013 September-October seismic sequence offshore Spain: a case of seismicity triggered by gas injection?, Geophys. J. Int., 198, 941-953, doi:10.1093/gji/ggu172.

Chabora, E., E. Zemach, P. Spielman, P. Drakos, S. Hickman, S. Lutz, K. Boyle, A. Falconer, A. Robertson-Tait, N. C. Davatzes, P. Rose, E. Majer, and S. Jarpe (2012), Hydraulic stimulation of Well 27-15, Desert Peak geothermal field, Nevada, U.S.A., Proceedings of the 37th Standford Geothermal Workshop, Stanford, CA.

Cladouhos, T., S. Petty, Y. Nordin, M. Moore, K. Grasso, M. Uddenberg, M. Swyer, B. Julian, and G. Foulger (2013), Microseismic monitoring of Newberry Volcano EGS Demonstration, Proceedings of the Thirty-Eighth Workshop on Geothermal Reservoir Engineering, Stanford University, Stanford, California, February 11-13, 2013.

Clarke, H., L. Eisner, P. Styles, and P. Turner (2014a), Felt seismicity associated with shale gas hydraulic fracturing: The first documented example in Europe, Geophys. Res. Lett., 41, 8308-8314, doi:10.1002/2014gl062047.

Clarke, H., L. Eisner, P. Styles, and P. Turner (2014b), Felt seismicity associated with shale gas hydraulic fracturing: The first documented example in Europe, Geophys. Res. Lett., 41, 8308–8314.

Cochran, E. S., J. Vidale, and S. Tanaka (2004), Earth tides can trigger shallow thrust fault earthquakes, Science, 306, 1164-1166.

Darold, A., A. A. Holland, C. Chen, and A. Youngblood (2014), Preliminary analysis of seismicity near Eagleton 1-29, Carter County, July 2014, pp 17, Oklahoma Geological Survey Open-File Report OF2-2014.

Davies, R., G. Foulger, A. Bindley, and P. Styles (2013), Induced seismicity and hydraulic fracturing for the recovery of hydrocarbons, Marine and Petroleum Geology, 45, 171-185, doi:10.1016/j.marpetgeo.2013.03.016.

Davis, S. D., and W. D. Pennington (1989), Induced seismic deformation in the Cogdell oil field of west Texas, Bull. seismol. Soc. Am., 79, 1477-1495.

Davis, S. D., and C. Frohlich (1993), Did (or will) fluid injection cause earthquakes? - Criteria for a rational assessment, Seismol. Res. Lett., 64, 207-224.

de Pater, C. J., and S. Baisch (2011), Geomechanical study of Bowland Shale seismicity. Synthesis report, pp 71, Report commissioned by Cuadrilla Resources Ltd., June 2011.

deBruyn, I. A., and F. G. Bell (1997), Mining and induced seismicity in South Africa: A survey, Proceedings of the International Symposium on Engineering Geology and the Environment, Athens, Greece, 23-27 June, pp. 2321-2326.

Deichmann, N., and J. Ernst (2009), Earthquake focal mechanisms of the induced seismicity in 2006 and 2007 below Basel (Switzerland), Swiss Journal of Geosciences, 102, 457-466, doi:10.1007/s00015-009-1336-y.

Dreger, D., S. R. Ford, and W. R. Walter (2008), Source analysis of the Crandall Canyon, Utah mine collapse, Science, 321, 217.

Durrheim, R. J. (2010), Mitigating the risk of rockbursts in the deep hard rock mines of South Africa: 100 years of research, *in* Extracting the Science: a century of mining research, edited by J. Brune, pp. 156-171, Society for Mining, Metallurgy, and Exploration, Inc.

Durrheim, R. J., D. Vogt, and M. Manzi (2013), Advances in geophysical technologies for the exploration and safe mining of deep gold ore bodies in the Witwatersrand basin, South Africa, *in* Mineral Deposit Research for a High-Tech World, edited by E. Jonsson, pp. 118-121.

Durrheim, R. J., R. L. Anderson, A. Cichowicz, R. Ebrahim-Trolloped, G. Hubert, A. Kijko, A. McGarr, W. Ortlepp, and N. van der Merwe (2006), The risks to miners, mines, and the public posed by large seismic events in the gold mining districts of South Africa, Proceedings of the Proceedings of the Third International Seminar on Deep and High Stress Mining, 2-4 October 2006, Quebec City, Canada.

Eberhart-Phillips, D., and D. H. Oppenheimer (1984), Induced seismicity in The Geysers geothermal area, California, J. Geophys. Res., 89, 1191-1207.

Ellsworth, W. L. (2013), Injection-induced earthquakes, Science, 341, 142-149.

Emanov, A. F., A. A. Emanov, A. V. Fateev, E. V. Leskova, E. V. Shevkunova, and V. G. Podkorytova (2014), Mining-induced seismicity at open pit mines in Kuzbass (Bachatsky earthquake on June 18, 2013), Journal of Mining Science, 50, 224-228, doi:10.1134/s1062739114020033.

Engdahl, E. R. (1972), Seismic effects of the MILROW and CANNIKIN nuclear explosions, Bull. seismol. Soc. Am., 62, 1411-1423.

Erzinger, J., and I. Stober (2005), Introduction to special issue: long-term fluid production in the KTB pilot hole, Germany, Geofluids, 5, 1-7, doi:10.1111/j.1468-8123.2004.00107.x.

Evans, D. M. (1966), The Denver area earthquakes and the Rocky Mountain Arsenal disposal well, The Mountain Geologist, 3, 23-36.

Evans, K. F., A. Zappone, T. Kraft, N. Deichmann, and F. Moia (2012), A survey of the induced seismic responses to fluid injection in geothermal and $CO_2$ reservoirs in Europe, Geothermics, 41, 30-54, doi:10.1016/j.geothermics.2011.08.002.

Farahbod, A. M., H. Kao, D. M. Walker, and J. F. Cassidy (2015), Investigation of regional seismicity before and after hydraulic fracturing in the Horn River Basin, northeast British Columbia, Canadian Journal of Earth Sciences, 52, 112-122, doi:10.1139/cjes-2014-0162.

Feignier, B., and R. P. Young (1992), Moment tensor inversion of induced microseismic events: Evidence of non-shear failures in the -4 < M < -2 moment magnitude range, Geophys. Res. Lett., 19, 1503-1506.

Ferrazzini, V., B. Chouet, M. Fehler, and K. Aki (1990), Quantitative analysis of long-period events recorded during hydrofracture experiments at Fenton Hill, New Mexico, J. Geophys. Res., 95, 21871-21884.

Fielitz, D., and U. Wegler (2015), Intrinsic and scattering attenuation as derived from fluid induced microseismicity at the German Continental Deep Drilling site, Geophys. J. Int., 201, 1346-1361, doi:10.1093/gji/ggv064.

Foulger, G. R. (1988a), Hengill triple junction, SW Iceland; 1. Tectonic structure and the spatial and temporal distribution of local earthquakes, J. Geophys. Res., 93, 13493-13506.

Foulger, G. R. (1988b), Hengill triple junction, SW Iceland; 2. Anomalous earthquake focal mechanisms and implications for process within the geothermal reservoir and at accretionary plate boundaries, J. Geophys. Res., 93, 13,507-513,523.

Foulger, G. R., and R. E. Long (1984), Anomalous focal mechanisms; tensile crack formation on an accreting plate boundary, Nature, 310, 43-45.

Foulger, G. R., and B. R. Julian (2014), Maximizing EGS earthquake location accuracies, Proceedings of the Thirty-Ninth Workshop on Geothermal Reservoir Engineering, Stanford, California, February 24-26, 2014, SGP-TR-202.

Foulger, G. R., R. E. Long, P. Einarsson, and A. Björnsson (1989), Implosive earthquakes at the active accretionary plate boundary in northern Iceland, Nature, 337, 640-642.

Foulger, G. R., C.-H. Jahn, G. Seeber, P. Einarsson, B. R. Julian, and K. Heki (1992), Post-rifting stress relaxation at the divergent plate boundary in Iceland, Nature, 358, 488-490.

Gaite, B., A. Ugalde, A. Villaseñor, and E. Blanch (2016), Improving the location of induced earthquakes associated with an underground gas storage in the Gulf of Valencia (Spain), Phys. Earth Planet. Int., 254, 46–59.

Gan, W., and C. Frohlich (2013), Gas injection may have triggered earthquakes in the Cogdell oil field, Texas, Proc. Nat. Acad. Sci., 110, 18786-18791, doi:10.1073/pnas.1311316110.

Gee, D., A. Sowter, A. Novellino, S. Marsh, and J. G. Gluyas (2016), Monitoring land motion due to natural gas extraction; validation of the Intermittent SBAS (ISBAS) DInSAR algorithm over gas fields of North Holland, the Netherlands, Marine and Petroleum Geology, 77, 1338-1354.

Glowacka, E., and F. A. Nava (1996), Major earthquakes in Mexicali Valley, Mexico, and fluid extraction at Cerro Prieto geothermal field, Bull. seismol. Soc. Am., 86, 93-105.

Gluyas, J., and R. Swarbrick (in press, 2016), Petroleum Geoscience, 2nd ed., Wiley-Blackwell.

Gluyas, J. G., and A. Peters (2010), Late field-life for oil reservoirs – a hydrogeological problem, paper presented at British Hydrological Society Third International Symposium, Managing Consequences of a Changing Global Environment.

Godano, M., E. Gaucher, T. Bardainne, M. Regnier, A. Deschamps, and M. Valette (2010), Assessment of focal mechanisms of microseismic events computed from two three-component receivers: application to the Arkema-Vauvert field (France), Geophysical Prospecting, 58, 772-787, doi:10.1111/j.1365-2478.2010.00906.x.

Goertz-Allmann, B. P., D. Kuhn, V. Oye, B. Bohloli, and E. Aker (2014), Combining microseismic and geomechanical observations to interpret storage integrity at the In Salah CCS site, Geophys. J. Int., 198, 447-461, doi:10.1093/gji/ggu010.

González, P. J., K. F. Tiampo, M. Palano, F. Cannavo, and J. Fernandez (2012), The 2011 Lorca earthquake slip distribution controlled by groundwater crustal unloading, Nature Geoscience, 5, 821-825, doi:10.1038/ngeo1610.

Got, J.-L., J. Frechet, and F. W. Klein (1994), Deep fault plane geometry inferred from multiplet relative relocation beneath the south flank of Kilauea, J. Geophys. Res., 99, 15375-15386.

Graham, S. P., M. Wilson, G. R. Foulger, and B. R. Julian (2017), Earthquake weather, in preparation.

Grasle, W., W. Kessels, H. J. Kumpel, and X. Li (2006), Hydraulic observations from a 1 year fluid production test in the 4000 m deep KTB pilot borehole, Geofluids, 6, 8-23, doi:10.1111/j.1468-8123.2006.00124.x.

Green, C. A., P. Styles, and B. J. Baptie (2012), Preese Hall shale gas fracturing. Review & recommendations for induced seismic mitigation, pp iv+26, UK Deparment of Energy and Climate Change.

Guglielmi, Y., F. Cappa, J.-P. Avouac, P. Henry, and D. Elsworth (2015), Seismicity triggered by fluid injection-induced aseismic slip, Science, 348, 1224-1226, doi:10.1126/science.aab0476.

Gupta, H. K. (2002), A review of recent studies of triggered earthquakes by artificial water reservoirs with special emphasis on earthquakes in Koyna, India, Earth-Science Reviews, 58, 279-310, doi:10.1016/s0012-8252(02)00063-6.

Hamilton, D. H., and R. L. Meehan (1971), Ground rupture in the Baldwin Hills, Science, 172, 333-344.

Hamilton, R. M., B. E. Smith, F. G. Fischer, and P. J. Papanek (1972), Earthquakes caused by underground nuclear explosions on Pahute Mesa, Nevada Test Site, Bull. seismol. Soc. Am., 62, 1319-1341.

Hanks, T. C. (1977), Earthquake stress drops, ambient tectonic stresses and stresses that drive plate motions, Pure Appl. Geophys., 115, 441-458.

Hanks, T. C., and H. Kanamori (1979), A moment magnitude scale, J. Geophys. Res., 84, 2348-2350.

Häring, M. O., U. Schanz, F. Ladner, and B. C. Dyer (2008), Characterisation of the Basel 1 enhanced geothermal system, Geothermics, 37, 469-495.

Harris, D. (2012), The impact of cultural and religious influences during natural disasters (volcano eruptions), http://earthquake-report.com/2012/09/27/the-impact-of-cultural-and-religious-influences-during-natural-disasters-volcano-eruptions/, September 27, 2012.

Hartline, C. (2014), Seismic Monitoring Advisory Committee Review, pp 44, Calpine Corporation.

Healy, J. H., W. W. Rubey, D. T. Griggs, and C. B. Raleigh (1968), The Denver earthquakes, Science, 61, 1301-1310.

Heesakkers, V., S. K. Murphy, G. van Aswegen, R. Domoney, S. Addams, T. Dewers, M. Zechmeister, and Z. Reches (2005), The rupture zone of the M=2.2 earthquake that

reactivated the ancient Pretorius Fault in TauTona Mine, South Africa, paper presented at Fall Meeting of the American Geophysical Union abstract S31B-04.

Heki, K., S. Miyazaki, and H. Tsuji (1997), Silent fault slip following an interplate thrust earthquake at the Japan Trench, Nature, 386, 595-598.

Heki, K., G. R. Foulger, B. R. Julian, and C.-H. Jahn (1993), Plate dynamics near divergent boundaries: Geophysical implications of postrifting crustal deformation in NE Iceland, J. Geophys. Res., 98, 14279-14297.

Herrmann, R. B. (1978), A seismological study of two Attica, New York earthquakes, Bull. seismol. Soc. Am., 68, 641-651.

Hill, D. P., P. A. Reasenberg, A. Michael, W. J. Arabasz, G. Beroza, D. Brumbaugh, J. N. Brune, R. Castro, S. Davis, D. dePolo, W. L. Ellsworth, J. Gomberg, S. Harmsen, L. House, S. M. Jackson, M. J. S. Johnston, L. Jones, R. Keller, S. Malone, L. Munguia, S. Nava, J. C. Pechmann, A. Sanford, R. W. Simpson, R. B. Smith, M. Stark, M. Stickney, A. Vidal, S. Walter, V. Wong, and J. Zollweg (1993), Seismicity remotely triggered by the magnitude 7.3 Landers, California, earthquake, Science, 260, 1617-1623.

Hitzman, M. W. (Ed.) (2013), Induced Seismicity Potential in Energy Technologies x+248 pp., National Academies Press, Washington, D.C.

Hough, S. E., and M. Page (2015), A Century of Induced Earthquakes in Oklahoma?, Bull. seismol. Soc. Am., 105, 2863-2870, doi:10.1785/0120150109.

Hsieh, P. A., and J. D. Bredehoeft (1981), A reservoir analysis of the Denver earthquakes: A case of induced seismicity, J. Geophys. Res., 86, 903-920.

Huaman, R. N. E., and T. X. Jun (2014), Energy related $CO_2$ emissions and the progress on CCS projects: a review, Renewable and Sustainable Energy Reviews, 31, 368-385.

Husen, S., C. Bachmann, and D. Giardini (2007), Locally triggered seismicity in the central Swiss Alps following the large rainfall event of August 2005, Geophys. J. Int., 171, 1126-1134, doi:10.1111/j.1365-246X.2007.03561.x.

Husen, S., E. Kissling, and A. von Deschwanden (2012), Induced seismicity during the construction of the Gotthard Base Tunnel, Switzerland: hypocenter locations and source dimensions, Journal of Seismology, 16, 195-213, doi:10.1007/s10950-011-9261-8.

Jahr, T., G. Jentzsch, H. Letz, and M. Sauter (2005), Fluid injection and surface deformation at the KTB location: Modelling of expected tilt effects, Geofluids, 5, 20-27, doi:10.1111/j.1468-8123.2004.00103.x.

Jahr, T., G. Jentzsch, H. Letz, and A. Gebauer (2007), Tilt observation around the KTB-site Germany: Monitoring and modelling of fluid induced deformation of the upper crust of the Earth, *in* Dynamic Planet: Monitoring and Understanding a Dynamic Planet with Geodetic and Oceanographic Tools, edited by P. Tregoning and C. Rizos, pp. 467-472.

Jahr, T., G. Jentzsch, A. Gebauer, and T. Lau (2008), Deformation, seismicity, and fluids: Results of the 2004/2005 water injection experiment at the KTB/Germany, J. Geophys. Res., 113, doi:10.1029/2008jb005610.

Jaku, E. P., A. J. Jager, and M. K. C. Roberts (2001), A review of rock-related fatality trends in the South African gold mining industry, *in* Rock Mechanics in the National Interest, edited by D. Elsworth, J. P. Tinucci and K. A. Heasley, pp. 467-471.

Johnston, A. C., and E. S. Schweig (1996), The enigma of the New Madrid earthquakes of 1811-1812, Ann. Rev. Earth Planet. Sci., 24, 339-384, doi:10.1146/annurev.earth.24.1.339.

Jost, M. L., T. Busselberg, O. Jost, and H. P. Harjes (1998), Source parameters of injection-induced microearthquakes at 9 km depth at the KTB deep drilling site, Germany, Bull. seismol. Soc. Am., 88, 815-832.

Julià, J., A. A. Nyblade, R. Durrheim, L. Linzer, R. Gök, P. Dirks, and W. Walter (2009), Source mechanisms of mine-related seismicity, Savuka mine, South Africa, Bull. seismol. Soc. Am., 99, 2801-2814.

Julian, B. R., G. R. Foulger, and K. Richards-Dinger (2004), The Coso Geothermal Area: A Laboratory for Advanced MEQ Studies for Geothermal Monitoring, Proceedings of the Geothermal Resources Council Annual Meeting, Palm Springs, August 2004.

Julian, B. R., G. R. Foulger, and F. Monastero (2007), Microearthquake moment tensors from the Coso Geothermal area, Proceedings of the Thirty-Second Workshop on Geothermal Reservoir Engineering, Stanford University, Stanford, California, January 22-24, pp. SGP-TR-183.

Julian, B. R., G. R. Foulger, F. C. Monastero, and S. Bjornstad (2010), Imaging hydraulic fractures in a geothermal reservoir, Geophys. Res. Lett., 37, doi:10.1029/2009GL040933.

Kaieda, H., S. Sasaki, and D. Wyborn (2010), Comparison of characteristics of micro-earthquakes observed during hydraulic stimulation operations in Ogachi, Hijiori and Cooper Basin HDR projects, Proceedings of the World Geothermal Congress, Bali, Indonesia, April 25 - 30.

Kao, H., A. M. Farahbod, J. F. Cassidy, M. Lamontagne, D. Snyder, and D. Lavoie (2015), Natural resources Canada's induced seismicity research, Proceedings of the Schatzalp Induced Seismicity Workshop, Davos, Switzerland, 10-13 March.

Kaven, J. O., S. H. Hickman, and N. C. Davatzes (2014), Micro-seismicity and seismic moment release within the Coso Geothermal Field, California, Proceedings of the Thirty-Ninth Workshop on Geothermal Reservoir Engineering, Stanford University, Stanford, California, February 24-26, 2014, pp. SGP-TR-202.

Kaven, J. O., S. H. Hickman, A. F. McGarr, and W. L. Ellsworth (2015), Surface monitoring of microseismicity at the Decatur, Illinois, $CO_2$ sequestration demonstration site, Seismol. Res. Lett., 86, 1096-1101.

Keiding, M., T. Arnadottir, S. Jonsson, J. Decriem, and A. Hooper (2010), Plate boundary deformation and man-made subsidence around geothermal fields on the Reykjanes Peninsula, Iceland, J. Volc. Geotherm. Res., 194, 139-149, doi:10.1016/j.jvolgeores.2010.04.011.

Keith, C. M., D. W. Simpson, and O. V. Soboleva (1982), Induced seismicity and style of deformation at Nurek reservoir, Tadjik SSR, J. Geophys. Res., 87, 4609-4624, doi:10.1029/JB087iB06p04609.

Keranen, K. M., H. M. Savage, G. A. Abers, and E. S. Cochran (2013), Potentially induced earthquakes in Oklahoma, USA: Links between wastewater injection and the 2011 Mw 5.7 earthquake sequence, Geology, 41, 699-702, doi:10.1130/g34045.1.

Keranen, K. M., M. Weingarten, G. A. Abers, B. A. Bekins, and S. Ge (2014), Sharp increase in central Oklahoma seismicity since 2008 induced by massive wastewater injection, Science, 345, 448-451, doi:10.1126/science.1255802.

King, G. C. P., R. S. Stein, and J. Lin (1994), Static stress changes and the triggering of earthquakes, Bull. seismol. Soc. Am., 84, 935-953.

King, V. M., L. V. Block, W. L. Yeck, C. K. Wood, and S. A. Derouin (2014), Geological structure of the Paradox Valley Region, Colorado, and relationship to seismicity induced by deep well injection, J. Geophys. Res., 119, 4955-4978, doi:10.1002/2013jb010651.

Kinscher, J., P. Bernard, I. Contrucci, A. Mangeney, J. P. Piguet, and P. Bigarre (2015), Location of microseismic swarms induced by salt solution mining, Geophys. J. Int., 200, 337-362, doi:10.1093/gji/ggu396.

Klein, F. W., P. Einarsson, and M. Wyss (1977), The Reykjanes Peninsula, Iceland, earthquake swarm of September 1972 and its tectonic significance, J. Geophys. Res., 82, 865-887.

Klose, C. D. (2007a), Geomechanical modeling of the nucleation process of Australia's 1989 M5.6 Newcastle earthquake, Earth planet. Sci. Lett., 256, 547-553, doi:10.1016/j.epsl.2007.02.009.

Klose, C. D. (2007b), Coastal land loss and gain as potential earthquake trigger mechanism in SCRs, Proceedings of the Fall Meeting of the American Geophysical Union abstract T51D-0759, San Francisco, 10–14 December.

Klose, C. D. (2012), Evidence for anthropogenic surface loading as trigger mechanism of the 2008 Wenchuan earthquake, Environmental Earth Sciences, 66, 1439-1447, doi:10.1007/s12665-011-1355-7.

Klose, C. D. (2013), Mechanical and statistical evidence of the causality of human-made mass shifts on the Earth's upper crust and the occurrence of earthquakes, Journal of Seismology, 17, 109-135, doi:10.1007/s10950-012-9321-8.

Knoll, P. (1990), The fluid-induced tectonic rock burst of March 13, 1989 in Werra potash mining district of the GDR (first results), Gerlands Beitrage zur Geophysik, 99, 239-245.

Kovach, R. L. (1974), Source mechanisms for Wilmington oil field, California, subsidence earthquakes, Bull. seismol. Soc. Am., 64, 699–711.

Kozlowska, M., B. Orlecka-Sikora, G. Kwiatek, M. S. Boettcher, and G. Dresen (2015), Nanoseismicity and picoseismicity rate changes from static stress triggering caused by a Mw 2.2 earthquake in Mponeng gold mine, South Africa, J. Geophys. Res., 120, 290-307, doi:10.1002/2014jb011410.

Kravania, S., F. Batini, A. Fiordelise, and G. F. Panza (2000), Full moment tensor retrieval from waveform inversion in the Larderello geothermal area, Pure Appl. Geophys., 157, 1379-1392.

Kundu, B., N. K. Vissa, and V. K. Gahalaut (2015), Influence of anthropogenic groundwater unloading in Indo-Gangetic plains on the 25 April 2015 Mw 7.8 Gorkha, Nepal earthquake, Geophys. Res. Lett., 42, 10607–10613.

Kundu, B., D. Legrand, K. Gahalaut, V. K. Gahalaut, P. Mahesh, K. A. K. Raju, J. K. Catherine, A. Ambikapthy, and R. K. Chadha (2012), The 2005 volcano-tectonic earthquake swarm in the Andaman Sea: Triggered by the 2004 great Sumatra-Andaman earthquake, Tectonics, 31, doi:10.1029/2012tc003138.

Kusznir, N. J., N. H. Al-Saigh, and D. P. Ashwin (1982), Induced seismicity generated by longwall coal mining in the North Staffordshire coal-field, U. K., Proceedings of the Procedings of the First International Congress on Rockbursts and Seismicity in Mines, Johannesburg, South Africa, pp. 153-160.

Latham, G., J. Dorman, F. Duennebier, M. Ewing, D. Lammlein, and Y. Nakamura (1973), Moonquakes, meteoroids, and the state of the lunar interior, Proceedings of the Third Lunar and Planetary Science Conference abstract, Houston, Texas, January 10-13.

Lei, X., G. Yu, S. Ma, X. Wen, and Q. Wang (2008), Earthquakes induced by water injection at ~3 km depth within the Rongchang gas field, Chongqing, China, J. Geophys. Res., 113, doi:10.1029/2008JB005604.

Lei, X., S. Ma, W. Chen, C. Pang, J. Zeng, and B. Jiang (2013), A detailed view of the injection-induced seismicity in a natural gas reservoir in Zigong, southwestern Sichuan Basin, China, J. Geophys. Res., 118, 4296-4311, doi:10.1002/jgrb.50310.

Leith, W., D. W. Simpson, and W. Alvarez (1981), Structure and permeability - geologic controls on induced seismicity at Nurek reservoir, Tadjikistan, USSR, Geology, 9, 440-444, doi:10.1130/0091-7613(1981)9<440:sapgco>2.0.co;2.

Li, G. (2011), World atlas of oil and gas basins, Wiley-Blackwell, 496 pp.

Li, T., M. F. Cai, and M. Cai (2007), A review of mining-induced seismicity in China, International Journal of Rock Mechanics and Mining Sciences, 44, 1149-1171, doi:10.1016/j.ijrmms.2007.06.002.

Lin, C. H. (2005), Seismicity increase after the construction of the world's tallest building: An active blind fault beneath the Taipei 101, Geophys. Res. Lett., 32, doi:10.1029/2005gl024223.

Lindh, A. G. (2005), Success and failure at Parkfield, Seismol. Res. Lett., 76, 3-6.

Lippmann-Pipke, J., J. Erzinger, M. Zimmer, C. Kujawa, M. Boettcher, E. Van Heerden, A. Bester, H. Moller, N. A. Stroncik, and Z. Reches (2011), Geogas transport in fractured hard rock - Correlations with mining seismicity at 3.54 km depth, TauTona gold mine, South Africa, Applied Geochemistry, 26, 2134-2146, doi:10.1016/j.apgeochem.2011.07.011.

Liu, C., A. T. Linde, and I. S. Sacks (2009), Slow earthquakes triggered by typhoons, Nature, 459, 833-836.

Liu, M., and S. Stein (2016), Mid-continental earthquakes: Spatiotemporal occurrences, causes, and hazards, Earth-Science Reviews, 162, 364-386.

Lofgren, B. E. (1978), Monitoring crustal deformation in The Geysers-Clear Lake geothermal area, California, Open-File Report 78-597, pp iv+26, 28 maps, U.S. Geological Survey, Washington, D.C.

Lofgren, B. E. (1981), Monitoring crustal deformation in the Geyser-Clear Lake region, *in* Research in the Geysers-Clear Lake geothermal area, Northern California, edited by R. J. McLaughlin and J. M. Donnelly-Nolan, p. viii+259, U.S. Geological Survey Professional Paper 1141, Washington, D.C.

Ma, X., Z. Li, P. Hua, J. Jiang, F. Zhao, C. Han, P. Yuan, S. Lu, and L. Peng (2015), Fluid-injection- induced seismicity experiment of the WFSD- 3P borehole, Acta Geologica Sinica (English Edition), 89, 1057-1058.

Majer, E. L., and T. V. McEvilly (1981), Detailed microearthquake studies at the Cerro Prieto Geothermal Field, Proceedings of the Third Symposium on the Cerro Prieto Geothermal Field, Baja California, Mexico, Lawrence Berkeley Laboratory, Berkeley, California, March 24-26, pp. 347-352.

Majer, E. L., and T. V. McEvilly (1982), Seismological studies at the Cerro Prieto Field: 1978-1982, Proceedings of the Fourth Symposium on the Cerro Prieto Geothermal Field, Baja California, Mexico, Lawrence Berkeley Laboratory, Berkeley, California, 10–12 August, pp. 145-151.

Majer, E. L., and J. E. Peterson (2007), The impact of injection on seismicity at The Geysers, California Geothermal Field, International Journal of Rock Mechanics and Mining Sciences, 44, 1079-1090, doi:10.1016/j.ijrmms.2007.07.023.

Majer, E. L., R. Baria, M. Stark, S. Oates, J. Bommer, B. Smith, and H. Asanuma (2007), Induced seismicity associated with enhanced geothermal systems, Geothermics, 36, 185-222, doi:10.1016/j.geothermics.2007.03.003.

Maxwell, S. C., and H. Fabriol (2004), Passive seismic imaging of $CO_2$ sequestration at Weyburn, Proceedings of the Society of Engineering Geophysicists International Exposition and 74th Annual Meeting, Denver, Colorado, 10-15 October.

McGarr, A. (1991), On a possible connection between three major earthquakes in California and oil production, Bull. seismol. Soc. Am., 81, 948-970.

McGarr, A. (1992a), Moment tensors of ten Witwatersrand mine tremors, Pure Appl. Geophys., 139, 781-800.

McGarr, A. (1992b), An implosive component in the seismic moment tensor of a mining-induced tremor, Geophys. Res. Lett., 19, 1579-1582.

McGarr, A. (2014), Maximum magnitude earthquakes induced by fluid injection, J. Geophys. Res., 119, 1008-1019, doi:10.1002/2013jb010597.

McGarr, A., D. Simpson, and L. Seeber (2002), Case histories of induced and triggered seismicity, *in* International Geophysics Series, International Handbook of Earthquake and Engineering Seismology, edited by W. H. Lee, P. Jennings, C. Kisslinger and H. Kanamori, pp. 647-664.

McKeown, F. A. (1975), Relation of geological structure to seismicity at Pahute Mesa, Nevada Test Site, Bull. seismol. Soc. Am., 65, 747-764.

McKeown, F. A., and D. D. Dickey (1969), Fault displacements and motion related to nuclear explosions, Bull. seismol. Soc. Am., 59, 2253-2269.

McNamara, D. E., H. M. Benz, R. B. Herrmann, E. A. Bergman, P. Earle, A. Holland, R. Baldwin, and A. Gassner (2015), Earthquake hypocenters and focal mechanisms in central Oklahoma reveal a complex system of reactivated subsurface strike-slip faulting, Geophys. Res. Lett., 42, 2742-2749, doi:10.1002/2014gl062730.

McNutt, S. R., and R. J. Beavan (1981), Volcanic earthquakes at Pavlof volcano correlated with the solid earth tide, Nature, 194, 615-618.

Mercerat, E. D., L. Driad-Lebeau, and P. Bernard (2010), Induced seismicity monitoring of an underground salt cavern prone to collapse, Pure Appl. Geophys., 167, 5-25, doi:10.1007/s00024-009-0008-1.

Milev, A. M., and S. M. Spottiswoode (2002), Effect of the rock properties on mining-induced seismicity around the Ventersdorp Contact Reef, Witwatersrand basin, South Africa, Pure Appl. Geophys., 159, 165-177, doi:10.1007/pl00001249.

Miller, A. D., G. R. Foulger, and B. R. Julian (1998a), Non-double-couple earthquakes II. Observations, Rev. Geophys., 36, 551-568.

Miller, A. D., B. R. Julian, and G. R. Foulger (1998b), Three-dimensional seismic structure and moment tensors of non-double-couple earthquakes at the Hengill-Grensdalur volcanic complex, Iceland, Geophys. J. Int., 133, 309-325.

Mogren, S. M., and M. Mukhopadhyay (2013), Study of seismogenic crust in the eastern province of Saudi Arabia and its relation to the seismicity of the Ghawar fields, paper presented at American Geophysical Union Fall Meeting, 9-13 December.

Monastero, F. C., A. M. Katzenstein, J. S. Miller, J. R. Unruh, M. C. Adams, and K. Richards-Dinger (2005), The Coso geothermal field: A nascent metamorphic core complex, Bull. Geol. Soc. Am., 117, 1534-1553.

Mossop, A., and P. Segall (1999), Volume strain within The Geysers geothermal field, J. Geophys. Res., 104, 29113-29131, doi:10.1029/1999jb900284.

Nagel, N. B. (2001), Compaction and subsidence issues within the petroleum industry: From Wilmington to Ekofisk and beyond, Physics and Chemistry of the Earth, 26, 3-14.

Newman, A., S. Stein, J. Weber, J. Engeln, A. Mao, and T. Dixon (1999), Slow deformation and low seismic hazard at the New Madrid seismic zone, Science, 284, 619-621.

Nicholson, C., and R. L. Wesson (1992), Triggered earthquakes and deep well activities, Pure Appl. Geophys., 139, 561-578.

Nicholson, C., E. Roeloffs, and R. L. Wesson (1988), The northeastern Ohio earthquake of 31 January 1986: Was it induced?, Bull. seismol. Soc. Am., 78, 188-217.

Nicol, A., R. Carne, M. Gerstenberger, and A. Christophersen (2011), Induced seismicity and its implications for $CO_2$ storage risk, *in* 10th International Conference on Greenhouse Gas Control Technologies, edited by J. Gale, C. Hendriks and W. Turkenberg, pp. 3699-3706.

Nielsen, S. B., R. Stephenson, and E. Thomsen (2007), Dynamics of Mid-Palaeocene North Atlantic rifting linked with European intra-plate deformations, Nature, 450, 1071-1074.

Obermeier, S. F. (1996), Use of liquefaction-induced features for paleoseismic analysis, Engineering Geology, 44, 1-76.

Odonne, F., I. Ménard, G. Massonat, and J.-P. Rolando (1999), Abnormal reverse faulting above a depleting reservoir, Geology, 27, 111–114.

Ohtake, M. (1974), Seismic activity induced by water injection at Matsushiro, Japan, Journal of Physics of the Earth, 22, 163-176.

Pavlovski, O. A. (1998), Radiological consequences of nuclear testing for the population of the former USSR (Input information, models, dose and risk estimates), *in* Atmopspheric Nuclear

Tests (Environmental and human consequences), Proceedings of the NATO Advanced Research Workshop, edited by C. S. Shapiro, pp. 219-260, Springer, Berlin.

Pennington, W. D., S. D. Davis, S. M. Carlson, J. DuPree, and T. E. Ewing (1986), The evolution of seismic barriers and asperities caused by the depressuring of fault planes in oil and gas fields of South Texas, Bull. seismol. Soc. Am., 76, 939-948.

Perea, H., E. Masana, and P. Santanach (2012), An active zone characterized by slow normal faults, the northwestern margin of the Valencia trough (NE Iberia): a review, Journal of Iberian Geology, 38, 31-52.

Plotnikova, I. M., B. S. Nurtaev, J. R. Grasso, L. M. Matasova, and R. Bossu (1996), The character and extent of seismic deformation in the focal zone of Gazli earthquakes of 1976 and 1984, M>7.0, Pure Appl. Geophys., 147, 377-387.

Pomeroy, P. W., D. W. Simpson, and M. L. Sbar (1976), Earthquakes triggered by surface quarrying-the Wappingers Falls, New York sequence of June, 1974, Bull. seismol. Soc. Am., 66, 685-700.

Pratt, W. E., and D. W. Johnson (1926), Local subsidence of the Goose Creek oil field, J. Geol., 34, 577-590.

Prioul, R., F. H. Cornet, C. Dorbath, L. Dorbath, M. Ogena, and E. Ramos (2000), An induced seismicity experiment across a creeping segment of the Philippine Fault, J. Geophys. Res., 105, 13595-13612, doi:10.1029/2000jb900052.

Purvis, K., K. E. Overshott, J. C. Madgett, and T. Niven (2010), The Ensign enigma: improving well deliverability in a tight gas reservoir, Proceedings of the Petroleum Geology: From Mature Basins to New Frontiers – Proceedings of the 7th Petroleum Geology Conference, London, pp. 325-336.

Raleigh, C. B., J. H. Healy, and J. D. Bredehoeft (1976), An experiment in earthquake control at Rangely, Colorado, Science, 191, 1230-1237.

Reasenberg, P. A., and R. W. Simpson (1992), Response of regional seismicity to the static stress change produced by the Loma Prieta earthquake, Science, 255, 1687-1690.

Richardson, E., and T. H. Jordan (2002), Seismicity in deep gold mines of South Africa: Implications for tectonic earthquakes, Bull. seismol. Soc. Am., 92, 1766-1782, doi:10.1785/0120000226.

Ross, A., G. R. Foulger, and B. R. Julian (1999), Source processes of industrially-induced earthquakes at The Geysers geothermal area, California, Geophysics, 64, 1877-1889.

Roth, P., N. Pavoni, and N. Deichmann (1992), Seismotectonics of the eastern Swiss Alps and evidence for precipitation-induced variations of seismic activity, Tectonophysics, 207, 183-197, doi:10.1016/0040-1951(92)90477-n.

Rudajev, V., and J. Sileny (1985), Seismic events with non-shear components: II Rockbursts with implosive source component, Pure Appl. Geophys., 123, 17-25.

Schultz, R., V. Stern, M. Novakovic, G. Atkinson, and Y. J. Gu (2015), Hydraulic fracturing and the Crooked Lake Sequences: Insights gleaned from regional seismic networks, Geophys. Res. Lett., 42, 2750-2758, doi:10.1002/2015gl063455.

Seeber, L., J. G. Armbruster, W.-Y. Kim, and N. Barstow (1998), The 1994 Cacoosing Valley earthquakes near Reading, Pennsylvania: A shallow rupture triggered by quarry unloading, J. Geophys. Res., 103, 24505-24521.

Segall, P. (1985), Stress and subsidence resulting from subsurface fluid withdrawal in the epicentral region of the 1983 Coalinga earthquake, J. Geophys. Res., 90, 6801-6816.

Segall, P. (1989), Earthquakes triggered by fluid extraction, Geology, 17, 942-946.

Segall, P. (1992), Induced stresses due to fluid extraction from axisymmetrical reservoirs, Pure Appl. Geophys., 139, 535-560, doi:10.1007/bf00879950.

Semmane, F., I. Abacha, A. K. Yelles-Chaouche, A. Haned, H. Beldjoudi, and A. Amrani (2012), The earthquake swarm of December 2007 in the Mila region of northeastern Algeria, Natural Hazards, 64, 1855-1871, doi:10.1007/s11069-012-0338-7.

Shapiro, S. A., J. Kummerow, C. Dinske, G. Asch, E. Rothert, J. Erzinger, H. J. Kumpel, and R. Kind (2006), Fluid induced seismicity guided by a continental fault: Injection experiment of 2004/2005 at the German Deep Drilling Site (KTB), Geophys. Res. Lett., 33, doi:10.1029/2005gl024659.

Simiyu, S. M., and G. R. Keller (2000), Seismic monitoring of the Olkaria Geothermal area, Kenya Rift valley, J. Volc. Geotherm. Res., 95, 197-208.

Simpson, D. W., and O. V. Soboleva (1977), Water level variations and reservoir-induced seismicity at Nurek, USSR, Transactions of the American Geophysical Union, 58, 1196.

Simpson, D. W., and S. K. Negmatullaev (1981), Induced seismicity at Nurek reservoir, Tadjikistan, USSR, Bull. seismol. Soc. Am., 71, 1561-1586.

Simpson, D. W., and W. Leith (1985), The 1976 and 1984 Gazli, USSR, earthquakes—were they induced?, Bull. seismol. Soc. Am., 75, 1465-1468.

Skoumal, R. J., M. R. Brudzinski, and B. S. Currie (2015), Earthquakes induced by hydraulic fracturing in Poland Township, Ohio, Bull. seismol. Soc. Am., 105, 189-197.

Stark, M. A. (1990), Imaging injected water in The Geysers reservoir using microearthquake data, Transactions of the Geothermal Resources Council, 17, 1697-1704.

Stein, S., M. Liu, E. Calais, and Q. Li (2009), Midcontinent earthquakes as a complex system, Seismol. Res. Lett., 80, 551-553.

Stein, S., M. Liu, T. Camelbeeck, M. Merino, A. Landgraf, E. Hintersberger, and S. Kuebler (2015), Challenges in assessing seismic hazard in intraplate Europe, *in* Seismicity, Fault Rupture and Earthquake Hazards in Slowly Deforming Regions, edited by A. Landgraf, S. Kuebler, E. Hintersberger and S. Stein, Geological Society, London, Special Publications, London.

Styles, P., P. Gasparini, E. Huenges, P. Scandone, S. Lasocki, and F. Terlizzese (2014), Report on the hydrocarbon exploration and seismicity in Emilia region, pp 213, International Commission on Hydrocarbon Exploration and Seismicity in the Emilia Region.

Suckale, J. (2009), Induced seismicity in hydrocarbon fields, Advances in Geophysics, 51, 55-106.

Suckale, J. (2010), Moderate-to-large seismicity induced by hydrocarbon production, The Leading Edge, 29, 310-319, doi:10.1190/1.3353728.

Tadokoro, K., M. Ando, and K. Nishigami (2000), Induced earthquakes accompanying the water injection experiment at the Nojima fault zone, Japan: Seismicity and its migration, J. Geophys. Res., 105, 6089-6104, doi:10.1029/1999jb900416.

Talwani, P. (1995), Speculation on the causes of continuing seismicity near Koyna reservoir, India, Pure Appl. Geophys., 145, 167-174, doi:10.1007/bf00879492.

Tang, C., J. W. Wang, and J. Zhang (2010), Preliminary engineering application of microseismic monitoring technique to rockburst prediction in tunneling of Jinping II project, Journal of Rock Mechanics and Geotechnical Engineering, 3, 193-208.

Tang, L., M. Zhang, L. Sun, and L. Wen (2015), Injection-induced seismicity in a natural gas reservoir in Hutubi, southern Junggar Basin, northwest China, Transactions of the American Geophysical Union, Abstract S13B-2847.

Terashima, T. (1981), Survey on induced seismicity at Mishraq area in Iraq, Journal of Physics of the Earth, 29, 371-375.

Tester, J. W., and e. al. (2006), The future of geothermal energy, pp 372, Massachusetts Institute of Technology, Cambridge, Massachusetts.

Toksöz, M. N., and H. K. Kehrer (1972), Tectonic strain release by underground nuclear explosions and its effect on seismic discrimination, Geophys. J. R. astron. Soc., 31, 141-161.

Turbitt, T., A. B. Walker, and C. W. A. Browitt (1983), Monitoring of the background and induced seismicity at the Cornwall geothermal energy site, Geophys. J. R. astron. Soc., 73, 299-299.

van der Elst, N. J., H. M. Savage, K. M. Keranen, and G. A. Abers (2013), Enhanced remote earthquake triggering at fluid-injection sites in the midwestern United States, Science, 341, 164-167.

van Eck, T., F. Goutbeek, H. Haak, and B. Dost (2006), Seismic hazard due to small-magnitude, shallow-source, induced earthquakes in The Netherlands, Engineering Geology, 87, 105-121.

Van Wees, J. D., L. Buijze, K. Van Thienen-Visser, M. Nepveu, B. B. T. Wassing, B. Orlic, and P. A. Fokker (2014), Geomechanics response and induced seismicity during gas field depletion in the Netherlands, Geothermics, 52, 206-219, doi:10.1016/j.geothermics.2014.05.004.

Vasco, D. W., J. Rutqvist, A. Ferretti, A. Rucci, F. Bellotti, P. Dobson, C. Oldenburg, J. Garcia, M. Walters, and C. Hartline (2013), Monitoring deformation at The Geysers Geothermal Field, California using C-band and X-band interferometric synthetic aperture radar, Geophys. Res. Lett., 40, 2567–2572, doi:doi:10.1002/grl.50314.

Verdon, J. P., J.-M. Kendall, A. L. Stork, R. A. Chadwick, D. J. White, and R. C. Bissell (2013), Comparison of geomechanical deformation induced by megatonne-scale $CO_2$ storage at Sleipner, Weyburn, and In Salah, Proceedings of the National Academy of Sciences, 110, E2762-E2771.

Villegas-Lanza, J. C., J.-M. Nocquet, F. Rolandone, M. Vallée, H. Tavera, F. Bondoux, T. Tran, X. Martin, and M. Chlieh (2016), A mixed seismic–aseismic stress release episode in the Andean subduction zone, Nature Geoscience, 9, 150–154, doi:10.1038/ngeo2620.

Waldhauser, F., and W. L. Ellsworth (2000), A double-difference earthquake location algorithm: Method and application to the northern Hayward Fault, California, Bull. seismol. Soc. Am., 90, 1353-1368.

Wallace, T., D. V. Helmberger, and G. R. Engen (1983), Evidence of tectonic release from underground nuclear explosions in long-period *P* waves, Bull. seismol. Soc. Am., 73, 593-613.

Walsh, F. R., and M. D. Zoback (2015), Oklahoma's recent earthquakes and saltwater disposal, Science Advances, 1, e1500195, doi:10.1126/sciadv.1500195.

Wang, P., M. J. Small, W. Harbert, and M. Pozzi (2016), A bayesian approach for assessing seismic transitions associated with wastewater injections, Bull. seismol. Soc. Am., 106, 832-845.

Wilson, M. P., G. R. Foulger, J. G. Gluyas, R. J. Davies, and B. R. Julian (2017), *HiQuake*: The Human-Induced Earthquake Database, Bull. seismol. Soc. Am., submitted.

Wilson, M. P., R. J. Davies, G. R. Foulger, B. R. Julian, P. Styles, J. G. Gluyas, and S. Almond (2015), Anthropogenic earthquakes in the UK: A national baseline prior to shale exploitation, Marine and Petroleum Geology, 68, 1-17, doi:10.1016/j.marpetgeo.2015.08.023.

Wong, I. G., and A. McGarr (1990), Implosional failure in mining-induced seismicity: A critical review, *in* Rockbursts and Seismicity in Mines, edited by C. Fairhurst, pp. 45-51, Bakema, Rotterdam.

Wong, I. G., J. R. Humphrey, J. A. Adams, and W. J. Silva (1989), Observations of mine seismicity in the eastern Wasatch Plateau, Utah, U. S. A.: A possible case of implosional failure, Pure Appl. Geophys., 129, 369-405.

Wright, C., E. M. Kgaswane, M. T. O. Kwadiba, R. E. Simon, T. K. Nguuri, and R. McRae-Samuel (2003), South African seismicity, April 1997 to April 1999, and regional variations in the crust and uppermost mantle of the Kaapvaal craton, Lithos, 71, 369-392, doi:10.1016/s0024-4937(03)00122-1.

Yabe, Y., M. Nakatani, M. Naoi, J. Philipp, C. Janssen, T. Watanabe, T. Katsura, H. Kawakata, D. Georg, and H. Ogasawara (2015), Nucleation process of an M2 earthquake in a deep gold mine in South Africa inferred from on-fault foreshock activity, J. Geophys. Res., 120, 5574-5594, doi:10.1002/2014jb011680.

Yakovlev, D. V., T. I. Lazarevich, and S. V. Tsirel (2013), Natural and induced seismic activity in Kuzbass, Journal of Mining Science, 49, 862-872.

Yeck, W. L., L. V. Block, C. K. Wood, and V. M. King (2015), Maximum magnitude estimations of induced earthquakes at Paradox Valley, Colorado, from cumulative injection volume and geometry of seismicity clusters, Geophys. J. Int., 200, 322-336, doi:10.1093/gji/ggu394.

Zaliapin, I., and Y. Ben-Zion (2016), Discriminating characteristics of tectonic and human-induced seismicity, Bull. seismol. Soc. Am., 106, 846-859.

Zang, A., E. Majer, and D. Bruhn (2014a), Analysis of induced seismicity in geothermal operations, Geothermics, 52, 1-5, doi:10.1016/j.geothermics.2014.07.006.

Zang, A., V. Oye, P. Jousset, N. Deichmann, R. Gritto, A. McGarr, E. Majer, and D. Bruhn (2014b), Analysis of induced seismicity in geothermal reservoirs - An overview, Geothermics, 52, 6-21, doi:10.1016/j.geothermics.2014.06.005.

Zedník, J., J. Pospíšil, B. Růžek, J. Horálek, A. Boušková, P. Jedlička, Z. Skácelová, V. Nehybka, K. Holub, and J. Rušajová (2001), Earthquakes in the Czech Republic and surrounding regions in 1995–1999, Studia Geophysica et Geodaetica, 45, 267-282.

Zhang, Y., W. Feng, L. Xu, C. Zhou, and Y. Chen (2008), Spatio-temporal rupture process of the 2008 great Wenchuan earthquake, Science in China Series D: Earth Sciences, 52, 145-154, doi:10.1007/s11430-008-0148-7.

Ziegler, M., K. Reiter, O. Heidbach, A. Zang, G. Kwiatek, D. Stromeyer, T. Dahm, G. Dresen, and G. Hofmann (2015), Mining-induced stress transfer and its relation to a 1.9 seismic event in an ultra-deep South African gold mine, Pure Appl. Geophys., 172, 2557-2570, doi:10.1007/s00024-015-1033-x.

Zoback, M. D., and J. H. Healy (1984), Friction, faulting, and insitu stress, Annales Geophysicae, 2, 689-698.

Zoback, M. D., and H. P. Harjes (1997), Injection-induced earthquakes and crustal stress at 9 km depth at the KTB deep drilling site, Germany, J. Geophys. Res., 102, 18477-18491, doi:10.1029/96jb02814.

Tables

Table 1: Data recorded in the database

| Column contents |
|---|
| Country |
| Project name |
| Project type (subclass) |
| Longitude |
| Latitude |
| Project end date |
| Project start date |
| End date of seismicity or monitoring |
| Start date of seismicity or monitoring |
| Magnitude type |
| Delay time |
| Date of largest earthquake |
| Depth of largest earthquake |
| Distance of largest earthquake from induction activity |
| Year of largest earthquake |
| Lithology/resource |
| Distance of furthest earthquake from induction activity |
| Depth of induction activity |
| Typical depth of earthquakes |
| Previous seismicity |
| Tectonic setting |
| Injection/extraction rate |
| Dam height |
| Total volume or mass injected/extracted |
| Units of injection/extraction rate |
| Maximum wellhead pressure during injection |
| Units of total volume or mass injected/extracted |
| Stress change postulated to have induced earthquake |
| Change in reservoir pressure |
| Bottom-hole temperature |
| Area of project |
| References |
| Notes |
| References used by Davies *et al.* [2013] |
| Project type |

Table 2: Classification categories of underground injection wells in The Code of Federal Regulations of the USA (40 CFR 144.6-Classification of wells)[23].

| Class of well | Purpose |
|---|---|
| Class I | Industrial and Municipal Waste Disposal Wells |
| Class II | Oil and Gas Related Injection Wells |
| Class III | Injection Wells for Solution Mining |
| Class IV | Shallow Hazardous and Radioactive Injection Wells |
| Class V | Wells for Injection of Non-Hazardous Fluids into or Above Underground Sources of Drinking Water |
| Class VI | Wells Used for Geologic Sequestration of $CO_2$ |

[23] https://www.epa.gov/uic/general-information-about-injection-wells#regulates

Table 3: Induced seismicity statistics for the total numbers of projects of different types, the number that are seismogenic, and related data.

| **Project type** | **# projects** | **# cases in the database** | **% projects that are seismogenic** | **Observed maximum magnitude ($M_{MAX}$)** | **# seismogenic projects reported by Hitzman et al., (2013)** | **Source for # projects** |
|---|---|---|---|---|---|---|
| CCS | 75 | 2 | 2.67 | 1.7 | - | Huaman and Jun (2014) |
| Construction | *unknown* | 2 | - | 4.2 | - | |
| Conventional oil and gas | 67,000 fields | 116 | 0.17 | 7.3 | 65 | Li (2011) |
| Fracking | 2,500,000 wells | 21 | 0.00 | 4.4 | 2 | King (2012) |
| Geothermal | *unknown* | 56 | - | 6.6 | 26 | Bertani (2010) |
| Groundwater extraction | *unknown* | 5 | - | 7.8 | - | |
| Mining | 13,262 currently active mines | 267 | 2.01 | 6.1 | 8 ("other") | http://mrdata.usgs.gov/ |
| Nuclear (Underground) | 1,352 tests | 22 | 1.63 | 4.9 | - | Pavlovski (1998) |
| Research | *unknown* | 13 | - | 3.1 | - | |
| Waste fluid injection wells (Class II wells) | 151,000 wells (USA only) | 33 | 0.02 | 5.7 | 11 | Hitzman *et al.*, (2013) |
| Water dam | 6,862 reservoirs (>0.1 $km^3$) | 168 | 2.45 | 7.9 | 44 | Lehner *et al.* (2011) |
| **Total** | | **705** | | | **156** | |

Table 4: Number of reported $M_{MAX}$ values and number predicted from downward extrapolation of the linear trend of earthquakes with $M_{MAX}$ 5 - 7 shown in Figure 111.

| $M_{MAX}$ | # reported earthquakes | # predicted earthquakes |
|---|---|---|
| 7 | 4 | 4 |
| 6 | 17 | 16 |
| 5 | 68 | 67 |
| 4 | 181 | ~250 |
| 3 | 371 | ~1000 |
| 2 | 497 | ~4000 |

Table 5: Conversions for commonly used units of pressure

| |
|---|
| 1 bar = 0.1 MPa, equivalent to ~4 m of rock overburden |
| 1 atmosphere = 0.1 MPa |
| 1 $kg/cm^2$ = 0.1 MPa |
| 1 $pound/inch^2$ (psi) = $6.9 \times 10^{-3}$ MPa |
| 1 acre-foot of water/football field[24] = $29 \times 10^{-6}$ MPa |
| Hydrostatic gradient = 10 MPa/km |
| Lithostatic gradient = ~25 MPa/km |

[24] American football, including end zones.

Table 6: Stress changes associated with some natural processes postulated to induce earthquakes.

| Effect | Stress change (MPa) |
|---|---|
| Earth tides | 0.05 |
| Seismic static stress changes | 0.03 |
| Remote triggering | ~0.5 |
| Typhoons | 0.003 |

Table 7: Seven questions proposed by Davis and Frohlich [1993] to diagnose earthquakes induced by fluid injection [from Davis & Frohlich, 1993].

| | Question | Earthquakes Clearly Not Induced | Earthquakes Clearly Induced | I Denver, Colorado | II Painesville, Ohio |
|---|---|---|---|---|---|
| | *Background Seismicity* | | | | |
| 1 | Are these events the first known earthquakes of this character in the region? | NO | YES | YES | NO |
| | *Temporal Correlation* | | | | |
| 2 | Is there a clear correlation between injection and seismicity | NO | YES | YES | NO |
| | *Spatial Correlation* | | | | |
| 3a | Are epicenters near wells (within 5 km)? | NO | YES | YES | YES? |
| 3b | Do some earthquakes occur at or near injection depths? | NO | YES | YES | YES? |
| 3c | If not, are there known geologic structures that may channel flow to sites of earthquakes? | NO | YES | NO? | NO? |
| | *Injection Practices* | | | | |
| 4a | Are changes in fluid pressure at well bottoms sufficient to encourage seismicity? | NO | YES | YES | YES |
| 4b | Are changes in fluid pressure at hypocentral locations sufficient to encourage seismicity? | NO | YES | YES | NO? |
| | **TOTAL "YES" ANSWERS** | **0** | **7** | **6** | **3** |

# SUPPLEMENTARY ONLINE MATERIAL

## A Method used to construct the database.

In performing the literature review on which our database is founded, we proceeded as follows:

1. A single-sheet Excel spreadsheet was constructed and the raw database of Davies *et al.* [2013] was imported. Additional columns were added for new types of data, *e.g.*, Earthquake Cause (main class) and Earthquake Cause (subclass);

2. The entries were checked and updated where necessary. References were added where lacking;

3. New cases were searched for using Google Scholar. Where possible (most cases) PDFs were downloaded, digitally filed, and entered into EndNote. Where a PDF of an entire paper or report was unobtainable, information from the abstract was used;

4. Where data are not available, *e.g.*, maximum magnitude, the relevant spreadsheet cell is left blank;

5. Entries in the database were double-checked;

6. Where conflicting information is published, *e.g.*, different magnitudes, we report moment magnitude ($M_W$). If $M_W$ is not available we report the largest magnitude from those available.

## B Description of the database

We have assembled 705 cases of industrial projects postulated to have induced earthquakes. These cases include a wide range of project types. For a large majority of industrial projects in all categories, there are no reports of seismogenesis. However, it is clear that there is large-scale under-reporting.

For the purpose of plotting figures, we divided the projects into the following categories:

*Carbon Capture and Storage (CCS)*

The implementation of CCS to combat climate change is still largely in the demonstration stage. To date there have been 75 CCS projects with eight of these on a commercial scale [Huaman & Jun, 2014]. Storage requires the injection of $CO_2$ into a subsurface formation. Two CCS projects are reported to have induced earthquakes–In Salah, Algeria and Decatur, Illinois, USA.

*Construction*

Projects where humans have built a structure or created artificial topography are classed as construction, with the exception of water dams which are categorized separately. Two such projects are reported to be linked to earthquakes, the erection of the Taipei 101, Taiwan, building and artificial accumulation of shingle deposits at Folkestone, UK. We searched for reports of earthquakes associated with the construction of nearby Samphire Hoe. This is a coastal park created using ~$10^{10}$ kg of chalk excavated on the English side of the Channel Tunnel, an order of magnitude greater than accumulated at Folkestone. However, we found none.

*Conventional oil and gas (including unspecified oil, gas and waste-water projects)*

There are approximately 67,000 oil- and gasfields globally. Our database contains 112 seismogenic projects in this category. The largest earthquake postulated to be related to such projects is the 1976 $M_S$ 7.3 earthquake near the Gazli Gasfield, Uzbekistan.

*Shale-gas hydrofracturing*

Hydraulic fracturing to increase oil and gas production has been practiced for several decades but its recent use to extract gas from shale has attracted media attention. Every successful hydrofracture job induces seismicity because the objective is to fracture rock. Despite the fact that ~2.5 million such jobs have been completed, our database contains only 21 cases of induced earthquakes. Of these cases, the largest earthquake reported was $M_W$ 4.4 and occurred in Canada in 2015.

*Geothermal exploitation*

There are 65 geothermal fields worldwide that produce >100 GW electric per year. Our database contains 51 cases that have been linked to earthquakes. The largest earthquake postulated to have been induced is the 1979 $M_L$ 6.6 earthquake near the Cerro Prieto Field, California.

*Groundwater extraction*

Our database contains five cases where earthquakes are postulated to be linked to large-scale groundwater extraction. The largest of these case is the 2015 $M_W$ 7.8 Gorkha, Nepal, earthquake, which resulted in ~8000 deaths and ~$10 billion of economic loss, ~50% of the Gross Domestic Product of Nepal.

*Mining*

Mining-related seismicity (gallery collapses, stope contractions, “rock bursts”, “coal bumps”, faulting) accounts for 38% (267 cases) of the cases in our database, the largest category. The U.S. Geological Survey estimates there are currently 13,262 active mines worldwide, in addition to inactive and historic mines. There is likely under-reporting of mining seismicity. The largest earthquake proposed to be induced by mining is the 2013 $M_L$ 6.1 earthquake, suggested to be linked to the Bachatsky open-cast coal mine, Russia. Other countries with $M \geq 5$ earthquakes postulated to be induced by mining include Australia, Canada, Germany, Poland, South Africa and the US.

*Underground nuclear explosions*

We exclude the initial explosions from our database but recognize two types of related induced seismicity:

a) earthquakes associated with the collapse of the underground cavity created by the explosion, and

b) earthquakes induced on local faults.

The largest recorded seismic event of type a) was $m_b$ 4.9 (the 5 Mt Cannikin test, Amchitka, Alaska, 1971). The largest reported event of type b) had $m_b$ 4.8 (the 27$^{th}$ October 1973 Novaya Zemlya test). Of 1,352 underground nuclear tests, 22 have been associated with earthquakes [Pavlovski, 1998].

*Research*

The database contains 13 projects classified as research. These involve injecting water into the

subsurface or flooding abandoned mines. One of the earliest of these was that at the Rangely Oilfield, Colorado, where the largest induced earthquake in this category occurred, the 1970 $M_L$ 3.1 event. Another notable project was the Kontinentales Tiefbohrprogramm der Bundesrepublik Deutschland (KTB), the German Continental Deep Drilling Program, in which small volumes of fluid were injected as deep as ~9 km, the deepest reported fluid injection to date.

*Waste fluid injection*

Seismicity induced by waste-fluid injection is increasing. Of the > 151,000 Class II waste-fluid injection wells in the USA, estimates for the rate of seismogenesis range from nine cases to > 18,000. Our database contains 33 cases in this category predominantly from the US and Canada. The largest earthquake postulated to be induced by this process is the 2011 $M_W$ 5.7 Prague, Oklahoma, earthquake.

*Water dams*

The database contains 168 cases of earthquakes possibly induced by impounding water behind dams. Approximately 2.5% of reservoirs with volumes > 0.1 $km^3$ are reported to be seismogenic. The largest postulated reservoir-related earthquake is the great 2008 $M_W$ ~8 Wenchuan, earthquake, China (Zipingpu dam) which caused ~90,000 fatalities.

## C Explanations of database column headings.

| Column Heading | Description |
|---|---|
| Country | Country where the project is/was geographically located |
| Eq cause (main class) | Overall project type, *e.g.*, geothermal, proposed to have caused the earthquake |
| Eq cause (subclass) | Type of project within the main class, *e.g.*, geothermal (injection), proposed to have caused the earthquake |
| Name | Project name |
| Latitude (˚N) | Project latitude |
| Longitude (˚W) | Project longitude |
| Start date of project | Start of project or main phase relevant to earthquakes |
| End date of project | End of project or main phase relevant to earthquakes |
| Start date of earthquakes or monitoring | Date of onset of seismicity (monitoring already in place) or the date monitoring commenced |
| End date of earthquakes or monitoring | Date seismicity ceased or the date monitoring equipment was removed |
| Delay time | Time between the start of the project and the onset of seismicity |
| No. eqs | Number of earthquakes recorded |
| Max magnitude ($M_{MAX}$) | Observed maximum magnitude reported |
| Mag type | Type of magnitude reported for the maximum magnitude earthquake. Moment magnitude is reported if available. If moment magnitude was not reported, the largest magnitude of any type was recorded |
| Depth of largest eq (m) | Hypocentral depth of largest earthquake |
| Date of largest eq | Date of the largest earthquake |

| | |
|---|---|
| Year of largest eq | Year of the largest earthquake |
| Distance of $M_{MAX}$ to project (m) | Horizontal distance of maximum magnitude earthquake from inducing project |
| Max distance to project (m) | Horizontal distance between the furthest observed earthquake (not necessarily the largest) and the inducing project |
| Lithology/resource | Reservoir lithology, *e.g.*, sandstone, or mining resource, *e.g.*, coal |
| Depth of most eq activity (m) | Depth at which most earthquake activity is observed |
| Depth of project (m) | Depth of the inducing activity, *e.g.*, the injection |
| Tectonic setting | Tectonic setting of project based on simple plate boundary model |
| Previous seismic activity | Notes on any seismicity prior to the start of the project |
| Dam height (m) | Height of the dam impounding the water reservoir |
| Injection/extraction rate (max unless stated, units in next column) | Rate of injection or extraction of material from the subsurface |
| Rate units | Units for rate of injection or extraction |
| Total volume or mass of material injected/extracted (units in next column | Total volume or mass of material injected into or extracted from the subsurface. For dams: the volume of the water reservoir |
| Volume or mass units | Units for volume or mass of material |
| Pressure (MPa) (max unless stated) | Maximum (unless stated) well head injection pressure during the project |
| Change in reservoir pressure (MPa) | Change in pressure of fluid in the subsurface reservoir |
| Stress change (MPa) | Change in stress postulated to have induced the earthquake |
| Area ($x10^6$ $m^2$) | Area of the project, *e.g.*, surface area of water reservoir |
| BHT (°C) | Bottom-hole temperature of borehole |
| Notes | Additional information about project or data |

| Reference(s) | Source of information on project |
|---|---|
| Reference(s) from Davies *et al.* [2013] | Source(s) used by Davies *et al.* (2013) for project |

## D List of the 705 entries in the database.

| Country | Eq cause (main class) | Eq cause (subclass) | Name | Max mag (Mmax) | Mag type | Date of largest eq |
|---|---|---|---|---|---|---|
| Algeria | CCS | CO2 injection | In Salah | 1.7 | MW | |
| USA | CCS | CO2 injection | Decatur, Illinois, demonstration site | 1.26 | MW | |
| UK | Construction | Coastal engineering (geoengineering) | Folkestone | 4.2 | ML | 2007/04/28 |
| Taiwan | Construction | Construction | Taipei 101 | 3.8 | ML | 2004/10/23 |
| Uzbekistan | Conventional Oil and Gas | Gas extraction and storage | Gazli | 7.3 | MS | 1976/04/08 |
| Canada | Conventional Oil and Gas | Secondary recovery (water injection) | Snipe Lake, Alberta | 5.1 | ML | 1970/03/08 |
| USA | Conventional Oil and Gas | Oil extraction | Long Beach (Wilmington and Huntington Beach oilfields), California | 6.3 | ML | 1933 |
| Iran | Conventional Oil and Gas | Oil extraction | Cheshmeh Khosh | 6.2 | | 2014/08/18 |
| Canada | Conventional Oil and Gas | Oil extraction and Secondary recovery (water injection) | Eagle/Eagle West | 4.3 | | 1994/05/22 |
| Canada | Conventional Oil and Gas | Secondary recovery | Gobles, Ontario | 3.4 | | |
| Canada | Conventional Oil and Gas | Secondary recovery and Waste disposal | Cold Lake, Alberta | 2 | ML | |
| Italy | Conventional Oil and Gas | Gas extraction | Caviaga, Po Valley | 5.5 | ML | 1951/05/15 |
| Canada | Conventional Oil and Gas | EOR (CO2 injection/part CCS project) | Weyburn, Saskatchewan | -1 | | |
| USA | Conventional Oil and Gas | Gas extraction | El Reno, Oklahoma | 5.2 | ML | 1952 |
| USA | Conventional Oil and Gas | Oil extraction | Wilmington, California | 5.1 | ML | 1949 |
| China | Conventional Oil and Gas | Secondary recovery (water injection) | Renqiu | 4.5 | ML | 1987/06/02 |
| USA | Conventional Oil and Gas | Oil extraction | Richland County, Illinois | 4.9 | ML | 1987 |
| China | Conventional Oil and Gas | Secondary recovery (water injection) | Shengli, Shandong Province | | | |
| USA | Conventional Oil and Gas | Gas extraction | Fashing, Texas | 4.8 | MW | 2011/10/20 |
| Denmark | Conventional Oil and Gas | Oil and Gas extraction and Secondary recovery | Dan | | | |

| | | | | | | |
|---|---|---|---|---|---|---|
| | | (water injection) | | | | |
| Russia | Conventional Oil and Gas | Oil extraction | Starogroznenskoe | 4.7 | ML | 1971/03/26 |
| Kuwait | Conventional Oil and Gas | Oil extraction and Burning | Minagish/Umm Gudair oil fields (for largest eq) | 4.7 | | 1993/06/02 |
| USA | Conventional Oil and Gas | Gas extraction | Catoosa, Oklahoma | 4.7 | ML | |
| Norway | Conventional Oil and Gas | Secondary recovery (unintentional water injection into overburden) | Ekofisk | 3 | ML | 2001/05/07 |
| Russia | Conventional Oil and Gas | Oil and gas extraction | Gudermes | 4.5 | | |
| Germany | Conventional Oil and Gas | Gas extraction | Rotenberg /Neuenkirchen | 4.4 | MW | 2004/10/20 |
| Norway | Conventional Oil and Gas | | Vishund | | | |
| Romania | Conventional Oil and Gas | Secondary recovery (water injection) | Tazlau | -1.5 | MW | |
| Spain | Conventional Oil and Gas | Gas storage | Castor | 4.3 | MW | 2013/10/01 |
| Saudi Arabia | Conventional Oil and Gas | Oil and gas extraction | Ghawar | 4.24 | ML | |
| France | Conventional Oil and Gas | Gas extraction | Lacq (Arette) | 4.2 | ML | 1978 |
| USA | Conventional Oil and Gas | Oil extraction | Wortham-Mexia, Texas | 4 | | 1932/04/09 |
| Canada | Conventional Oil and Gas | Gas extraction | Strachan, Alberta | 4 | ML | |
| Russia | Conventional Oil and Gas | Oil extraction and Secondary recovery (water injection) | Romashkinskoye (Romashkino field), Volga-Ural | 4 | ML | 1991/10/28 |
| Russia | Conventional Oil and Gas | Oil extraction and Secondary recovery? | Grozny, Chechen Republic | 3.3 | ML | |
| Germany | Conventional Oil and Gas | Gas extraction | Soltau | 4 | ML | 1977/06/02 |
| Russia | Conventional Oil and Gas | Oil extraction and Secondary recovery (water injection) | Novo-Elkhovskoye, Volga-Ural | | | |
| USA | Conventional Oil and Gas | Oil and Gas extraction | Alice (Stratton field), Texas | 3.9 | mbLG | 2010/04/25 |
| Germany | Conventional Oil and Gas | Gas extraction | Skye (Bassum, Niedersachsen) | 3.8 | ML | 2005/07/15 |
| Turkmenistan | Conventional Oil and Gas | Oil extraction and Secondary recovery (water injection) | Barsa-Gelmes-Vishka | 6 | | 1984 |
| USA | Conventional Oil and Gas | Oil extraction and Secondary recovery (water injection) | Coalinga, California | 6.5 | ML | 1983 |
| China | Conventional Oil and Gas | Gas extraction and storage | Hutubi, Southern Junggar Basin | 3.6 | ML | |
| USA | Conventional Oil and Gas | Oil extraction and Secondary recovery | Kettleman North Dome, California | 6.1 | MW | 1985 |

| | | | | | | |
|---|---|---|---|---|---|---|
| | | (water injection) | | | | |
| USA | Conventional Oil and Gas | Oil extraction and Secondary recovery (water injection) | Montebello (Whittier Narrows), California | 5.9 | ML | 1987 |
| Netherlands | Conventional Oil and Gas | Gas extraction | Bergermeer (Alkmaar) | 3.5 | MW | 2001/09/09 |
| USA | Conventional Oil and Gas | Gas extraction | East Durant, Oklahoma | 3.5 | ML | |
| USA | Conventional Oil and Gas | Secondary recovery (water injection) | Cogdell Field, Texas | 5.3 | ML | 1978/06/16 |
| Netherlands | Conventional Oil and Gas | Gas extraction | Groningen | 3.4 | ML | 2012/08/06 |
| USA | Conventional Oil and Gas | Oil extraction and Secondary recovery (water injection) | Brewton (Big Escambia Creek, Little Rock, and Sizemore Creek fields), Alabama | 4.9 | MW | 1997/10/24 |
| USA | Conventional Oil and Gas | Oil extraction and Stimulation | Orcutt, California | 3.5 | ML | |
| USA | Conventional Oil and Gas | Oil extraction and Secondary recovery (water injection) | East Texas (Gladewater), Texas | 4.7 | | 1957/03/19 |
| Netherlands | Conventional Oil and Gas | Gas extraction | Roswinkel | 3.4 | ML | 1997/02/19 |
| USA | Conventional Oil and Gas | EOR (CO2 injection) | Cogdell Field, Texas | 4.4 | MW | 2011/09/11 |
| USA | Conventional Oil and Gas | Secondary recovery | Kermit, Texas | 4 | ML | |
| USA | Conventional Oil and Gas | Oil and Gas extraction and Secondary recovery (water injection) | Imogene (Pleasanton), Texas | 3.9 | ML | 1984/03/03 |
| USA | Conventional Oil and Gas | Oil and gas extraction | War-Wink, Texas | 3 | ML | 1975 |
| USA | Conventional Oil and Gas | Production and Secondary recovery | Inglewood, California | 3.7 | ML | 1962 |
| USA | Conventional Oil and Gas | Oil extraction and Secondary recovery (water injection) | Falls City, Texas | 3.6 | mbLg | 1991/07/20 |
| USA | Conventional Oil and Gas | Gas/Brine extraction and Wastewater (injection) | Azle/Reno,Texas | 3.6 | | |
| USA | Conventional Oil and Gas | Secondary recovery | Hunt, Alabama /Mississippi | 3.6 | ML | |
| Germany | Conventional Oil and Gas | Gas extraction | Visselhövede | 2.9 | ML | 2012/02/13 |
| Germany | Conventional Oil and Gas | Gas extraction | Völkersen | 2.9 | ML | 2012/11/22 |
| USA | Conventional Oil and Gas | Secondary recovery | Dollarhide, Texas/New Mexico | 3.5 | ML | |
| Germany | Conventional Oil and Gas | Gas extraction | Langwedel | 2.8 | ML | 2008/04/03 |
| Netherlands | Conventional Oil and Gas | Gas extraction | Eleveld | 2.8 | ML | 1986/12/26 |

| | | | | | | |
|---|---|---|---|---|---|---|
| Netherlands | Conventional Oil and Gas | Gas extraction | Assen | 2.8 | ML | 1986 |
| USA | Conventional Oil and Gas | Secondary recovery | Keystone I&II, Texas | 3.5 | ML | |
| Netherlands | Conventional Oil and Gas | Gas extraction | Middelie | 2.7 | ML | 1989/12/01 |
| Netherlands | Conventional Oil and Gas | Gas extraction | Bergen | 2.7 | ML | 2001/10/10 |
| Germany | Conventional Oil and Gas | Gas extraction | Verden | 2.5 | ML | 2011/05/02 |
| Netherlands | Conventional Oil and Gas | Gas extraction | Annerveen | 2.3 | ML | 1994/08/16 |
| Netherlands | Conventional Oil and Gas | Gas extraction | Appelscha | 2.3 | ML | 2003/06/16 |
| Netherlands | Conventional Oil and Gas | Gas extraction | Dalen | 2.2 | ML | 1996/11/17 |
| Netherlands | Conventional Oil and Gas | Gas extraction | Roden | 2.1 | ML | 1996/09/02 |
| France | Conventional Oil and Gas | Well collapse/Water injection | Lacq (Arette) | 1.9 | ML | 1996/09/18 |
| Oman | Conventional Oil and Gas | Gas extraction | Shuiba reservoir | 2.05 | ML | 2001/03/04 |
| Netherlands | Conventional Oil and Gas | Gas extraction | Emmen | 2 | ML | 1991/02/15 |
| USA | Conventional Oil and Gas | Secondary recovery | Ward-Estes, Texas | 3.5 | ML | |
| USA | Conventional Oil and Gas | Secondary recovery | North Panhandle (Lambert), Texas | 3.4 | ML | |
| Netherlands | Conventional Oil and Gas | Gas extraction | VriesNoord | 1.9 | | 1996 (Dec.) |
| USA | Conventional Oil and Gas | Secondary recovery | Ward-South, Texas | 3 | ML | |
| Netherlands | Conventional Oil and Gas | Gas extraction | Emmen-Nieuw Amsterdam | 1.7 | | 1994 (Sep.) |
| Czech Republic | Conventional Oil and Gas | Gas storage | Příbram (Háje) | 1.5 | ML | |
| Netherlands | Conventional Oil and Gas | Gas extraction | Schoonebeek | 1.4 | | 2002 (Dec.) |
| Netherlands | Conventional Oil and Gas | Gas extraction | Coevorden | 1.2 | | 1997 (Feb.) |
| Netherlands | Conventional Oil and Gas | Gas extraction | Ureterp | 1 | | 1999 (Apr.) |
| Netherlands | Conventional Oil and Gas | Gas extraction | VriesCentraal | 1 | | 2000 (July) |
| USA | Conventional Oil and Gas | Oil extraction | Seventy Six oil field, Clinton County, Kentucky | 0.9 | MW | |
| Netherlands | Conventional Oil and Gas | Gas storage | Bergermeer | 0.7 | | 2013 (Oct.) |
| USA | Conventional Oil and Gas | Secondary recovery | Dora Roberts, Texas | 3 | ML | |
| USA | Conventional | Secondary recovery | Monahans, Texas | 3 | ML | |

| | | | | | | |
|---|---|---|---|---|---|---|
| | Oil and Gas | | | | | |
| Norway | Conventional Oil and Gas | Oil extraction | Valhall | | | |
| USA | Conventional Oil and Gas | Secondary recovery | Sleepy Hollow, Nebraska | 2.9 | ML | |
| USA | Conventional Oil and Gas | Secondary recovery and Stimulation | Love County, Oklahoma | 2.8 | ML | |
| USA | Conventional Oil and Gas | Oil and Gas extraction and Secondary recovery | Apollo-Hendrick, Texas | 2 | MD | |
| USA | Conventional Oil and Gas | Oil and gas extraction | South Houston, Texas | | | |
| USA | Conventional Oil and Gas | Oil and gas extraction | Clinton, Texas | | | |
| USA | Conventional Oil and Gas | Oil and gas extraction | MyKawa, Texas | | | |
| USA | Conventional Oil and Gas | Oil and gas extraction | Blue Ridge, Texas | | | |
| USA | Conventional Oil and Gas | Oil and gas extraction | Webster, Texas | | | |
| USA | Conventional Oil and Gas | Oil and gas extraction | Goose Creek, Texas | | | |
| Venezuela | Conventional Oil and Gas | Oil and gas extraction | Costa Oriental, Lake Maracaibo | | | |
| USA | Conventional Oil and Gas | Oil extraction and Secondary recovery (water injection) | New Harmony, Indiana | 1.8 | MW | |
| USA | Conventional Oil and Gas | Secondary recovery (water injection) | South Eugene Island, Louisianna | | | |
| France | Conventional Oil and Gas | Gas extraction | Meillon | | | |
| Netherlands | Conventional Oil and Gas | Gas Storage | Norg | | | |
| Netherlands | Conventional Oil and Gas | Gas Storage | Grijpskerk | | | |
| USA | Conventional Oil and Gas | Stimulation | Austin Chalk, Giddings Field, Texas | | | |
| Canada | Fracking | Fracking (injection) | Northern Montney Earthquake, British Columbia | 4.4 | MW | 2014/08/04 |
| Canada | Fracking | Fracking (injection) | Crooked Lake (Fox Creek), Alberta (Waskahigan and McKinley fields) | 4.4 | ML | 2015/01/23 |
| Canada | Fracking | Fracking (injection) | Septimus (Montney Trend) | 4.2 | ML | 2013/05/27 |
| Canada | Fracking | Fracking (injection) | Fox Creek, Alberta | 3.9 | MW | 2015/06/13 |
| Canada | Fracking | Fracking (injection) | Horn River Basin | 3.8 | ML | 2011/05/19 |
| Canada | Fracking | Fracking (injection) | Beg-Town (Montney Trend) | 3.4 | ML | 2013/08/21 |
| Canada | Fracking | Fracking (injection) | Caribou (Montney Trend) | 3.2 | ML | 2014/03 |

| | | | | | | |
|---|---|---|---|---|---|---|
| | | | | | | /02 |
| Canada | Fracking | Fracking (injection) | Cardston, Alberta (Ninastoko field) | 3 | ML | 2011/12 /04 |
| Canada | Fracking | Fracking (injection) | Doe-Dawson (Montney Trend) | 2.8 | ML | 2013/10 /23 |
| Canada | Fracking | Fracking (injection) | Altares (Montney Trend) | 2.2 | ML | 2013/11 /05 |
| Canada | Fracking | Fracking (injection) | Montney Trend | -0.4 | MW | |
| Canada | Fracking | Fracking (injection) | Western Canada | -2.2 | MW | 2006 |
| UK | Fracking | Fracking (injection) | Preese Hall | 2.3 | ML | 2011/04 /01 |
| USA | Fracking | Fracking (injection) | Eagleton 1-29, Oklahoma | 3.2 | ML | 2014/07 /07 |
| USA | Fracking | Fracking (injection) | Poland Township, Ohio | 3 | ML | 2014/03 /10 |
| USA | Fracking | Fracking (injection) | Oklahoma (Eola-Robberson field) | 2.9 | ML | 2011/01 /18 |
| USA | Fracking | Fracking (injection) | Harrison County, Ohio | 2 | MW | 2013/10 /02 |
| USA | Fracking | Fracking (injection+production ?) | Bienville Parish, Louisiana | 1.9 | ML | 2011/10 /15 |
| USA | Fracking | Fracking (injection) | Cotton Valley, Texas | -0.2 | MW | 1997/05 /14 |
| USA | Fracking | Fracking (injection) | Jonah, Wyoming | -1.2 | | |
| USA | Fracking | Fracking (injection) | Hughes County, Oklahoma | -1.9 | | 2007 |
| Mexico | Geothermal | Geothermal (extraction) | Cerro Prieto (Imperial Valley) | 6.6 | ML | 1979/10 /15 |
| USA | Geothermal | EGS (circulation) | Salton Sea, California | 5.1 | | 2005 |
| USA | Geothermal | EGS (circulation) | The Geysers | 4.6 | | 1982 |
| Mexico | Geothermal | EGS (circulation) | Los Humeros | 4.6 | Md | 1994/11 /25 |
| El Salvador | Geothermal | EGS (injection) | Berlín | 4.4 | ML | 2003/09 /16 |
| Australia | Geothermal | EGS (injection) | Cooper Basin (Habanero 1) | 3.7 | MW | 2003/11 /14 |
| Italy | Geothermal | EGS (circulation) | Monte Amiata | 3.5 | ML | 1983 |
| Switzerland | Geothermal | EGS (injection) | Basel | 3.4 | ML | 2006/12 /08 |
| Switzerland | Geothermal | EGS (injection) | St. Gallen | 3.3 | MW | 2013/07 /20 |
| New Zealand | Geothermal | Geothermal (reinjection) | Rotokawa | 3.3 | | 2012 (Feb.) |
| Italy | Geothermal | EGS (circulation) | Larderello-Travale | 3.2 | ML | 1982 |
| New Zealand | Geothermal | Geothermal (reinjection) | Mokai | 3.2 | | |
| Italy | Geothermal | EGS (injection) | Torre Alfina | 3 | ML | 1977 |
| El Salvador | Geothermal | EGS (injection) | Ahuachapan | 3 | ML | 1991 |

| | | | | | | |
|---|---|---|---|---|---|---|
| Iceland | Geothermal | Geothermal (extraction) | Reykjanes | 3 | ML | 2006 |
| Australia | Geothermal | EGS (injection) | Cooper Basin (Habanero 4) | 3 | ML | |
| Italy | Geothermal | EGS (injection) | Latera | 2.9 | ML | 1984/12/09 |
| France | Geothermal | EGS (injection) | Soultz (GPK-3) | 2.9 | ML | 2003/06/10 |
| Australia | Geothermal | EGS (injection) | Cooper Basin (Habanero 1 restimulation) | 2.9 | ML | 2005 |
| USA | Geothermal | EGS (stimulation) | Coso | 2.8 | | 2004 (Aug.) |
| Germany | Geothermal | EGS (circulation) | Landau | 2.7 | ML | 2009/08/15 |
| New Zealand | Geothermal | Geothermal (reinjection) | Ngatamariki | 2.7 | | |
| Australia | Geothermal | EGS (injection) | Paralana 2 | 2.5 | MW | 2011/11/13 |
| Kenya | Geothermal | Geothermal (extraction) | Olkaria | 2.5 | Md | 1996 |
| Philippines | Geothermal | Geothermal (reinjection) | Puhagan | 2.4 | ML | 1983 (Feb.) |
| France | Geothermal | EGS (injection) | Soultz (GPK-2) | 2.4 | MW | 2000/07/16 |
| Germany | Geothermal | EGS (circulation) | Unterhaching | 2.4 | ML | 2008 (July) |
| Germany | Geothermal | EGS (injection) | Insheim | 2.4 | ML | 2010 (Apr.) |
| Iceland | Geothermal | EGS (injection) | Hellisheidi | 2.4 | ML | |
| USA | Geothermal | EGS (injection) | Newberry | 2.39 | MW | 2012/07/12 |
| Italy | Geothermal | EGS (injection) | Cesano | 2 | ML | 1978 |
| UK | Geothermal | EGS (circulation) | Rosemanowes | 2 | ML | 1987/07/12 |
| Iceland | Geothermal | EGS (circulation) | Krafla | 2 | ML | |
| Japan | Geothermal | EGS (injection) | Ogachi (OGC-1) | 2 | MW | |
| Indonesia | Geothermal | EGS (circulation) | Lahendong | 2 | | |
| Mexico | Geothermal | EGS (injection) | Los Azufres | 1.9 | Md | |
| Germany | Geothermal | EGS (injection) | Bad Urach | 1.8 | MW | 2002 |
| USA | Geothermal | EGS (injection) | Desert Peak, Nevada | 1.7 | ML | |
| France | Geothermal | EGS (injection) | Rittersshoffen, Alsace | 1.6 | Mlv | 2013/07/02 |
| Australia | Geothermal | EGS (injection) | Cooper Basin (Jolokia 1) | 1.6 | ML | |
| Australia | Geothermal | EGS (injection) | Paralana 2 DFIT | 1.4 | ML | |
| USA | Geothermal | EGS (injection) | Fenton Hill, New Mexico | 1.3 | | 1983 |
| Germany | Geothermal | EGS (injection) | GeneSys, Hannover | 0 | ML | |

| | | | | | | |
|---|---|---|---|---|---|---|
| Sweden | Geothermal | EGS (injection) | Fjällbacka | -0.2 | ML | |
| Japan | Geothermal | EGS (injection) | Hijiori (SKG-2 injection/stimulation) | -1 | | 1988 |
| Germany | Geothermal | EGS (injection) | Groß-Schönebeck | -1 | MW | 2007 |
| Iceland | Geothermal | EGS (circulation) | Laugaland | -1 | ML | |
| Iceland | Geothermal | EGS (injection) | Svartsengi | -1 | ML | |
| Japan | Geothermal | EGS (circulation) | Hijiori (SkG-2 circulation) | -1 | | |
| USA | Geothermal | EGS (injection) | Baca, New Mexico | -2 | | 1982 (May) |
| Mexico | Geothermal | Drilling, Stimulation and Production tests | Tres Virgenes, LV-06 | | | |
| Turkey | Geothermal | EGS (circulation) | Salavatli, Aydin | | | |
| USA | Geothermal | EGS (circulation) | Brady, Nevada | | | |
| Indonesia | Geothermal | EGS (injection) | Darajat | | | |
| Indonesia | Geothermal | EGS (injection) | Wayang Windu | | | |
| USA | Geothermal | EGS (circulation) | Raft River, Idaho | | | |
| Nepal | Groundwater extraction | Groundwater (extraction) | Gorkha earthquake, Indo-Gangetic plains | 7.8 | MW | 2015/04/25 |
| Spain | Groundwater extraction | Groundwater (extraction) | Lorca | 5.1 | MW | 2011/05/11 |
| Spain | Groundwater extraction | Groundwater extraction/Water dam | Jaen (Giribaile reservoir) | 3.72 | MW | 2013/05/02 |
| Brazil | Groundwater extraction | Groundwater (extraction) | Bebedouro, Paraná Basin | 2.9 | | 2005 (Mar.) |
| USA | Groundwater extraction | Groundwater extraction | San Joaquin Valley | | | |
| Russia | Mining | Mining | Bachatsky, Kuzbass | 6.1 | ML | 2013/06/18 |
| Germany | Mining | Mining (collapse/fluid-induced rockburst) | Volkershausen (Ernst Thaelmann/Merkers mine) | 5.6 | ML | 1989/03/13 |
| Australia | Mining | Mining and Groundwater extraction | Newcastle | 5.6 | ML | 1989/12/27 |
| South Africa | Mining | Mining | President Brand Mine, Welkom | 5.6 | mb | 1994/10/30 |
| Australia | Mining | Mining | Ellalong | 5.4 | ML | 1994/08/06 |
| Australia | Mining | Mining | Maitland | 5.3 | ML | 18/06/1868 |
| Australia | Mining | Mining | Boolaroo | 5.3 | ML | 1925/12/18 |
| South Africa | Mining | Mining | Klerksdorp (DRDGold's North West Operations) | 5.3 | ML | 2005/03/09 |
| USA | Mining | Mining (solution) | Attica, New York | 5.2 | ML | 1929/08/12 |

| | | | | | | |
|---|---|---|---|---|---|---|
| Germany | Mining | Mining | Sunna (Suenna) | 5.2 | ML | 1975/06/23 |
| South Africa | Mining | Mining | Welkom | 5.2 | ML | 1976/12/08 |
| USA | Mining | Mining (collapse) | Solvay mine, Wyoming | 5.2 | mb | 1995/02/03 |
| Russia | Mining | Mining (rock burst) | Umbozero Mine | 5.1 | ML | 1999/08/17 |
| Germany | Mining | Mining | Heringen | 5 | ML | |
| Poland | Mining | Mining | Lubin mine | 5 | ML | 1977/03/24 |
| South Africa | Mining | Mining | Hartebeesfontein | 5 | ML | 1997/08/21 |
| Australia | Mining | Mining | Kalgoorlie Super Pit | 5 | ML | 2010/04/20 |
| Canada | Mining | Mining (rockburst) | Wright-Hargreaves mine, Ontario | 5 | | 1905/05/17 |
| South Africa | Mining | Mining | Free State Goldfield | 4.7 | ML | 1989/01/25 |
| South Africa | Mining | Mining | Carletonville | 4.7 | ML | 1992/03/07 |
| Russia | Mining | Mining (collapse) | Solikamsk, Upper Kama | 4.7 | | 1994/01/05 |
| Germany | Mining | Mining (collapse) | Saale (Halle) (Teutschental mine) | 4.6 | MW | 42/5/1940 |
| China | Mining | Mining (solution) | Salt mine, Zigong, Sichuan | 4.6 | ML | 1985/03/29 |
| Germany | Mining | Mining | Ibbenbüren | 4.6 | ML | 1991/05/16 |
| USA | Mining | Mining | Moss No. 2, Virginia | 4.5 | ML | 1972/05/20 |
| USA | Mining | Mining (extraction and abandonment) | Cacoosing Valley (Sinking Springs), Pennsylvania | 4.4 | ML | 1994/01/16 |
| Russia | Mining | Mining (rock burst) | SKRU-2, Ural Mountains | 4.4 | | 1995/01/05 |
| Australia | Mining | Mining | Appin, Tower and West Cliff Collieries | 4.4 | | 1999/03/17 |
| Belarus | Mining | Mining | Soligorsk (Starobin deposit) | 4.4 | | 2003/12/18 |
| South Africa | Mining | Mining | Savuka, Carletonville | 4.4 | ML | 2007 |
| China | Mining | Mining | Taiji mine, Beipiao, Liaoning | 4.3 | ML | 1977/04/28 |
| China | Mining | Mining | Chayuan mine, Shizhu, Sichuan | 4.3 | ML | 1987/07/02 |
| Russia | Mining | Mining (rock burst) | Kurgazakskaya Mine | 4.3 | ML | 1990/05/28 |
| China | Mining | Mining | Louguanshan #4 well, South Bureau, Sichuan | 4.3 | ML | 1994/04/15 |

| | | | | | | |
|---|---|---|---|---|---|---|
| China | Mining | Mining | Weixi mine, Leshan, Sichuan | 4.2 | ML | 1979/08/15 |
| China | Mining | Mining | Mentougou mine, Beijing, Beijing | 4.2 | ML | 1994/05/19 |
| USA | Mining | Mining | Willow Creek, Utah | 4.2 | ML | 2000/03/07 |
| Poland | Mining | Mining | Rudna mine | 4.2 | ML | 2013/03/19 |
| Germany | Mining | Mining | Ruhr area | 4.1 | MW | 1936/11/03 |
| China | Mining | Mining | Huachu mine, Liuzhi, Guizhou | 4.1 | ML | 1982/03/20 |
| Russia | Mining | Mining (rock burst) | Kirovsky Mine, Khibiny Massif (Kola Peninsula) | 4.1 | ML | 1989/04/16 |
| Russia | Mining | Mining (rock burst) | Blinovo-Kamensky Mine | 4.1 | ML | 1994/07/29 |
| Canada | Mining | Mining | Creighton, Ontario | 4.1 | MN | 2006/11/29 |
| France | Mining | Mining | Lorraine | 4 | MW | 1973/04/20 |
| USA | Mining | Mining | Buchanan No. 1, Virginia | 4 | ML | 1988/04/14 |
| USA | Mining | Mining | Lynch mine, Kentucky | 4 | | 1995/03/11 |
| South Africa | Mining | Mining | Western Deep Levels East | 4 | ML | 1996/05/05 |
| Germany | Mining | Mining | Saar (Primsmulde), Saarland | 4 | ML | 2008/02/23 |
| South Africa | Mining | Mining | Kloof | 4 | ML | |
| Italy | Mining | Mining (tunneling) and hydrologic changes | Gran Sasso | 3.9 | | 1992/08/25 |
| South Africa | Mining | Mining | Deelkraal | 3.9 | ML | |
| South Africa | Mining | Mining | East Driefontain | 3.9 | ML | |
| Germany | Mining | Mining | Peissenberg | 3.8 | MW | 1967/09/16 |
| China | Mining | Mining | Wacang/Shimacao/ Chenjiapo mines, Yichang, Hubei | 3.8 | ML | 1971/06/17 |
| USA | Mining | Mining (collapse) | King #4, Utah | 3.8 | ML | 1981/05/14 |
| USA | Mining | Mining | Lynch No. 37, Kentucky | 3.8 | ML | 1994/08/03 |
| China | Mining | Mining | Wulong mine, Fuxin, Liaoning | 3.8 | ML | 2004/06/16 |
| Canada | Mining | Mining | Copper Cliff North, Ontario | 3.8 | MN | 2008/09/11 |
| Canada | Mining | Mining | Kidd Creek, Ontario | 3.8 | MN | 2009/01/06 |
| South Africa | Mining | Mining | Elandsrand | 3.8 | ML | |

| | | | | | | |
|---|---|---|---|---|---|---|
| Czech Republic | Mining | Mining | CSA Mine, Ostrava-Karvina Coal Basin | 3.75 | | 1983/04/27 |
| China | Mining | Mining | Nanshan mine, Hegang, Heilongjiang | 3.7 | ML | 2001/02/01 |
| China | Mining | Mining | Laohutai mine, Fushun, Liaoning | 3.7 | ML | 2002/01/26 |
| Germany | Mining | Mining | Saar/Lorraine | 3.7 | MW | 2008/02/23 |
| South Africa | Mining | Mining | Mponeng | 3.7 | ML | |
| South Africa | Mining | Mining | Leeudoorn | 3.7 | ML | |
| China | Mining | Mining | Huaibaoshi mine, Zigui, Yichang, Hubei | 3.6 | ML | 1972/03/13 |
| Poland | Mining | Mining | Belchatow | 3.6 | ML | 1979/08/17 |
| China | Mining | Mining | Taozhuang mine, Zaozhuang, Shandong | 3.6 | ML | 1982/01/07 |
| USA | Mining | Mining (collapse and rockburst) | Jim Walter Resources, Inc., No. 4, Alabama | 3.6 | ML | 1986/05/07 |
| China | Mining | Mining | Liu zhi mine, Yingpan, Liuzhi, Guizhou | 3.6 | ML | 1991/07/09 |
| China | Mining | Mining | Bingshuijing mine, Yingpan, Liuzhi, Guizhou | 3.6 | ML | 1991/07/09 |
| USA | Mining | Mining | Soldier Creek, Utah | 3.6 | ML | 1993/01/21 |
| USA | Mining | Mining (collapse) | Retsof, New York | 3.6 | | 1994/03/12 |
| USA | Mining | Mining (collapse) | Genesseo, New York | 3.6 | | 1994 |
| Russia | Mining | Mining (rock burst) | Tashtagol Mine | 3.6 | ML | 1999/10/24 |
| China | Mining | Mining (collapse) | Shunyuan mine, Zaozhuang, Shandong | 3.6 | ML | 2002/05/20 |
| Russia | Mining | Mining (rock burst) | Karnasurt Mine | 3.6 | ML | 2002/12/17 |
| USA | Mining | Mining (collapse) | Cottonwood, Utah | 3.5 | ML | 1992/07/05 |
| Germany | Mining | Mining | Saar (Dilsburg Ost), Saarland | 3.5 | ML | 2000 (Nov.) |
| Russia | Mining | Mining | Mine 15-15bis | 3.5 | ML | 2010/02/13 |
| Australia | Mining | Mining | Olympia Dam | 3.5 | | 2013/05/01 |
| USA | Mining | Mining | Lucky Friday Mine, Idaho | 3.5 | | |
| USA | Mining | Mining | Olga, West Virginia | 3.4 | ML | 1965/04 |

| | | | | | | |
|---|---|---|---|---|---|---|
| | | | | | | /26 |
| UK | Mining | Mining (extraction and collapse) | North Staffordshire (Stoke on Trent) | 3.4 | mb | 1975/07/15 |
| USA | Mining | Mining (collapse) | Sunnyside #3, Utah | 3.4 | ML | 1981/09/21 |
| China | Mining | Mining | Xujiadong 711 mine, Chenzhou, Hunan | 3.4 | ML | 1998/03/12 |
| China | Mining | Mining | San he jian mine, Xuzhou, Jiangsu | 3.4 | ML | 2003/05/08 |
| China | Mining | Mining | Chengzi mine, Beijing, Beijing | 3.4 | ML | |
| USA | Mining | Mining | Wappingers Falls, New York | 3.3 | mbn | 1974/06/07 |
| USA | Mining | Mining | Trail Mountain, Utah | 3.3 | ML | 1987/12/16 |
| Germany | Mining | Mining (tunneling) | Saar (Primsmulde), Saarland (Roadway construction) | 3.3 | ML | 2005 (May) |
| Canada | Mining | Mining | Garson, Ontario | 3.3 | MN | 2008/12/05 |
| China | Mining | Mining | Huating mine, Pingliang, Gansu | 3.3 | ML | |
| Canada | Mining | Mining (rockburst) | Campbell mine, Ontario | 3.3 | MN | |
| UK | Mining | Mining | Nottinghamshire | 3.2 | ML | 1984/03/22 |
| China | Mining | Mining | Niumasi mine, Shaoyang, Hunan | 3.2 | ML | 1994/09/04 |
| Russia | Mining | Mining (rock burst) | Mine 14-14bis | 3.2 | ML | 2004/03/25 |
| Sweden | Mining | Mining (rock burst) | Grängesberg ore mine | 3.1 | ML | 1974/08/30 |
| Germany | Mining | Mining | S-Harz | 3.1 | MW | 1983/07/02 |
| China | Mining | Mining | Xifeng Nan shan mine, Lindong, Guizhou | 3.1 | ML | 1991/04/06 |
| USA | Mining | Mining (collapse) | Star Point #2, Utah | 3.1 | ML | 1991/02/06 |
| Bulgaria | Mining | Mining (solution) | Provadia | 3.1 | MD | 1994/06/20 |
| China | Mining | Mining | Qixingjiezhen mine, Lianyuan, Hunan | 3.1 | ML | 1996/03/28 |
| China | Mining | Mining | Shanjiaocun mine, Panjiang, Guizhou | 3.1 | ML | 1997/12/05 |
| China | Mining | Mining | Yueliangtian mine, Panjiang, Guizhou | 3.1 | ML | 1997/12/05 |
| Canada | Mining | Mining | Macassa, Ontario | 3.1 | MN | 2008/07/12 |
| India | Mining | Mining (abandonment) | Champion Reef, Kolar Gold field | 3.09 | ML | |

| | | | | | | |
|---|---|---|---|---|---|---|
| Canada | Mining | Mining | Cory Mine, Saskatchewan | 3 | mb | 1980/02/29 |
| USA | Mining | Mining (collapse) | Deer Creek, Utah | 3 | ML | 1984/03/21 |
| USA | Mining | Mining (collapse) | Castle Gate #3, Utah | 3 | ML | 1986/10/30 |
| USA | Mining | Mining | VP No. 3, Virginia | 3 | ML | 1987/03/04 |
| China | Mining | Mining | Xindong mine, Shaoyang, Hunan | 3 | ML | 1994/11/20 |
| USA | Mining | Mining | Skyline #3, Utah | 3 | ML | 1996/06/02 |
| China | Mining | Mining | Fangshan mine, Beijing, Beijing | 3 | ML | 1997/02/18 |
| USA | Mining | Mining (solution) | Cleveland, Ohio | 3 | ML | |
| USA | Mining | Mining (abandonment and flooding) | Mineville, New York | 3 | Mc | |
| USA | Mining | Mining | Galena mine, Idaho | 3 | ML | |
| Canada | Mining | Mining (rockburst) | Quirke mine, Ontario | 3 | | |
| Poland | Mining | Mining | Polkowice mine | 3 | MW | |
| China | Mining | Mining | En kou mine, Lowde, Hunan | 2.9 | ML | 1976/01/08 |
| USA | Mining | Mining | Dillsburg, Pennsylvania | 2.9 | ML | 2009/04/24 |
| China | Mining | Mining | Huayazi mine, Zigui, Yichang, Hubei | 2.8 | ML | 1973 (Mar.) |
| China | Mining | Mining | Sheng li mine, Fushun, Liaoning | 2.8 | ML | 1978/09/21 |
| China | Mining | Mining | Da he bian mine, Shiucheng, Guizhou | 2.8 | ML | 1985/07/09 |
| UK | Mining | Mining | Midlothian | 2.8 | ML | 1986/10/09 |
| China | Mining | Mining | Mei tan ba mine, Xifenglun, Hunan | 2.8 | ML | 1991/04/23 |
| China | Mining | Mining | Niwan mine, Xiangtan, Hunan | 2.8 | ML | 2003/01/17 |
| China | Mining | Mining | Benxi Caitun mine, Shenyang, Liaoning | 2.8 | ML | 2004/04/13 |
| China | Mining | Mining | Baidong mine, Datong, Shanxi | 2.7 | ML | 1983 (Sep.) |
| China | Mining | Mining | Sijiaotian mine, Yingpan, Liuzhi, Guizhou | 2.7 | ML | 1985/01/21 |
| China | Mining | Mining | Dizong mine, Yingpan, Liuzhi, Guizhou | 2.7 | ML | 1985/01/21 |
| China | Mining | Mining | Dayong mine, | 2.7 | ML | 1985/01 |

| | | | | | | |
|---|---|---|---|---|---|---|
| | | | Yingpan, Liuzhi, Guizhou | | | /21 |
| Canada | Mining | Mining | Strathcona, Ontario | 2.7 | mN | 1988/06 /19 |
| China | Mining | Mining | Dahuatang mine, Shaoyang, Hunan | 2.7 | ML | 1997/12 /04 |
| China | Mining | Mining | Qingshan mine, Lianyuan, Hunan | 2.6 | ML | 1996/07 /01 |
| Sweden | Mining | Mining | Zingruvan | 2.6 | MW | |
| China | Mining | Mining | Longfeng mine, Fushun, Liaoning | 2.5 | ML | 1981/02 /16 |
| China | Mining | Mining | Doulishan mine, Lowde, Hunan | 2.5 | ML | 1985/03 /04 |
| China | Mining | Mining | Yan guan mine, Zigui, Yichang, Hubei | 2.5 | ML | 1988/05 /14 |
| France | Mining | Mining (abandonment and flooding) | Gardanne | 2.5 | | 2005 (Nov.) |
| Spain | Mining | Mining (collapse) | Lo Tacón (Torre Pacheco) | 2.4 | MW | 1998/05 /02 |
| Switzerland | Mining | Mining (tunneling) | MFS Faido (Gotthard basetunnel) | 2.4 | ML | 2006/03 /25 |
| Canada | Mining | Mining | Fraser, Ontario | 2.4 | MN | 2008/10 /16 |
| Korea | Mining | Mining | Dogye | 2.4 | ML | |
| USA | Mining | Mining | Lompoc diatomite mine, California | 2.3 | MD | 1995/04 /05 |
| USA | Mining | Mining | Florida, New York | 2.3 | | 2003 |
| China | Mining | Mining | Gangdong mine, Shuangyashan, Heilongjiang | 2.3 | ML | |
| Sweden | Mining | Mining | Dannemora | 2.27 | MD | |
| China | Mining | Mining | Qiao tou he mine, Lowde, Hunan | 2.2 | ML | 1974/05 /31 |
| UK | Mining | Mining | Rotherham (Yorkshire) | 2.2 | ML | 1988/10 /14 |
| China | Mining | Mining | Kaiyang mine, Jinzhong, Kaiyang, Guizhou | 2.2 | ML | 1990/10 /23 |
| UK | Mining | Mining | Bargoed Mid Glamorgan (South Wales) | 2.2 | ML | 1992/08 /17 |
| South Africa | Mining | Mining | TauTona, Carletonville | 2.2 | | 2004/12 /12 |
| Canada | Mining | Mining | Craig, Ontario | 2.2 | MN | 2007/06 /22 |
| Poland | Mining | Mining | Wujek mine | 2.2 | MW | |
| Poland | Mining | Mining | Ziemowit mine | 2.2 | MW | |
| Japan | Mining | Mining (hydraulic extraction rockburst) | Sunagawa mine | 2.1 | ML | 1986/01 |

| | | | | | | |
|---|---|---|---|---|---|---|
| | | | | | | /29 |
| UK | Mining | Mining | Buxton (Derbyshire) | 2.1 | ML | 1989/09/04 |
| China | Mining | Mining | Jinhuagong mine, Datong, Shanxi | 2.1 | ML | |
| UK | Mining | Mining | Sunderland (Durham and Northumberland) | 2 | ML | 1988/05/05 |
| China | Mining | Mining | Shuikoushan mine, Hengnan, Hunan | 2 | ML | |
| Czech Republic | Mining | Mining | Mayrau mine | 2 | ML | |
| UK | Mining | Mining | Bolton (Lancashire) | 1.7 | ML | 1989/03/11 |
| China | Mining | Mining | Shi xia jiang mine, Shaoyang, Hunan | 1.6 | ML | 1991 (Dec.) |
| Finland | Mining | Mining | Pyhäsalmi | 1.2 | MW | |
| USA | Mining | Mining | Beatrice, Virginia | 1 | ML | 1974/05/15 |
| USA | Mining | Mining (solution) | Dale, New York | 1 | ML | |
| Australia | Mining | Mining (rock fracture) | Moonee Colliery | 0.6 | MW | 1998 |
| USA | Mining | Mining (collapse) | Springfield Pike Quarry, Pennsylvania | 0.2 | MW | 2000/02/21 |
| China | Mining | Mining | Dagandsham Hydropower Station | -0.2 | MW | |
| France | Mining | Mining (solution) | Arkema-Vauvert | -0.24 | MW | |
| Canada | Mining | Shaft excavation | Underground Research Laboratory, Manitoba | -1.9 | MW | |
| South Africa | Mining | Mining (collapse) | Ophirton | | | 1908 |
| USA | Mining | Mining (collapse) | Wilkes-Barre, Pennsylvania | | | 1954 (Feb.) |
| China | Mining | Mining (tunneling rock burst) | Dongguashan (Shizishan copper mine), Tongling, Hunan (Roadway construction) | | | 1999 (Mar.) |
| China | Mining | Mining (tunneling rock burst) | Tianshengqiao II Hydropower Station (Head race tunnel construction) | | | 1990/12/11 |
| Chile | Mining | Mining | El Teniente | | | 1992 (Mar.) |
| India | Mining | Mining | Chinakuri Colliery | | | |
| Russia | Mining | Mining | Gluboky Mine, Streltsovsk | | | |
| Australia | Mining | Mining | Mount Charlotte Mine | | | |
| Russia | Mining | Mining (collapse) | Berezniki-1 Mine | | | |
| Kazakhstan | Mining | Mining | Zhezkazgan Mine | | | |

| | | | |
|---|---|---|---|
| Australia | Mining | Mining | Southern Colliery, German Creek |
| Japan | Mining | Mining | Horonai |
| Norway | Mining | Mining (tunneling rock burst) | Road tunnel |
| Sweden | Mining | Mining (tunneling rock burst) | Head race tunnel |
| Iraq | Mining | Mining (solution) | Mishraq |
| Sweden | Mining | Mining | Malmberget |
| Switzerland/Italy | Mining | Mining (tunneling rock burst) | Simplon Tunnel |
| Japan | Mining | Mining (tunneling rock burst) | Shimizu Tunnel |
| Japan | Mining | Mining (tunneling rock burst) | Kanetsu (Kan-Etsu) Tunnel |
| Sweden | Mining | Mining (tunneling rock burst) | Forsmark Nuclear Plant (Hydraulic tunnels construction) |
| Sweden | Mining | Mining (tunneling rock burst) | Ritsem Traffic Tunnel |
| China | Mining | Mining (tunneling rock burst) | Yuzixi I Hydropower Station (Head race tunnel construction) |
| China | Mining | Mining (tunneling rock burst) | Erlangshan Tunnel (Sichuan-Tibet Highway) |
| China | Mining | Mining (tunneling rock burst) | Qinling Railway Tunnel |
| China | Mining | Mining (tunneling rock burst) | Cangling Tunnel (Taizhou-Jiyun Highway) |
| China | Mining | Mining (tunneling rock burst) | Pubugou Hydropower Station |
| China | Mining | Mining (tunneling rock burst) | Jinping II Hydropower Station (Auxiliary tunnel) |
| China | Mining | Mining | Fuli mine, Hegang, Heilongjiang |
| China | Mining | Mining | Zhenxing mine, Hegang, Heilongjiang |
| China | Mining | Mining | Didao mine, Jixi, Heilongjiang |
| China | Mining | Mining | Yingcheng mine, Shulang, Jilin |
| China | Mining | Mining | Xian mine, Liaoyuan, Jilin |
| China | Mining | Mining | Tai xin mine, Liaoyuan, Jilin |
| China | Mining | Mining | Tiechang mine, Tonghua, Jilin |
| China | Mining | Mining | Hongtoushan mine, |

| | | | |
|---|---|---|---|
| | | | Fushun, Liaoning |
| China | Mining | Mining | Gaode mine, Fuxin, Liaoning |
| China | Mining | Mining | Dongliang mine, Fuxin, Liaoning |
| China | Mining | Mining | Guanshan mine, Beipiao, Liaoning |
| China | Mining | Mining | Benxi Niu xin tai mine, Shenyang, Liaoning |
| China | Mining | Mining | Binggou mine, Jianchang county, Liaoning |
| China | Mining | Mining | Chang/Zhang gou yu mine, Beijing, Beijing |
| China | Mining | Mining | Datai mine, Beijing, Beijing |
| China | Mining | Mining | Muchengjian mine, Beijing, Beijing |
| China | Mining | Mining | Tang shan mine, Kailuan, Hebei |
| China | Mining | Mining | Guan tai mine, Cixian, Hebei |
| China | Mining | Mining | Tongjialiang mine, Datong, Shanxi |
| China | Mining | Mining | Xin zhou yao mine, Datong, Shanxi |
| China | Mining | Mining | Meiyukou mine, Datong, Shanxi |
| China | Mining | Mining | Yongdingzhuang mine, Datong, Shanxi |
| China | Mining | Mining | Bayi mine, Zaozhuang, Shandong |
| China | Mining | Mining | Chaili mine, Zaozhuang, Shandong |
| China | Mining | Mining | Huafeng mine, Xinwen, Shandong |
| China | Mining | Mining | Sun cun mine, Xinwen, Shandong |
| China | Mining | Mining | Zhangzhuan mine, Xinwen, Shandong |
| China | Mining | Mining | Pan xi mine, Xinwen, Shandong |
| China | Mining | Mining | Dong tan mine, Yankuang, Shandong |
| China | Mining | Mining | Bao dian mine, Yankuang, Shandong |
| China | Mining | Mining | #2 mine, Weishanhu, |

| | | | |
|---|---|---|---|
| | | | Shandong |
| China | Mining | Mining | Qianqiu mine, Yima, Henan |
| China | Mining | Mining | Wumei mine, Hebi, Henan |
| China | Mining | Mining | Shier (Shi'er kuang?) mine, Pingdingshan, Henan |
| China | Mining | Mining | Quantai mine, Xuzhou, Jiangsu |
| China | Mining | Mining | Qishan mine, Xuzhou, Jiangsu |
| China | Mining | Mining | Zhangxiaolou mine, Xuzhou, Jiangsu |
| China | Mining | Mining | Zhangji mine, Xuzhou, Jiangsu |
| China | Mining | Mining | Yaoqiao mine, Datun, Jiangsu |
| China | Mining | Mining | Kong zhuang mine, Datun, Jiangsu |
| China | Mining | Mining | Leigu mine, Mianyang |
| China | Mining | Mining | Beichuan, Sichuan |
| China | Mining | Mining | Wuyi mine, Shanxi |
| China | Mining | Mining | Tianchi mine, Mianzhu, Sichuan |
| China | Mining | Mining | Yanshitai mine, Wansheng district, Nantong, Chongqing |
| China | Mining | Mining | Nantong mine, Nantong, Chongqing |
| China | Mining | Mining | Hua gu shan mine, Xinyu, Jiangxi |
| China | Mining | Mining | Bajing mine, Gaoan, Jiangxi |
| China | Mining | Mining | Tungsten ore mine, Jiangxi |
| China | Mining | Mining | Manganese mine, Zunyi, Guizhou |
| China | Mining | Mining | Dongguashan (Shizishan copper mine), Tongling, Hunan |
| China | Mining | Mining | South manganese mine, Huayuan, Hunan |
| China | Mining | Mining | Manganese mine, Taojiang, Hunan |
| China | Mining | Mining | Phosphorus mine, Yichang, Hubei |
| China | Mining | Mining | Fengdouyan, Jiupanshan, |

| | | | | | |
|---|---|---|---|---|---|
| China | Mining | Mining | Qishuping and Beitou mines, Jiupanshan, Yichang, Hubei | | |
| China | Mining | Mining | Yangmuxi mine, Changyang, Yichang, Hubei | | |
| China | Mining | Mining | Songyi mine, Yichang, Hubei | | |
| China | Mining | Mining | Gaofeng mine, Dachangjingtian, Guangxi | | |
| China | Mining | Mining | Tongkeng mine, Dachangjingtian, Guangxi | | |
| China | Mining | Mining | Manganese mine, Dounan, Yunnan | | |
| China | Mining | Mining | Manganese mine, Heqing, Yunnan | | |
| China | Mining | Mining (tunneling rock burst) | Lujialiang Tunnel (Chongqing-Yichang Highway) | | |
| Australia | Mining | Mining | Cadia | | |
| Australia | Mining | Mining | Queenstown, Tasmania | | |
| Canada | Mining | Mining (rockburst) | Brunswick No. 12 mine | | |
| Canada | Mining | Mining (rockburst) | Denison mine, Ontario | | |
| Poland | Mining | Mining | Pstrowski mine | | |
| Japan | Mining | Mining (rock burst) | Miike mine | | |
| USA | Nuclear | Seismicity/faulting following nuclear detonation | Cannikin | 4.9 | mb |
| Russia | Nuclear | Seismicity/faulting following nuclear detonation | Novaya Zemlya site | 4.8 | mb |
| USA | Nuclear | Seismicity/faulting following nuclear detonation | Milrow | 4.3 | mb |
| USA | Nuclear | Seismicity/faulting following nuclear detonation | Benham, Nevada | 4.2 | ML |
| USA | Nuclear | Seismicity/faulting following nuclear detonation | Jorum, Nevada | 3 | ML |
| USA | Nuclear | Seismicity/faulting following nuclear detonation | Purse, Nevada | 2 | ML |
| USA | Nuclear | Seismicity/faulting following nuclear detonation | Handley, Nevada | 2 | ML |
| USA | Nuclear | Seismicity/faulting following nuclear detonation | Faultless | | |

| | | | | | |
|---|---|---|---|---|---|
| USA | Nuclear | Seismicity/faulting following nuclear detonation | Hard Hat, Nevada | | |
| USA | Nuclear | Seismicity/faulting following nuclear detonation | Rex, Nevada | | |
| USA | Nuclear | Seismicity/faulting following nuclear detonation | Halfbeak, Nevada | | |
| USA | Nuclear | Seismicity/faulting following nuclear detonation | Greeley, Nevada | | |
| USA | Nuclear | Seismicity/faulting following nuclear detonation | Bourbon, Nevada | | |
| USA | Nuclear | Seismicity/faulting following nuclear detonation | Buff, Nevada | | |
| USA | Nuclear | Seismicity/faulting following nuclear detonation | Charcoal, Nevada | | |
| USA | Nuclear | Seismicity/faulting following nuclear detonation | Chartreuse | | |
| USA | Nuclear | Seismicity/faulting following nuclear detonation | Nash, Nevada | | |
| USA | Nuclear | Seismicity/faulting following nuclear detonation | Dumont, Nevada | | |
| USA | Nuclear | Seismicity/faulting following nuclear detonation | Tan, Nevada | | |
| USA | Nuclear | Seismicity/faulting following nuclear detonation | Boxcar, Nevada | | |
| USA | Nuclear | Seismicity/faulting following nuclear detonation | Duryea, Nevada | | |
| USA | Nuclear | Seismicity/faulting following nuclear detonation | Scotch, Nevada | | |
| USA | Oil and Gas | Oil and Water extraction | Fashing Region (D Cluster) | 3 | 2010/12/21 |
| USA | Oil and Gas | Oil and Water extraction | Dimmit County (K Cluster), Texas | 2.98 | 2010/03/08 |
| USA | Oil and Gas | Oil and Water extraction | Dimmit County (M Cluster), Texas | 2.72 | 2011/06/26 |
| USA | Oil and Gas | Oil and Water extraction | Fashing Region (H Cluster) | 2.62 | 2011/05/22 |
| USA | Oil and Gas | Oil and Water extraction | Fashing Region (G Cluster) | 2.4 | 2011/04/09 |
| USA | Oil and Gas | Oil and Water extraction | Fashing Region (C Cluster) | 2.12 | 2011/07/05 |

| | | | | | | |
|---|---|---|---|---|---|---|
| USA | Oil and Gas | Oil and Water extraction | Fashing Region (Event B) | 1.94 | | 2011/01/15 |
| USA | Oil and Gas | Oil and Water extraction | Dimmit County (L Cluster), Texas | 1.83 | | 2010/04/26 |
| Italy | Oil and Gas/Waste fluid injection | Oil and Gas/Wastewater injection | Cavone and San Giacomo fields, Mirandola License (Emilia sequence) | 5.9 | ML | 2012/05/20 |
| USA | Oil and Gas/Waste fluid injection | Oil and Gas/Wastewater injection | Fashing Region (F Cluster), Texas | 3 | | 2010/03/08 |
| USA | Oil and Gas/Waste fluid injection | Oil and Gas/Wastewater injection | Bakken, North Dakota | 2.5 | | 2010/03/21 |
| USA | Oil and Gas/Waste fluid injection | Oil and Gas/Wastewater injection | Cedar Creek Anticline, Montana | 2.1 | | 2010/04/27 |
| USA | Research | Research and Secondary recovery (water injection) | Rangely, Colorado | 3.1 | ML | 1970/04/21 |
| New Zealand | Research | Water injection | Wairakei | 3 | | 1984 (June) |
| Philippines | Research | Research (injection) | Tongonan Geothermal field | 3 | mc | |
| Japan | Research | Water injection | Matsushiro | 2.8 | | 1970/01/25 |
| Germany | Research | Brine (KBr, KCl) injection | KTB | 1.2 | ML | 1994 |
| China | Research | Research (injection) | WFSD-3P | 1 | | |
| Germany | Research | Fluid injection | KTB | 0.7 | ML | |
| Japan | Research | Research (injection) | Nojima | 0.6 | | 1997 |
| Germany | Research | Water injection | KTB | 0.5 | ML | 2000 |
| France | Research | Research (solution mining) | Cerville-Buissoncourt | -0.8 | MW | |
| France | Research | Research (injection) | Laboratoire Souterrain à Bas Bruit | | | |
| Germany | Research | Mine flooding | Hope mine | | | |
| USA | Research | Waste disposal | Frio Formation, Beaumont, near Jasper County, Texas | | | |
| USA | Waste fluid injection | Wastewater (injection) | Prague, Oklahoma | 5.7 | MW | 2011/11/06 |
| USA | Waste fluid injection | Waste disposal | Rocky Mountain Arsenal (Denver), Colorado | 5.5 | ML | 1967 |
| USA | Waste fluid injection | Wastewater (injection) | Raton Basin, Colorado and New Mexico | 5.3 | MW | 2011/08/23 |
| China | Waste fluid injection | Wastewater (injection) | Rongchang gas field | 5.2 | ML | 1997/08/13 |
| USA | Waste fluid | Wastewater | Oklahoma | 5.1 | | 2016/02 |

| | | | | | | |
|---|---|---|---|---|---|---|
| | injection | (injection) | | | | /13 |
| USA | Waste fluid injection | Wastewater (injection) | Painesville (Perry), Ohio | 4.9 | MW | 1986/01 /31 |
| USA | Waste fluid injection | Wastewater (injection) | Timpson, East Texas | 4.8 | MWrm t | 2012/05 /17 |
| USA | Waste fluid injection | Wastewater (injection) | Arkansas | 4.7 | | 2011/02 /27 |
| USA | Waste fluid injection | Wastewater (injection) | Central Valley (WWF), California | 4.6 | MW | 2005/09 /22 |
| China | Waste fluid injection | Wastewater (injection) | Huangjiachang gas field | 4.4 | ML | 2009/02 /16 |
| USA | Waste fluid injection | Brine injection | Paradox Valley, Colorado | 4.3 | | 2000/05 /27 |
| USA | Waste fluid injection | Waste disposal | Ashtabula, Ohio | 4.3 | Mblg | 2001/01 /26 |
| USA | Waste fluid injection | Wastewater injection | Cushing, Oklahoma | 4.3 | MW | 2014 (Oct.) |
| USA | Waste fluid injection | Wastewater (injection) | Dagger Draw, New Mexico | 4.1 | MW | 2005 (Dec.) |
| Canada | Waste fluid injection | Wastewater (injection) | Cordel (Brazeau Cluster) | 4 | ML | 1997/03 /31 |
| Canada | Waste fluid injection | Wastewater (injection) | Graham (Montney Trend) | 4 | ML | 2010 |
| USA | Waste fluid injection | Wastewater injection | Marcotte oil field (Palco), Kansas | 4 | | 1989 |
| USA | Waste fluid injection | Wastewater injection | Guthrie, Oklahoma | 4 | | 2014 |
| USA | Waste fluid injection | Wastewater (injection) | Jones, Oklahoma | 4 | | 2008? |
| USA | Waste fluid injection | Wastewater (injection) | Youngstown, Ohio | 3.88 | MW | 2011/12 /31 |
| USA | Waste fluid injection | Waste disposal | Lake Charles, Louisiana | 3.8 | ML | |
| USA | Waste fluid injection | Wastewater (injection) | Dallas-Fort Worth, Texas | 3.3 | mb | 2009/05 /16 |
| USA | Waste fluid injection | Wastewater (injection) | Greeley, Colorado | 3.2 | | 2014/06 /01 |
| Canada | Waste fluid injection | Wastewater (injection) | Pintail (Montney Trend) | 3.1 | ML | 2014 |
| USA | Waste fluid injection | Waste disposal | El Dorado, Arkansas | 3 | ML | 1983 |
| USA | Waste fluid injection | Wastewater (injection) | Lillian (J-A cluster), Barnett Shale, Texas | 3 | | 2011/07 /17 |
| USA | Waste fluid injection | Deep fluid injection | Avoca, New York | 2.9 | Mblg | 2001 |
| USA | Waste fluid injection | Wastewater (injection) | Cleburne, Texas | 2.8 | MbLg | 2009/06 /09 |
| Italy | Waste fluid injection | Wastewater injection | Val d'Agri oil field (CM2 well) | 2.2 | ML | 2006 |
| USA | Waste fluid injection | Wastewater injection | Fashing Region (A Cluster), Texas | 1.82 | | 2011/08 /26 |

| | | | | | | |
|---|---|---|---|---|---|---|
| USA | Waste fluid injection | Wastewater injection | Dimmit County (Event J), Texas | 1.52 | | 2010/11/29 |
| USA | Waste fluid injection | Wastewater injection | Center, Texas | 1.5 | ML | 2010/12/01 |
| USA | Waste fluid injection | Wastewater injection | Cedar Creek Anticline, North Dakota | 1.4 | | 2010/06/14 |
| China | Water dam | Water dam | Zipingpu (Wenchuan earthquake) | 7.9 | MW | 2008/05/12 |
| USA | Water dam | Water dam | Lake Hebgen, Montana | 7.1 | MS | 1959/08/17 |
| Greece | Water dam | Water dam | Polyphyto | 6.5 | MS | 1995/05/13 |
| India | Water dam | Water dam | Koyna | 6.3 | MS | 1967/12/10 |
| Zambia–Zimbabwe | Water dam | Water dam | Kariba | 6.2 | | 1963/09/23 |
| Greece | Water dam | Water dam | Kremasta | 6.2 | | 1966/02/05 |
| China | Water dam | Water dam | Hsinfengkiang (Hsingfengchiang, Xinfengjiang) | 6.1 | MS | 1962/03/18 |
| India | Water dam | Water dam | Killari | 6.1 | MW | 1993/09/30 |
| Thailand | Water dam | Water dam | Srinagarind | 5.9 | ML | 1983 |
| USA | Water dam | Water dam | Oroville, California | 5.8 | ML | 1975/08/01 |
| Greece | Water dam | Water dam | Marathon | 5.7 | | 1938/07/20 |
| Egypt | Water dam | Water dam | Aswan | 5.7 | ML | 1981/11/14 |
| Greece | Water dam | Water dam | Pournari | 5.6 | ML | 1981/03/10 |
| Australia | Water dam | Water dam | Warragamba (Varragamba) | 5.5 | | 1973/03/09 |
| Greece | Water dam | Water dam | Asomata | 5.4 | MS | 1984/10/25 |
| France | Water dam | Water dam | Monteynard | 5.3 | ML | 1962 |
| Ghana | Water dam | Water dam | Akosombo | 5.3 | | 1964 (Nov.) |
| India | Water dam | Water dam | Kinnersani | 5.3 | | 1969/04/13 |
| Uzbekistan | Water dam | Water dam | Charvak | 5.3 | ML | 1977/03/15 |
| USA | Water dam | Water dam | Coyote Valley (Leroy Anderson?), California | 5.2 | | 1962/06/06 |
| China | Water dam | Water dam | Shenwo/Shenwu | 5.2 | ML | 1974/12/02 |
| Greece | Water dam | Water dam | Sfikia | 5.2 | MS | 1986/02/18 |

| | | | | | | |
|---|---|---|---|---|---|---|
| USA | Water dam | Water dam | Hoover (Lake Mead), Nevada/Arizona | 5 | ML | 1939 |
| Australia | Water dam | Water dam | Eucumbene | 5 | | 1959/05/18 |
| New Zealand | Water dam | Water dam | Benmore | 5 | ML | 1966/07/07 |
| India | Water dam | Water dam | Warna (Warana) | 5 | | 1993 |
| Australia | Water dam | Water dam | Thomson | 5 | ML | 1996 |
| Zambia | Water dam | Water dam | Itezhi-Tezhi | 5 | | 2011/07/21 |
| Japan | Water dam | Water dam | Kurobe | 4.9 | MS | 1961/08/19 |
| Serbia | Water dam | Water dam | Bajina Basta | 4.9 | ML | 1967/07/03 |
| USA | Water dam | Water dam | Kerr, Montana | 4.9 | | 1971/07/28 |
| India | Water dam | Water dam | Bhatsa | 4.9 | ML | 1983/09/15 |
| Vietnam | Water dam | Water dam | Hoa Binh | 4.9 | | 1989 |
| Russia | Water dam | Water dam | Lake Baikal | 4.8 | | |
| Spain | Water dam | Water dam | Canelles | 4.7 | | 1962/06/09 |
| Iran | Water dam | Water dam | Sefia Rud | 4.7 | | 1968/08/02 |
| Canada | Water dam | Water dam | McNaughton (Mica) | 4.7 | ML | 1973 |
| China | Water dam | Water dam | Danjiangkou | 4.7 | ML | 1973/11/29 |
| USA | Water dam | Water dam | Anderson, Idaho | 4.7 | ML | 1973 |
| Vietnam | Water dam | Water dam | Song Tranh 2 | 4.7 | | 2012/11/15 |
| Georgia | Water dam | Water dam | Enguri (Inguri) | 4.7 | | |
| Greece | Water dam | Water dam | Kastraki | 4.6 | ML | 1969 |
| Tadjikistan | Water dam | Water dam | Nurek | 4.6 | MS | 1972/11/27 |
| Kyrgyzstan | Water dam | Water dam | Toktogul | 4.6 | ML | 1977 |
| New Zealand | Water dam | Water dam | Lake Pukaki | 4.6 | ML | 1978/12/17 |
| Spain | Water dam | Water dam | Itoiz | 4.6 | mbLg | 2004/09/18 |
| China | Water dam | Water dam | Three Gorges | 4.6 | ML | 2008/11/22 |
| France | Water dam | Water dam | Vouglans | 4.5 | MW | 1971/06/21 |
| China | Water dam | Water dam | Foziling | 4.5 | | 1973/08/11 |
| China | Water dam | Water dam | Dahua | 4.5 | | 1993 |
| Italy | Water dam | Water dam | Pieve de Cadore | 4.4 | | 1960/01/13 |

| | | | | | | |
|---|---|---|---|---|---|---|
| Italy | Water dam | Water dam | Piastra | 4.4 | | 1966/04/07 |
| China | Water dam | Water dam | Dongjing/Dongqing | 4.4 | | 2010/01/17 |
| USA | Water dam | Water dam | Clark Hill, South Carolina/Georgia | 4.3 | ML | 1974/08/02 |
| Iran | Water dam | Water dam | Karun III | 4.3 | ML | 2006/05/12 |
| Brazil | Water dam | Water dam | P. Colombia/Volta Grande | 4.2 | | 1974/02/24 |
| Armenia | Water dam | Water dam | Tolors | 4.2 | | 1982 |
| Albania | Water dam | Water dam | Komani | 4.2 | ML | 1986 |
| Russia | Water dam | Water dam | Bratsk | 4.2 | | 1996 |
| China | Water dam | Water dam | Longtan | 4.2 | ML | 2007/07/17 |
| Spain | Water dam | Water dam | Camarillas | 4.1 | | 1964/04/15 |
| Canada | Water dam | Water dam | Mica | 4.1 | | 1974/01/05 |
| Canada | Water dam | Water dam | Manic-3, Quebec | 4.1 | mbLg | 1975/10/23 |
| Brazil | Water dam | Water dam | Nova Ponte | 4 | mb | 1998 (May) |
| Spain | Water dam | Water dam | Tous New | 4 | mb | 2000/10/08 |
| USA | Water dam | Water dam | Jocassee, South Carolina | 3.9 | ML | 1979/08/25 |
| Paraguay | Water dam | Water dam | Yacyreta | 3.9 | mR | 2000/04/28 |
| Algeria | Water dam | Leakage from pumping between reservoirs (unintentional injection) | Beni Haroun dam/reservoir and the Oued Athmania reservoir | 3.9 | Md | 2007/12/18 |
| China | Water dam | Water dam | Xiaowan | 3.9 | ML | 2012/09/16 |
| USA | Water dam | Water dam | Keowee, South Carolina | 3.8 | | 1971/07/13 |
| India | Water dam | Water dam | Dhamni | 3.8 | ML | 1994 |
| USA | Water dam | Water dam | Palisades, Idaho | 3.7 | | 1966/06/10 |
| Brazil | Water dam | Water dam | Carmo do Cajuru | 3.7 | | 1972/01/23 |
| Brazil | Water dam | Water dam | Capivara | 3.7 | | 27/3/1979, 07/01/1989 |
| Canada | Water dam | Water dam | LG 3, Quebec | 3.7 | ML | 1983 |
| Pakistan | Water dam | Water dam | Mangla | 3.6 | ML | 1967/05/28 |

| | | | | | | |
|---|---|---|---|---|---|---|
| China | Water dam | Water dam | Shengjiaxia (Shenjia Xiashuiku) | 3.6 | | 1984 |
| Switzerland | Water dam | Water dam | Lac de Salanfe | 3.5 | MW | 1953/10/17 |
| Australia | Water dam | Water dam | Blowering | 3.5 | | 1973/01/06 |
| Australia | Water dam | Water dam | Talbingo | 3.5 | | 1973/01/06 |
| Turkey | Water dam | Water dam | Keban | 3.5 | | 1973 |
| Switzerland | Water dam | Water dam | Emosson | 3.5 | ML | 1974 |
| India | Water dam | Water dam | Idukki | 3.5 | | 1977/07/02 |
| India | Water dam | Water dam | Gandipet (Osman Sagar) | 3.5 | ML | 1982 |
| Italy | Water dam | Water dam | Ridracoli | 3.5 | | 1988 |
| China | Water dam | Water dam | Yantan | 3.5 | | 1994 |
| Poland | Water dam | Water dam | Czorsztyn Lake | 3.5 | | 2013/03/01 |
| France | Water dam | Water dam | Eguzon | 3.5 | | |
| India | Water dam | Water dam | Nagarjuna Sagar | 3.5 | | |
| Japan | Water dam | Water dam | Hitotsuse | 3.5 | | |
| Japan | Water dam | Water dam | Arimine | 3.5 | | |
| Japan | Water dam | Water dam | Kuzuryu | 3.5 | | |
| Japan | Water dam | Water dam | Midono | 3.5 | | |
| Japan | Water dam | Water dam | Makio | 3.5 | | |
| Japan | Water dam | Water dam | Miomote | 3.5 | | |
| Japan | Water dam | Water dam | Nagawado | 3.5 | | |
| Japan | Water dam | Water dam | Narugo | 3.5 | | |
| Japan | Water dam | Water dam | Ohkura | 3.5 | | |
| Japan | Water dam | Water dam | Tohri (Tori) | 3.5 | | |
| Japan | Water dam | Water dam | Uchikawa | 3.5 | | |
| Japan | Water dam | Water dam | Yuda | 3.5 | | |
| Brazil | Water dam | Water dam | Tucurui | 3.4 | | 1985 |
| China | Water dam | Water dam | Wujiangdu | 3.4 | ML | 1985 |
| China | Water dam | Water dam | Lubuge | 3.4 | | 1988 |
| Brazil | Water dam | Water dam | Balbina | 3.4 | mb | 1990/03/25 |
| France | Water dam | Water dam | Serre-Poncen | 3.3 | | 1966/08/23 |
| China | Water dam | Water dam | Zhelin | 3.2 | ML | 1972/10/14 |
| India | Water dam | Water dam | Sriramsagar | 3.2 | | 1984/07/21 |
| China | Water dam | Water dam | Shuikou | 3.2 | | 1994 |
| Lesotho | Water dam | Water dam | Katse | 3.1 | | 1996 |
| Algeria | Water dam | Water dam | Oued Fodda | 3 | | 1933 (May) |

| | | | | | | |
|---|---|---|---|---|---|---|
| USA | Water dam | Water dam | Shasta, California | 3 | | 1944 |
| Italy | Water dam | Water dam | Vajont | 3 | ML | 1960 |
| India | Water dam | Water dam | Mangalam | 3 | | 1963 |
| Switzerland | Water dam | Water dam | Contra | 3 | | 1965 (Oct.) |
| Bosnia and Herzegovina | Water dam | Water dam | Grancarevo | 3 | | 1967 |
| Japan | Water dam | Water dam | Kamafusa | 3 | | 1970 |
| China | Water dam | Water dam | Qianjin | 3 | | 1971/10/20 |
| Brazil | Water dam | Water dam | Paraibuna–Paraitinga | 3 | | 1977 |
| Brazil | Water dam | Water dam | Jaguari | 3 | mb | 1985/12/17 |
| Cyprus | Water dam | Water dam | Kouris | 3 | | 1994-1995 |
| Brazil | Water dam | Water dam | Irapé | 3 | ML | 2006/05/14 |
| India | Water dam | Water dam | Rihand | 3 | | |
| India | Water dam | Water dam | Parambikulam | 3 | | |
| India | Water dam | Water dam | Ukai | 3 | | |
| Pakistan | Water dam | Water dam | Tarbela | 3 | | |
| Thailand | Water dam | Water dam | Tsengwen (Zengwen) | 3 | | |
| USA | Water dam | Water dam | Monticello (Fairfield), California | 2.9 | | 1978 (Oct.) |
| China | Water dam | Water dam | Tongjiezi | 2.9 | | 1992 |
| China | Water dam | Water dam | Nanchong | 2.8 | | 1974/07/25 |
| China | Water dam | Water dam | Hunanzhen | 2.8 | | 1979 |
| Brazil | Water dam | Water dam | Açu | 2.8 | | 1994 |
| Romania | Water dam | Water dam | Vidra Lotru | 2.8 | | |
| Romania | Water dam | Water dam | Vidraru-Arges | 2.8 | | |
| Japan | Water dam | Water dam | Takase | 2.7 | | 1982 |
| USA | Water dam | Water dam | Heron, New Mexico | 2.7 | ML | |
| Albania | Water dam | Water dam | Fierza | 2.6 | | 1981 |
| India | Water dam | Water dam | Kadana | 2.5 | | |
| Brazil | Water dam | Water dam | Miranda | 2.4 | mb | 1998/04/07 |
| China | Water dam | Water dam | Nanshui | 2.3 | | 1970 |
| China | Water dam | Water dam | Huangshi | 2.3 | | 1974/09/21 |
| Brazil | Water dam | Water dam | Serra da Mesa | 2.2 | mb | 1999/06/13 |
| France | Water dam | Water dam | Sainte-Croix | 2.2 | | |
| Italy | Water dam | Water dam | Pertusillio | 2.1 | ML | |

| | | | | | | |
|---|---|---|---|---|---|---|
| USA | Water dam | Water dam | Cabin Creek, Colorado | 2 | | 1968 |
| South Africa | Water dam | Water dam | Hendrik Verwoerd (Gariep) | 2 | | 1971 |
| Spain | Water dam | Water dam | Almendra | 2 | | 1972 (Jan.) |
| Austria | Water dam | Water dam | Schlegeis | 2 | | 1973 (Apr.) |
| Brazil | Water dam | Water dam | Marimbondo | 2 | ML | 1978/07/25 |
| Brazil | Water dam | Water dam | Sobradinho | 2 | | 1979 |
| Brazil | Water dam | Water dam | Emborcacao | 2 | | 1984 |
| India | Water dam | Water dam | Sholayar | 2 | | |
| India | Water dam | Water dam | Sharavathi (Sharavati) | 2 | | |
| Romania | Water dam | Water dam | Ievorul Muntelui-Bicaz | 2 | | |
| Brazil | Water dam | Water dam | Xingó | 1.7 | mb | 1994/07/20 |
| India | Water dam | Water dam | Mula | 1.5 | | 1972 |
| Canada | Water dam | Water dam | Toulnustouc | 1.4 | mN | 2005/02/26 |
| Brazil | Water dam | Water dam | Castanhão | 1.4 | mb | |
| Canada | Water dam | Hydroelectric tunnel | Toulnustouc | 0.8 | mN | 2005/04/09 |
| France | Water dam | Water dam | Grandval | | | 1963/08/05 |
| Spain | Water dam | Water dam | El Cenajo | | | 1973 |
| Australia | Water dam | Water dam | Gordon River Power Development Storage | | | |
| Indonesia | Water dam | Water dam | Saguling-Cirata | | | |
| Spain | Water dam | Water dam | El Grado | | | |
| Spain | Water dam | Water dam | La Cohilla | | | 1975 |
| USA | Water dam | Water dam | Rocky Reach, Washington | | | |
| USA | Water dam | Water dam | San Luis, California | | | |
| USA | Water dam | Water dam | Sanford, Michigan | | | |

# E Bibliography

Adams, R. D. (1969), Seismic effects at Mangla Dam, Pakistan, Nature, 222, 1153-1155.

Adushkin, V. V., V. Rodionov, N, S. Turuntaev, and A. E. Yudin (2000), Seismicity in the oil field.

Adushkin, V. V., and A. Spivak (2015), Underground explosions, DTIC Document.

Ake, J., K. Mahrer, D. O'Connell, and L. Block (2005), Deep-injection and closely monitored induced seismicity at Paradox Valley, Colorado, Bulletin of the Seismological Society of America, 95, 664-683.

Albaric, J., V. Oye, N. Langet, M. Hasting, I. Lecomte, K. Iranpour, M. Messeiller, and P. Reid (2014), Monitoring of induced seismicity during the first geothermal reservoir stimulation at Paralana, Australia, Geothermics, 52, 120-131.

Alcott, J. M., P. K. Kaiser, and B. P. Simser (1998), Use of microseismic source parameters for rockburst hazard assessment, in Seismicity caused by mines, fluid injections, reservoirs, and oil extraction, pp. 41-65, Springer.

Al-Enezi, A., L. Petrat, R. Abdel-Fattah, and G. D. M. Technologie (2008), Induced seismicity and surface deformation within Kuwait's oil fields, paper presented at Proc. Int. Conf. Geol. Seismol.

Allis, R. G., S. A. Currie, J. D. Leaver, and S. Sherburn (1985), Results of injection testing at Wairakei geothermal field, New Zealand, Trans. GRC, 289-294.

Alvarez-Garcia, I. N., F. L. Ramos-Lopez, C. Gonzalez-Nicieza, M. I. Alvarez-Fernandez, and A. E. Alvarez-Vigil (2013), The mine collapse at Lo Tacón (Murcia, Spain), possible cause of the Torre Pacheco earthquake (2nd May 1998, se Spain), Engineering Failure Analysis, 28, 115-133.

Amidzic, D., S. K. Murphy, and G. Van Aswegen (1999), Case study of a large seismic event at a South African gold mine, paper presented at 9th ISRM Congress, International Society for Rock Mechanics.

Amos, C. B., P. Audet, W. C. Hammond, R. Bürgmann, I. A. Johanson, and G. Blewitt (2014), Uplift and seismicity driven by groundwater depletion in central California, Nature, 509, 483-486.

Arabasz, W. J., J. Ake, M. K. McCarter, and A. McGarr (2002), Mining-induced seismicity near Joes Valley dam: Summary of ground-motion studies and assessment of probable maximum magnitude, Technical Report, University of Utah Seismograph Stations, Salt Lake City, Utah, 35 pp. Accessible online at www/seis. utah. edu/Reports/sitla2002b.

Arabasz, W. J., S. J. Nava, M. K. McCarter, K. L. Pankow, J. C. Pechmann, J. Ake, and A. McGarr (2005), Coal-mining seismicity and ground-shaking hazard: A case study in the Trail Mountain area, Emery County, Utah, Bulletin of the Seismological Society of America, 95, 18-30.

Arkhipova, E. V., A. D. Zhigalin, L. I. Morozova, and A. V. Nikolaev (2012), The Van earthquake on October 23, 2011: Natural and technogenic causes, paper presented at Doklady Earth Sciences, Springer.

Armbruster, J. G., D. W. Steeples, and L. Seeber (1989), The 1989 earthquake sequence near Palco, Kansas: A possible example of induced seismicity (abstract), Seismological Research Letters, 60, 141.

Asanuma, H., N. Soma, H. Kaieda, Y. Kumano, T. Izumi, K. Tezuka, H. Niitsuma, and D. Wyborn (2005), Microseismic monitoring of hydraulic stimulation at the Australian HDR project in Cooper Basin, paper presented at Proceedings World Geothermal Congress.

Assumpção, M., V. Marza, L. Barros, C. Chimpliganond, J. E. Soares, J. Carvalho, D. Caixeta, A. Amorim, and E. Cabral (2002), Reservoir-induced seismicity in Brazil, in The mechanism of induced seismicity, pp. 597-617, Springer.

Assumpção, M., T. H. Yamabe, J. R. Barbosa, V. Hamza, A. E. V. Lopes, L. Balancin, and M. B. Bianchi (2010), Seismic activity triggered by water wells in the Paraná Basin, Brazil, Water Resources Research, 46.

Avouac, J.-P. (2012), Earthquakes: Human-induced shaking, Nature Geoscience, 5, 763-764.

Awad, M., and M. Mizoue (1995), Earthquake activity in the Aswan region, Egypt, in Induced seismicity, pp. 69-86, Springer.

Baecher, G. B., and R. L. Keeney (1982), Statistical examination of reservoir-induced seismicity, Bulletin of the Seismological Society of America, 72, 553-569.

Baisch, S., E. Rothert, H. Stang, R. Vörös, C. Koch, and A. McMahon (2015), Continued geothermal reservoir stimulation experiments in the Cooper Basin (Australia), Bulletin of the Seismological Society of America.

Baisch, S., and R. Vörös (2011), Geomechanical study of Blackpool seismicity.

Baisch, S., R. Vörös, R. Weidler, and D. Wyborn (2009), Investigation of fault mechanisms during geothermal reservoir stimulation experiments in the Cooper Basin, Australia, Bulletin of the Seismological Society of America, 99, 148-158.

Baisch, S., R. Weidler, R. Vörös, D. Wyborn, and L. de Graaf (2006), Induced seismicity during the stimulation of a geothermal HFR reservoir in the Cooper Basin, Australia, Bulletin of the Seismological Society of America, 96, 2242-2256.

Baker, K., D. Hollett, and A. Coy (2014, February), Geothermal technologies office 2013 peer review report.

Balassanian, S. Y. (2005), Earthquakes induced by deep penetrating bombing?, Acta Seismologica Sinica, 18, 741-745.

Balfour, N., E. Borleis, C. Bugden, V. Dent, D. H. Glanville, D. Hardy, D. Love, M. Salmon, M. Sambridge, and A. Wallace (2014), Australian seismological report 2013.

Bardainne, T., N. Dubos-Sallée, G. Sénéchal, P. Gaillot, and H. Perroud (2008), Analysis of the induced seismicity of the Lacq gas field (southwestern France) and model of deformation, Geophysical Journal International, 172, 1151-1162.

Bardainne, T., P. Gaillot, N. Dubos-Sallée, J. Blanco, and G. Sénéchal (2006), Characterization of seismic waveforms and classification of seismic events using chirplet atomic decomposition. Example from the Lacq gas field (western Pyrenees, France), Geophysical Journal International, 166, 699-718.

Basham, P. W. (1969), Canadian magnitudes of earthquakes and nuclear explosions in south-western North America, Geophysical Journal International, 17, 1-13.

Bella, F., P. F. Biagi, M. Caputo, E. Cozzi, G. Della Monica, A. Ermini, W. Plastino, and V. Sgrigna (1998), Aquifer-induced seismicity in the central Apennines (Italy), Pure and applied geophysics, 153, 179-194.

Bennett, T. J., M. E. Marshall, K. L. Mclaughlin, B. W. Barker, and J. R. Murphy (1995), Seismic characteristics and mechanisms of rockbursts, DTIC Document.

Bennett, T. J., K. L. McLaughlin, M. E. Marshall, B. W. Barker, and J. R. Murphy (1995), Investigations of the seismic characteristics of rockbursts, DTIC Document.

Benz, H. M., N. D. McMahon, R. C. Aster, D. E. McNamara, and D. B. Harris (2015), Hundreds of earthquakes per day: The 2014 Guthrie, Oklahoma, earthquake sequence, Seismological Research Letters, 86, 1318-1325.

Bertani, R. (2012), Geothermal power generation in the world 2005–2010 update report, Geothermics, 41, 1-29.

Bertini, G., M. Casini, G. Gianelli, and E. Pandeli (2006), Geological structure of a long- living geothermal system, Larderello, Italy, Terra Nova, 18, 163-169.

Białoń, W., E. Zarzycka, and S. Lasocki (2015), Seismicity of Czorsztyn Lake region: A case of reservoir triggered seismic process?, Acta Geophysica, 63, 1080-1089.

Bischoff, M., A. Cete, R. Fritschen, and T. Meier (2010), Coal mining induced seismicity in the Ruhr area, Germany, Pure and applied geophysics, 167, 63-75.

Bommer, J. J., S. Oates, J. M. Cepeda, C. Lindholm, J. Bird, R. Torres, G. Marroquín, and J. Rivas (2006), Control of hazard due to seismicity induced by a hot fractured rock geothermal project, Engineering Geology, 83, 287-306.

Boucher, G., A. Ryall, and A. E. Jones (1969), Earthquakes associated with underground nuclear explosions, Journal of Geophysical Research, 74, 3808-3820.

Bou- Rabee, F. (1994), Earthquake recurrence in Kuwait induced by oil and gas extraction, Journal of Petroleum Geology, 17, 473-480.

Bou-Rabee, F., and A. Nur (2002), The 1993 M4.7 Kuwait earthquake: Induced by the burning of the oil fields, Kuwait J. Sci. Eng, 29, 155-163.

Bourne, S. J., and S. J. Oates (2014), An activity rate model of induced seismicity within the Groningen field.

Bowers, D. (1997), The October 30, 1994, seismic disturbance in South Africa: Earthquake or large rock burst?, Journal of Geophysical Research: Solid Earth, 102, 9843-9857.

Breede, K., K. Dzebisashvili, X. Liu, and G. Falcone (2013), A systematic review of enhanced (or engineered) geothermal systems: Past, present and future, Geothermal Energy, 1, 1-27.

British Columbia Oil and Gas Commission (BCOGC) (2012), Investigation of observed seismicity in the Horn River Basin.

British Columbia Oil and Gas Commission (BCOGC) (2014), Investigation of observed seismicity in the Montney trend.

Brodsky, E. E., and L. J. Lajoie (2013), Anthropogenic seismicity rates and operational parameters at the Salton Sea geothermal field, Science, 341, 543-546.

Bromley, C. J., C. F. Pearson, and D. M. Rigor (1987), Microearthquakes at the Puhagan geothermal field, Philippines—a case of induced seismicity, Journal of volcanology and geothermal research, 31, 293-311.

Brune, J. N., and P. W. Pomeroy (1963), Surface wave radiation patterns for underground nuclear explosions and small- magnitude earthquakes, Journal of Geophysical Research, 68, 5005-5028.

Bukchin, B. G., A. Z. Mostinsky, A. A. Egorkin, A. L. Levshin, and M. H. Ritzwoller (2001), Isotropic and nonisotropic components of earthquakes and nuclear explosions on the Lop Nor test site, China, in Monitoring the comprehensive nuclear-test-ban treaty: Surface waves, pp. 1497-1515, Springer.

Calò, M., C. Dorbath, and M. Frogneux (2014), Injection tests at the EGS reservoir of Soultz-Sous-Forêts. Seismic response of the GPK4 stimulations, Geothermics, 52, 50-58.

Caloi, P., M. De Panfilis, D. Di Filippo, L. Marcelli, and M. C. Spadea (1956), Terremoti della Val Padana del 15-16 Maggio 1951, Annals of Geophysics, 9, 63-105.

Carder, D. S. (1945), Seismic investigations in the Boulder dam area, 1940-1944, and the influence of reservoir loading on local earthquake activity, Bulletin of the Seismological Society of America, 35, 175-192.

Carpenter, P. J., and I. W. El-Hussain, Reservoir induced seismicity near Heron and El Vado reservoirs, northern New Mexico, and implications for fluid injection within the San Juan Basin, paper presented at AAPG Annual Convention and Exhibition.

Cesca, S., F. Grigoli, S. Heimann, Á. González, E. Buforn, S. Maghsoudi, E. Blanch, and T. Dahm (2014), The 2013 September–October seismic sequence offshore Spain: A case of seismicity triggered by gas injection?, Geophysical Journal International, 198, 941-953.

Chadha, R. K. (1995), Role of dykes in induced seismicity at Bhatsa reservoir, Maharashtra, India, in Induced seismicity, pp. 155-165, Springer.

Chen, L., and P. Talwani (1998), Reservoir-induced seismicity in China, Pure and applied geophysics, 153, 133-149.

Chouhan, R. K. S. (1986), Induced seismicity of Indian coal mines, Physics of the earth and planetary interiors, 44, 82-86.

Chouhan, R. K. S. (1992), Combating the rockburst problem - a seismological approach, in Induced seismicity, edited by P. Knoll, Balkema, Rotterdam.

Číž, R., and B. Růžek (1997), Periodicity of mining and induced seismicity in the Mayrau mine, Czech Republic, Studia Geophysica et Geodaetica, 41, 29-44.

Cladouhos, T. T., S. Petty, Y. Nordin, M. Moore, K. Grasso, M. Uddenberg, M. Swyer, B. Julian, and G. Foulger (2013), Microseismic monitoring of Newberry volcano EGS demonstration, paper presented at Proceedings of the 38th Workshop on Geothermal Reservoir Engineering, Stanford, CA.

Clark, D. (2009), Potential geologic sources of seismic hazard in the Sydney Basin, Proceedings volume of a one day workshop. Geoscience Australia Record 2009/11. 115pp.

Clarke, H., L. Eisner, P. Styles, and P. Turner (2014), Felt seismicity associated with shale gas hydraulic fracturing: The first documented example in Europe, Geophysical Research Letters, 41, 8308-8314.

Dahm, T., S. Cesca, S. Hainzl, T. Braun, and F. Krüger (2015), Discrimination between induced, triggered, and natural earthquakes close to hydrocarbon reservoirs: A probabilistic approach based on the modeling of depletion- induced stress changes and seismological source parameters, Journal of Geophysical Research: Solid Earth, 120, 2491-2509.

Dahm, T., F. Krüger, K. Stammler, K. Klinge, R. Kind, K. Wylegalla, and J.-R. Grasso (2007), The 2004 Mw 4.4 Rotenburg, northern Germany, earthquake and its possible relationship with gas recovery, Bulletin of the Seismological Society of America, 97, 691-704.

Darold, A., A. A. Holland, C. Chen, and A. Youngblood (2014), Preliminary analysis of seismicity near Eagleton 1-- 29, Carter County, July 2014.

Davies, R., G. Foulger, A. Bindley, and P. Styles (2013), Induced seismicity and hydraulic fracturing for the recovery of hydrocarbons, Marine and Petroleum Geology, 45, 171-185.

Davis, S. D., and C. Frohlich (1993), Did (or will) fluid injection cause earthquakes?-criteria for a rational assessment, Seismological Research Letters, 64, 207-224.

Davis, S. D., P. A. Nyffenegger, and C. Frohlich (1995), The 9 April 1993 earthquake in south-central Texas: Was it induced by fluid withdrawal?, Bulletin of the Seismological Society of America, 85, 1888-1895.

Davis, S. D., and W. D. Pennington (1989), Induced seismic deformation in the Cogdell oil field of west Texas, Bulletin of the Seismological Society of America, 79, 1477-1495.

De Pater, C. J., and S. Baisch (2011), Geomechanical study of Bowland Shale seismicity, Synthesis Report, 57.

Deichmann, N., and J. Ernst (2009), Earthquake focal mechanisms of the induced seismicity in 2006 and 2007 below Basel (Switzerland), Swiss Journal of Geosciences, 102, 457-466.

Diaz, A. R., E. Kaya, and S. J. Zarrouk (2016), Reinjection in geothermal fields− a worldwide review update, Renewable and Sustainable Energy Reviews, 53, 105-162.

Doblas, M., N. Youbi, J. De Las Doblas, and A. J. Galindo (2014), The 2012/2014 swarmquakes of Jaen, Spain: A working hypothesis involving hydroseismicity associated with the hydrologic cycle and anthropogenic activity, Natural hazards, 74, 1223-1261.

Doornenbal, H., and A. Stevenson (2010), Petroleum geological atlas of the southern Permian Basin area, EAGE.

Doser, D. I., M. R. Baker, M. Luo, P. Marroquin, L. Ballesteros, J. Kingwell, H. L. Diaz, and G. Kaip (1992), The not so simple relationship between seismicity and oil production in the Permian Basin, west Texas, Pure and applied geophysics, 139, 481-506.

Dost, B., and J. Spetzler (2015), Probabilistic seismic hazard analysis for induced earthquakes in Groningen; update 2015.

Downing, J. A., Y. T. Prairie, J. J. Cole, C. M. Duarte, L. J. Tranvik, R. G. Striegl, W. H. McDowell, P. Kortelainen, N. F. Caraco, and J. M. Melack (2006), The global abundance and size distribution of lakes, ponds, and impoundments, Limnology and Oceanography, 51, 2388-2397.

Dreger, D. S., S. R. Ford, and W. R. Walter (2008), Source analysis of the Crandall Canyon, Utah, mine collapse, Science, 321, 217-217.

Durrheim, R. J. (2010), Mitigating the risk of rockbursts in the deep hard rock mines of South Africa: 100 years of research, in Extracting the science: A century of mining research, Brune, J. (eds), Society for Mining, Metallurgy, and Exploration, Inc, pp. 156-171.

Durrheim, R. J., R. L. Anderson, A. Cichowicz, R. Ebrahim-Trolloped, G. Hubert, A. Kijko, A. McGarr, W. Ortlepp, and N. van der Merwe (2006), The risks to miners, mines, and the public posed by large seismic events in the gold mining districts of South Africa, paper presented at Proceedings of the Third International Seminar on Deep and High Stress Mining, 2-4 October 2006, Quebec City, Canada.

Durrheim, R. J., R. L. Anderson, A. Cichowicz, R. Ebrahim-Trolloped, G. Hubert, A. Kijko, A. McGarr, W. D. Ortlepp, and N. van der Merwe (2006), Investigation into the risks to miners, mines, and the public associated with large seismic events in gold mining districts, Department of Minerals and Energy.

Eagar, K. C., G. L. Pavlis, and M. W. Hamburger (2006), Evidence of possible induced seismicity in the Wabash Valley seismic zone from improved microearthquake locations, Bulletin of the Seismological Society of America, 96, 1718-1728.

El-Hussain, I. W., and P. J. Carpenter (1990), Reservoir induced seismicity near Heron and El Vado reservoirs, northern New Mexico, Bulletin of the Association of Engineering Geologists, 27, 51-59.

Ellsworth, W. L. (2013), Injection-induced earthquakes, Science, 341, 1225942.

Emanov, A. F., A. A. Emanov, A. V. Fateev, E. V. Leskova, E. V. Shevkunova, and V. G. Podkorytova (2014), Mining-induced seismicity at open pit mines in Kuzbass (Bachatsky earthquake on June 18, 2013), Journal of Mining Science, 50, 224-228.

Engdahl, E. R. (1972), Seismic effects of the Milrow and Cannikin nuclear explosions, Bulletin of the Seismological Society of America, 62, 1411-1423.

Eremenko, V. A., A. A. Eremenko, S. V. Rasheva, and S. B. Turuntaev (2009), Blasting and the man-made seismicity in the Tashtagol mining area, Journal of mining science, 45, 468-474.

Evans, K. F., A. Zappone, T. Kraft, N. Deichmann, and F. Moia (2012), A survey of the induced seismic responses to fluid injection in geothermal and CO2 reservoirs in Europe, Geothermics, 41, 30-54.

Fabriol, H., and A. Beauce (1997), Temporal and spatial distribution of local seismicity in the Chipilapa-Ahuachapán geothermal area, El Salvador, Geothermics, 26, 681-699.

Fajklewicz, Z., and K. Jakiel (1989), Induced gravity anomalies and seismic energy as a basis for prediction of mining tremors, in Seismicity in mines, pp. 535-552, Springer.

Farahbod, A. M., H. Kao, D. M. Walker, J. F. Cassidy, and A. Calvert (2015), Investigation of regional seismicity before and after hydraulic fracturing in the Horn River Basin, northeast British Columbia, Canadian Journal of Earth Sciences, 52, 112-122.

Feng, Q., and J. M. Lees (1998), Microseismicity, stress, and fracture in the Coso geothermal field, California, Tectonophysics, 289, 221-238.

Ferguson, G. (2015), Deep injection of waste water in the Western Canada Sedimentary Basin, Groundwater, 53, 187-194.

Ferreira, J. M., G. S. França, C. S. Vilar, A. F. do Nascimento, F. H. R. Bezerra, and M. Assumpção (2008), Induced seismicity in the Castanhão reservoir, ne Brazil—preliminary results, Tectonophysics, 456, 103-110.

Fletcher, J. B., and L. R. Sykes (1977), Earthquakes related to hydraulic mining and natural seismic activity in western New York state, Journal of Geophysical Research, 82, 3767-3780.

Folger, P. F., and M. Tiemann (2014), Human-induced earthquakes from deep-well injection: A brief overview, Congressional Research Service.

Ford, S. R., D. S. Dreger, and W. R. Walter (2008), Source characterization of the 6 August 2007 Crandall Canyon mine seismic event in central Utah, Seismological Research Letters, 79, 637-644.

Friberg, P. A., G. M. Besana- Ostman, and I. Dricker (2014), Characterization of an earthquake sequence triggered by hydraulic fracturing in Harrison County, Ohio, Seismological Research Letters.

Fritschen, R. (2010), Mining-induced seismicity in the Saarland, Germany, Pure and applied geophysics, 167, 77-89.

Frohlich, C. (2012), Two-year survey comparing earthquake activity and injection-well locations in the Barnett Shale, Texas, Proceedings of the National Academy of Sciences, 109, 13934-13938.

Frohlich, C., and M. Brunt (2013), Two-year survey of earthquakes and injection/production wells in the Eagle Ford Shale, Texas, prior to the Mw4.8 20 October 2011 earthquake, Earth and Planetary Science Letters, 379, 56-63.

Frohlich, C., and S. D. Davis (2002), Texas earthquakes, University of Texas Press.

Frohlich, C., W. Ellsworth, W. A. Brown, M. Brunt, J. Luetgert, T. MacDonald, and S. Walter (2014), The 17 May 2012 M4.8 earthquake near Timpson, east Texas: An event possibly triggered by fluid injection, Journal of Geophysical Research: Solid Earth, 119, 581-593.

Frohlich, C., J. Glidewell, and M. Brunt (2012), Location and felt reports for the 25 April 2010 mbLg 3.9 earthquake near Alice, Texas: Was it induced by petroleum production?, Bulletin of the Seismological Society of America, 102, 457-466.

Frohlich, C., C. Hayward, B. Stump, and E. Potter (2011), The Dallas–Fort Worth earthquake sequence: October 2008 through May 2009, Bulletin of the Seismological Society of America, 101, 327-340.

Frohlich, C., and E. Potter (2013), What further research could teach us about "close encounters of the third kind": Intraplate earthquakes associated with fluid injection.

Frohlich, C., J. I. Walter, and J. F. W. Gale (2015), Analysis of transportable array (USarray) data shows earthquakes are scarce near injection wells in the Williston Basin, 2008–2011, Seismological Research Letters.

Gahalaut, K., V. K. Gahalaut, and M. R. Pandey (2007), A new case of reservoir triggered seismicity: Govind Ballav Pant reservoir (Rihand dam), central India, Tectonophysics, 439, 171-178.

Gaite, B., A. Ugalde, A. Villaseñor, and E. Blanch (2016), Improving the location of induced earthquakes associated with an underground gas storage in the Gulf of Valencia (Spain), Physics of the Earth and Planetary Interiors, 254, 46-59.

Galybin, A. N., S. S. Grigoryan, and S. A. Mukhamediev (1998), Model of induced seismicity caused by water injection, paper presented at SPE/ISRM Rock Mechanics in Petroleum Engineering, Society of Petroleum Engineers.

Gan, W., and C. Frohlich (2013), Gas injection may have triggered earthquakes in the Cogdell oil field, Texas, Proceedings of the National Academy of Sciences, 110, 18786-18791.

Gasparini, P., P. Styles, S. Lasocki, P. Scandone, E. Huenges, F. Terlizzese, and S. Esposito (2015), The ICHESE report on the relationship between hydrocarbon exploration and the May 2012 earthquakes in the Emilia region (Italy) and their consequences.

Gaucher, E., M. Schoenball, O. Heidbach, A. Zang, P. A. Fokker, J.-D. van Wees, and T. Kohl (2015), Induced seismicity in geothermal reservoirs: A review of forecasting approaches, Renewable and Sustainable Energy Reviews, 52, 1473-1490.

Ge, S., M. Liu, N. Lu, J. W. Godt, and G. Luo (2009), Did the Zipingpu reservoir trigger the 2008 Wenchuan earthquake?, Geophysical Research Letters, 36.

Gendzwill, D. J., R. B. Horner, and H. S. Hasegawa (1982), Induced earthquakes at a potash mine near Saskatoon, Canada, Canadian Journal of Earth Sciences, 19, 466-475.

Genmo, Z., C. Huaran, M. Shuqin, and Z. Deyuan (1995), Research on earthquakes induced by water injection in China, in Induced seismicity, pp. 59-68, Springer.

German, V. I. (2014), Rock failure prediction in mines by seismic monitoring data, Journal of Mining Science, 50, 288-297.

Gestermann, N., T. Plenefisch, U. Schwaderer, and M. Joswig (2015), Induced seismicity at the natural gas fields in northern Germany, in Schatzalp Induced Seismicity Workshop, 10-13 March 2015, Davos, Switzerland.

Gibowicz, S. J. (1998), Partial stress drop and frictional overshoot mechanism of seismic events induced by mining, in Seismicity caused by mines, fluid injections, reservoirs, and oil extraction, pp. 5-20, Springer.

Gibowicz, S. J., A. Bober, A. Cichowicz, Z. Droste, Z. Dychtowicz, J. Hordejuk, M. Kazimierczyk, and A. Kijko (1979), Source study of the Lubin, Poland, tremor of 24 March 1977, Acta Geophys. Pol, 27, 3-38.

Gibowicz, S. J., Z. Droste, B. Guterch, and J. Hordejuk (1981), The Belchatow, Poland, earthquakes of 1979 and 1980 induced by surface mining, Engineering Geology, 17, 257-271.

Gibowicz, S. J., R. P. Young, S. Talebi, and D. J. Rawlence (1991), Source parameters of seismic events at the Underground Research Laboratory in Manitoba, Canada: Scaling relations for events with moment magnitude smaller than −2, Bulletin of the Seismological Society of America, 81, 1157-1182.

Gibson, G., and M. Sandiford (2013), Seismicity and induced earthquakes, Office of the New South Wales Chief Scientist and Engineer.

Gilyarov, V. L., E. E. Damaskinskaya, A. G. Kadomtsev, and I. Y. Rasskazov (2014), Analysis of statistic parameters of geoacoustic monitoring data for the Antey Uranium Deposit, Journal of Mining Science, 50, 443-447.

Glowacka, E., and F. A. Nava (1996), Major earthquakes in Mexicali valley, Mexico, and fluid extraction at Cerro Prieto geothermal field, Bulletin of the Seismological Society of America, 86, 93-105.

Göbel, T. (2015), A comparison of seismicity rates and fluid-injection operations in Oklahoma and California: Implications for crustal stresses, The Leading Edge, 34, 640-648.

Godano, M., E. Gaucher, T. Bardainne, M. Regnier, A. Deschamps, and M. Valette (2010), Assessment of focal mechanisms of microseismic events computed from two three-component receivers: Application to the Arkema- Vauvert field (France), Geophysical prospecting, 58, 775-790.

Goebel, T. H. W., S. M. Hosseini, F. Cappa, E. Hauksson, J. P. Ampuero, F. Aminzadeh, and J. B. Saleeby (2016), Wastewater disposal and earthquake swarm activity at the southern end of the Central Valley, California, Geophysical Research Letters.

Goldbach, O. D. (2009), Flooding-induced seismicity in mines, paper presented at 11th SAGA Biennial Technical Meeting and Exhibition.

Gomberg, J., and L. Wolf (1999), Possible cause for an improbable earthquake: The 1997 Mw 4.9 southern Alabama earthquake and hydrocarbon recovery, Geology, 27, 367-370.

González, P. J., K. F. Tiampo, M. Palano, F. Cannavó, and J. Fernández (2012), The 2011 Lorca earthquake slip distribution controlled by groundwater crustal unloading, Nature Geoscience, 5, 821-825.

Gough, D. I., and W. I. Gough (1970), Load-induced earthquakes at Lake Kariba—II, Geophysical Journal International, 21, 79-101.

Grasso, J.-R. (1992), Mechanics of seismic instabilities induced by the recovery of hydrocarbons, Pure and applied geophysics, 139, 507-534.

Green, C. A., P. Styles, and B. J. Baptie (2012), Preese Hall shale gas fracturing review & recommendations for induced seismic mitigation: UK department of energy and climate change.

Groos, J., J. Zeiß, M. Grund, and J. Ritter (2013), Microseismicity at two geothermal power plants at Landau and Insheim in the Upper Rhine Graben, Germany, paper presented at EGU General Assembly Conference Abstracts.

Ground Water Research & Education Foundation (GWREF) (2013), White paper II summarizing a special session on induced seismicity.

Grünthal, G. (2014), Induced seismicity related to geothermal projects versus natural tectonic earthquakes and other types of induced seismic events in central Europe, Geothermics, 52, 22-35.

Guglielmi, Y., F. Cappa, J.-P. Avouac, P. Henry, and D. Elsworth (2015), Seismicity triggered by fluid injection–induced aseismic slip, Science, 348, 1224-1226.

Guha, S. K., and D. N. Patil (1990), Large water-reservoir-related induced seismicity, Gerlands Beitr Geophys, 99, 265-288.

Gupta, H. K. (2002), A review of recent studies of triggered earthquakes by artificial water reservoirs with special emphasis on earthquakes in Koyna, India, Earth-Science Reviews, 58, 279-310.

Gupta, H. K. (2011), Artificial water reservoir triggered earthquakes, Encyclopedia of Solid Earth Geophysics, 15-24.

Hamilton, R. M., B. E. Smith, F. G. Fischer, and P. J. Papanek (1972), Earthquakes caused by underground nuclear explosions on Pahute Mesa, Nevada test site, Bulletin of the Seismological Society of America, 62, 1319-1341.

Haney, F., J. Kummerow, C. Langenbruch, C. Dinske, S. A. Shapiro, and F. Scherbaum (2011), Magnitude estimation for microseismicity induced during the KTB 2004/2005 injection experiment, Geophysics, 76, WC47-WC53.

Hasegawa, H. S., R. J. Wetmiller, and D. J. Gendzwill (1989), Induced seismicity in mines in Canada—an overview, Pure and applied geophysics, 129, 423-453.

Hauksson, E., T. Göbel, J.-P. Ampuero, and E. Cochran (2015), A century of oil-field operations and earthquakes in the Greater Los Angeles Basin, southern California, The Leading Edge, 34, 650-656.

Heck, N. H., and R. R. Bodle (1931), United States earthquakes 1929, US Coast and Geodetic Survey, Serial.

Hedley, D. G. F., and J. E. Udd (1989), The Canada-Ontario-industry rockburst project, in Seismicity in mines, pp. 661-672, Springer.

Heesakkers, V., S. K. Murphy, G. van Aswegen, R. Domoney, S. Addams, T. Dewers, M. Zechmeister, and Z. Reches (2005), The rupture zone of the M= 2.2 earthquake that reactivated the ancient Pretorius fault in Tautona mine, South Africa, paper presented at AGU Fall Meeting Abstracts.

Heick, C., and D. Flach (1989), Microseismicity in a flooded potash mine, the Hope mine, Federal Republic of Germany, in Seismicity in mines, pp. 475-496, Springer.

Herrmann, R. B. (1978), A seismological study of two Attica, New York earthquakes, Bulletin of the Seismological Society of America, 68, 641-651.

Hill, D. P., P. A. Reasenberg, A. Michael, W. J. Arabaz, G. Beroza, D. Brumbaugh, J. N. Brune, R. Castro, S. Davis, and W. L. Ellsworth (1993), Seismicity remotely triggered by the magnitude 7.3 Landers, California, earthquake, Science, 260, 1617-1623.

Holland, A. (2011), Examination of possibly induced seismicity from hydraulic fracturing in the Eola field, Garvin County, Oklahoma.

Holland, A. A. (2013), Earthquakes triggered by hydraulic fracturing in south- central Oklahoma, Bulletin of the Seismological Society of America, 103, 1784-1792.

Holmgren, J. (2015), Induced seismicity in the Dannemora mine, Sweden, Uppsala Universitet.

Holschneider, M., G. Zöller, and S. Hainzl (2011), Estimation of the maximum possible magnitude in the framework of a doubly truncated Gutenberg–Richter model, Bulletin of the Seismological Society of America, 101, 1649-1659.

Holub, K., J. Holečko, J. Rušajová, and A. Dombkova (2012), Long-term development of seismic monitoring networks in the Ostrava-Karviná coal mine district, Acta Geodynamica et Geomaterialia, 9, 115-132.

Hong, T. K., C. E. Baag, H. Choi, and D. H. Sheen (2008), Regional seismic observations of the 9 October 2006 underground nuclear explosion in North Korea and the influence of crustal structure on regional phases, Journal of Geophysical Research: Solid Earth, 113.

Hornbach, M. J., H. R. DeShon, W. L. Ellsworth, B. W. Stump, C. Hayward, C. Frohlich, H. R. Oldham, J. E. Olson, M. B. Magnani, and C. Brokaw (2015), Causal factors for seismicity near Azle, Texas, Nature communications, 6.

Horner, R. B., J. E. Barclay, and J. M. MacRae (1994), Earthquakes and hydrocarbon production in the Fort St. John area of northeastern British Columbia, Canadian Journal of Exploration Geophysics, 30, 39-50.

Horton, S. (2012), Disposal of hydrofracking waste fluid by injection into subsurface aquifers triggers earthquake swarm in central Arkansas with potential for damaging earthquake, Seismological Research Letters, 83, 250-260.

Hough, S. E., and M. Page (2015), A century of induced earthquakes in Oklahoma?, Bulletin of the Seismological Society of America, 105, 2863-2870.

Hsieh, P. A., and J. D. Bredehoeft (1981), A reservoir analysis of the Denver earthquakes: A case of induced seismicity, Journal of Geophysical Research: Solid Earth, 86, 903-920.

Hsiung, S. M., W. Blake, A. H. Chowdhury, and T. J. Williams (1992), Effects of mining-induced seismic events on a deep underground mine, Pure and applied geophysics, 139, 741-762.

Hua, W., Z. Chen, S. Zheng, and C. Yan (2013), Reservoir-induced seismicity in the Longtan reservoir, southwestern China, Journal of seismology, 17, 667-681.

Hua, W., H. Fu, Z. Chen, S. Zheng, and C. Yan (2015), Reservoir-induced seismicity in high seismicity region—a case study of the Xiaowan reservoir in Yunnan province, China, Journal of Seismology, 19, 567-584.

Hua, W., S. Zheng, C. Yan, and Z. Chen (2013), Attenuation, site effects, and source parameters in the Three Gorges reservoir area, China, Bulletin of the Seismological Society of America, 103, 371-382.

Huaman, R. N. E., and T. X. Jun (2014), Energy related CO2 emissions and the progress on CCS projects: A review, Renewable and Sustainable Energy Reviews, 31, 368-385.

Husen, S., E. Kissling, and A. von Deschwanden (2012), Induced seismicity during the construction of the Gotthard Base Tunnel, Switzerland: Hypocenter locations and source dimensions, Journal of seismology, 16, 195-213.

Iannacchione, A. T., and J. C. Zelanko (1995), Occurrence and remediation of coal mine bumps: A historical review, Paper in Proceedings: Mechanics and Mitigation of Violent Failure in Coal and Hard-Rock Mines. US Bureau of Mines Spec. Publ, 01-95.

Improta, L., L. Valoroso, D. Piccinini, C. Chiarabba, and M. Buttinelli (2015), A detailed analysis of initial seismicity induced by wastewater injection in the Val d'Agri oil field (Italy), in Schatzalp Induced Seismicity Workshop, 10-13 March 2015, Davos, Switzerland.

Jaku, E. P., A. Z. Toper, and A. J. Jager (2001), Updating and maintaining the accident database, Safety in Mines Research Advisory Committee.

Jiménez, A., K. F. Tiampo, A. M. Posadas, F. Luzón, and R. Donner (2009), Analysis of complex networks associated to seismic clusters near the Itoiz reservoir dam, The European Physical Journal Special Topics, 174, 181-195.

Julià, J., A. A. Nyblade, R. Durrheim, L. Linzer, R. Gök, P. Dirks, and W. Walter (2009), Source mechanisms of mine-related seismicity, Savuka mine, South Africa, Bulletin of the Seismological Society of America, 99, 2801-2814.

Julian, B. R., G. R. Foulger, and F. C. Monastero (2009), Seismic monitoring of EGS stimulation tests at the Coso geothermal field, California, using microearthquake locations and moment tensors, paper presented at Thirty-Fourth Workshop on Geothermal Reservoir Engineering, Stanford University, Stanford, California, February.

Julian, B. R., A. Ross, G. R. Foulger, and J. R. Evans (1996), Three- dimensional seismic image of a geothermal reservoir: The Geysers, California, Geophysical Research Letters, 23, 685-688.

Jupe, A. J., A. S. P. Green, and T. Wallroth (1992), Induced microseismicity and reservoir growth at the Fjällbacka hot dry rocks project, Sweden, International journal of rock mechanics and mining sciences & geomechanics abstracts, 29, 343-354.

Justinic, A. H., B. Stump, C. Hayward, and C. Frohlich (2013), Analysis of the Cleburne, Texas, earthquake sequence from June 2009 to June 2010, Bulletin of the Seismological Society of America, 103, 3083-3093.

Kaieda, H., H. Ito, K. Kiho, K. Suzuki, H. Suenaga, and K. Shin (2005), Review of the Ogachi HDR project in Japan, paper presented at World Geothermal Congress.

Kaieda, H., S. Sasaki, and D. Wyborn (2010), Comparison of characteristics of micro-earthquakes observed during hydraulic stimulation operations in Ogachi, Hijiori and Cooper Basin HDR projects, paper presented at World Geothermal Congress.

Kalkan, E. (2016), An automatic P- phase arrival- time picker, Bulletin of the Seismological Society of America.

Kalkan, E., C. Gurbuz, and E. Zor (2014), The usage of correlation method for micro-earthquake analysis at Salavatli geothermal area, Aydin, Turkey, paper presented at AGU Fall Meeting Abstracts.

Kaneko, K., K. Sugawara, and Y. Obara (1989), Microseismic monitoring for coal burst prediction in the Miike coal mine, Gerlands Beitrage zur Geophysik, 98, 447-460.

Kangi, A., and N. Heidari (2008), Reservoir-induced seismicity in Karun III dam (southwestern Iran), Journal of Seismology, 12, 519-527.

Kao, H., A. M. Farahbod, J. F. Cassidy, M. Lamontagne, D. Snyder, and D. Lavoie (2015), Natural resources Canada's induced seismicity research, in Schatzalp Induced Seismicity Workshop, 10-13 March 2015, Davos, Switzerland.

Kaven, J. O., S. H. Hickman, A. F. McGarr, and W. L. Ellsworth (2015), Surface monitoring of microseismicity at the Decatur, Illinois, CO2 sequestration demonstration site, Seismological Research Letters, 86, 1096-1101.

Keck, R. G., and R. J. Withers (1994), A field demonstration of hydraulic fracturing for solids waste injection with real-time passive seismic monitoring, paper presented at SPE Annual Technical Conference and Exhibition, Society of Petroleum Engineers.

Keiding, M., T. Árnadóttir, S. Jonsson, J. Decriem, and A. Hooper (2010), Plate boundary deformation and man-made subsidence around geothermal fields on the Reykjanes Peninsula, Iceland, Journal of Volcanology and Geothermal Research, 194, 139-149.

Keranen, K. M., C. Hogan, H. M. Savage, G. A. Abers, and N. van der Elst (2013), Variable seismic response to fluid injection in central Oklahoma, paper presented at AGU Fall Meeting Abstracts.

Keranen, K. M., H. M. Savage, G. A. Abers, and E. S. Cochran (2013), Potentially induced earthquakes in Oklahoma, USA: Links between wastewater injection and the 2011 Mw 5.7 earthquake sequence, Geology, 41, 699-702.

Keranen, K. M., M. Weingarten, G. A. Abers, B. A. Bekins, and S. Ge (2014), Sharp increase in central Oklahoma seismicity since 2008 induced by massive wastewater injection, Science, 345, 448-451.

Kerr, R. A. (2009), After the quake, in search of the science—or even a good prediction, Science, 324, 322-322.

Kerr, R. A., and R. Stone (2009), A human trigger for the great quake of Sichuan?, Science, 323, 322-322.

Kertapati, E. K. (1987), Saguling-Cirata water reservoirs along Citarum river west Java, Indonesia as reservoir induced seismicity, YY1-YY9.

Kim, W. Y. (2013), Induced seismicity associated with fluid injection into a deep well in Youngstown, Ohio, Journal of Geophysical Research: Solid Earth, 118, 3506-3518.

Kim, W.-Y., M. Gold, C. Schamberger, J. Jones, and H. Delano (2009), The 2008-2009 earthquake swarm near Dillsburg, Pennsylvania.

King, G. C. P., R. S. Stein, and J. Lin (1994), Static stress changes and the triggering of earthquakes, Bulletin of the Seismological Society of America, 84, 935-953.

King, G. E. (2012), Hydraulic fracturing 101: What every representative, environmentalist, regulator, reporter, investor, university researcher, neighbor and engineer should know about estimating frac risk and improving frac performance in unconventional gas and oil wells, paper presented at SPE Hydraulic Fracturing Technology Conference, Society of Petroleum Engineers.

Kinscher, J., P. Bernard, I. Contrucci, A. Mangeney, J. P. Piguet, and P. Bigarre (2015), Location of microseismic swarms induced by salt solution mining, Geophysical Journal International, 200, 337-362.

Király, E., V. Gischig, D. Karvounis, and S. Wiemer (2014), Validating models to forecasting induced seismicity related to deep geothermal energy projects, paper presented at Proceedings, 39th Workshop on Geothermal Reservoir Engineering.

Kitano, K., Y. Hori, and H. Kaieda (2000), Outline of the Ogachi HDR project and character of the reservoirs, paper presented at World Geothermal Congress, Kyushu-Tohoku, Japan, May 28-June 10

Klose, C. D. (2007), Coastal land loss and gain as potential earthquake trigger mechanism in SCRs, paper presented at AGU Fall Meeting Abstracts.

Klose, C. D. (2007), Geomechanical modeling of the nucleation process of Australia's 1989 M5.6 Newcastle earthquake, Earth and Planetary Science Letters, 256, 547-553.

Klose, C. D. (2007), Mine water discharge and flooding: A cause of severe earthquakes, Mine Water and the Environment, 26, 172-180.

Klose, C. D. (2010), Human-triggered earthquakes and their impacts on human security, Achieving Environmental Security: Ecosystem Services and Human Welfare, 13-19.

Klose, C. D. (2012), Evidence for anthropogenic surface loading as trigger mechanism of the 2008 Wenchuan earthquake, Environmental Earth Sciences, 66, 1439-1447.

Klose, C. D. (2013), Mechanical and statistical evidence of the causality of human-made mass shifts on the Earth's upper crust and the occurrence of earthquakes, Journal of Seismology, 17, 109-135.

Klose, C. D., and L. Seeber (2007), Shallow seismicity in stable continental regions, Seismological Research Letters, 78, 554-562.

Knoll, P., G. Kowalle, K. Rother, B. Schreiber, and I. Paskaleva (1996), Analysis of microtremors within the Provadia region near a salt leaching mine, in Induced seismic events, pp. 389-407, Springer.

Kouznetsov, O., V. Sidorov, S. Katz, and G. Chilingarian (1995), Interrelationships among seismic and short-term tectonic activity, oil and gas production, and gas migration to the surface, Journal of Petroleum Science and Engineering, 13, 57-63.

Kovach, R. L. (1974), Source mechanisms for Wilmington oil field, California, subsidence earthquakes, Bulletin of the Seismological Society of America, 64, 699-711.

Kraaijpoel, D., D. Nieuwland, B. Wassing, and B. Dost (2012), Induced seismicity at an underground gas storage facility in the Netherlands, paper presented at EGU General Assembly Conference Abstracts.

Kreitler, C. W. (1976), Faulting and land subsidence from ground-water and hydrocarbon production, Houston-Galveston, Texas, paper presented at Proceedings of the Anaheim Symposium.

Kremenetskaya, E. O., and V. M. Trjapitsin (1995), Induced seismicity in the Khibiny Massif (Kola Peninsula), in Induced seismicity, pp. 29-37, Springer.

Kundu, B., N. K. Vissa, and V. K. Gahalaut (2015), Influence of anthropogenic groundwater unloading in Indo- Gangetic Plains on the 25 April 2015 Mw 7.8 Gorkha, Nepal earthquake, Geophysical Research Letters, 42.

Kwee, J. (2012), Micro-seismicity in the Bergermeer gas storage field, University of Utrecht, The Netherlands.

Kwiatek, G., M. Bohnhoff, G. Dresen, A. Schulze, T. Schulte, G. Zimmermann, and E. Huenges (2010), Microseismicity induced during fluid-injection: A case study from the geothermal site at Groß Schönebeck, North German Basin, Acta Geophysica, 58, 995-1020.

Lamontagne, M., Y. Hammamji, and V. Peci (2008), Reservoir-triggered seismicity at the Toulnustouc hydroelectric project, Quebec north shore, Canada, Bulletin of the Seismological Society of America, 98, 2543-2552.

Leblanc, G., and F. Anglin (1978), Induced seismicity at the Manic 3 reservoir, Quebec, Bulletin of the Seismological Society of America, 68, 1469-1485.

Lee, M. F., P. Mikula, and E. Kinnersly (2006), In situ rock stress measurements and stress change monitoring at Mt Charlotte gold mine, western Australia, paper presented at In-Situ Rock Stress: International Symposium on In-Situ Rock Stress, Trondheim, Norway, 19-21 June 2006, CRC Press.

Lehner, B., C. R. Liermann, C. Revenga, C. Vörösmarty, B. Fekete, P. Crouzet, P. Döll, M. Endejan, K. Frenken, and J. Magome (2011), High-resolution mapping of the world's reservoirs and dams for sustainable river-flow management, Frontiers in Ecology and the Environment, 9, 494-502.

Lei, X., S. Ma, W. Chen, C. Pang, J. Zeng, and B. Jiang (2013), A detailed view of the injection- induced seismicity in a natural gas reservoir in Zigong, southwestern Sichuan Basin, China, Journal of Geophysical Research: Solid Earth, 118, 4296-4311.

Lei, X., G. Yu, S. Ma, X. Wen, and Q. Wang (2008), Earthquakes induced by water injection at ~3 km depth within the Rongchang gas field, Chongqing, China, Journal of Geophysical Research: Solid Earth, 113.

Li, T., M. F. Cai, and M. Cai (2007), A review of mining-induced seismicity in China, International Journal of Rock Mechanics and Mining Sciences, 44, 1149-1171.

Lin, C. H. (2005), Seismicity increase after the construction of the world's tallest building: An active blind fault beneath the Taipei 101, Geophysical Research Letters, 32.

Lizurek, G., Ł. Rudziński, and B. Plesiewicz (2015), Mining induced seismic event on an inactive fault, Acta Geophysica, 63, 176-200.

Llenos, A. L., and A. J. Michael (2013), Modeling earthquake rate changes in Oklahoma and Arkansas: Possible signatures of induced seismicity, Bulletin of the Seismological Society of America, 103, 2850-2861.

Lockridge, J. S., M. J. Fouch, and J. R. Arrowsmith (2012), Seismicity within Arizona during the deployment of the Earthscope USarray transportable array, Bulletin of the Seismological Society of America, 102, 1850-1863.

Long, L. T., and C. W. Copeland (1989), The Alabama, USA, seismic event and strata collapse of May 7, 1986, Pure and applied geophysics, 129, 415-421.

Lorenz, J. C. (2001), The stimulation of hydrocarbon reservoirs with subsurface nuclear explosions, Oil-Industry History, 2, 56-63.

Lovchikov, A. V. (2013), Review of the strongest rockbursts and mining-induced earthquakes in Russia, Journal of Mining Science, 49, 572-575.

Ma, T. H., C. A. Tang, L. X. Tang, W. D. Zhang, and L. Wang (2015), Rockburst characteristics and microseismic monitoring of deep-buried tunnels for Jinping II hydropower station, Tunnelling and Underground Space Technology, 49, 345-368.

Ma, W. (2012), Analysis on the disaster mechanism of rock collapse of M4.4 reservoir-induced earthquake on January 17, 2010, at Dongjing reservoir in Guizhou Province, China, Natural hazards, 62, 141-148.

Maggi, A., J. A. Jackson, D. Mckenzie, and K. Priestley (2000), Earthquake focal depths, effective elastic thickness, and the strength of the continental lithosphere, Geology, 28, 495-498.

Mahdi, S. K. (1988), Tarbela reservoir a question of induced seismicity, in International Conference on Case Histories in Geotechnical Engineering.

Majer, E. L. (2011), Workshop on induced seismicity due to fluid injection/production from energy-related applications, Lawrence Berkeley National Laboratory.

Majer, E. L., R. Baria, M. Stark, S. Oates, J. Bommer, B. Smith, and H. Asanuma (2007), Induced seismicity associated with enhanced geothermal systems, Geothermics, 36, 185-222.

Majer, E. L., and J. E. Peterson (2008), The impact of injection on seismicity at The Geysers, California geothermal field, International Journal of Rock Mechanics and Mining Sciences, 44, 1079-1090.

Malovichko, D., R. Dyagilev, D. Y. Shulakov, P. Butyrin, and S. V. Glebov (2009), Seismic monitoring of large-scale karst processes in a potash mine, Controlling seismic hazard and sustainable development of deep mines, 2, 989-1002.

Matrullo, E., I. Contrucci, P. Dominique, M. Bennani, H. Aochi, J. Kinsher, P. Bernard, and P. Bigarré (2015), Analysis and interpretation of induced micro-seismicity by flooding of the Gardanne Coal Basin (Provence–southern France), paper presented at 77th EAGE Conference and Exhibition-Workshops.

Maurer, V., N. Cuenot, E. Gaucher, M. Grunberg, J. Vergne, H. Wodling, M. Lehujeur, and J. Schmittbuhl (2015), Seismic monitoring of the Rittershoffen EGS project (Alsace, France), paper presented at World Geothermal Congress.

Maxwell, S. C., D. Cho, T. L. Pope, M. Jones, C. L. Cipolla, M. G. Mack, F. Henery, M. Norton, and J. A. Leonard (2011), Enhanced reservoir characterization using hydraulic fracture microseismicity, paper presented at SPE Hydraulic Fracturing Technology Conference, Society of Petroleum Engineers.

Maxwell, S. C., and H. Fabriol (2004), Passive seismic imaging of CO2 sequestration at Weyburn.

Maxwell, S. C., U. Zimmer, R. W. Gusek, and D. J. Quirk (2009), Evidence of a horizontal hydraulic fracture from stress rotations across a thrust fault, SPE Production & Operations, 24, 312-319.

Mazzoldi, A., A. Borgia, M. Ripepe, E. Marchetti, G. Ulivieri, M. della Schiava, and C. Allocca (2015), Faults strengthening and seismicity induced by geothermal exploitation on a spreading volcano, Mt. Amiata, Italia, Journal of Volcanology and Geothermal Research, 301, 159-168.

McClure, M. W., and R. N. Horne (2014), Correlations between formation properties and induced seismicity during high pressure injection into granitic rock, Engineering Geology, 175, 74-80.

McGarr, A. (1991), On a possible connection between three major earthquakes in California and oil production, Bulletin of the Seismological Society of America, 81, 948-970.

McGarr, A. (2014), Maximum magnitude earthquakes induced by fluid injection, Journal of Geophysical Research: Solid Earth, 119, 1008-1019.

McGarr, A., B. Bekins, N. Burkardt, J. Dewey, P. Earle, W. Ellsworth, S. Ge, S. Hickman, A. Holland, and E. Majer (2015), Coping with earthquakes induced by fluid injection, Science, 347, 830-831.

McGarr, A., and D. Simpson (1997), A broad look at induced and triggered seismicity, Rockbursts and Seismicity in Mines, 385-396.

McGarr, A., D. Simpson, and L. Seeber (2002), Case histories of induced and triggered seismicity, in International geophysics series, international handbook of earthquake and engineering seismology, pp. 647-664.

McKavanagh, B., B. Boreham, K. McCue, G. Gibson, J. Hafner, and G. Klenowski (1995), The CQU regional seismic network and applications to underground mining in Central Queensland, Australia, Pure and applied geophysics, 145, 39-57.

McKeown, F. A. (1975), Relation of geological structure to seismicity at Pahute Mesa, Nevada test site, Bulletin of the Seismological Society of America, 65, 747-764.

McKeown, F. A., and D. D. Dickey (1969), Fault displacements and motion related to nuclear explosions, Bulletin of the Seismological Society of America, 59, 2253-2269.

McNamara, D. E., H. M. Benz, R. B. Herrmann, E. A. Bergman, P. Earle, A. Holland, R. Baldwin, and A. Gassner (2015), Earthquake hypocenters and focal mechanisms in central Oklahoma reveal a complex system of reactivated subsurface strike- slip faulting, Geophysical Research Letters, 42, 2742-2749.

McNamara, D. E., G. P. Hayes, H. M. Benz, R. A. Williams, N. D. McMahon, R. C. Aster, A. Holland, T. Sickbert, R. Herrmann, and R. Briggs (2015), Reactivated faulting near Cushing, Oklahoma: Increased potential for a triggered earthquake in an area of United States strategic infrastructure, Geophysical Research Letters, 42, 8328-8332.

Mercerat, E. D., L. Driad-Lebeau, and P. Bernard (2010), Induced seismicity monitoring of an underground salt cavern prone to collapse, Pure and applied geophysics, 167, 5-25.

Mereu, R. F., J. Brunet, K. Morrissey, B. Price, and A. Yapp (1986), A study of the microearthquakes of the Gobles oil field area of southwestern Ontario, Bulletin of the Seismological Society of America, 76, 1215-1223.

Milev, A. M., and S. M. Spottiswoode (2002), Effect of the rock properties on mining-induced seismicity around the Ventersdorp Contact Reef, Witwatersrand Basin, South Africa, in The mechanism of induced seismicity, pp. 165-177, Springer.

Milne, W. G., and M. J. Berry (1976), Induced seismicity in Canada, Engineering Geology, 10, 219-226.

Mirzoev, K. M., A. V. Nikolaev, A. A. Lukk, and S. L. Yunga (2009), Induced seismicity and the possibilities of controlled relaxation of tectonic stresses in the Earth's crust, Izvestiya, Physics of the Solid Earth, 45, 885-904.

Moeck, I., T. Bloch, R. Graf, S. Heuberger, P. Kuhn, H. Naef, M. Sonderegger, S. Uhlig, and M. Wolfgramm (2015), The St. Gallen project: Development of fault controlled geothermal systems in urban areas, paper presented at World Geothermal Congress.

Mogren, S., and M. Mukhopadhyay (2013), Study of seismogenic crust in the eastern province of Saudi Arabia and its relation to the seismicity of the Ghawar fields, paper presented at AGU Fall Meeting Abstracts.

Morrison, D. M. (1989), Rockburst research at Falconbridge's Strathcona mine, Sudbury, Canada, Pure and applied geophysics, 129, 619-645.

Mossop, A., and P. Segall (1999), Volume strain within The Geysers geothermal field, Journal of Geophysical Research: Solid Earth, 104, 29113-29131.

Mulargia, F., and A. Bizzarri (2014), Anthropogenic triggering of large earthquakes, Scientific Reports, 4.

Mulyadi (2010), Case study: Hydraulic fracturing experiment in the Wayang Windu geothermal field, paper presented at World Geothermal Congress, Bali, Indonesia, 25-29 April 2010.

National Research Council (NRC) (2013), Induced seismicity potential in energy technologies, National Academies Press, Committee on Induced Seismicity Potential in Energy Technologies.

Neuhaus, C. W., and J. L. Miskimins (2012), Analysis of surface and downhole microseismic monitoring coupled with hydraulic fracture modeling in the Woodford Shale, paper presented at SPE Europec/EAGE Annual Conference, Society of Petroleum Engineers.

Nicholson, C., E. Roeloffs, and R. L. Wesson (1988), The northeastern Ohio earthquake of 31 January 1986: Was it induced?, Bulletin of the Seismological Society of America, 78, 188-217.

Nicholson, C., and R. L. Wesson (1992), Triggered earthquakes and deep well activities, Pure and applied geophysics, 139, 561-578.

Nicholson, C. J. (1992), Earthquakes associated with deep well activities-comments and case histories, paper presented at The 33th US Symposium on Rock Mechanics (USRMS), American Rock Mechanics Association.

Nicol, A., R. Carne, M. Gerstenberger, and A. Christophersen (2011), Induced seismicity and its implications for CO2 storage risk, Energy Procedia, 4, 3699-3706.

Nuannin, P., O. Kulhanek, L. Persson, and T. Askemur (2005), Inverse correlation between induced seismicity and b-value, observed in the Zingruvan mine, Sweden, Acta Geodynamica et Geomaterialia, 2, 5.

Ohtake, M. (1974), Seismic activity induced by water injection at Matsushiro, Japan, Journal of Physics of the Earth, 22, 163-176.

Orlic, B., B. B. T. Wassing, and C. R. Geel (2013), Field scale geomechanical modeling for prediction of fault stability during underground gas storage operations in a depleted gas field in the Netherlands, paper presented at 47th US Rock Mechanics/Geomechanics Symposium, American Rock Mechanics Association.

Orzol, J., R. Jung, R. Jatho, T. Tischner, and P. Kehrer (2005), The Genesys-Project: Extraction of geothermal heat from tight sediments, paper presented at World Geothermal Congress.

Ottemöller, L., H. H. Nielsen, K. Atakan, J. Braunmiller, and J. Havskov (2005), The 7 May 2001 induced seismic event in the Ekofisk oil field, North Sea, Journal of Geophysical Research: Solid Earth, 110.

Oye, V., E. Aker, T. M. Daley, D. Kühn, B. Bohloli, and V. Korneev (2013), Microseismic monitoring and interpretation of injection data from the In Salah CO2 storage site (Krechba), Algeria, Energy Procedia, 37, 4191-4198.

Oye, V., and M. Roth (2005), Source parameters of microearthquakes from the 1.5 km deep Pyhäsalmi ore mine, Finland, paper presented at Proceedings, Thirtieth Workshop on Geothermal Reservoir Engineering, Stanford University, Stanford, California, January.

Paskaleva, I., A. G. Aronov, R. R. Seroglazov, and T. I. Aronova (2006), Characteristic features of induced seismic processes in mining regions exemplified by the potassium salt deposits in Belarus and Bulgaria, Acta Geodaetica et Geophysica Hungarica, 41, 293-303.

Pavlou, K., G. Drakatos, V. Kouskouna, K. Makropoulos, and H. Kranis (2016), Seismicity study in Pournari reservoir area (w. Greece) 1981–2010, Journal of Seismology, 20, 701-710.

Pavlou, K., G. Kaviris, K. Chousianitis, G. Drakatos, V. Kouskouna, and K. Makropoulos (2013), Seismic hazard assessment in Polyphyto dam area (nw Greece) and its relation with the “unexpected” earthquake of 13 May 1995 (Ms= 6.5, nw Greece), Nat. Hazards Earth Sys. Sci, 13, 141-149.

Pavlovski, O. A. (1998), Radiological consequences of nuclear testing for the population of the former USSR (input information, models, dose, and risk estimates), in Atmospheric nuclear tests, pp. 219-260, Springer.

Pechmann, J. C., W. J. Arabasz, K. L. Pankow, R. Burlacu, and M. K. McCarter (2008), Seismological report on the 6 August 2007 Crandall Canyon mine collapse in Utah, Seismological Research Letters, 79, 620-636.

Pennington, W. D., S. D. Davis, S. M. Carlson, J. DuPree, and T. E. Ewing (1986), The evolution of seismic barriers and asperities caused by the depressuring of fault planes in oil and gas fields of south Texas, Bulletin of the Seismological Society of America, 76, 939-948.

Petersen, M. D., C. S. Mueller, M. P. Moschetti, S. M. Hoover, A. L. Llenos, W. L. Ellsworth, A. J. Michael, J. L. Rubinstein, A. F. McGarr, and K. S. Rukstales (2016), One-year seismic hazard forecast for the central and eastern United States from induced and natural earthquakes, US Geological Survey.

Petersen, M. D., C. S. Mueller, M. P. Moschetti, S. M. Hoover, J. L. Rubinstein, A. L. Llenos, A. J. Michael, W. L. Ellsworth, A. McGarr, and A. A. Holland (2015), Incorporating induced seismicity in the 2014 United States national seismic hazard model: Results of 2014 workshop and sensitivity studies, US Department of the Interior, US Geological Survey.

Phillips, W. S., T. D. Fairbanks, J. T. Rutledge, and D. W. Anderson (1998), Induced microearthquake patterns and oil-producing fracture systems in the Austin Chalk, Tectonophysics, 289, 153-169.

Phillips, W. S., J. T. Rutledge, L. S. House, and M. C. Fehler (2002), Induced microearthquake patterns in hydrocarbon and geothermal reservoirs: Six case studies, in The mechanism of induced seismicity, pp. 345-369, Springer.

Piccinelli, F. G., M. Mucciarelli, P. Federici, and D. Albarello (1995), The microseismic network of the Ridracoli dam, north Italy: Data and interpretations, Pure and applied geophysics, 145, 97-108.

Plotnikova, L. M., B. S. Nurtaev, J. R. Grasso, L. M. Matasova, and R. Bossu (1996), The character and extent of seismic deformation in the focal zone of Gazli earthquakes of 1976 and 1984, M> 7.0, in Induced seismic events, pp. 377-387, Springer.

Pomeroy, P. W., D. W. Simpson, and M. L. Sbar (1976), Earthquakes triggered by surface quarrying-the Wappingers falls, New York sequence of June, 1974, Bulletin of the Seismological Society of America, 66, 685-700.

Pramono, B., and D. Colombo (2005), Microearthquake characteristics in Darajat geothermal field, Indonesia, paper presented at World Geothermal Congress 2005, Antalya, Turkey, 24–29 April, 2005.

Prioul, R., F. H. Cornet, C. Dorbath, I. Dorbath, M. Ogena, and E. Ramos (2000), An induced seismicity experiment across a creeping segment of the Philippine fault, Journal of geophysical research, 105, 13,595-513,612.

Rajendran, K. (1995), Sensitivity of a seismically active reservoir to low-amplitude fluctuations: Observations from Lake Jocassee, South Carolina, Pure and applied geophysics, 145, 87-95.

Raleigh, C. B., J. H. Healy, and J. D. Bredehoeft (1976), An experiment in earthquake control at Rangely, Colorado, Science, 191, 1230-1237.

Rastogi, B. K., C. V. R. K. Rao, R. K. Chadha, and H. K. Gupta (1986), Microearthquakes near Osmansagar reservoir, Hyderabad, India, Physics of the earth and planetary interiors, 44, 134-141.

Redmayne, D. W. (1988), Mining induced seismicity in UK coalfields identified on the BGS national seismograph network, Geological Society, London, Engineering Geology Special Publications, 5, 405-413.

Reyners, M. (1988), Reservoir-induced seismicity at Lake Pukaki, New Zealand, Geophysical Journal International, 93, 127-135.

Ringdal, F., P. D. Marshall, and R. W. Alewine (1992), Seismic yield determination of Soviet underground nuclear explosions at the Shagan River test site, Geophysical Journal International, 109, 65-77.

Rojas, E., P. Cavieres, R. Dunlop, and S. Gaete (2000), Control of induced seismicity at El Teniente mine Codelco-Chile, Proceeding, Massmin 2000, 777-781.

Ross, A., G. R. Foulger, and B. R. Julian (1999), Source processes of industrially-induced earthquakes at The Geysers geothermal area, California, Geophysics, 64, 1877-1889.

Rubinstein, J. L., W. L. Ellsworth, and A. McGarr (2012), The 2001-present triggered seismicity sequence in the Raton Basin of southern Colorado/northern New Mexico, paper presented at AGU Fall Meeting Abstracts.

Rubinstein, J. L., W. L. Ellsworth, A. McGarr, and H. M. Benz (2014), The 2001–present induced earthquake sequence in the Raton Basin of northern New Mexico and southern Colorado, Bulletin of the Seismological Society of America.

Rubinstein, J. L., and A. B. Mahani (2015), Myths and facts on wastewater injection, hydraulic fracturing, enhanced oil recovery, and induced seismicity, Seismological Research Letters, 86, 1060-1067.

Rutledge, J. T., W. S. Phillips, and B. K. Schuessler (1998), Reservoir characterization using oil-production-induced microseismicity, Clinton County, Kentucky, Tectonophysics, 289, 129-152.

Sanford, A. R., T. M. Mayeau, J. W. Schlue, R. C. Aster, and L. H. Jaksha (2006), Earthquake catalogs for New Mexico and bordering areas II: 1999–2004, New Mexico Geology, 28.

Sargsyan, L. S. (2009), Reservoir-triggered seismicity in Armenian large dams, Journal of Seismology and Earthquake Engineering, 11, 153.

Sasaki, S. (1998), Characteristics of microseismic events induced during hydraulic fracturing experiments at the Hijiori hot dry rock geothermal energy site, Yamagata, Japan, Tectonophysics, 289, 171-188.

Sato, K., and Y. Fujii (1988), Induced seismicity associated with longwall coal mining, paper presented at International Journal of Rock Mechanics and Mining Sciences & Geomechanics Abstracts, Elsevier.

Sato, K., and Y. Fujii (1989), Source mechanism of a large scale gas outburst at Sunagawa coal mine in Japan, Pure and applied geophysics, 129, 325-343.

Sato, K., T. Isobe, N. Mori, and T. Goto (1986), 9. Microseismic activity associated with hydraulic mining, paper presented at International Journal of Rock Mechanics and Mining Sciences & Geomechanics Abstracts, Elsevier.

Schlutz, R., V. Stern, and Y. J. Gu (2014), An investigation of seismicity clustered near the Cordel field, west central Alberta, and its relation to a nearby disposal well, Journal of Geophysical Research: Solid Earth, 119, 3410-3423, doi:10.1002/2013JB010836.

Schultz, R., S. Mei, D. Pană, V. Stern, Y. J. Gu, A. Kim, and D. Eaton (2015), The Cardston earthquake swarm and hydraulic fracturing of the Exshaw Formation (Alberta Bakken Play), Bulletin of the Seismological Society of America.

Schultz, R., V. Stern, M. Novakovic, G. Atkinson, and Y. J. Gu (2015), Hydraulic fracturing and the Crooked Lake sequences: Insights gleaned from regional seismic networks, Geophysical Research Letters, 42, 2750-2758.

Seeber, L., J. G. Armbruster, and W.-Y. Kim (2004), A fluid-injection-triggered earthquake sequence in Ashtabula, Ohio: Implications for seismogenesis in stable continental regions, Bulletin of the Seismological Society of America, 94, 76-87.

Seeber, L., J. G. Armbruster, W. Y. Kim, N. Barstow, and C. Scharnberger (1998), The 1994 Cacoosing Valley earthquakes near Reading, Pennsylvania: A shallow rupture triggered by quarry unloading, Journal of Geophysical Research: Solid Earth, 103, 24505-24521.

Segall, P. (1985), Stress and subsidence resulting from subsurface fluid withdrawal in the epicentral region of the 1983 Coalinga earthquake, Journal of Geophysical Research: Solid Earth, 90, 6801-6816.

Segall, P. (1989), Earthquakes triggered by fluid extraction, Geology, 17, 942-946.

Semmane, F., I. Abacha, A. K. Yelles-Chaouche, A. Haned, H. Beldjoudi, and A. Amrani (2012), The earthquake swarm of December 2007 in the Mila region of northeastern Algeria, Natural hazards, 64, 1855-1871.

Shapiro, S. A., C. Dinske, C. Langenbruch, and F. Wenzel (2010), Seismogenic index and magnitude probability of earthquakes induced during reservoir fluid stimulations, The Leading Edge, 29, 304-309.

Shapiro, S. A., J. Kummerow, C. Dinske, G. Asch, E. Rothert, J. Erzinger, H. J. Kümpel, and R. Kind (2006), Fluid induced seismicity guided by a continental fault: Injection experiment of 2004/2005 at the German deep drilling site (KTB), Geophysical Research Letters, 33.

Sherburn, S., S. Bourguignon, S. Bannister, S. Sewell, B. Cumming, C. Bardsley, J. Quinao, and I. Wallis (2013), Microseismicity at Rotokawa geothermal field, 2008 to 2012, paper presented at Proceedings of the 35th New Zealand geothermal workshop. Rotorua, New Zealand.

Sherburn, S., C. Bromley, S. Bannister, S. Sewell, and S. Bourguignon (2015), New Zealand geothermal induced seismicity: An overview.

Shirley, J. E. (1980), Tasmanian seismicity—natural and reservoir-induced, Bulletin of the Seismological Society of America, 70, 2203-2220.

Shivakumar, K., M. V. M. S. Rao, C. Srinivasan, and K. Kusunose (1996), Multifractal analysis of the spatial distribution of area rockbursts at Kolar gold mines, paper presented at International journal of rock mechanics and mining sciences & geomechanics abstracts, Elsevier.

Silitonga, T. H., E. E. Siahaan, and Suroso (2005), A Poisson's ratio distribution from Wadati diagram as indicator of fracturing of Lahendong geothermal field, north Sulawesi, Indonesia, paper presented at World Geothermal Congress 2005, Antalya, Turkey, 24–29 April, 2005.

Simiyu, S. M., and G. R. Keller (2000), Seismic monitoring of the Olkaria geothermal area, Kenya Rift Valley, Journal of volcanology and geothermal research, 95, 197-208.

Simpson, D. W., and W. Leith (1985), The 1976 and 1984 Gazli, USSR, earthquakes—were they induced?, Bulletin of the Seismological Society of America, 75, 1465-1468.

Simpson, D. W., and S. K. Negmatullaev (1981), Induced seismicity at Nurek reservoir, Tadjikistan, USSR, Bulletin of the Seismological Society of America, 71, 1561-1586.

Skoumal, R. J., M. R. Brudzinski, and B. S. Currie (2015), Earthquakes induced by hydraulic fracturing in Poland Township, Ohio, Bulletin of the Seismological Society of America, 105, 189-197.

Son, M. (2015), Microevent detection based on waveform cross-correlation in the Dogye mining area, Korea, paper presented at 2015 AGU Fall Meeting.

Stein, S., M. Liu, T. Camelbeeck, M. Merino, A. Landgraf, E. Hintersberger, and S. Kuebler (2015), Challenges in assessing seismic hazard in intraplate Europe, Geological Society, London, Special Publications, 432, SP432. 437.

Stork, A. L., J. P. Verdon, and J.-M. Kendall (2015), The microseismic response at the In Salah carbon capture and storage (CCS) site, International Journal of Greenhouse Gas Control, 32, 159-171.

Styles, P., P. Gasparini, E. Huenges, P. Scandone, S. Lasocki, and F. Terlizzese (2014), Report on the hydrocarbon exploration and seismicity in Emilia region, 1-213.

Suckale, J. (2009), Induced seismicity in hydrocarbon fields, Advances in geophysics, 51, 55-106.

Sumy, D. F., E. S. Cochran, K. M. Keranen, M. Wei, and G. A. Abers (2014), Observations of static coulomb stress triggering of the November 2011 M5.7 Oklahoma earthquake sequence, Journal of Geophysical Research: Solid Earth, 119, 1904-1923.

Sun, X., and S. Hartzell (2014), Finite- fault slip model of the 2011 Mw 5.6 Prague, Oklahoma earthquake from regional waveforms, Geophysical Research Letters, 41, 4207-4213.

Swanson, P. L. (1992), Mining-induced seismicity in faulted geologic structures: An analysis of seismicity-induced slip potential, Pure and applied geophysics, 139, 657-676.

Sylvester, A. G., and J. Heinemann (1996), Preseismic tilt and triggered reverse faulting due to unloading in a diatomite quarry near Lompoc, California, Seismological Research Letters, 67, 11-18.

Sze, E. K.-M. (2005), Induced seismicity analysis for reservoir characterization at a petroleum field in Oman, Massachusetts Institute of Technology.

Tadokoro, K., M. Ando, and K. y. Nishigami (2000), Induced earthquakes accompanying the water injection experiment at the Nojima fault zone, Japan: Seismicity and its migration, Journal of Geophysical Research: Solid Earth, 105, 6089-6104.

Talwani, P. (1995), Speculation on the causes of continuing seismicity near Koyna reservoir, India, Pure and applied geophysics, 145, 167-174.

Tang, C., T. Ma, and X. Ding (2009), On stress-forecasting strategy of earthquakes from stress buildup, stress shadow and stress transfer (SSS) based on numerical approach, Earthquake Science, 22, 53-62.

Tang, C. a., J. Wang, and J. Zhang (2010), Preliminary engineering application of microseismic monitoring technique to rockburst prediction in tunneling of Jinping II project, Journal of Rock Mechanics and Geotechnical Engineering, 2, 193-208.

Taylor, O.-D. S., T. A. Lee III, and A. P. Lester (2015), Hazard and risk potential of unconventional hydrocarbon development-induced seismicity within the central United States, Natural Hazards Review, 16, 04015008.

Taylor, O.-D. S., A. P. Lester, and T. A. Lee III (2015), Unconventional hydrocarbon development hazards within the central United States. Report 1: Overview and potential risk to infrastructure, DTIC Document.

Telesca, L., T. Matcharasvili, T. Chelidze, and N. Zhukova (2012), Relationship between seismicity and water level in the Enguri high dam area (Georgia) using the singular spectrum analysis, Natural Hazards and Earth System Science, 12, 2479-2485.

Terakawa, T., S. A. Miller, and N. Deichmann (2012), High fluid pressure and triggered earthquakes in the enhanced geothermal system in Basel, Switzerland, Journal of Geophysical Research: Solid Earth, 117.

Terashima, T. (1981), Survey on induced seismicity at Mishraq area in Iraq, Journal of Physics of the Earth, 29, 371-375.

Teyssoneyre, V., B. Feignier, J. Šilény, and O. Coutant (2002), Moment tensor inversion of regional phases: Application to a mine collapse, in The mechanism of induced seismicity, pp. 111-130, Springer.

Tiira, T. (1996), Discrimination of nuclear explosions and earthquakes from teleseismic distances with a local network of short period seismic stations using artificial neural networks, Physics of the Earth and Planetary Interiors, 97, 247-268.

TNO (2014), Literature review on injection-related induced seismicity and its relevance to nitrogen injection.

Torcal, F., I. Serrano, J. Havskov, J. L. Utrillas, and J. Valero (2005), Induced seismicity around the Tous New dam (Spain), Geophysical Journal International, 160, 144-160.

Townend, J., and M. D. Zoback (2000), How faulting keeps the crust strong, Geology, 28, 399-402.

Trifu, C.-I., T. I. Urbancic, and R. P. Young (1995), Source parameters of mining-induced seismic events: An evaluation of homogeneous and inhomogeneous faulting models for assessing damage potential, Pure and applied geophysics, 145, 3-27.

Trippi, M. H., H. E. Belkin, S. Dai, S. J. Tewalt, and C.-J. Chou (2014), USGS compilation of geographic information system (GIS) data representing coal mines and coal-bearing areas in China, US Geological Survey.

Turbitt, T. (1988), Bulletin of British earthquakes. British Geological Survey technical report wl/88/11.

Turuntaev, S. B. (1994), Temporal and spatial structures of triggered seismicity in Romashkinskoye oil-field, paper presented at Rock Mechanics in Petroleum Engineering, Society of Petroleum Engineers.

Urban, E., and J. F. Lermo (2012), Relationship of local seismic activity, injection wells and active faults in the geothermal fields of Mexico, paper presented at Proceedings of Thirty-Seventh Workshop on Geothermal Reservoir Engineering, Stanford University, Stanford, CA, SGP-TR-194.

Urban, E., and J. F. Lermo (2013), Local seismicity in the exploitation of Los Humeros geothermal field, Mexico, paper presented at Proceedings of the Thirty-Eighth Workshop on Geothermal Reservoir Engineering.

Urbancic, T. I. J., V. J. Shumila, J. T. J. Rutledge, and R. J. J. Zinno (1999), Determining hydraulic fracture behavior using microseismicity, paper presented at Vail Rocks 1999, The 37th US Symposium on Rock Mechanics (USRMS), American Rock Mechanics Association.

Vallejos, J. A., and S. D. McKinnon (2011), Correlations between mining and seismicity for re-entry protocol development, International Journal of Rock Mechanics and Mining Sciences, 48, 616-625.

Valoroso, L., L. Improta, L. Chiaraluce, R. Di Stefano, L. Ferranti, A. Govoni, and C. Chiarabba (2009), Active faults and induced seismicity in the Val d'Agri area (southern Apennines, Italy), Geophysical Journal International, 178, 488-502.

van der Elst, N. J., H. M. Savage, K. M. Keranen, and G. A. Abers (2013), Enhanced remote earthquake triggering at fluid-injection sites in the midwestern United States, Science, 341, 164-167.

van der Voort, N., and F. Vanclay (2015), Social impacts of earthquakes caused by gas extraction in the province of Groningen, the Netherlands, Environmental Impact Assessment Review, 50, 1-15.

Van Eck, T., F. Goutbeek, H. Haak, and B. Dost (2006), Seismic hazard due to small-magnitude, shallow-source, induced earthquakes in the Netherlands, Engineering Geology, 87, 105-121.

Van Eijs, R. M. H. E., F. M. M. Mulders, M. Nepveu, C. J. Kenter, and B. C. Scheffers (2006), Correlation between hydrocarbon reservoir properties and induced seismicity in the Netherlands, Engineering Geology, 84, 99-111.

Van Wees, J. D., L. Buijze, K. Van Thienen-Visser, M. Nepveu, B. B. T. Wassing, B. Orlic, and P. A. Fokker (2014), Geomechanics response and induced seismicity during gas field depletion in the Netherlands, Geothermics, 52, 206-219.

Verdon, J. P. (2014), Significance for secure CO2 storage of earthquakes induced by fluid injection, Environmental Research Letters, 9, 064022.

Verdon, J. P., J.-M. Kendall, A. L. Stork, R. A. Chadwick, D. J. White, and R. C. Bissell (2013), Comparison of geomechanical deformation induced by megatonne-scale CO2 storage at Sleipner, Weyburn, and In Salah, Proceedings of the National Academy of Sciences, 110, E2762-E2771.

Walsh, F. R., and M. D. Zoback (2015), Oklahoma's recent earthquakes and saltwater disposal, Science advances, 1, e1500195.

Walter, J. I., P. J. Dotray, C. Frohlich, and J. F. W. Gale (2016), Earthquakes in northwest Louisiana and the Texas–Louisiana border possibly induced by energy resource activities within the Haynesville Shale Play, Seismological Research Letters, 87, 285-294.

Wang, P., M. J. Small, W. Harbert, and M. Pozzi (2016), A Bayesian approach for assessing seismic transitions associated with wastewater injections, Bulletin of the Seismological Society of America.

Wang, R., Y. J. Gu, R. Schultz, A. Kim, and G. Atkinson (2016), Source analysis of a potential hydraulic fracturing induced earthquake near Fox Creek, Alberta, Geophysical Research Letters.

Wang, W., X. Meng, Z. Peng, Q. F. Chen, and N. Liu (2015), Increasing background seismicity and dynamic triggering behaviors with nearby mining activities around Fangshan pluton in Beijing, china, Journal of Geophysical Research: Solid Earth, 120, 5624-5638.

Wang, Z., C. N. Tang, T. H. Ma, L. C. Li, and Y. F. Yang (2012), Research on the surrounding rock damage of deep hard rock tunnels caused by bottom excavation, paper presented at Applied Mechanics and Materials, Trans Tech Publ.

Weingarten, M., S. Ge, J. W. Godt, B. A. Bekins, and J. L. Rubinstein (2015), High-rate injection is associated with the increase in US mid-continent seismicity, Science, 348, 1336-1340.

Weiser, D. A. (2016), Maximum magnitude and probabilities of induced earthquakes in California geothermal fields: Applications for a science-based decision framework, University of California.

Westbrook, G. K., N. J. Kusznir, C. W. A. Browitt, and B. K. Holdsworth (1980), Seismicity induced by coal mining in Stoke-on-Trent (UK), Engineering Geology, 16, 225-241.

Wettainen, T., and J. Martinsson (2014), Estimation of future ground vibration levels in Malmberget town due to mining-induced seismic activity, Journal of the Southern African Institute of Mining and Metallurgy, 114, 835-843.

Wheeler, R. L. (2009), Sizes of the largest possible earthquakes in the central and eastern United States-summary of a workshop, September 8-9, 2008, Golden, Colorado, US Geological Survey.

Wilson, M. P., R. J. Davies, G. R. Foulger, B. R. Julian, P. Styles, J. G. Gluyas, and S. Almond (2015), Anthropogenic earthquakes in the UK: A national baseline prior to shale exploitation, Marine and Petroleum Geology, 30, e17.

Windsor, C. R., P. Caviares, E. Villaescusa, and J. Pereira (2006), Reconciliation of strain, structure and stress in the El Teniente mine region, Chile, paper presented at Proceedings of International Symposium on In Situ Rock Stress, Trondheim, Norway.

Wiszniowski, J., N. Van Giang, B. Plesiewicz, G. Lizurek, D. Q. Van, L. Q. Khoi, and S. Lasocki (2015), Preliminary results of anthropogenic seismicity monitoring in the region of Song Tranh 2 reservoir, central Vietnam, Acta Geophysica, 63, 843-862.

Wolhart, S. L., T. A. Harting, J. E. Dahlem, T. Young, M. J. Mayerhofer, and E. P. Lolon (2006), Hydraulic fracture diagnostics used to optimize development in the Jonah field, paper presented at SPE Annual Technical Conference and Exhibition, Society of Petroleum Engineers.

Xie, L., K.-B. Min, and Y. Song (2015), Observations of hydraulic stimulations in seven enhanced geothermal system projects, Renewable Energy, 79, 56-65.

Xiumin, M. A., L. I. Zhen, P. E. N. G. Hua, J. I. A. N. G. Jingjie, Z. H. A. O. Fang, H. A. N. Chaopu, Y. U. A. N. Pengxiang, L. U. Shengzhou, and P. E. N. G. Liguo (2015), Fluid-

injection- induced seismicity experiment of the WFSD- 3P borehole, Acta Geologica Sinica (English Edition), 89, 1057-1058.

Xu, N.-w., C.-a. Tang, H. Li, F. Dai, K. Ma, J.-d. Shao, and J.-c. Wu (2012), Excavation-induced microseismicity: Microseismic monitoring and numerical simulation, Journal of Zhejiang University SCIENCE A, 13, 445-460.

Yeck, W. L., A. F. Sheehan, M. Weingarten, J. Nakai, and S. Ge (2014), The 2014 Greeley, Colorado earthquakes: Science, industry, regulation, and media, paper presented at AGU Fall Meeting Abstracts.

Younger, P. L., J. G. Gluyas, and W. E. Stephens (2012), Development of deep geothermal energy resources in the UK, Proceedings of the Institution of Civil Engineers-Energy, 165, 19-32.

Yu, Q., C.-A. Tang, L. Li, G. Cheng, and L.-X. Tang (2015), Study on rockburst nucleation process of deep-buried tunnels based on microseismic monitoring, Shock and Vibration, 501, 685437.

Zaliapin, I., and Y. Ben- Zion (2016), Discriminating characteristics of tectonic and human- induced seismicity, Bulletin of the Seismological Society of America.

Zang, A., V. Oye, P. Jousset, N. Deichmann, R. Gritto, A. McGarr, E. Majer, and D. Bruhn (2014), Analysis of induced seismicity in geothermal reservoirs–an overview, Geothermics, 52, 6-21.

Zedník, J., and J. Pazdírková (2014), Seismic activity in the Czech Republic in 2012, Studia Geophysica et Geodaetica, 58, 342.

Zedník, J., J. Pospíšil, B. Růžek, J. Horálek, A. Boušková, P. Jedlička, Z. Skácelová, V. Nehybka, K. Holub, and J. Rušajová (2001), Earthquakes in the Czech Republic and surrounding regions in 1995–1999, Studia Geophysica et Geodaetica, 45, 267-282.

Zhang, W.-d., and T.-h. Ma (2013), Research on characteristic of rockburst and rules of microseismic monitoring at headrace tunnels in Jinping II hydropower station, paper presented at Digital Manufacturing and Automation (ICDMA), 2013 Fourth International Conference on, IEEE.

Zhang, Y., W. Feng, L. Xu, C. Zhou, and Y. Chen (2009), Spatio-temporal rupture process of the 2008 great Wenchuan earthquake, Science in China Series D: Earth Sciences, 52, 145-154.

Zhang, Y., M. Person, J. Rupp, K. Ellett, M. A. Celia, C. W. Gable, B. Bowen, J. Evans, K. Bandilla, and P. Mozley (2013), Hydrogeologic controls on induced seismicity in crystalline basement rocks due to fluid injection into basal reservoirs, Groundwater, 51, 525-538.

Zoback, M. D., and S. M. Gorelick (2012), Earthquake triggering and large-scale geologic storage of carbon dioxide, Proceedings of the National Academy of Sciences, 109, 10164-10168.

Zoback, M. D., and H. P. Harjes (1997), Injection- induced earthquakes and crustal stress at 9 km depth at the KTB deep drilling site, Germany, Journal of Geophysical Research: Solid Earth, 102, 18477-18491.

Zoback, M. D., and J. C. Zinke (2002), Production-induced normal faulting in the Valhall and Ekofisk oil fields, in The mechanism of induced seismicity, pp. 403-420, Springer.